



# Proceedings of the International Academic Forum **AMO – SPITSE – NESEFF**

**20–25 June 2016**  
**Moscow – Smolensk**



**Proceedings of the  
International Academic Forum  
AMO – SPITSE – NESEFF**

**Russia,  
Moscow — Smolensk  
2016**

УДК 621.3+621.37+004  
И74

**INTERNATIONAL ACADEMIC FORUM AMO – SPITSE – NESEFF**  
(20–25 June 2016, Moscow – Smolensk): Proceedings of the International Academic Forum AMO – SPITSE – NESEFF. –Smolensk: Publishing «Universum». – 2016. – 156 c.

ISBN 978-5-91412-313-7

The proceedings include the works of the International Academic Forum AMO – SPITSE – NESEFF, held on 20–25 June 2016 in National Research University "Moscow Power Engineering Institute" in Moscow and Smolensk, that present the results of the original research and development work in the field of electricity, electronics and information technology, and reflect the issues of international cooperation in the field of education and science.

The publication is intended for researchers and university professors, graduate and post-graduate students engaged in research in the field of electricity, electronics and information technology.

As a rule, author's original papers are presented, but in some cases, corrections of a technical nature were made.

**INTERNATIONAL COMMITTEE**

Nikolay Rogalev, MPEI Rector  
Vladimir Kutuzov, ETU "LETI" Rector  
Vladimir Zamolodchikov, MPEI Vice-Rector  
Viktor Tupik, ETU "LETI" Vice-Rector  
Matthias Hein, TU Ilmenau  
Peter Biegel, BTU Cottbus-Senftenberg  
Hannes Töpfer, TU Ilmenau  
Karel Fraňa, TU Liberec  
Marek Młyńczak, Wrocław Univ. of Tech.  
Oleg Duhlev, TU Sofia

**ORGANIZING COMMITTEE**

Maxim Goncharov, MPEI Smolensk branch  
Deputy Director  
Maksim Dli, MPEI Smolensk branch Deputy Director  
Igor Zhelbakov, MPEI  
Valeriy Lunin, MPEI  
Sylvio Simon, BTU Cottbus-Senftenberg  
Pavel Varshavskiy, MPEI  
Ekaterina Zhigulina, MPEI  
Vera Barat, MPEI  
Natalia Savchenkova, MPEI  
Alexander Tarasov, MPEI

ISBN 978-5-91412-313-7

© Авторы, 2016  
© «Универсум»  
© филиал МЭИ в г. Смоленске, 2016

# **XXI AMO Conference 2016**



## **AMO - Association of International Offices of Higher Education Institutions**

The mission of AMO is integration of efforts and creative potential of international departments of higher educational institutions staff for solution relevant organizational, methodical, economical and social problems related to modernization of international relations directed to development of academic, scientific, economic and cultural activity.

Aims and tasks are all possible support to academic exchange, keeping and development of existing relations between higher educational institutions

This Association is non-governmental non-commercial public organization establishing on the free-will basis.

Association activity is based on official documents of international rights, position of UN on the human rights and intends coordinate its efforts with activity of UNESCO, UNIDO and other humanitarian international organizations.

The Association is an open organization and is ready to accept those who share aims and tasks of Association and agree with its Charter.

Working languages are Russian, English, German.

The Association is ready for cooperation with any similar organization which support ideal of humanism and progress.

# Ассоциация международных отделов: история создания, цели, планы и перспективы

Замолодчиков Владимир Николаевич  
Проректор по международным связям НИУ "МЭИ"  
Москва, Россия  
ZamolodchikVN@mpei.ru

Тарасов Александр Евгеньевич<sup>1</sup>,  
Гуличева Елена Геннадьевна<sup>2</sup>  
Отдел международного сотрудничества НИУ "МЭИ"  
Москва, Россия  
<sup>1</sup>oms.mpei@gmail.com, <sup>2</sup>egulicheva@gmail.com

**Abstract**—В статье рассмотрены особенности, связанные с организаций международного сотрудничества в области науки и образования посредством добровольного объединения представителей международных подразделений университетов стран мира в рамках Ассоциации международных отделов (АМО).

**Abstract**—In the article features connected with organization of international cooperation in science and education through voluntary association of representatives of universities international offices of various countries within the Association of the International Departments (AMO) are considered.

**Keywords**—international cooperation, internationalization of education, joint educational programs

На пути интеграции университетов в мировое научное и образовательное пространство наиболее актуально для каждого из вузов и, прежде всего, ведущих университетов, их подключение в разработку совместных с зарубежными вузами образовательных услуг. Одним из способов активизации данной деятельности является участие университетов в работе межвузовских объединений, в том числе и международных.

В качестве примера такого межвузовского объединения можно привести Ассоциацию международных отделов вузов (АМО). АМО была создана 25 лет назад, для сохранения сложившихся в советское время связей вузов России и Восточной Европы.

На заре создания АМО вузы России, Беларуси, Болгарии, Венгрии, Германии, Литвы, Польши, Словакии, Украины и Чехии в лице представителей международных подразделений своих университетов объединили свои усилия и творческий потенциал для решения актуальных организационных, методических, экономических и социальных проблем, связанных с совершенствованием международных связей, направленных на развитие образования, науки, техники, экономики и культуры. Ради этой высокой цели была создана ассоциация международных отделов высших учебных заведений, которая успешно функционирует и сейчас.

Ассоциация является неправительственной, некоммерческой общественной организацией, созданной

на добровольной основе. Членами АМО могут быть физические и юридические лица, проявившие себя в развитии международных связей и содействующие деятельности АМО [1].

За годы существования АМО её членами была организована 21 международная конференция для сотрудников международных отделов. АМО доказала свою эффективность: проведены многочисленные академические обмены, десятки преподавателей и сотрудников повысили квалификацию в партнерских вузах. Самое главное достижение – неформальные, дружественные связи между конкретными людьми, которые позволили не только сохранить, но укрепить и развить имеющийся потенциал. Именно личные связи между сотрудниками международных служб позволяют находить неординарные решения, предлагать новые программы.

В эпоху интернационализации образования перед Ассоциацией встает задача расширения сотрудничества за пределы России и Восточной Европы, увеличения вузов-участников. Согласно новым перспективным направлениям сотрудничества между вузами и концепции непрерывного образования, деятельность ассоциации должна быть направлена также и на создание международных летних школ, участие в национальных государственных и европейских стипендиальных программах, создание конкурентоспособных заявок в рамках программы Эразмус Плюс (Erasmus+). Немаловажным направлением развития в условиях информационного общества является использование социальных сетей и создание единой информационной площадки. Деятельность университета в рамках АМО позволяет оперативно реагировать на вызовы, связанные с глобализацией, решать задачи как саморазвития, так и развития своего региона и страны. Современный опыт международного сотрудничества показывает, что стратегия интеграции является эффективным способом повышения конкурентоспособности вуза в глобальном обществе.

[1] Устав АМО. Электронный ресурс // Режим доступа: <http://mpei.ru/internationalactivities/partnership/Pages/amo.aspx>. – 2016.

# О реализации права университета по самостоятельному осуществлению признания иностранных образований и иностранной квалификации

Замолодчиков Владимир Николаевич  
Проректор по международным связям  
НИУ "МЭИ"  
Москва, Россия  
UVS@mpei.ru

Житникова Марина Николаевна  
Отдел экспертизы иностранных документов  
НИУ "МЭИ"  
Москва, Россия  
recognition@mpei.ru

**Abstract**—В данной статье обсуждаются вопросы реализации российскими университетами права, предоставленного им российским законодательством в области образования, по самостоятельному осуществлению признания иностранного образования.

**Abstract**—This article discusses the realization of the Russian universities the right granted to them by the Russian legislation in the field of education for the implementation of self-recognition of foreign education.

**Keywords**—education; credentials; recognition; evaluation

Вступивший в силу 01 сентября 2013 года Федеральный закон "Об образовании в Российской Федерации" [1] создал новую законодательную основу российского образования. Этим законом были введены новые определения и термины, внесены изменения в структуру уровней образования. Отдельная статья регулирует в этом законе вопросы признания иностранного образования и (или) иностранной квалификации — одного из основных инструментов академической мобильности. Настоящим законом осуществлен по сути революционный прорыв в российской системе признания, формирование которой происходило в правовых рамках действовавших последние двадцать лет российских нормативных актов. Все эти годы в России действовала строго централизованная схема, в которой любой обладатель иностранной квалификации, планировавший продолжить обучение в российском университете, приступить к профессиональной деятельности, вынужден был ожидать официального решения о признании, которое принималось исключительно на государственном уровне — в стенах Министерства образования или Федеральной службы по надзору в сфере образования и науки РФ. С момента вступления в силу нового закона право осуществлять признание иностранного образования и(или) квалификации, а также иностранной ученой степени, иностранного ученого звания получили и некоторые университеты, однако с оговоркой — только для целей

обеспечения доступа к образовательным программам или профессиональной деятельности исключительно в данном конкретном университете. К этим университетам относятся вузы нескольких категорий: МГУ, СПбГУ, "федеральные" и "национальные исследовательские" университеты, а также вузы, перечень которых утверждается указом Президента РФ. В настоящее время таких образовательных организаций насчитывается сорок шесть. Эти вузы, реализовав такое право на самостоятельную деятельность в области признания, должны проинформировать о принятых в них порядках признания Национальный информационный центр по вопросам признания образования и (или) квалификации, ученых степеней и званий, полученных в иностранном государстве, функции которого Распоряжением Правительства РФ от 27.02.2014 № 272-р [2] возложено на ФГБНУ "Главэкспертцентр". К настоящему моменту (весна 2016г.) 28 российских вузов из 46 сообщили о принятых в них нормативных актах, устанавливающих порядки признания [3]. Не удивительно, что эти документы, разработанные в вузах, имеют свои уникальные особенности. Каждый вуз выстраивал в рамках действующего законодательства свою локальную систему признания, опираясь на имеющуюся практику международного сотрудничества, опыт обучения иностранных студентов, учитывая кадровые возможности — наличие сотрудников, прошедших повышение квалификации по программам оценки и экспертизы иностранных документов об образовании.

НИУ "МЭИ" имеет категорию национального исследовательского университета с 2010г. [4]. И, следовательно, получил возможность воспользоваться правом, предоставленным новым законом об образовании. Университет разработал Порядок признания иностранного образования и(или) квалификации одним из первых — документ вступил в университете в действие в марте 2014г., что позволило достаточно успешно подготовиться к началу приемной кампании.

Российский закон об образовании устанавливает, что признание иностранного образования и(или) квалификации – это официальное подтверждение значимости уровня образования и(или) квалификации, подпадающих по действие международных договоров по признанию или выданных иностранными организациями, включенными в Перечень Правительства [1], наделяющее обладателя такого образования правами, которые имеют обладатели российских документов об образовании соответствующего уровня. Однако ни в законе, ни в подготовленных для его реализации подзаконных актах не содержится персонифицированной ответственности за принятие такого официального решения. Следует отметить, что в соответствии с международной практикой ответственность за признание лежит на принимающем первоначально на обучение, а затем выпускающем (выдающем документы об образовании) вузе. Основываясь на таком постулате, в НИУ "МЭИ" было принято решение проводить оценку всех документов об образовании, свидетельствующих о получении иностранного образования и(или) квалификации. Такая экспертная оценка включает фактологический анализ документа, установление принадлежности иностранного образования и(или) квалификации национальной системе образования, а именно, выполнение требований по лицензированию, аттестации, аккредитации образовательной организации и образовательной программы, или иному способу признания иностранного образования и(или) квалификации в качестве составляющей этой национальной системы образования, определение уровня полученного образования, выполнения требований доступа к этому уровню образования в национальной системе образования, условий доступа к последующему уровню образования или профессиональной деятельности. И только при положительных результатах такой проверки устанавливается, подпадает или нет под действие международного договора представленные к признанию иностранное образование и(или) квалификация, указан ли в утвержденном Правительством РФ Перечне иностранный вуз, перечислен ли в этом Перечне уровень образования и (или) квалификации и соответствующий им российский уровень образования и квалификация. Для иностранного образования и(или) квалификации, не подпадающих по действие договоров или не включенных в перечень, Статьей 107 Закона [1] предусмотрено проведение экспертизы. Наделение университета правом по вынесению официального решения о признании позволяет в большинстве случаев проводить предварительную экспертную оценку иностранного образования и(или) квалификации потенциальных абитуриентов по их запросам, поступающим в течение всего учебного года, консультировать их по вопросам требований к оформлению документов об иностранном образовании и(или) квалификации при поступлении в

российские вузы, а в жаркое время приемной кампании принимать оперативно, основываясь на результатах уже проведенной оценки, решения о признании. Наличие в университете собственных структурных подразделений или отдельных квалифицированных экспертов по вопросам признания иностранного образования и(или) квалификации, принятого порядка признания позволяет минимизировать стрессовые состояния у абитуриентов, которым в ограниченный срок перед началом приемной кампании требуется подготовить удовлетворяющие установленным требованиям документы и пройти процедуру признания. Для абитуриентов таких вузов, как и, например, НИУ "МЭИ" процедура признания проходит практически незаметно. Все формальные вопросы решаются на уровне взаимодействия подразделений университета: приемной комиссии и структурного подразделения, ответственного за проведение процедуры признания. Совсем иные переживания у абитуриентов вузов, которые не наделены правом признания иностранного образования и(или) квалификации, или тех университетов из числа сорока шести, которые не воспользовались еще своим правом. Наибольшие сложности в таком случае испытывают выпускники иностранных школ и вузов текущего года – время на прохождение такой процедуры и получения официального свидетельства, выдаваемого Рособрнадзором, у них весьма ограничено, а значит абитуриент может не успеть предъявить в установленные правилами приема в вуз сроки свидетельство о признании установленного образца, а значит не будет в итоге принят на обучение.

Хочется надеяться, что опыт университетов, воспользовавшихся правом, предоставленным им новым законом, по осуществлению признания ИОК для целей продолжения обучения или профессиональной деятельности в таком вузе, будет изучен, проанализирован, и в недалеком будущем либерализация вопросов признания иностранного образования и(или) квалификации коснется всех российских университетов.

- [1] Федеральный закон от 29.12.2012 N 273-ФЗ (ред. от 02.03.2016) "Об образовании в Российской Федерации". КонсультантПлюс, [www.consultant.ru](http://www.consultant.ru).
- [2] Распоряжение Правительства РФ от 27.02.2014 № 272-р "Об уполномоченной организации, осуществляющей функции национального информационного центра по информационному обеспечению признания в Российской Федерации образования и (или) квалификации, ученых степеней и ученых званий, полученных в иностранном государстве". КонсультантПлюс, [www.consultant.ru](http://www.consultant.ru).
- [3] Официальный сайт Национального информационного центра по информационному обеспечению признания в Российской Федерации образования и (или) квалификации, ученых степеней и ученых званий, полученных в иностранном государстве. <http://www.nic.gov.ru>.

# DAAD resource platform as a tool in formation the students' professional and cultural motivation in SFD

T. Izvekova

Dept. of Linguistics and International Communications  
Novosibirsk State Medical University  
Novosibirsk, Russia  
izvekova01@gmail.com

**Abstract**—international academic mobility is an integral part of intellectual potential existence and an exceptionally important process for personal and professional development. It is one of the important parts of universities and science integration process in international educational space. The article considers logistic organizing international academic mobility programs.

**Keywords**—academic mobility programs; financing and organizing programs; global educational space

## I. INTRODUCTION

Geographically Siberian Federal District is located in the central part of the Russian Federation. Such location of SFD has a number of both advantages and disadvantages connected with opportunities of getting around the world.

Students and teaching staff international academic mobility is an integral part of modern university development and its constant work. Besides the informative part as a rule mostly depending on partner university organizing international academic mobility programs comprises organizational part engaging logistics and documentation. The article focuses on organizing international academic mobility programs in the Novosibirsk State Medical University.

## II. MAIN PART

As to the fact Novosibirsk is located in the geographical center of Russia, there are practically no transfer flights into European and Asian countries. Consequently the flight cost is rather impressive. The above mentioned reasons cause some peculiarities in financing international academic mobility programs. Due to high flight cost it is possible to organize some programs although university potential and the number of partner agreements bring more resources for that. The flight from Novosibirsk to Europe is much more expensive than from European part of Russia.

Programs of German Academic Exchange Service for students, postgraduate students and teaching staff give new opportunities for realizing exchange programs and mobility programs as well.

Novosibirsk State Medical University is a participant of DAAD grant receiving contests and many programs for students are realized due to this collaboration.

Students academic mobility is exceptionally important process for their personal and professional development, for everybody having taken part in exchange program faces the necessity to analyze and solve educational tasks and reality situations from the point of view of native and “foreign” culture. Studying at the foreign university, being in other cultural environment students will become not only objects of definite cultural traditions, standards, values influence, and also subjects, translators of their native culture into other society. Having completed their studies the students will get not only new knowledge, but they will be able to use this knowledge and “foreign” culture elements. Academic mobility is an integral part of intellectual potential existence reflecting realization of primary need of the environmental movement in social, economic, cultural, political interrelationships and interconnections. [1] It is one of the most important parts of universities and science integration process into international educational space, DAAD being an important part of it.

## III. CONCLUSION

Process of using foreign experience in the field of higher education is the aim of its quality improvement, effectiveness; focus of higher education according to international standard promotes forming common educational space. Also, the best features of Russian education continue to develop with the help of German Academic Exchange Service (DAAD).

## REFERENCES

- [1] Chistokhvalov V. N., Filipov V. M. Condition, tendencies and problems of academic mobility in European space of higher education. Training aid. Moscow, RUDN University, 2008, 162 p.
- [2] Ivanov V. G. Intercultural communications and students academic mobility of SHOC Universities. Pedagogical magazine of Bashkortostan, №3, 2015, pp. 80-86.
- [3] Antonenko S. World opened for learning: academic mobility and global educational environment, №3, Education quality. 2012, pp. 4-9.
- [4] Izvekova T. F., Pushkareva N. V. Linguistic competence as a part of professional success. Innovative development of Russia: conditions, contradictions, priorities. Part III. IX international science conference proceedings, Moscow, 2013, pp. 260-263.

**3rd International Scientific Symposium  
“Sense. Enable. SPITSE.” 2016**



## 3rd International Scientific Symposium “Sense. Enable. SPITSE.” 2016

The project **SPITSE** is the trilateral Strategic Partnership of engineering science departments of Ilmenau University of Technology (Germany), St. Petersburg Electrotechnical University "LETI" (Russia), and the National Research University "Moscow Power Engineering Institute" (Russia) for joint education and research.

The International Scientific Symposium "**Sense. Enable. SPITSE.**" is the main annual event of the Strategic Partnership. The Symposium combines a Scientific Conference and a Summer School for young researchers.

### CONFERENCE TOPICS:

1. Novel technologies for RF, microwave, and optical sensors and devices
2. Antennas for RF and microwave sensing
3. Energy efficient frontends, wireless power transfer
4. Smart sensors, sensor signal acquisition, HW/SW co-design
5. Biomedical diagnostics
6. Wireless devices and strategies for intelligent traffic systems (ITS)
7. Nonlinear dynamic system modeling, analog and digital signal processing, dirty RF
8. Wireless sensor networks, network security
9. Data fusion and data mining
10. Embedded software engineering

# A Wide Dynamic Range Microwave Spectrum Sensor for Cognitive Radio

Kurt Blau, Debalina Chatterjee and Matthias A. Hein

RF and Microwave Research Laboratory, Technische Universität Ilmenau, Ilmenau, Germany

kurt.blau@tu-ilmenau.de

**Abstract**—Microwave frequency discriminators based on six-port architecture are becoming increasingly popular for a multitude of applications in sensing and identification of spectrum holes e.g. for cognitive radio applications. This paper proposes the use of logarithmic detectors for the detector stage of the six-port receiver which enables a dynamic range of up to 80 dB.

**Keywords**—Six-port, cognitive radio, logarithmic detectors.

## I. INTRODUCTION

In order to mitigate the problem of spectrum scarcity, Mitola proposed cognitive radio (CR) [1] as a possible solution where the efficiency of spectrum utilization is enhanced through opportunistic spectrum sharing. Six-port receivers are becoming increasingly popular due to their simple architecture, favorable frequency bandwidth (usually limited to one octave) and low power consumption [2], [3]. Such receivers are generally used in direction finding and radar sensor calibration [4], [5]. With respect to spectrum sensing in CR, an example of such an approach is described in [6] where spectrum sensing is carried out through a combination of a pre-amplifier employing gain control, a tunable pre-selector (e.g., a single resonator YIG filter), and a six-port receiver. It is worth noting that the precision of the frequency measurement is determined by the six-port circuit and not by the pre-selector. However, these six-port receivers are primarily limited by their large footprint area (which is proportional to the operating wavelength) and narrow dynamic range [7]. Since the operating principle of such a six-port receiver is based on the use of square-law detectors (SD), its dynamic range is mainly restricted by the available dynamic range of the detector and the accuracy of its calibration, which is limited to about 20 to 30 dB [6], [8]. The dynamic range of the six-port receiver could be increased by using automatic gain-controlled (AGC) low-noise amplifiers (LNA) in front of the spectrum sensor, though at the expense of introducing unwanted non-linearity into the receiver circuit.

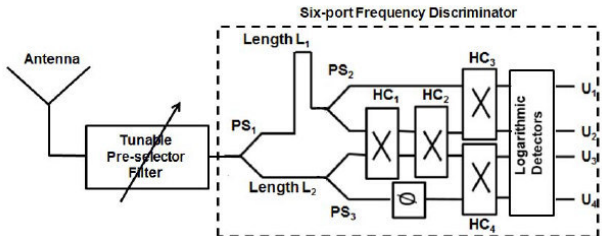


Fig. 1. Block diagram of the complete interferometer comprising antenna, tunable pre-selector and six-port circuit consisting of power splitters, transmission lines, couplers, phase shifter and logarithmic detectors, delivering 4 DC voltages  $U_1$ , through  $U_4$ . Further details are given in the text.

Also, the feedback loop required for gain control causes stability problems along with increased response time.

In contrast, this paper proposes to use logarithmic detectors (LD) in place of square-law detectors for increasing the effective dynamic range of the six-port receiver. Some commercially available LDs such as ADL5513 from Analog Devices offer a dynamic range of 80 dB at operating frequencies from 1 to 2 GHz, hence making it comparable to that of ultra wide-band heterodyne receivers without any pre-amplification. Therefore, the stand-alone spectrum sensor consisting of just a pre-selector filter and the LD-based six-port receiver can be used for detecting spectrum holes in CR, thus omitting the need of using pre-amplification with gain control as part of the measurement set-up. Additionally, the sensitivity of such a LD reaches -70 dBm, thus making this an extremely promising approach to be used in CR systems where low-power signal sensing is imperative for avoiding interference with primary users [1]. It is mandatory to mention that the operating principle of the six-port receiver is considerably modified by using LD instead of SD in the detector circuit, and so far we have not seen any previous attempt of sensing the incoming signal using this novel technique. It is worth noting that signal detection can also be essentially carried out using a four-port circuit. However, as compared to the four-port circuit, the six-port circuit helps in precise measurement of the incoming signal frequency by reducing the quadrature error [9].

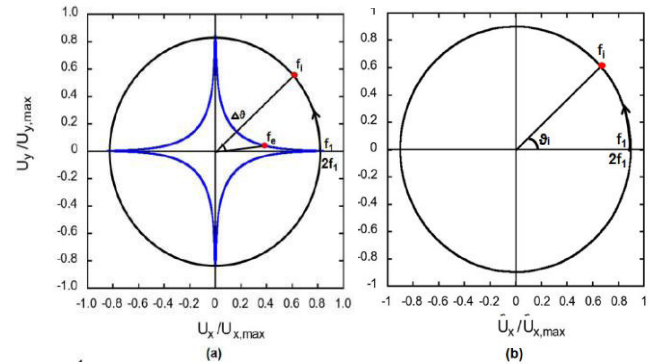


Fig. 2. Frequency discrimination in polar format for a single harmonic source at the antenna input, swept between frequencies  $f_i$  and  $2f_i$  (the arrows depict the direction of increasing frequency). Panel (a) shows the plot for normalized difference voltages from equations (3), (4) for SD depicted by circle and for LD depicted by blue super-ellipse.  $f_i$  and  $f_e$  represent the accurate and erroneous frequency respectively and  $\Delta\theta$  depicts the phase difference error. Panel (b) shows the result after minimizing the measurement error for the normalized difference voltages. The input signal frequency and phase difference are represented by  $f_i$  and  $\Delta\theta$  respectively.

## II. ARCHITECTURE AND OPERATING PRINCIPLE

Fig. 1 displays the block diagram of the proposed microwave frequency discriminator. The antenna receives a signal from the environment which is passed to the tunable pre-selector and the six-port circuit consisting of three symmetric power splitters ( $PS_1$  through  $PS_3$ ), two transmission lines of different lengths  $L_1$  and  $L_2$ , four hybrid couplers ( $HC_1$  through  $HC_4$ ) and four LDs. Additionally, the phase shifter  $\phi$  is used for precise tuning of the center frequency of the discriminator. The frequency  $f_i$  of the incoming signal is converted into a corresponding phase difference  $\delta_i$  through the delay lines as the key components, and the couplers in combination with the LDs translate the phase difference  $\delta_i$  into four complementary output voltages  $U_1$  through  $U_4$ . In general, the operating principle of the six-port interferometer is essentially based on the use of SD and can be described by the following equations which describe the resultant output voltages at the SDs [2], where  $U$  denotes the amplitude of the incoming signal and  $k$  denotes the transfer parameter of the detector and the six-port circuit:

$$U_{1,2} = \frac{1}{2}kU^2[1 \pm \cos(\vartheta_i)], \quad (1)$$

$$U_{3,4} = \frac{1}{2}kU^2[1 \mp \sin(\vartheta_i)], \quad (2)$$

The difference voltages can then be calculated as:

$$U_x = U_1 - U_2 = kU^2 \cos(\vartheta_i), \quad (3)$$

$$U_y = U_4 - U_3 = kU^2 \sin(\vartheta_i). \quad (4)$$

It is worth noting that equations (3) and (4) represent parametric equations of a circle. This is shown by the circle in Fig. 2a which depicts a hypothetical detector result in polar format using the difference voltages from equations (3) and (4) when there is only one sinusoidal signal source at the input of the antenna. The figure is based on numerical simulations and is performed with the ideal component models available in ADS 2011.05 for a single source of constant output power swept over one octave starting at  $f_i = 1$  GHz.

## III. MEASUREMENT RESULTS

Some measurements have been carried out at frequencies between 1 to 2 GHz, using a commercial six-port circuit from TRW and logarithmic detectors ADL 5513 from Analog Devices. The measurement set-up comprises a single CW carrier signal source with constant output power at the input of the six-port circuit alone (without pre-selector) and the logarithmic detectors. Fig. 3 shows the measured result in polar format and the frequency measurement error. It is seen that the maximum achieved error within this range is about + 70 MHz to - 85 MHz. It is worth noting that the simulated error is only +/- 51 MHz. The large difference is due to the real values in transmission coefficients between the direct and coupled ports of the hybrid couplers and the non-ideal transfer characteristic of the logarithmic detectors with a measured maximum error over the entire frequency range of +/- 3 dB.

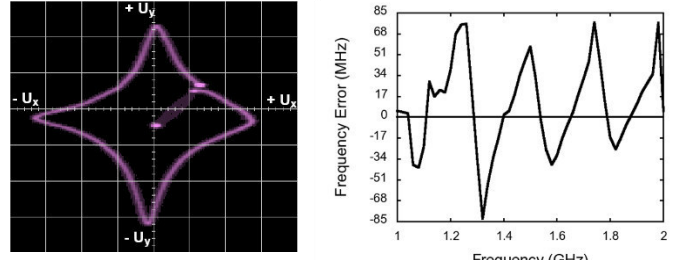


Fig. 3. The left panel shows the measurement result in polar format for a single source (0 dBm constant power) swept from 1 GHz to 2 GHz using LD's and the right panel depicts the resultant measured frequency error.

## IV. CONCLUSIONS

This paper describes a suitable technique for sensing an incoming signal spanning a very wide dynamic range using a six-port receiver employing logarithmic instead of square-law diode detectors. Such a technique provides low-power spectral sensing in CR over a very large dynamic range without pre-amplifier. It is worth noting that for all practical purposes considering the losses due to the pre-selector and the six-port circuit, the usable dynamic range is about 70 dB in the frequency range of 1 to 2 GHz.

## ACKNOWLEDGMENT

This work has been performed within the Cognitive Radio Network Lab associated with the International Graduate School on Mobile Communications (Mobicom), and has been supported in part by the Carl Zeiss Foundation and the German Research Foundation (GRK1487).

## REFERENCES

- [1] J. Mitola, III, and G. Q. Maquire, Jr., *Cognitive radio: making software radios more personal*, IEEE Pers Commun., vol. 6, no. 4, pp. 13-18, Aug. 1999.
- [2] A. Koelpin, G. Vinci, B. Laemmle, D. Kissinger, and R. Weigel, *The six-port in modern society*, IEEE Microw. Mag, vol. 11, no. 7, pp. 3543, Dec. 2010.
- [3] F. M. Ghannouchi and A. Mohammadi, *The Six-Port Technique with Microwave and Wireless Applications*, Artech House, 2009.
- [4] G. Vinci, B. Laemmle, F. Barbon, R. Weigel, and A. Koelpin, *A 77 GHz direction of arrival detector system with SiGe integrated six-port receiver*, Proc. IEEE Topical Meeting on Wireless Sensors and Sensor Networks (WiSNET), pp. 2932, 2012.
- [5] G. Vinci, A. Koelpin, and R. Weigel, *Employing six-port technology for phase-measurement-based calibration of automotive radar*, Proc. Asia-Pacific Microwave Conf. (APMC), pp. 329332, 2009.
- [6] D. Chatterjee, K. Blau, and M. Hein, *Highly Linear Microwave Signal Detection for Cognitive Radio*, German Microwaves Conference GeMiC, VDE-Verl. (2014), insges. 4 S, March 2014.
- [7] C. de la Morena-Alvarez-Palencia, and M. Burgos-Garcia, *Experimental performance comparison of six-port and conventional zero-IF/low-IF receivers for software defined radio*, Progress Electrom. Research B, vol. 42, pp. 311333, 2012.
- [8] A. Rutkowski, and B. Stec, *A planar microwave frequency discriminator*, Microwaves and Radar Conference MIKON, vol. 2, pp. 368-372, May 1998.
- [9] D. Chatterje, K. Blau, and M. Hein, *A Wide Dynamic Range Frequency Discriminator for Cognitive Radio*, Proceedings of the 45<sup>th</sup> Microwave Conference (EuMC), pp. 889-892, Paris 2015.

# Design Verification of a Passive, Tuneable, Transistor-based RF Inductance

S. Loracher, K. Blau, U. Stehr, R. Stephan, and M. A. Hein

RF & Microwave Research Laboratory, Technische Universität Ilmenau, 98693 Ilmenau, Germany

E-Mail: stefanie.loracher@tu-ilmenau.de

**Abstract**—An innovative approach for tuneable reactances using the example of electronic inductances is introduced and the operation principle affirmed by measurement. Hitherto solutions for variable inductances often lack applicability in serial paths or do not exhibit passive behaviour. Complementary to previous ideas of tuneable reactive elements, initial numerical and experimental studies of the transistor-based approach described here reveal a passive, reciprocal tuneable inductance. Even though it is transistor-based, the behaviour shown at the output terminals is that of a passive, reactive element, over a limited frequency range. Due to its possible implementations in series paths, new applications become feasible and result in more degrees-of-freedom in circuit design. Through its tuneability and degree of integrability, new possibilities for interesting applications open up, e.g., in integrated oscillator and amplifier circuits for a multitude of relevant applications in sensing and mobile communications.

**Keywords**— Tunable circuits and devices, Tuneable inductance, Transistor-based reactance, Tuneable reactance

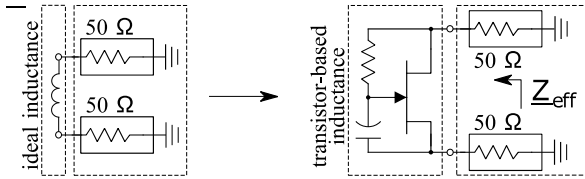


Fig. 1. Inductances in a 2-port setup: Comparison of the circuit diagram of an ideal inductance (left-hand part) measured as a 2-port device, and the corresponding ideal transistor-based inductance circuit (right-hand part), that displays inductive behaviour at its terminals.

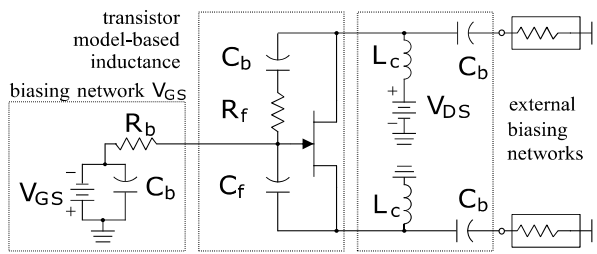


Fig. 2. Circuit diagram of the JFET-based inductance with feedback elements R<sub>f</sub> and C<sub>f</sub>. The biasing was included in the simulation but implemented externally.

## I. INTRODUCTION

Out of four basic tuneable reactance circuits [1], the topology of the basic transistor-based inductance as depicted in Fig. 1 is of highest interest and has been investigated further. It consists of the transistor and two passive feedback elements. The inductance circuit illustrated in Fig. 2 yields S-parameters for every biasing condition. Based on the S-parameters, the effective inductance value L and the resulting  $Z_{\text{eff}} = R_L + j X_L$  and inductance  $L = X_L/\omega$  can be evaluated. The tuneability of the inductance is achieved through a variation of the biasing condition of the transistor, causing a variation of the time invariant forward transconductance  $S = \delta I_{\text{out}}/\delta V_{\text{in}}$ . As a result, the impedance  $Z_{\text{eff}}$  at the output varies, displaying a variation of the inductive value L, but keeping at the same time a frequency-dependent fixed resistance value  $R_L$  [1]. As the transistor-based inductance utilises an active element, passivity and reciprocity must be verified, to give reason to the application as a stable tuneable inductance not only in shunt but series paths as well. Therefore, an inductance measured as a 2-port device, as shown in Fig. 1 and Fig. 2, was the preferred setup for simulations and experimental verification. On one hand, it offers higher measurement accuracy and dynamic range in terms of S-parameters, and on the other hand it facilitates the discussion of symmetry and reciprocity, based on formal considerations of the 2x2 scattering matrix. Reciprocity and passivity are often attributed to the same circuit but are not identical terms. The passive behaviour of the inductance circuit was analytically proven in [1] and is obvious from both simulated and measured data: The sum of the squared absolute values remains below one:  $|S_{11}|^2 + |S_{12}|^2 \leq 1$ . Reciprocity, on the other side, is defined as identical forward and backward transmission  $S_{12} = S_{21}$  and symmetry is achieved when additionally, the reflection parameters are identical,  $S_{11} = S_{22}$  [1]. Reciprocity and symmetry both are satisfactorily shown for simulation and as shown in the measurement of the test board in Fig. 3. This is a main feature of the transistor circuit introduced here, closing a long existing gap in circuit design.

## II. SIMULATION RESULTS

To illustrate the potential of the inductance circuit, initially simulation results of ideal inductances were compared with those of the reactance circuit-based inductance in terms of reflection and transmission parameters for different values of the forward transconductance. The results reveal strong similarity between the ideal case and the electronic circuit, as well as its symmetric transmission properties. results

revealed strong similarity between the ideal case and the electronic circuit, as well as its symmetric transmission properties. Later, this behaviour was confirmed again through a comparison of the simulated and measured results. The variation of the feedback elements  $R_f$  and  $C_f$  showed that magnitude and frequency dependence are strongly influenced by them. It became also apparent that the resistive part  $R_L$  of  $Z_{\text{eff}}$  is especially high at smaller  $S$  values, whereas larger  $S$  values cause a smaller  $R_L$  over a broader frequency range. It is imperative in the design of a useful inductive circuit to keep  $R_L$  small, as it compromises the quality factor  $Q$  as well as the transmission and reflection characteristics. However, the existing differences between ideal and transistor-based inductance, e.g., increasing resistive part over frequency, lower quality factor and so on, are based on the transistor characteristics, therefore being limiting factors in implementation. The drain-gate capacitance  $C_{dg}$  acting as a feedback capacitance parallel to  $R_f$  was identified in the simulations to be one of the most influencing parameters as it lowers the reactive part of the transistor circuit. Small capacitances in the transistor, especially  $C_{dg}$  and  $C_{gs}$ , high resistances  $R_{in}$  and  $R_{out}$ , as well as a high forward transconductance  $S$  are essential for optimal results. As the selection of the transistor influences reciprocity, tuning range, and achievable  $Q$ -factors, the significance of an optimal choice of the transistor element must be emphasized to gain the best possible results.

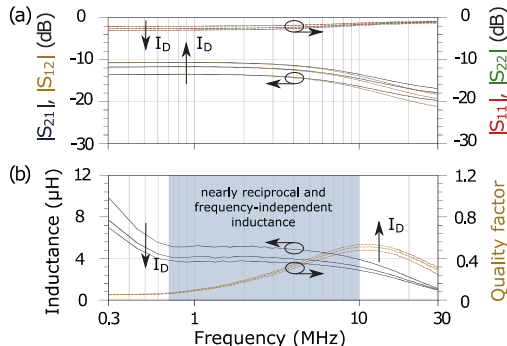


Fig. 3. Measured results of the BF545A-based electronic inductance: Experimental proof-of-principle is achieved by variation of inductance values as well as those being constant over a frequency range across which reciprocity is fulfilled (blue-shaded region).

### III. FABRICATION AND MEASUREMENT OF THE TEST BOARD

In reference to the simulation of the ideal FET model, a vendor transistor model-based circuit was devised in Keysight ADS [2] as shown in Fig. 2. It consists of the electronic inductance and the biasing networks with the RF choke inductance  $L_c$  and the blocking capacitance  $C_b$ . The readily available n-channel junction field-effect transistor (JFET) BF545A was chosen, due to its inherent symmetric structure and parameters that promise a high input resistance  $R_{in}$  [3]. Transit and cut-off frequencies were not focused on at this point, but instead the value of the generated inductance, its  $Q$ -factor, and especially the achievable tuning range through  $I_D$ . The vendor model of

the BF545A is included in the ADS 2014.01 component library, its biasing network is realised as ideal elements in the simulation and the bias conditions are chosen according to the datasheet. The resulting transmission and reflection parameters derived from the ideal reactance circuit simulation confirm the expected reciprocity and symmetry. However, contrary to the simulations of the idealised circuits, the simulation of the model-based inductance reveals a limited operational frequency range and higher resistive than reactive parts of  $Z_{\text{eff}}$ , leading to low  $Q$ -factors. This behaviour was found for all transistor types investigated (pHEMT, Dual-Gate FET, JFET, BJT). Leaving further improvement to a future step of our work, the circuit depicted in Fig. 2 was fabricated for evaluation of the principle-of-operation, with different feedback element value combinations, of which  $C_f = 1 \text{ pF}$  and  $R_f = 5.1 \text{ k}\Omega$  is presented here. The test board was evaluated using the vector network analyser HP8753C and its test set HP85046A. In contrast to the conducted simulations of the vendor model-based circuit, the measurement of the test board, as can be seen in Fig. 3(a) and (b), shows that the reciprocity and symmetry conditions are met over a limited frequency range (nearly-reciprocal behaviour). Countermeasures to prevent the non-reciprocal behaviour at higher frequencies are one focus of further investigation. Figure 3 reveals a strong similarity between the simulated and the measured results. Across the frequency range, for which the inductance value remains constant, the reciprocal behaviour is preserved, while the symmetrical reflection is seen over the full frequency range. As expected from the simulation, while the reflection is high,  $|S_{11}| = |S_{22}|$ . The inductance value is varied from  $3.4 \mu\text{H}$  to  $5.1 \mu\text{H}$  with a decrease of  $I_D$ , mirrored also in the slight change of the  $Q$ -factor. The inductance is constant over a broader frequency range with a smaller  $R_f = 1.5 \text{ k}\Omega$ , but the tuning range also tends to decrease.

### IV. CONCLUSIONS

A promising approach to tuneable inductances based on a transistor circuit was introduced, and an experimental implementation proved the operation principle. Closing the existing gap of passive, reciprocal, and electronically tuneable inductances makes this an important step to new degrees in circuit design. We have identified potential solutions to the limited  $Q$ -factor, which will be subject to further investigation.

### ACKNOWLEDGMENT

This work has been funded by the German Research Foundation (DFG) in the project "Miniaturised active radio frequency metamaterial circuits" (HE 3642/8-1).

### REFERENCES

- [1] S.Kühn, R.Stephan, K.Blau, M. A. Hein, "Passive Reciprocal Transistor-based RF Tuneable Inductances", German Microwave Conference, 2015.
- [2] Keysight.com. "Vendor Component Libraries | Keysight (Agilent)", 2016. [Online]. Available: <http://www.keysight.com/find/eesof-vendor-libraries>. [Accessed: Feb- 2016].
- [3] D.Ehrhardt, "Verstärkertechnik", Vieweg, Braunschweig, Germany, 1992.

# An Over-The-Air Wave Field Synthesis Testbed for Multi-GNSS Systems – Setup and Verification

Christopher Schirmer<sup>§</sup>, Alexander Rügamer<sup>\*</sup>, Mario Lorenz<sup>§</sup>, Simon Taschke<sup>\*</sup>,  
Marcus Grossmann<sup>+</sup>, Markus Landmann<sup>+</sup>, Wolfgang Felber<sup>\*</sup>, Giovanni Del Galdo<sup>†§</sup>

<sup>§</sup>Technische Universität Ilmenau, Germany

<sup>†</sup>Fraunhofer IIS, Ilmenau, <sup>\*</sup>Fraunhofer IIS, Nuremberg, Germany

**Abstract**—In this paper, we present an Over-The-Air (OTA) testbed that uses wave field synthesis (WFS) to realistically emulate a virtual electromagnetic environment in the context of global navigation satellite systems (GNSS). We will describe the software/hardware setup, system calibration, and the final test procedure with discussion of the measurement results.

When conventional test procedures employ conducted test methods for device and system tests, the realistic spatial radio channel as well as the antenna radiation pattern with possible coupling effects are not considered. The approach presented here emulates a realistic spatio-temporal electromagnetic field inside an anechoic chamber where the desired field properties are present inside a so called sweet spot. Having a known and reproducible electromagnetic field, we are able to test different systems under the same conditions for the evaluation of receiver performance, especially for the evaluation of multiantenna/beamforming receivers.

After we outlined the architecture and hardware setup, we will present the used 2D WFS-OTA setup and give an outlook to the upcoming 3D version.

**Index Terms**—Satellite navigation systems, Global Positioning System, Over-the-Air Testing, Wave Field Synthesis Introduction

## I. INTRODUCTION

In contrast to conventionally conducted and open field device testing, the over-the-air (OTA) test represents a novel approach that allows, by the use of wave-field synthesis (WFS), the realistic emulation of real world scenarios under controllable and repeatable conditions inside an anechoic chamber, see Figure 1. The benefits of such a controlled test environment are the realistic performance assessment and the product evaluation of different wireless technologies, without the need for special frequency licensing or other interference restraints required for open field tests [1], [2].

Recently, interference mitigation techniques utilizing antenna arrays have attracted a lot of interest in global navigation satellite system (GNSS) applications. The main advantage of directional steerable antennas in GNSS systems is the suppression of jammers and spoofers as well as the higher reception signal quality in multi-path fading channel environments. However, this advantage comes at the cost of increased device testing effort. In this regard, traditional device test measurement procedures such as the conducted measurement test are not able to cover the spatial dimension of the propagation channel as the air interface is bridged by cables towards the device tester. Coping with that issue, the

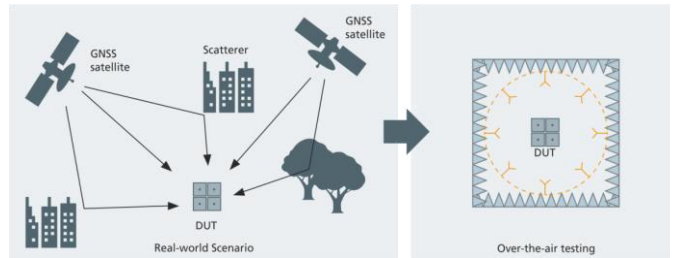


Figure 1 Principle of Over-the-air testing inside an anechoic chamber

two-stage conducted testing approach that includes the effects of the propagation channel and the antenna radiation pattern has been developed, see [3]. However, a drawback of this procedure is the inaccessibility of small and compact antennas in integrated devices, as it is not always possible to access the antenna ports without destroying the device under test (DUT), or at least significantly altering its electromagnetic properties.

In comparison to the well-known methods for device testing, the wave-field synthesis (WFS) Over-The-Air (OTA) approach provides the opportunity to test a device in an holistic way [4]. The DUT is placed in an anechoic chamber surrounded by an antenna ring or (hemi)-sphere to recreate the electromagnetic environment virtually in the chamber, as depicted in Figure 1. The advantages of the OTA method are the device testing without unmounting the device antennas. Multiple devices of the same or of different types can be tested using exactly the same measurement environment.

No electromagnetic disturbance from the outside to the test environment and vice versa has to be taken care of. Therefore, even jamming and spoofing can be investigated for single-element of CRPA antennas which is not allowed to be carried out in the free field without permission. Finally, the propagation channel conditions (e.g. multipath) of GNSS signals but also of jammers and spoofers can be emulated in great detail.

## II. OVER-THE-AIR TESTING FOR GNSS SYSTEMS

Figure 2 is showing the measurement setup inside the anechoic chamber. As a device under test (DUT), we used a NavXperience 3G+C geodetic multi-GNSS antenna that was developed by Fraunhofer IIS [5]. The DUT antenna is surrounded by 24 OTA emulation antennas, which emulate the GPS satellite positions relative to the DUT using wave field synthesis. A mapping is performed to project the GPS satellite

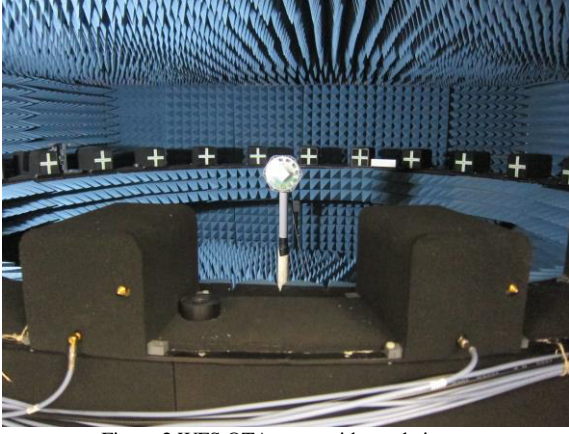


Figure 2 WFS OTA setup with geodetic antenna

positions onto the corresponding positions on the OTA ring plane. The GPS signals are emulated using the Spirent GSS9000 GNSS emulator, where we defined different scenarios, a static one, where the GPS position stays constant, a circular, and a rectangular movement scenario. The received signals were analyzed using a Septentrio receiver, that delivers i.a. the positioning information (PVT) and the C/N0 ratio for each satellite.

To have a valid comparison of the WFS OTA setup, we repeated the measurement without the antenna in a conducted test, where the gain of the DUT antenna was programmed into the Spirent satellite emulator. This means that low elevation satellites result in less signal power, because of the antenna radiation pattern, which has its main lobe looking towards the zenith. Hence, we can achieve comparable results. Figure 3 shows first measurement results, where we can compare the positioning errors for both the WFS OTA, and the conducted case. It can be seen, that we achieve similar results in both cases. Even though the mean error in the WFS OTA case is with 5.4cm larger than the conducted case with just 0.1cm, the standard deviation is with 15.4cm and 16.5cm is the same region.

The full paper will contain a detailed description of the measurement setup, calibration, and an analysis with different measurement scenarios.

#### REFERENCES

- [1] A. Rügamer, G. Del Galdo, J. Mahr, G. Rohmer, G. Siegert, and M. Landmann, "GNSS Over-the-Air Testing using Wave Field Synthesis," in *Proceedings of the 26th International Technical Meeting of The Satellite Division of the Institute of Navigation (ION GNSS+ 2013)*, Nashville, TN, September 2013, pp. 1931-1943, September 2013.
- [2] G. Siegert, M. Landmann, A. Rügamer, F. Klier, J. Mahr, G. Del Galdo, and G. Rohmer, "Multi-directional Over The Air Testbed for Robustness Testing of GNSS Receivers against Jammers and Spoofers," in *Proceedings of the 31st AIAA International Communications Satellite Systems Conference - ICSSC 2013*, 2013.

- [3] M. Rumney, R. Pirkl, M. H. Landmann, and D. A. Sanchez-Hernandez, "MIMO over-the-air research, development, and testing", *International Journal of Antennas and Propagation*, vol. 2012, 2012.
- [4] R. K. Sharma, W. Kotterman, M. H. Landmann, C. Schirmer, C. Schneider, F. Wollenschläger, G. Del Galdo, M. Hein, and R. S. Thomä, "Over-the-air testing of cognitive radio nodes in a virtual electromagnetic environment", *International Journal of Antennas and Propagation*, vol. 2013, 2013.
- [5] A. Popugaev, R. Wansch, and S. Urquijo, "A Novel High Performance Antenna for GNSS Applications", in *Antennas and Propagation, 2007. EuCAP 2007. The Second European Conference on*, Nov. 2007, pp. 1 –5

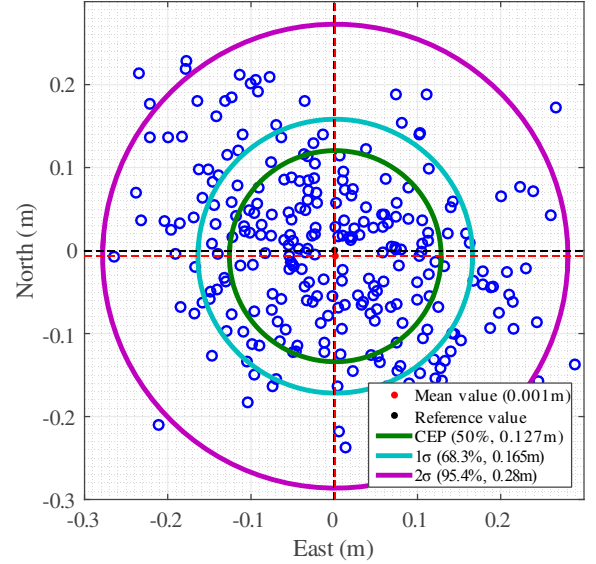
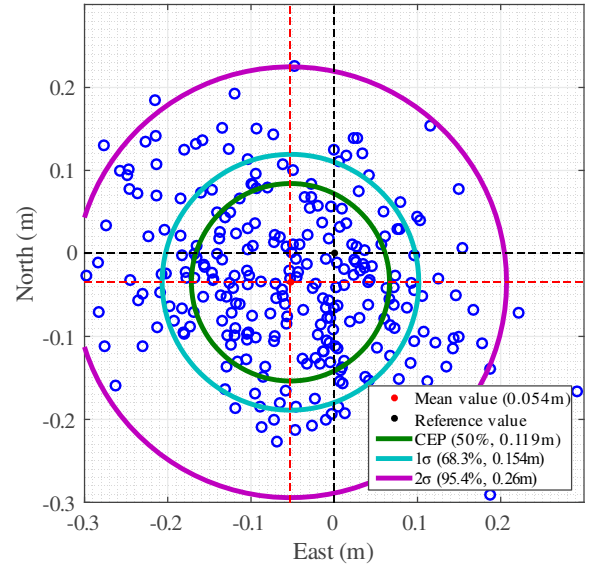


Figure 3 Static GPS scenario. Positioning error for the WFS OTA testbed (top), and conducted test including antenna pattern (bottom)

# Operating Characteristics Of The Vortex Spin Transfer Nano-Oscillator

Pavel A. Stremoukhov

Dept. of Formation and Processing of Radio Signals  
Moscow Power Engineering Institute  
Moscow, Russia  
1opavel1@mail.ru

**Abstract**—Based on the Thiele equation for the vortex spin transfer nano-oscillator (STNO) we obtain truncated equations for the output amplitude and phase of the oscillator. On the basis of the resistive equivalent circuit we consider operating characteristics of the STNO and find the optimal parameter values satisfying the maximum output power at the load. Based on this model it we find the tuning frequency range of STNO.

**Keywords**—spin transfer vortex nano-oscillator; vortex dynamics; power optimization

## I. INTRODUCTION

In modern electronics and communication systems, there are three important trends, such as: consolidation of the frequency spectrum used in a means of communication, the growing number of wireless standards in various devices, and the appearance of wearable electronics. We can conclude that today there is a serious demand to develop and manufacture low-cost, portable, integrated into the chip, tunable oscillators. However, with the development of spintronics it became possible to solve such problems. At present, the spin transfer nano-oscillators (STNO) exceed the widely used voltage-controlled oscillators (VCO) for all of the above characteristics.

Studies in the field of microwave generation by nanoscale structures with magnetic multilayers began with theoretical studies of J. Slonczewski and L. Berger [1,2]. It was shown that in simple structures consisting of two magnetic layers and one non-magnetic, for sufficiently high current densities (around  $10^7\text{-}10^8$  A/cm), can be observed the effect of spin transfer torque from one layer to another, which leads to a precession of the magnetization in the microwave range [3].

Vortex spin transfer nano-oscillators (STNO) based on such magnetic structures, have a number of positive qualities, such as: a wide range of carrier frequency, adjustment, integrated with the technological cycle of producing CMOS-circuits, low working voltages, small time of transition, almost linear dependence of the output frequency of the input control current.

## II. FORMULATION

However, despite the large number of positive qualities and the prospects of using vortex STNO, there is a lack limiting its use at this stage of technological development, it is associated with a low output level (in the best case to 0.5  $\mu\text{W}$ ).

In this regard, researchers have proposed a variety of synchronization mechanisms of networks of vortex STNO: by a common current [4], by spin waves [5], by a common magneto-dipolar field [6] and due to dipole interaction forces.

Despite the large number of works on the STNO, there are no studies in the literature relating to such technical issues as the selection of maximum output power of a single generator, selection of material parameters, selection of load and operating current to the frequency tuning range. These

Ansar R. Safin

Dept. of Formation and Processing of Radio Signals  
Moscow Power Engineering Institute  
Moscow, Russia  
arsafin@gmail.com

objectives are highly relevant for the calculation of the optimal mode of addition of power for STNO ensembles.

This report consider the problem of obtaining the maximum power of oscillation at the load, and the influence of the operating current on the frequency tuning range.

## III. MAIN RESULT

Typical STNO consists of three layers: a layer with a fixed magnetization, layer with a free magnetization and non-magnetic intermediate spacer layer. To analyze the processes in the free layer, it is convenient to use the Thiele equation for the vortex core , which is as follows :

$$G[\vec{e}_z \times \vec{X}] - D \cdot \vec{X} - \frac{\partial W}{\partial \vec{X}} - \chi[\vec{X} \times \vec{e}_z] = 0. \quad (1)$$

For further analysis of oscillations in the system is convenient to go to the truncated equations. For this we represent in the following form:

$$\vec{X} = x\vec{i} + y\vec{j}. \quad (2)$$

We introduce the complex amplitude and the complex conjugate to it:

$$A = x - jy, A^* = x + jy \quad (3)$$

Analyzing equation (1) we have got the truncated equations for the amplitude and phase oscillations in the vortex STNO, for the nonlinear regime :

$$\begin{cases} \dot{U} = -\frac{\chi G - \kappa_0 D}{G^2 + D^2} \cdot U + \frac{a \kappa_0 D}{G^2 + D^2} \cdot U^3 \\ \dot{\phi} = \frac{\chi D + \kappa_0 G}{G^2 + D^2} + \frac{a \kappa_0 G}{G^2 + D^2} \cdot U^2 \end{cases} \quad (4)$$

Nonlinear mode is taken into account with the coefficient characterizing the conservative energy of the vortex in the form of the following function [8]:

$$\kappa = -\kappa_0 [1 + aU^2] \quad (5)$$

We conduct an analysis of the obtained equations in the phase plane. For sufficiently small currents, a stable point is a stable focus, above the critical current taking place an Andronov-Hopf bifurcation and stable focus becomes unstable, with a stable limit cycle is born. This is consistent with the physics of the processes observed in the experiments [9]. The boundary where it is possible to increase the current is a natural limit related to the limited STNO sample's radius. Note that the derivation of the equations for the radius and phase of the vortex met in the literature [10], but the dynamics of the vortex STNO from the position of the phase space was not studied at all.

Solving equation (4) with respect to a stationary amplitude and phase we obtain expressions for the stationary amplitude and frequency:

$$U_0 = \sqrt{\frac{\zeta - 1}{a}}, \quad (6)$$

$$\omega_0 = \frac{\chi}{D}, \quad (7)$$

where  $\zeta = \chi G / \kappa_0 D$ .

Using standard radio engineering formula for the power of oscillations and expression (3), we obtain an expression for the power allocated to the load, which takes into account the physical parameters of STNO and resistance of the load :

$$P_L = \frac{R_L^3 \cdot \Delta R_0^2 \cdot I_0^2}{2 \cdot (R_0 + R_L)^4} \cdot \frac{I_0 \cdot \chi_0 \cdot \mu \cdot G - \kappa_0 D}{a \kappa_0 D} \cdot \cos(\gamma_p). \quad (8)$$

Using the expression for the power (8) it could be determine the minimum resistance value of the load required for generating vibrations and the optimum value of load resistance, whereby the load power is maximum.

$$R_{\min} = -\left( \frac{R_0 - \Delta R_0 - 2FR_0}{2 \cdot (1 - F)} \right) + \left( \frac{\sqrt{(R_0 - \Delta R_0 - 2FR)^2 + 4FR_0^2} \cdot (1 - F)}{2 \cdot (1 - F)} \right) \quad (9)$$

$$R_{opt} = -\frac{b + \sqrt{b^2 - 4 \cdot m}}{2v}, \quad (10)$$

where  $F = \sqrt{\zeta}$ .

Vortex STNO is a "hard" oscillating system , so a certain threshold by the initial impact must be overcome in order to start generating oscillations in this case, this is a threshold  $I_{th} = \frac{\kappa_0 D}{\chi_0 G}$ . On the other hand, diameter of each STNO has a boundary, it limits the current that can be passed through the oscillator, while maintaining the vortex dynamics thus appears  $I_{cr} = \frac{\kappa_0 D}{\chi_0 G} \cdot (a + 1)$ .

Solving equation (7) with considering expressions for  $I_{th}$  and  $I_{cr}$  we can estimate relative and absolute frequency tuning range:

$$\Delta f_{rel} = f_2 - f_1 = \frac{\kappa_0 \mu}{2\pi G} \cdot a \quad (11)$$

$$\Delta f_{abs} = \frac{\Delta f_{rel}}{f_1} = a \quad (12)$$

From (12) it follows that the absolute frequency tuning range is completely determined by the value of the nonlinearity parameter  $a$  of the system, which essentially depends on the properties of the STNO sample.

#### IV. CONCLUSION

We obtain the truncated equations for slowly varying amplitude and phase of the vortex STNO. For the first time obtained an analytical dependence of the output power for the first harmonic oscillation on various parameters of the system.

Estimates of the frequency tuning range STNO oscillations and changes in the range of operating currents. These characteristics qualitatively consistent with the results of experiments conducted in [9] and need for further investigation of STNO ensembles.

#### REFERENCES

- [1] Slonczewski J.C. Current-driven excitation of magnetic multilayers Journal of Magnetism and Magnetic Materials, 1996, 159, L1-L7.
- [2] Berger L. Emission of spin waves by a magnetic multilayer traversed by a current PHYSICAL REVIEW B, 1996, 54, № 13, 9353–9358.
- [3] Slavin A., Tiberkevich V. Nonlinear Auto-Oscillator Theory of Microwave Generation by Spin-Polarized Current IEEE Trans. Mag., 2009, 45, 1875 –1918.
- [4] Grollier J., Cros V., Fert A. Synchronization of spin-transfer oscillators driven by stimulated microwave currents PHYSICAL REVIEW B, 2006, 73, 060409(R).
- [5] Safin A.R., Udalov N.N., Kapranov M.V. Mutual Phase Locking of Very Nonidentical Spin Torque Nanooscillators via Spin Wave Interaction Eur. Phys. J. Appl. Phys., 2014, 67: 20601.
- [6] Belanovsky A.D., Locatelli N., Skirdkov P.N., Abreu Araujo F., Zvezdin K. A., Grollier J., Cros V., Zvezdin A. K. Appl. Phys. Lett., 2013, 103, 122405.
- [7] Junyeon Kim & Sug-Bong Choe Simple Harmonic Oscillation of Ferromagnetic Vortex Core Journal of Magnetics, 2007, 12(3), 113-117.
- [8] Gaididei Yuri, Kravchuk Volodymyr, Sheka Denis Magnetic Vortex Dynamics Induced by an Electrical Current International Journal of Quantum Chemistry, 2009, Vol. 110, 83–97.
- [9] Khvalkovskiy A. V., Grollier J., Dussaux A., Zvezdin K. A., Cros V. Vortex oscillations induced by spin-polarized current in a magnetic nanopillar: Analytical versus micromagnetic calculations PHYSICAL REVIEW B, 2009, 80, 140401(R).
- [10] Skirdkov P. N., Zvezdin K. A., Belanovsky A. D., George J. M., Wu J. C., Cros V., Zvezdin A. K. Large amplitude vortex gyration in permalloy/Bi<sub>2</sub>Se<sub>3</sub>-like heterostructures PHYSICAL REVIEW B, 2015, 92, 094432.

# Optical setup for spectral analysis of microscopic specimens in extreme conditions by means of acousto-optical spectrometers

A. Bykov, P. Zinin

Scientific and Technological Center of Unique  
Instrumentation of the Russian Academy of Sciences  
Russia, Moscow  
bykov@ntcup.ru, zosimpvz@mail.ru

**Abstract**—In this study, we report on the development of a setup for multipurpose analysis of microscopic specimens at extremely high pressures and temperatures. It includes a diamond anvil cell (DAC) heated by a laser, optical coupling components and acousto-optical (AO) spectrometers for the analysis of radiation emitted by a sample in DAC. It is shown that AO devices have significant advantages over other techniques and can be effectively used for accurate spectral measurements and temperature distribution evaluation.

**Keywords**—high pressure, high temperature, diamond anvil cell, spectral measurements, temperature distribution, acousto-optical spectrometers.

## I. INTRODUCTION

Laser-based techniques are widely used for thin film deposition, crystallization of amorphous materials, surface treatment, alloying and the modification of material properties. Material processing tools, such as lasers, are used in advanced manufacturing systems because of their precision, low cost, localized processing, and high speed of operation. Laser heating is one of the main tools in the study of minerals and synthesis of new materials under high pressure and high temperature in DAC. Progress of high pressure physics and minerals is closely associated with the development of new methods of laser heating of samples in DAC [1]. DAC is the only experimental method that can compress static agents to 6 Mbar at temperatures up to 6000 K [2]. That is why the analysis of optical properties in these conditions is of a great interest.

## II. ACOUSTO-OPTIC SPECTROMETRY

Spectral systems based on AO tunable filters provide a unique collection of features such as random spectral access, programmability and image transmission with high image quality (less than 1% distortion in the visible spectral range). Rather narrow bandwidth (down to 0.1 nm) and high spatial resolution (up to 1000×1000 dots), fast spectral tuning (~10 µs), compactness and absence of any moving elements make them a precise and ergonomic analytical tool capable of working even in out-of-lab environment.

In this study, we describe how AO spectrometers may be effectively used for DAC applications. Numerous experiments show that the use of the spectral devices of this type provides an accurate temperature distribution evaluation inside DAC and spectral measurements of the sample. Proposed approach can be widely used in geophysical studies, the synthesis of new superhard and superconductive materials and other tasks. This paper describes unique setup for studying of optical

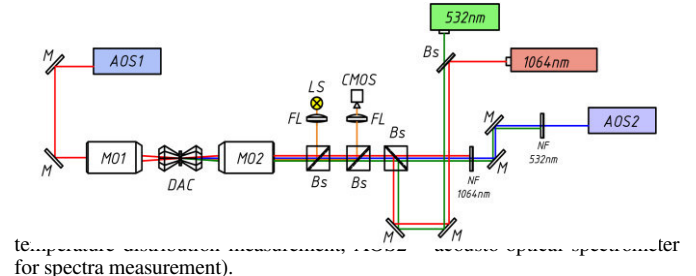
A. Machikhin

National Research University  
“Moscow Power Engineering Institute”  
Russia, Moscow  
MachikhinAS@mpei.ru

properties of materials under extreme temperatures and pressure including a channel for multispectral imaging radiometry based on the tandem AO filtration.

The setup is shown in Fig.1. It includes two lasers (1064 nm – for heating the sample in DAC and 532 nm – for spectral measurements). For wide-band imaging and adjusting the setup white light source LS and the color CMOS camera are used. For the spectral measurements (either fluorescence or Raman) acousto-optical spectrometer AOS1 is used. Acousto-optical imaging system AOS2 is utilized for the measurement of the temperature distribution in the sample under laser heating [3].

Figure 1. Scheme of proposed setup (M - mirrors, MO - microobjectives, BS – beam splitter, FL - focusing lenses, LS - wide-band light source, CMOS - CMOS camera, NF - notch filter, AOS1 – acousto-optical imaging system for



## III. CONCLUSION

We described a new multi-purpose setup based on acousto-optical spectral elements. It allows to carry out multiple measurements of the microscopic specimens under high pressure and temperature.

## IV. ACKNOWLEDGMENTS

This work is supported by Russian Foundation for Basic Research (grant 15-37-20646).

## REFERENCES

- [1] S. Odake, P. V. Zinin, E. Hellebrand, V. Prakapenka, Y. Liu, S. Hong, K. Burgess, L.C. Ming. "Formation of the high pressure graphite and BC8 phases in a cold compression experiment by Raman scattering". *Journal of Raman Spectroscopy*, 44(11), 1596-1602 (2013).
- [2] S. Odake, P. V. Zinin, L. C. Ming. "Raman Spectroscopy of Melamine at High Pressures up to 60 GPa". *High Pressure Research*, 33(2) 392-398 (2013).
- [3] A.S. Machikhin, P. V. Zinin and A. V. Shurygin "Acousto-optic imaging system for in-situ measurement of the high temperature distribution in micron-size specimens." *Physics Procedia*, 70, 733-736 (2015).

# Reconfigurable Industry-level Ka-band Switch Matrix Module for Geostationary Satellite Operation

Alexander Ebert\*, Jens Müller\*, Ralf Stephan\*, Dirk Stöpel\*, Tobias Kässer†, Willibald Konrath†, and Matthias A. Hein\*

\*Institute for Micro- and Nanotechnologies, Technische Universität Ilmenau, P.O. Box 100565,  
98684 Ilmenau, Germany

†Tesat-Spacecom GmbH Co. KG, P.O. Box 1120, 71501 Backnang, Germany

**Abstract**—In this paper we describe the development of a compact and lightweight reconfigurable 4x4 switch matrix module for geostationary satellite communications in Ka-band (17...22 GHz), where signal routing becomes more and more relevant. The module is based on a space-qualified low-temperature co-fired ceramic multilayer technology. Following a successful on-orbit verification aboard a low-earth orbit satellite mission, the switch matrix has undergone major design revisions, aiming at an industry-scale manufacturability without compromising the advanced functional performance. By applying a system-in-package approach including automated hybrid assembly, a fully operational breadboard version has been developed, which upon further space qualification steps is intended to become part of a reconfigurable input multiplexer aboard the geostationary Heinrich Hertz satellite. The dimensions of the module measure 126 mm x 87 mm x 11 mm with a weight of 193 g, corresponding to a reduction of 60 % in volume and 40 % in mass compared to a previous electronic version, and orders-of-magnitude better than coaxial switch matrices.

**Keywords**—Ceramics, LTCC, microwave switches, space application, switch matrix, SiP, automated hybrid assembly.

## I. INTRODUCTION

In previous research, we have developed a reconfigurable 4×4 switch matrix (RSM) for the Ka-band downlink frequencies (17...22 GHz) utilizing LTCC technology. Starting from a first-generation technology demonstrator (RSM-1G), a miniaturized version (RSM-2G) was successfully space-qualified and its fully operational performance verified in a low-earth orbit mission, thus achieving the highest possible technology-readiness-level (TRL = 9) for low-earth orbit applications [1]. Further design issues led to increased functional density and reliability, integrating the bias-circuitry into the core module of the switch matrix (RSM-3G), and a redundancy network, which bypasses the switches in case of onboard power failure (RSM-4G) [2]. The most recent implementation of the switch matrix (RSM-5G) has been designed for manufacturability and adopted to become an integral part of a flexible Ka-band input multiplexer aboard the geostationary Heinrich Hertz communications satellite. This module was fabricated, packaged, and assembled in a space qualified system-in-package, suitable for fully automated hybrid assembly. In comparison to its predecessor modules, this leads to higher reliability and reduced manufacturing costs

of the module itself while keeping the well-advanced combination of compact size and high functional density.

## II. SWITCH MATRIX FOR THE RECONFIGURABLE INPUT MULTIPLEXER

Fig. 1 depicts an optical photograph of the RSM, showing the ceramic package and the printed circuit board (PCB), acting as an interface, inside the housing. The housing is fabricated from aluminum and plated with gold in a post-processing step. The ceramic package is mounted on a molybdenum heat-sink, which mitigates the thermal mismatch between the ceramic material and the aluminum housing. The interface PCB connects the LTCC microwave module and the DC-bias and control circuitry, which is, for reasons of modularity and risk minimization, not integrated in the ceramic package. The overall dimensions of the switch matrix module measure 126 mm × 87 mm × 11 mm. The total mass of the switch matrix amounts to 193 g. The microwave interface to the payload is achieved by means of K-type coaxial connectors.

The switching operation matrix is based on a single-pole multiple-throw architecture, utilizing eight PIN-diode based single-pole quadruple-throw (SP4T) switch ICs. The ceramic package contains all microwave components needed for the electronic switching functionality, i.e. the SP4T-switch ICs, the PIN-diode drivers, and blocking capacitors. The footprint area of the ceramic package measures 58 mm × 58 mm.

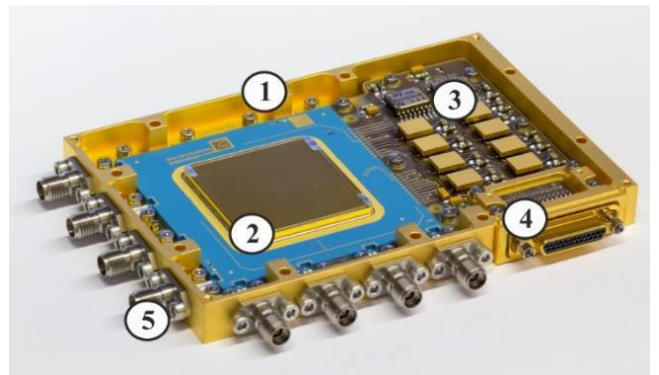


Fig. 1. Optical photograph of the compact and fully equipped switch matrix module (RSM-5G), with mechanical housing (1), LTCC-based ceramic package (2), interface PCB (3), interface connector (4), and coaxial K-type connectors (5).

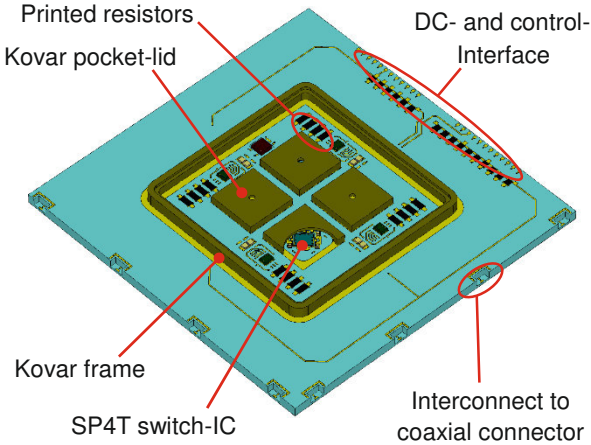


Fig. 2. Schematic view of the ceramic package of the RSM-5G designed for industry-scale manufacturability, with kovar frame, interconnects for microwave signals, power supply and control, as well as the SP4T-switch ICs covered by kovar pocket-lids.

Since the SP4T switch ICs are controlled by bipolar bias currents, bare-die PIN-diode driver ICs are integrated into the package, which convert the TTL-level control signals to the required analogue bipolar currents. To adjust the bias currents, printed resistors are incorporated, which are fine-adjusted by laser trimming to a value of  $300 \Omega \pm 2\%$ . The total DC power consumption of the switch matrix amounts to 2 W.

A three-dimensional view of the ceramic package is depicted in Fig. 2. For the hermetic sealing of the bare-die components employed, gold-plated kovar frames with inner dimensions of  $34 \text{ mm} \times 34 \text{ mm} \times 1.5 \text{ mm}$  were soldered on both sides, and sealed by laser-welding kovar lids on top. Since the sealed kovar frame is electrically large at the operating frequencies with wavelengths around 15 mm, small kovar pocket-lids are placed around each switch-IC, ensuring electromagnetic shielding and good isolation. The inner dimensions of the pocket-lids were carefully chosen to  $7 \text{ mm} \times 7 \text{ mm} \times 0.8 \text{ mm}$ , shifting the fundamental resonance to  $f = 27.1 \text{ GHz}$ , well above the Ka-band downlink frequencies ( $17 \dots 22 \text{ GHz}$ ) [4].

### III. MICROWAVE QUALIFICATION

A breadboard of the complete module as shown in Fig. 3 was fabricated and measured. Additionally, the ceramic package was characterized separately by on-wafer measurements. A comparison of the simulated and measured scattering parameters of the ceramic package alone and the measured scattering parameters of the breadboard for one exemplary signal path in transmission state, is shown in Fig. 4. The measured insertion loss of 17 dB conforms well with the simulated value of 14.5 dB for the ceramic package in the frequency range of interest. For the breadboard, the insertion loss amounts to 18 dB, reflecting the additional losses of the coaxial interfaces. The return loss remains above 11.5 dB for both simulated and measured results of the ceramic package, and above 13.5 dB for the breadboard. The isolation is better than 57 dB for the on-wafer measured ceramic package and remains above 50 dB for the breadboard.

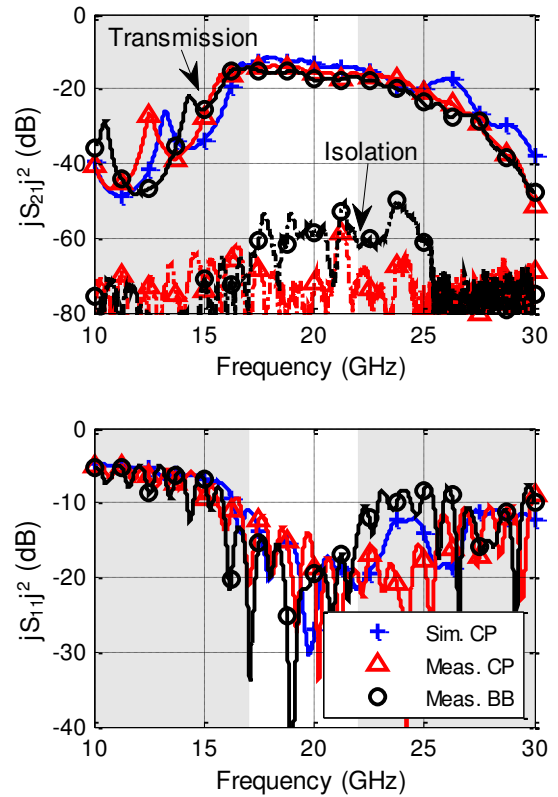


Fig. 3. Comparison of the simulated and measured scattering parameters of the ceramic package (CP) and the complete breadboard (BB), for transmission-state and isolation-state as indicated.

### IV. CONCLUSIONS

The compact, electronically reconfigurable,  $4 \times 4$  switch matrix, previously demonstrated in a low earth orbit technology verification, was thoroughly re-designed for manufacturability and adapted to an industry-level automated hybrid assembly. A breadboard of the switch matrix was fabricated and measured, revealing an insertion loss of less than 18 dB and a return loss better than 13.5 dB, and an isolation remaining higher than 50 dB, from 17 to 22 GHz. This performance was incorporated into link budget of the entire payload module and found well suited for realistic payload operation.

### REFERENCES

- [1] S. Humbla, R. Stephan, D. Stöpel, J. Müller, and M.A. Hein, "Low-Earth-Orbit Verification of a Reconfigurable  $4 \times 4$  Switch Matrix and Potential Applications for Satellite Communications," IEEE-APS Topical Conference on Antennas and Propagation in Wireless Communications, pp. 851-854, September 2013.
- [2] S. Kaleem, S. Rentsch, S. Humbla, D. Stöpel, R. Stephan, J. Müller, and M.A. Hein, "Highly integrated reconfigurable microwave switch matrix module for geostationary satellites," Proceedings of the 44th European Microwave Conference, pp. 992-995, October 2014.
- [3] A. Ebert S. Kaleem, J. Müller, R. Stephan, D. Stöpel, T. Kässer, W. Konrath, and M.A. Hein, "An Industry-level Implementation of a Compact Microwave Diode Switch Matrix for Flexible Input Multiplexing of a Geo-stationary Satellite Payload," International Conference on Microwaves, Communications, Antennas and Electronics Systems (COMCAS), November 2015.

# A Leaky-Wave Antenna Based on a Dual-Layer Frequency Selective Surface for Mobile Satellite Communications in Ka-Band

Alexander Krauss, Hendrik Bayer, Ralf Stephan, Matthias A. Hein  
RF & Microwave Research Laboratory, Technische Universität Ilmenau, Germany  
E-mail: alexander.krauss@tu-ilmenau.de

**Abstract**—This publication presents a leaky-wave antenna panel comprised of a dual-layer frequency selective surface (FSS) intended for transmit and receive operation in Ka-band. Several of these panels are installed on the outdoor-unit of a low-profile user-terminal intended for satellite communication on the move during emergency scenarios. Due to widely separated up- and downlink-frequencies in Ka-band the antenna panel provides a dual-band behaviour and offers circular polarisation. This paper presents the design of the antenna in detail and discusses simulation and measurement results.

**Index Terms**—Mobile Satellite Communications, Ka-Band, User-Terminal, Low-Profile Antenna, Dual-Band Leaky-Wave Antenna, Partially Reflective Surface.

## I. INTRODUCTION

The growing interest in bi-directional satellite communications in Ka-band necessitates an antenna design, which is capable of handling dual-band operation given the widely separated down- and uplink frequencies within this communication band (downlink: 19.7-20.2 GHz and uplink: 29.5-30.0 GHz). Especially in the case of satcom on-the-move at the event of catastrophes or disaster situations, a compact and robust antenna design with high reliability, that addresses circular polarisation, is needed. As the communication of public authorities and rescue forces would no longer be feasible due to destroyed terrestrial networks, nomadic and mobile satcom user-terminals become very important. This alternative provides the connection of portable terminals as well as of vehicles on the move via Ka-band satellite links. Because of the spot-beam architecture available in this frequency range, the link budgets are relaxed and compact antennas with moderate directivity enable voice communication, the transmission of situation reports, geographical and positioning data as well as images. A number of the antenna panels presented here are intended to be installed on our low-profile antenna outdoor-unit as depicted in Fig. 1. This mobile user-terminal antenna operates in heterogeneous satellite communication networks and involves a hybrid mechanical-electronic tracking method [1-2].



Fig. 1. Photograph of the low-profile antenna terminal outdoor-unit for mobile satellite communications in Ka-band. The radome is indicated by the transparent frame.

## II. KA-BAND ANTENNA PANEL DESIGN

The leaky-wave antenna panel based on 2D-periodic cell structures applies a dual-layer frequency selective surface (FSS) [3-4] to enable the functionality at 20 and 30 GHz simultaneously. As depicted in Fig. 2, a top-layer (20 GHz FSS) and a bottom-layer (30 GHz FSS) of periodically arranged unit cells (Fig. 3) are printed on a microwave substrate, e.g., Rogers laminate. Depending on the effective permittivity of the substrate and air, both are located at approximately half of an effective wavelength over a ground-plane with an integrated dual-band slot radiator array operating as primary source. The intention is to create a frequency-selective [5] dual-layer arrangement, where only one FSS layer offers its partially reflective (partially reflective surface - PRS) behaviour at one frequency band while it leaves the radiation pattern at the respective other frequency essentially unaffected.

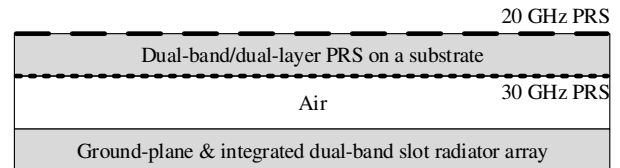


Fig. 2. Layer build-up of the dual-layer FSS antenna panel with a ground-plane and integrated dual-band slot radiator arrays as primary source.

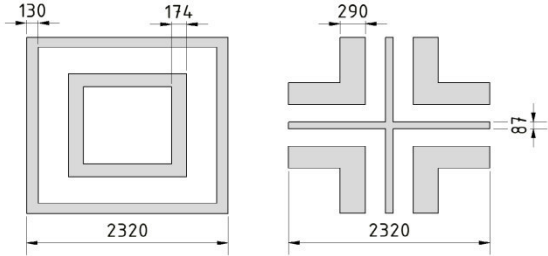


Fig. 3. 20 GHz unit-cell on the top-layer (left-hand side) and 30 GHz unit-cell on the bottom-layer (right-hand side) of the dual-layer FSS (dimensions in  $\mu\text{m}$ ).

Fig. 4 shows a CAD model of the Ka-band panel without the dual-layer FSS to illustrate the design of the primary source. Compared to mono-band excitations [6] the novel development is the realisation of rectangular waveguide feeds, for both, 20 and 30 GHz milled into one panel ground-plane. The guided waves excite circularly polarised radiation enabled by a precise laser-cut X-slot array [7], located on the top of the rectangular waveguides. For 20 GHz excitation, a 20-slot array was implemented, with slot lengths differing from 6.8 mm to 7.0 mm, centrally fed by two rectangular waveguides and combined by a network on the panel backside (green, lower panel of Fig. 4). As 30 GHz source, an array of 16 slots was realised with lengths from 4.375 mm to 4.800 mm and fed by one integrated waveguide.

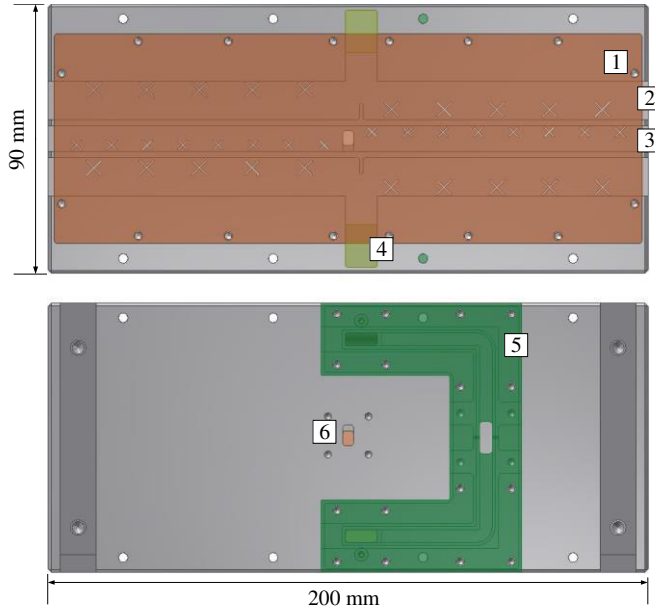


Fig. 4. CAD model of the Ka-band antenna panel (top- and bottom-view, depicted without the dual-layer FSS) comprising a brass-plate with 20 & 30 GHz slot radiator arrays (1) as the primary source of the leaky-wave antenna, 20 GHz (2) and a 30 GHz (3) waveguide feed networks, waveguide bends to the panel backside (4), a rectangular waveguide junction and several bends to provide a common 20 GHz standard flange on the panel backside (5), and the 30 GHz standard flange (6).

### III. IMPLEMENTATION & RESULTS

The manufactured Ka-band antenna panel comprising a dual-layer FSS for dual-band operation is depicted in Fig. 5. The maximum LHCP gain amounts to 22.4 dBi at 19.8 GHz. A main-beam gain above 20.0 dBi is observed over a 900 MHz wide band, from 19.2 to 20.1 GHz. The maximal co-polarisation gain of 22.1 dBi was measured at 30.0 GHz. The main-beam gain in that case remained above 21 dBi over a 1.1 GHz wide band, from 29.2 to 30.3 GHz. A cross-polarisation discrimination (XPD) of more than 15 dB is achieved in the up- and downlink bands. Simulation and measurement results are in a good agreement and will be presented graphically and discussed in detail in the final paper.

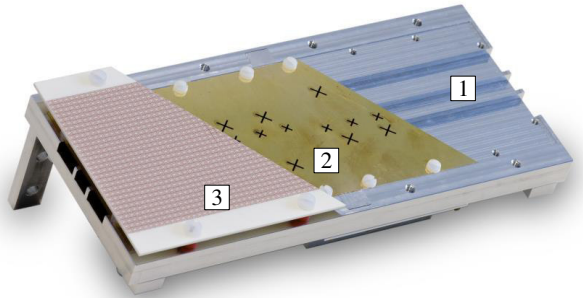


Fig. 5. Photograph showing an exploded view of a full dual-band antenna panel consisting of a ground-plane with integrated waveguide feed structure (1) and a slot radiator array as primary source (2) below the dual-layer FSS realised on Rogers laminate.

### ACKNOWLEDGMENTS

The authors would like to thank M. Huhn and M. Zocher for providing technical assistance, as well as all project partners. This work has been supported by the German space agency, project acronyms MOSAKA and KASYMOSA (contracts 50YB0913, 50YB1319).

### REFERENCES

- [1] M.A. Hein, H. Bayer, A. Krauss, et al., "Perspectives for Mobile Satellite Communications in Ka-Band (MoSaKa)," in *Proc. EuCAP'2010*, Barcelona, Spain, 2010.
- [2] A. Krauss, H. Bayer, C. Volmer, et al., "Low-Profile Antenna for Mobile Ka-Band Satellite Communications," in *Proc. 32nd ESA Antenna Workshop*, Noordwijk, The Netherlands, 2010.
- [3] A.A. Oliner and D.R. Jackson, "Leaky-wave, antennas," *Antenna Engineering Handbook*, 4th ed., McGraw-Hill, ch. 11, 2007.
- [4] T. Zhao, D.R. Jackson, J.T. Williams, et al., "2-D periodic leaky-wave antennas – Part I & Part II," in *IEEE Trans. on Antennas and Propagation*, vol. 53, no. 11, 2005, pp. 3505–3524.
- [5] B. Munk, "Frequency Selective Surfaces, Theory and Design," Wiley & Sons, 2000.
- [6] A. Krauss, H. Bayer, R. Stephan, and M.A. Hein, "Low-Profile Ka-Band Satellite Terminal Antenna Based on a Dual-Band Partially Reflective Surface", in *Proc. EuCAP'2012*, Prague, Czech Republic, 2012.
- A.J. Simmons, "Circularly Polarized Slot Radiators," in *IRE Trans. on Antennas and Propagation*, vol. 5, 1957, pp. 31-36.

# Reliability of sensors and measurement results in chemical monitoring systems

Andrushin A.V., Dolbikova N.S., Kiet S.V., Merzlikina E.I., Nikitina I.S.

Department of Automated Control Systems for Thermal Process

NRU MPEI

Moscow, Russia

MerzlikinaYI@Mpei.ru

**Abstract**—In this paper a model of chemical control system is considered. Great attention is paid to the chemical sensors reliability and measurements reliability, some methods that can improve it are described. The methods are applied on a laboratory bench representing a model of a water circuit and chemical monitoring system and are being tested at the moment.

**Keywords**—*smart sensors, chemical monitoring, control systems models, reliability.*

## I. INTRODUCTION

In the modern world great attention is paid to the environmental protection and safety of industrial devices, for example, power plant units. Safe and reliable performance of the units depends on many factors, the chemical composition of heat carriers, i.e., steam and water being one of them. It is important to have necessary chemical composition of the heat carriers, to predict future changes of the composition and to inform immediately the power plant personnel about any potentially dangerous situation, chemical sensor failures and so on. Because of these reasons modern chemical monitoring systems must work in the real-time mode and be an integral part of the control system of the whole power plant, the measurement results must be reliable and the unit operators must be informed immediately about any possible unreliability of the measurements or abnormal performance of the sensors.

This paper deals with some problems of the measurements and sensors reliability, let us consider chemical sensors for water only.

## II. COMMON APPROACHES TO THE RELIABILITY OF SENSORS AND MEASUREMENT RESULTS

Reliability of any measurement results and sensors is important at power plants. It is obvious that all the devices must be reliable and meet modern standards, but any device can be broken. When it is important to know exactly which device is broken, three devices can be installed at one point instead of one. The values measured by each of them are compared to each other and if one value is different from the other two, that means that the device is faulty.

If it is not possible to install three devices, for example, because of economic or technical reasons, the values measured can be compared with standard values or with the previous measurements and then it may be estimated if the value under consideration can change so quickly and so on. The

measurement results can also be compared with certain limit values and if the results are not in the limits that means that the measuring device or the whole unit works improperly. Some values can be calculated as a result in indirect measurement based on the results of direct measurements [1] and measured and calculated values can be compared. If they differ from each other considerably, the measuring device also works improperly.

## III. CHEMICAL MONITORING SYSTEMS: SPECIAL FEATURES AND RELIABILITY

Chemical sensors are very complex and expensive devices that must be maintained and serviced according to certain rather strict rules, some parts of the devices must be replaced periodically or if it is necessary, some devices must be adjusted periodically or after the part (for example, electrodes) replacement [2]. Some of the devices work with considerable error, some chemical values can be controlled by laboratory devices only. All these factors make the matter of the chemical monitoring system reliability rather difficult and controversial.

As it has already been said, many of the chemical devices are rather expensive and each of them has to be equipped with certain software, which is expensive too. Because of these it is impossible to use three devices instead of one, though the measurement result reliability is very important. So, what can be done?

Modern chemical systems are equipped with smart elements and can be considered as smart sensors [2], all of them have a special microprocessor module performing certain functions, some of them are important for the chemical monitoring systems. In the devices [2] the microprocessor module generates the following signals, which can be used to determine the reliability of the sensor or measurements:

- calibration error;
- measurement error;
- calculation error (for example, the isopotential coordinate is wrong);
- no signal from the smart sensor;
- measured value is out of limits (for example, pH is negative);
- the sensor temperature is too high and so on.

All these data are stored in the microprocessor module, so they can be transferred to the operator's PC, for example, on the operator's demand.

Modern chemical smart sensors are also able to work out automatically when electrodes must be replaced, to work out when the sensor must be calibrate (or even calibrate it automatically) and so on. The information about it is stored in the microprocessor module, so it can be obtained from it in the way previously described.

Because it is impossible to put, for example, several conductometers or pH-meters at one point, other methods have to be used. Let us consider one of them. For certain work modes of the power plant units three values are in the single-valued correspondence [4] – pH, concentration of  $\text{NH}_3$  and electric conductivity, so if one of them is known the others can be calculated. This idea can be used in many practically important cases. For example, if a conductometer is installed anywhere, pH at this point can be calculated. If a pH-meter is installed next to the conductometer, two values, the measured one and the calculated one can be compared and if they are very different, the operator is informed.

The chemical monitoring system model using the principles described above is now under construction at Department of Automated Control Systems for Thermal Process (NRU MPEI). The laboratory bench [3] under construction represents a part of a boiler water circuit (let us assume that it is the part with the feed water). Several chemical valued are controlled, they are pH, electrical conductivity, pNa, concentration of oxygen, concentration of carbon total organic, water hardness. Some other parameters are water temperature, pressure and flow, they are controlled in the sample preparation device of the model, the temperature is also controlled in all the devices, the pressure is controlled in some of them.

So, the problem of the measurement results reliability and the sensors reliability may be solved in the following way. The devices are installed sequentially in a water pipe, so the water temperature in the pipe must fall gradually. If the temperature falls too fast or does not fall at all (or even rises), the operator is informed (Fig. 1).

In Fig. 1 a part of the system is shown, the water in the pipe goes from sensor 1 (T1) to sensor 4 (T4), all data are gathered by the controller and sent to the operator's PC. In the operator's PC software the data are processed, for example, the temperature values are compared with each other. If temperature T3 is higher than temperature T2, the operator is informed. It may mean, that temperature sensor T3 is faulty, or (less probable) temperature sensor T2 is faulty, or the whole chemical sensor number 2 or 3 is faulty. In this system it cannot be determined exactly but nevertheless the operator knows that something IS wrong and where something is wrong.

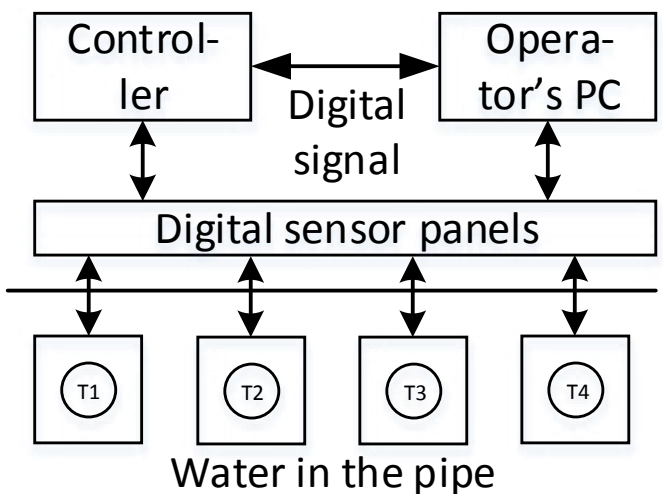


Fig. 1. System of temperature sensors reliability control.

Almost the same thing can be done, for example, with pH. There is a pH-meter and a conductometer in the system. From the pH-meter the computer gets the measured pH value and from the conductometer it get the calculated pH value, after that they are compared by the software. If the values are different, the operator knows that one of the sensors is faulty. He still does not know what exactly is wrong, but he is informed that one of two sensors (or both of them) is faulty and can send a worker to check the sensors or take other necessary measures.

#### IV. CONCLUSION

Reliability of sensors and measurement results is very important now at power plants, because any accident can have grave environmental, social and economic consequences. One of the ways of improving the reliability is to inform the operator about deviations and errors in the control and monitoring systems. In this case the operator can notice a potentially accident situation on time and take measures prevent it.

That is why it is important to develop control and monitoring systems which can predict a dangerous situation or inform about it. This system can have noticeable economic and technical effect.

#### REFERENCES

- [1] Иванова Г.М., Кузнецов Н.Д., Чистяков В.С. Теплотехнические измерения и приборы. –М.: Издательство МЭИ, 2005. – 460 стр.
- [2] «Technopribor»'s site, URL-address <http://www.tehnopribor.ru/>.
- [3] Андрюшин А.В., Киет С.В., Мерзликина Е.И., Никитина И.С. Экспериментально-обучающий стенд кафедры АСУТП НИУ МЭИ, оснащенный приборами химического контроля теплоносителя ТЭС и АЭС. Доклады БГУИР, №2, 2015, стр. 238-240.
- [4] Мартынова О.И., Живилова Л.М., Рогацкин Б.С., Субботина Н.П. Химический контроль на тепловых и атомных электростанциях. – М.: Энергия, 1980. – 320 с.

# Simulation of Mold Metal Level Sensor's Signals With Pulsed Excitation

E. Slavinskaya

Dept. of Automation and Computer Engineering  
Moscow Power Engineering Institute  
Moscow, Russia  
slavinskaya@inbox.ru

**Abstract**— Pulsed excitation for mold metal level sensors is researched in this paper. Proposed signal processing algorithm allows determining mold metal level in a continuous casting process. The method used is based on time-integration of function attenuation of eddy currents in mold wall.

**Keywords**—mold level sensor, pulsed excitation, dynamic correction

## I. INTRODUCTION

At present, the continuous casting of steel is a widely used technology in heavy industry. Continuous casting is the process whereby molten metal is drained into a copper mold. The mold is water-cooled to solidify the hot metal directly in contact with it. Then "semifinished" billet passes through straightening rolls and withdrawal rolls. It is necessary to carry out the control metal level in the mold to ensure trouble-free operation during casting. Eddy current testing is one of contactless testing methods used for metal level control sensors. This method is realized through signal distribution of the electromagnetic sensor over the height of the mold [1]. Metal level is determined indirectly by the temperature gradient along the inner wall of the mold. The temperature of the outer wall of the mold characterized by a large transient time constant than the inner. Hence, signal from the inner wall is the most important for correct metal level control tasks.

Nowadays eddy current level sensors are excited via alternating voltage of one or more frequencies. Their main problem is the presence of the large primary signal during the measurement. This signal randomly depends on external hindering factors so detuning from this influence is difficult. At present requirements for the quality of the metal are growing so there is need automatic stabilization of technological process. It determines the need to increase the accuracy and stability of the readings of devices. Metal level sensor with pulsed excitation has a number of advantages over the harmonic type sensor - precedence and independence processes of excitation and measurement, high sensitivity to the conductivity, possibility of layer-by-layer control and simple design.

## II. SIMULATION RESULTS

The object of investigation is model of eddy current level sensor with a pulsed excitation embedded in the wall of the mold. Design of the device is a sensor matrix in the form of inductance coils and extended excitation winding. In the study static and dynamic mode of heating the mold wall is simulated. Signals of measurement coils are registered to evaluate technical properties of developed device. The time-domain features such as the time integral, signal duration and the time constant of the approximating function of detected signals are

I. Terekhin

Dept. of Automation and Computer Engineering  
Moscow Power Engineering Institute  
Moscow, Russia  
terekhin.iv@mail.ru

analyzed to obtain an optimum parameter to measure conductivity of mold wall [2,3,4].

## III. PROPOSED ALGORITHM

The goal of the signal processing algorithm is to determine a mold level using pulsed excitation of eddy current. Measuring integral from time of a signal will provide information about the mold wall conductivity layer-by-layer. The main point is to start integrating with 20-30ms from the initial time. It allows to receive data about the most heated layers of mold wall. According to the distribution of the value of the integral over the matrix of the sensor coils is calculated coordinate metal level in the mold at each measurement cycle.

The method of dynamic correction is proposed to improve system performance. It consists in detuning information on the upper layers, contained in further layers around 20-30ms. Application of the correction algorithm improves performance - after only 0.5 s after the jump metal level informative parameter reaches a value close to the temperature of the inner wall, which is about half times faster than that of the curve further integral without detuning from the surface layer. This achieves the maximum approximation to the inner wall of the mold heating exponential curve close to the molten steel. With these settings, a reaction to changes in the level of metal in the mold will be most rapid.

## IV. CONCLUSION

In this paper signal processing algorithm and method of dynamic correction of the metal level trend are proposed.

The dynamic correction algorithm based on the subtraction of the integral on the end part integral to the initial segment is proposed and tested on simulated data. The procedure yielded good results, and the corrected dynamic curve coincide to the temperature distribution on the inner wall of the mold.

## REFERENCES

- [1] D.Moermann, J.schmid, S.SPAGNUL “Recent progress in fast and accurate meniscus level measurement for continuous casting machines”, 2011
- [2] C.S. Angani, D.G. Park, G.D. Kim, C.G. Kim, and Y.M.Cheong; “Differential pulsed eddy current sensor for the detection of wall thinning in an insulated stainless steel pipe”, 2010
- [3] Deqiang Zhou, Gui Yun Tian, Binqiang Zhang, Maxim Morozov and Haito Wang; “Optimal features combination for pulsed eddy current NDT”, 2008
- [4] Jesús A. Vega , Alain Gauthier S. “On the signal features analysis of a pulse induction metal detector prototype”, 2012

# Problems of Eddy Current Sensor Imbedded Type in Mould Level Control

I.Savin, I.Terekhin

Institute of Automation and Computer Engineering

Moscow Power Engineering Institute

Moscow, Russia

Igorkoff@inbox.ru, terekhin.iv@mail.ru

**Abstract —** Introduced in the paper main problems of eddy current sensor embedded type are discussed. Methods to reduce the errors are developed. The efficiency of the methods proved in the industrial experience.

**Keywords —** Eddy current sensor, mould, metal level.

## I. INTRODUCTION

The use of eddy current sensors for mould level measurement in continuous casting of steel is a worldwide common practice. There are three types of mould level sensors: suspended type, edge type and imbedded type (built-in) [1]. In recent years, the most in demand type is built-in sensors. They are mounted opposite the copper mould wall. Level measured by the temperature distribution in it (thermal profile). Imbedded eddy current sensor consists of inducing coils and measuring coils matrix. The main advantage of the sensor built-in type is that it is protected from overflow of melt and does not interfere with maintenance personnel during casting.

Imbedded type sensor is characterized by three types of errors: thermal inertia, the influence of the electromagnetic stirrer and unstable of the temperature profile.

## II. THERMAL INERTIA

Built-in eddy current sensor measure thermal profile in the mould. Thermal profile has a maximum. Maximum of thermal profile correlates with the metal level. When level change the mold temperature varies with delay. The delay increases with the thickness of the mold wall. A large thermal delay makes it impossible process control level.

To reduce the delay of the sensor signal can be used links dynamic correction. These units are described in the theory of automatic control.

You can also use the nonlinear properties of the locus level change signal for dynamic correction. This is possible since depending on the level of the rate of change has a different shape of the hodograph. But such a dynamic correction is complicated by the fact that the dynamic component of the locus is small (about 5 % of the static).

## III. ELECTROMAGNETIC STIRRER (EMS)

For improving the quality of steel molds equipped with EMS. EMS is AC machine stator that generates a rotating magnetic field. Rotating field frequency is 2-5 Hz. EMS field induces voltage in the measuring coil.

To tune out interferences EMS should use digital bandpass filter. The industrial experience used elliptic filter tuned to the frequency of the sensor supply.

Furthermore, when changing EMS current the magnetic permeability of the magnetic objects surrounding the sensor changes. Changing magnetic permeability occurs at twice the frequency EMS. As a result the sensor signal appears at the same frequency interference.

To tune out the interference caused by the magnetic permeability change of the environment should be further developed mold. Industrial experience shows that stainless steel also changes the magnetic permeability. With a specific design of the mold (bloom mold) should establish an electromagnetic shield.

## IV. THE INSTABILITY OF THE TEMPERATURE PROFILE

Level control built-in sensor is carried out by the temperature distribution in the copper wall of the mold. Most of the casting time the temperature profile maximum indirectly reflects the melt level. But during casting processes are when produced false temperature highs not characterize the level position (eg , at local contact ingot) . Thus the temperature profile maximum may not be characteristic the level. Therefore, the level should be monitored on the front which characterizes the transition from the hot to the cold area of the mold.

## V. CONCLUSION

In this paper, an analysis of the impact of each of these errors in the measurement of the melt level . Methods to reduce these errors are developed. The efficiency of the proposed methods in the approbation of their industrial experience in a metallurgical plant.

## VI. ACKNOWLEDGMENT

This work was supported "Foundation for Assistance to Small Innovative Enterprises in Science and Technology".  
<http://www.fasie.ru/>

## REFERENCES

- [1] D. Mörmann, J. Schmid, S. Spagnul. Recent progress in fast and accurate meniscus level measurement for continuous casting machines Proc. 7th European Continuous Casting Conference (ECCC) 2011, 27 June — 1 July 2011, Dusseldorf. 2012

# Experimental Study of Color Doppler Twinkling Artifact

Denis V. Leonov<sup>1,2</sup>, V.A. Fin<sup>3</sup>, N. S. Kulberg<sup>2</sup>

<sup>1</sup>Radio Engineering Fundamentals Department, Moscow Power Engineering Institute

<sup>2</sup>Scientific Practical Center of Medical Radiology of Moscow

<sup>3</sup>Scientific Research Institute of Precision Instruments

Moscow, Russia

LeonovDV@mpei.ru

**Abstract**—In this research we investigate the twinkling artifact phenomenon observed in hyperechoic regions presenting as rapidly changing colors seen posterior to a reflector and try to experimentally check the underlying cause which we believe is its pendulum motion. We also introduce a signal processing technique allowing better visualization of calculi.

**Keywords**—Ultrasound; Color Doppler; Twinkling Artifact; Lithiasis; Acoustic Resonance Imaging; Pendulum Hypothesis.

## I. INTRODUCTION

There are two main reasons to study this artifact. First, we should know its properties and features to be able to distinguish its rapid color alteration from the real blood flow. This sort of confusion may result in inaccurate diagnosis [1]. Second, ultrasound machines have several advantages in comparison with common tools for lithiasis diagnosis. These are the absence of ionizing radiation and greater mobility and availability.

Conventionally calculi are observed on B-mode images through shadows immediately behind a stationary echogenic object. However, this method lacks accuracy [2]. It was proposed to use color flow mapping (CFM) to improve reliability [3].

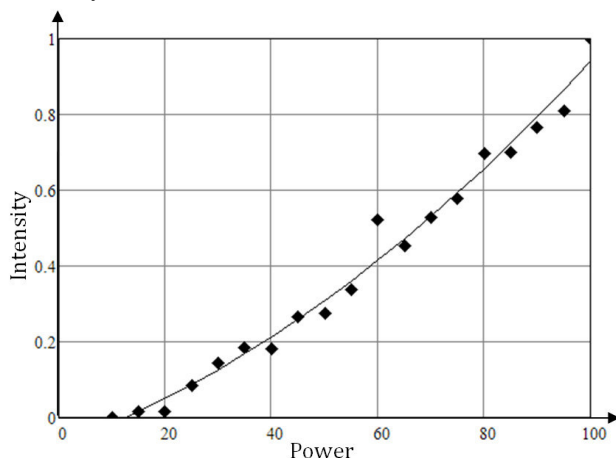


Fig. 1. Intensity of twinkling artifact increases with power of emitted radiation.

## II. MATERIALS AND METHODS

All scans were made using a Medison Sonoace 8000 EX Prime sonography machine with an L5-9EC liner array probe and a Sonomed-500 machine with a 7.5 L38 probe. The transducer was fixed with a test tube clamp attached to a retort stand. Holding the probe in a clamp ensured that the probe was stationary and, therefore, did not affect or contribute the twinkling artifact.

For the experiment a numbers of phantoms were made from gelatin, agar and silicone. As inhomogeneities we used smooth and rusty wires, stone fragments, calculi and less dense materials, such as wood. Proportions of ingredients were chosen to ensure that phantoms properties are close to a human body.

## III. RESULTS

Many researchers found that twinkling artifact depends on material and roughness of inhomogeneities [2;4–6]. We tried a smooth wire, a rusty one, stones with different surfaces. Twinkling artifact accrued much more often on rough surfaces and had a tendency to increase with roughness. We also examined a wooden match, but in CFM-mode it did not produce any twinkling. It is a fact in favour of a pendulum hypothesis. This hypothesis states that colored pixels are seen because inhomogeneities are actually moving.

Our experiment also confirmed that twinkling artifact intensity, which was evaluated by the number of color pixels in the color box, positively depends on power of emitted ultrasound (Fig.1). We compared two ultrasound machines and found that a Medison has greater power of emitted pulses than a Sonomed. In our experiment twinkling artifact was more easily detected on a Medison machine.

Chances of observing twinkling artifact are higher when calculi are in focus [5]. In Fig.2 there are four pictures for four focal lengths in descending order with the first picture representing the furthest focal position, and the fourth — the

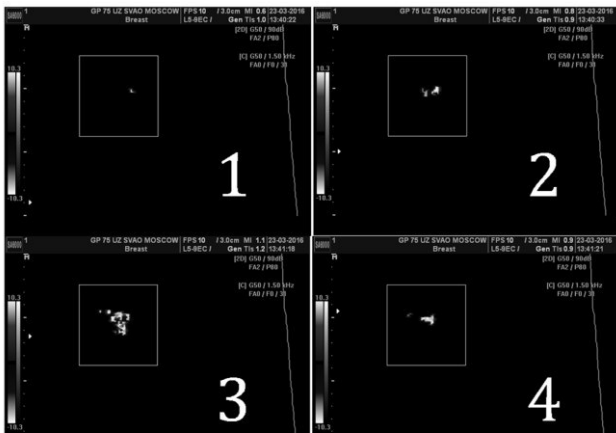


Fig. 2. Color Doppler sonogram shows twinkling artifact changes with focal length. Note amount of twinkling artifact riches its maximum when the stone is in focus.

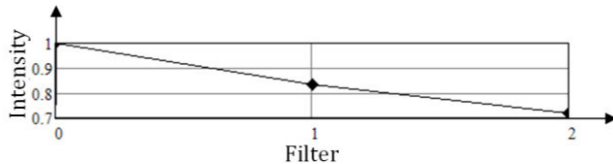


Fig. 3. Graph shows intensity going down with cutoff frequency being changed from 0.04 PRF to 0.272 PRF.

closest to the probe. In the third picture calculi are in focus, and the artifact is at its peak intensity.

Twinkling artifact intensity negatively correlates with a cutoff frequency (Fig.3). Interestingly, our results were not in accord with [2], who found that twinkling artifact intensity was stronger under a higher wall filter.

Found relationship between intensity and pulse repetition frequency (PRF) was very complex. By varying PRF we automatically alter wall filter cutoff frequency, which should downturn intensity. Observed peaks could mean that calculi have their special resonance frequencies.

If we imagine that our inhomogeneity is a pendulum and its surrounding substance is a spring then we can apply the laws of mechanics to describe its motion and find its resonance. There is a technique [7–8] in which acoustic resonance is used to visualize calcifications. The resonance frequency depends on the size of the calcifications and the binding strength with the surrounding tissues in which they are embedded.

Acoustic resonance was used to find calculi in phantoms in which they were not seen in conventional CFM-mode. As an additional excitation source we used a regular audio speaker with an amplifier driven by a signal generator. Frequency was varied up to 1 kHz. Particles became visible on frequencies from 340 to 550 Hz. It was also observed that intensity was steadily increasing with volume until it reached its maximum and leveled off with some slight fluctuations.

In one of the recent experiments we have measured magnitudes and deviations of signals reflected from a piece of wood and a wire. Magnitudes were almost the same, but the deviation from the wire was considerably stronger. We believe this observation might be evidence supporting the pendulum hypothesis. Although some researchers claim to find evidence in favour of other hypotheses [9–11], the particle motion can be a cause for their results.

#### IV. CONCLUSIONS

1. Twinkling artifact deserves to be called a clinical sign rather than an artifact, as its appearance usually means the presence of calculi and shall not be ignored.
2. Intensity of this artifact strongly correlates with the surface roughness. It is far more likely to be observed on a rusty wire than on one with a smooth exterior.
3. Twinkling artifact intensity highly depends on machine settings, especially transmitting power and focal position.
4. The pulse repetition frequency and sensitivity influence is not so obvious, though peaks on a PRF graph might be a sign of resonance frequencies.
5. An additional excitation source is a handy tool substantially increasing the probability of calculi detection in dense media.

#### REFERENCES

- [1] M.S.Hirsch, T.B.Palavcino, B.R.Leon. Color doppler twinkling artifact: A misunderstood and useful sign//Revista Chilena de Radiologia. Vol. 17 № 2, 2011, pp. 82-84.
- [2] M.Wang et al. Systematic Analysis of Factors Related to Display of the Twinkling Artifact by a Phantom//Ultrasound Med. Vol. 30, 2011, pp. 1449-1457.
- [3] M.D.Sorensen et al. B-mode Ultrasound Versus Coor Doppler Twinkling Artifact in Detecting Kidney Stones//Journal of endourology. Vol. 27, № 2, 2013, pp. 149-153.
- [4] A.I.Gromov, S.J.Cubova. Ultrasound Artifacts. Moscow: Vidar-M, 2007 (In Russian).
- [5] A.Jamzad, S.K.Setarehdan. A Novel Approach for Quantification and Analysis of the Color Doppler Twinkling Artifact With Application in Noninvasive Surface Roughness Characterization. An In Vltro Phantom Study//Ultrasound Med. Vol. 33, 2014, pp. 597-610.
- [6] E.Ghersin, M.Soundack. Twinkling Artifact in Gallbladder Adenomyomatosis//Ultrasound Med. Vol. 22, 2003, pp. 229-231.
- [7] C.Seghal. Apparatus for imaging an element within a tissue and method therefor. United States Patent № 5,997,477. 1999.
- [8] C.Seghal et al. Microcalcifications in Breast Tissue Phantoms Visualized with Acoustic Resonance Coupled with Power Doppler US: Initial Observations//Radiology. July 2002, pp. 265-269.
- [9] S.K.Ahmad, M.M.Abdallah. The diagnostic value of the twinkle sign in color Doppler imaging of urinary stones//The Egyptian Journal of Radiology and Nuclear Medicine. Feb. 2014, pp. 569-574.
- [10] W.Lu et al. Evidence for trapped surface bubbles as the cause for the twinkling artifact in ultrasound imaging//Ultrasound Med. Vol. 39, 2013, pp. 1026-1038.
- [11] A.Kamaya et al. Twinkling Artifact on Color Doppler Sonography: Dependence on Machine Parameters and Underlying Cause//American Roentgen Ray Society. January 2003, pp. 215-222.

# Determination of the current state of human retina using algorithms of multistep binary classification

Olga Titova<sup>1</sup>, Dmitry Anisimov<sup>1</sup>, Oleg Kolosov<sup>1</sup>

<sup>1</sup>Institute of Automatic and Computer Engineering, Moscow  
Power Engineering Institute  
Moscow, Russian Federation

Irina Tsapenko<sup>2</sup>, Marina Zueva<sup>2</sup>

<sup>2</sup>Moscow Scientific Research Institute of Eye Diseases  
“Helmholtz” of Russian Ministry of Health  
Moscow, Russian Federation

**Abstract**— The ERG (electroretinogram) is a test used worldwide to assess the status of the retina in eye diseases in human patients and in laboratory animals used as models of retinal disease. In the present study we aim to develop algorithm for determining the state of the human retina on the basis of the ERG. We analyze standard ERG and apply its characteristic features in a modified binary classification.

**Keywords**—classification, retina, ERG, diagnostic system

## I. INTRODUCTION

Diagnosis of the current state of complex dynamic objects and systems is a well-known problem. These objects can be characterized by the absence of sufficiently complete mathematical description, limited number of registered parameters, large dimension, nonlinear static characteristics or parallel structure of the system. [1]

An example of such a complex object is a human retina, which can be represented as a dynamic object with parallel structure defined by retinal cell structure. Diagnosis of pathologies of the retina is provided on the basis of characteristic points of the transition process also known as electroretinogram (ERG). It is a mass electrical response of the retina to photic stimulation. The ERG records total response of all parallel layers of the retina [2]. It is technically impossible to determine the contribution of each layer. [3]

Modern medicine knows limited number of possible diseases (pathologies) and their combinations. Furthermore, due to the stochastic nature of pathological processes in biological objects physiological parameters vary greatly. In the case of finite number of outcomes to solve problems of medical and technical diagnostics there are often used diagnostic systems based on classification algorithms [4].

## II. METHOD

As the initial data we used ERG, produced by specialists of the Institute of Eye Diseases “Helmholtz” for the period from 2009 to 2012. On the basis of ERG data we made an object description in form of a matrix of parameters. Using these parameters we provided the training of classifier. Registration of ERG has been implemented on the electrophysiological system TOMEY EP-1000 (Japan). Six different pathologies were investigated during the study. With respect to the classes of problems when characteristic parameters of the various diseases are highly intersected it was mentioned, that classical classification algorithms are not sufficiently effective.

Therefore it was necessary to develop the modification of standard classification algorithm [6]. The idea was to apply the same type classifier consistently using in each different sets of parameters and classification rules.

As the classifying parameters we selected the most uniquely characterizing the certain state of the object. [5] At the same time in one iteration only one disease is classified, and if no disease is diagnosed, the classification repeats. The classifier is applied (n-1) times, where n is the number of diseases. This technique allows diagnosing single diseases, without increasing excessively the dimension of the diagnostic system.

## III. RESULTS

The obtained results showed that the developed method is quite effective when applied to the problem of determining of pathologies of the human retina and can be used widely applied to the tasks of medical and technical diagnostics. The problem of the method is the inability of complete formalization of the first stage of diagnosis. In matters of medical diagnosis an individual approach is often used, and methods of statistical analysis only work for classical cases. This technique can be used in the developing of expert systems when used in conjunction with the experience of professionals.

## ACKNOWLEDGMENT

This paper was prepared with the financial support of Russian Foundation for Basic Research (Project № 16-01-0054).

## REFERENCES

- [1] Д.В. Вершинин, Диагностика текущего состояния сложных динамических объектов с использованием параметров имитационной модели, дис... канд. техн. наук, 2011, с. 132
- [2] M. F. Marmor, A. B. Fulton, G. E. Holder, Y. Miyake, M. Brigell and M. Bach, “ISCEV Standard for full-field clinical electroretinography (2008 update)”, Doc Ophthalmol, 2009, vol. 118, pp. 69–77
- [3] Ido Perlman. The Electroretinogram: ERG by Ido Perlman. Webvision, 2011.
- [4] Hastie T., Tibshirani R., Friedman J. The Elements of Statistical Learning, Springer, 2001, pp. 533
- [5] Айвазян С. А., Бухштабер В. М., Енюков И. С., Мешалкин Л. Д. Прикладная статистика: классификация и снижение размерности, М.: Финансы и статистика, 1989, с. 607
- [6] Dembele D., Kastner P. C-means method for clustering microarray data, Bioinformatics, 2003, vol. 19(8), pp. 973–98

# The effect of rocker sole design variation on lower limb kinetics, kinematics and muscle function: implications for patients with intermittent claudication

Aksenov A.Y., Klishkovskaya T.A., Drozdova M.D.

Department of bioengineering systems  
Saint-Petersburg Electrotechnical University "LETI"  
St. Petersburg, Russia  
andreynet83@hotmail.com

**Abstract**—Intermittent claudication results in significant gait impairment due to lack of blood supply in calf muscle. The best treatment for claudicants is walking exercise. By changing design and shape of rocker soles, it is possible to offload calf muscle and increase walking distance for people with intermittent claudication. Therefore, adapted footwear features can help enhance rehabilitation process for patients with peripheral arterial disease.

**Keywords:** *kinematic, kinetic, muscle function, calf muscle, rocker sole, intermittent claudication*

## I. INTRODUCTION

Intermittent claudication (IC) is a condition which affects people with peripheral arterial disease in the lower limbs and causes calf muscle pain and limping due to the lack of blood supply to the gastrocnemius muscle in particular [1]. This limits the distance people with IC (known as claudicants) can walk before having to stop because of the pain. The accepted best treatment currently is enrolment onto supervised exercise regimes, but these provide limited improvement and do not alter their antalgic gait [2-5]. This study aims to investigate the effect of specific footwear designs on gait and lower limb muscle function with the intention of identifying which features would be recommended for inclusion in footwear designed to relieve their painful symptoms by offloading the calf muscles.

## II. METHODS

Fifteen volunteer healthy subjects, age range 20-29 years (mean  $25.3 \pm 2.73$ ) undertook a series of gait laboratory trials with shoes adapted with specifically-chosen outsole features. High street shoes were adapted with the test conditions which included shoes with five different heel heights (varying from a 1.5cm to 5.5cm heels), two heel profile conditions (curved and semi curved heels), three traditional (angled) rocker soles with varying apex positions (55%, 62.5% and 70% of shoe length) and three with varying apex angles (10, 15, and 20 deg.), plus three with different forepart sole stiffness (solid, semi-flexible and flexible). The baseline shoe was taken as being one with no heel curve, a heel height of 3.5mm, an apex position of 62.5% of shoe length, and apex angle of 15 deg. and a stiff forepart to the shoe. Measurement and comparisons were taken of lower limb kinetics and kinematics (Qualysis, Sweden) plus electromyographical (EMG) activity (Noraxon USA) of medial

gastrocnemius, soleus, tibialis anterior, rectus femoris and biceps femoris during walking trials where the walking speed was controlled using timing gaits. Data were analysed using Visual3D and OpenSim software to enable interpretation of EMG activity to enable calculation of lower limb muscle function during gait.

## III. RESULTS

Changes from the baseline shoe were taken as being at a level of significance of  $p<0.05$ . The most effective footwear test condition in regards to offloading of the calf muscles compared to the control shoe was that with a 4.5cm heel, a 55% of shoe length apex position, and a 20 deg. rocker apex angle; which demonstrated significant offloading to the calf muscles. The 55% apex position had a significant offloading influence on the calf muscles whilst at the same time not significantly altering knee and hip kinematics.

## IV. CONCLUSION

This study demonstrates that a potentially useful shoe design was identified for treatment of claudicant calf pain which did not adversely affect more proximal joint kinematics and kinematics.

## REFERENCES

- [1] A. V. Meru, S. Mittra, B. Thyagarajan, and A. Chugh, "Intermittent claudication: An overview," *Atherosclerosis*, vol. 187, pp. 221-237, 2006.
- [2] W. Al-Jundi, K. Madbak, J. D. Beard, S. Nawaz, and G. A. Tew, "Systematic Review of Home-based Exercise Programmes for Individuals with Intermittent Claudication," *European Journal of Vascular and Endovascular Surgery*, vol. 46, pp. 690-706, 2013.
- [3] L. M. Kruidenier, S. P. Nicolaï, E. J. Hendriks, E. C. Bollen, M. H. Prins, and J. A. W. Teijink, "Supervised exercise therapy for intermittent claudication in daily practice," *Journal of Vascular Surgery*, vol. 49, pp. 363-370, 2009.
- [4] R. G. Crowther, W. L. Spinks, A. S. Leicht, K. Sangla, F. Quigley, and J. Golledge, "The influence of a long term exercise program on lower limb movement variability and walking performance in patients with peripheral arterial disease," *Human Movement Science*, vol. 28, pp. 494-503, 2009.
- [5] W. Gardner, S. Montgomery, M. Ritti-Dias, and L. Forrester, "The effect of claudication pain on temporal and spatial gait measures during self-paced ambulation," *Vascular Medicine*, vol. 15, pp. 21-26, 2010.

# Decision support system for finding surgical incision location for the gallbladder remove operation for patients with overweight

A. Zahharova

St. Petersburg Electrotechnical University "LETI"  
Saint Petersburg, Russia

**Abstract—** In this research decision support system for finding surgical incision location in order to remove the gallbladder for patient with overweight is developed. The anatomic geometry was used to find dependence between gallbladder location and patient body type. To prove the results 3D models were built. The decision support system takes into account body type, sex and obesity type to find the perfect incision location for the surgery.

**Keywords—** Gallbladder, decision support system, body type, anatomical geometry, 3D modeling.

## I. INTRODUCTION

The determination of the correct location and the size of a cut is very important, especially for patient with obesity as it is known that fat tissue heals very badly and big fat layer complicates the surgeon work. The study is based on depending of the gallbladder location on human body type. On the collected CT images data base statistics of gallbladder location was researched. The collected statistics about bladder location depending on the body type is the basis of the anatomical geometry and confirmed by 3D models. The result of the research is an information system, which determines the location and magnitude of the cut for the most convenient surgical access. This supporting system will advise the doctor the position to make cut, calculate the length of the cut and show 3D model of patient body type when needed. This system will allow a doctor to make cuts smaller what will lead to patient faster recovering and decreasing of amount of complications.

Determinants of making the decision of the gallbladder location

There are some main factors that influent on gallbladder location:

- sex;
- body type (depends on angle between ribs);
- type of obesity;
- gallbladder inflammation (when gallbladder is inflamed it is closer to the anterior abdominal wall).

There are three types of human body:

- Asthenic - ribs angle is less than 85°
- Normosthenic - ribs angle is between 85° and 95°
- Hypersthenic - ribs angle is greater than 95°

The goal is to find the dependency between all determinants and bladder location. The main determinant is body type.

## II. CT-BASED RESEARCH

In order to observe bladder location CT-images were used. For that aim CT images data base was created on base of North-Western State Medical University named after I.I Mechnikov. Data base contains 205 patients of both sexes, different body types and obesity.

Using DICOM viewing programs 6 distances for every patient were measured. A fat layer thickness near navel and in the place of the cut were measured in order to determinate the type of obesity. The distance to bile ducts was measured in order to get statistics about occurrence depth. Using anatomical geometry it was decided to use triangle to describe bladder location. Three sides of anatomical triangle (distance from navel to intercostal space, distance from navel to bladder projection and distance from intercostal space to bladder projection) were measured in order to find position of bile ducts projections to the abdominal wall depending on body type. By defining the distances and angles between them average value for each body type was found. It is clear that distances depend on body high, but angles, calculated using them, are variable in certain range for every body type.

With CT-research two main information blocks were discovered: location of the cut (using anatomical triangle described above) and size of the cut (using knowledge about fat layer thickness and gallbladder occurrence depth depending on the body type).

## III. 3D MODELING

To visualize the research 3D models for every body type of each sex were created. Each model consists of skeleton, gallbladder, liver and fat layer. 3D models were created with MIMICS program.

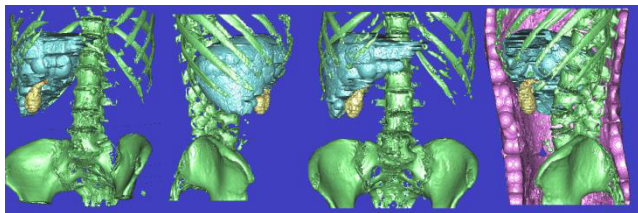


Fig. 6. Fig. 1 Woman asthenic with obesity

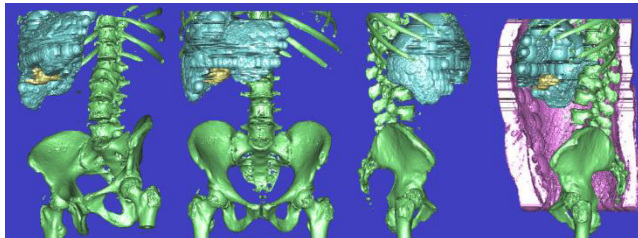


Fig. 7. Fig. 2 Woman hypersthenic with obesity.

3D models give the opportunity to proof the correctness of calculated location of gallbladder. It also allows to calculate gallbladder volume and size parameters for further research.

#### IV. PROGRAMM DEVELOPING

Program consists of many moduls. The first one is patient registration. The second allows to register body parameters in order to calculate the type of body and obesity. The third modul calculates cut length based on the operation angle prefered by surgeon and gallbladder location depth. The forth modul calculates the point of projection of gallbladder to the abdominal wall. Those two blocks allow to give an advise to the surgeon about place and length of the cut. Fifth module shows the 3D model if necessary.

#### V. RESULT VALIDATION

To test the developed method training system was used. For training the system statistics of 75% of the patient form one group were accumulated. System was tested on other 25%. A testing algorithm was next:

- Determination of the body type and sex.
- Determination of the obesity.
- Finding recommended location on the CT-image.
- Marking the cut on the CT-image.
- Measuring the distance between recommended point and gallbladder projection to the abdominal wall.
- Estimation of error mean value.

#### VI. CONCLUSION

In this study decision support system prototype for operation on gallbladder was developed. All calculation made in this study are based on statistics of anatomical location of gallbladder received from CT-based research.

#### REFERENCES

- [1] Aleksandrovich A.A. (2010) Kliniko-ekspertnyie kriterii dlya minilaparotomnoy holetsistektomii u bolnyih s zhelchnokamennoy boleznyu. Stavropol (in Russian)
- [2] Grigoreva, I. N. Osnovnyie faktoryi riska zhelchnokamennoy bolezni (2007) p.17 - 21. (in Russian)
- [3] Makarov S.S. Modelirovaniye i informatsionnoe obespechenie meditsinskikh uchrezhdeniy. 2005 MGUP. (in Russian)
- [4] Lyalin P.P. Sistemyi podderzhki prinyatiya resheniy v meditsine (2006) Moskva (in Russian)

# Research of NMR relaxation efficiency of composite magnetic nanoparticles for biomedical diagnostics

Yu.V. Bogachev, A.V. Nikitina, A.A. Kostina, V.A. Sabitova, K.G. Gareev  
Department of Physics  
Saint-Petersburg Electrotechnical University "LETI"  
Saint-Petersburg, Russia  
e-mail: Yu.Bogachev@mail.ru

V.V. Pankov, V.O. Natarov, E.G. Petrova, D.A. Kotikov, T.G. Shutova  
Department of Chemistry  
Belarusian State University  
Minsk, Republic of Belarus  
e-mail: val\_natarov@mail.ru

**Abstract** –Results of proton NMR relaxation measurements in aqueous solutions of iron oxide composite magnetic nanoparticles are discussed. It is shown that their  $r_2$  relaxation efficiency coefficient is much higher than  $r_1$  relaxation efficiency coefficient and depends on the composition, method of MNPs synthesis. It allows to use this parameter to assess the stability of MNPs in aqueous solutions and estimate their aggregation behavior.

**Key words** – *NMR relaxation, magnetic nanoparticles (MNPs), magnetic resonance.*

## I. INTRODUCTION

Magnetic nanoparticles (MNPs) is currently finding increasingly wide application in medicine and biology for diagnostics, magnetic separation, hyperthermia, drug delivery, etc. [1]. Particular interest is aroused by use of MNPs in magnetic resonance (MR) diagnostics as *in vivo* [2] and *in vitro* [3]. The magnetic nanoparticles should have certain magnetic characteristics, to be stable (have low aggregation capacity), biocompatible, non-toxic, have the ability of functionalization to interact or bind with specific biological objects. Composite MNPs and functional systems based on them are promise materials for the MR-diagnostics. One of the most common methods for the synthesis of iron oxide MNPs is the co-precipitation method. Due to the high sensitivity to different parameters (nature of the precipitant, concentration of reagents, temperature of synthesis, pH of the reaction medium, etc.), it allows to widely vary the size and properties of the resulting nanoparticles.

The aim of this paper is research the NMR relaxation properties of protons in aqueous solutions of composite nanoparticles based on solid solutions of zinc ferrites, magnesium and iron (magnetite).

## II. EXPERIMENTAL METHODS

Composite MNPs substituted with zinc and/or magnesium magnetite were obtained by co-precipitation method from solutions of the corresponding salts using different precipitants – NaOH and Na<sub>2</sub>CO<sub>3</sub>. The solution taken in stoichiometric ratio of initial reagents at room temperature was introduced into the solution of precipitator, taken with some excess, and stood for 1 h with intensive mixing until the completion of

crystallization processes. The pH of the system during the reaction was maintained at ~ 11, due to which it is managed to achieve full deprotonation of aqua complexes ions of all metals, but to prevent the formation of water-soluble hydroxocomplexes. In the event carbonate co-precipitation, the reaction mixture was rapidly heated to a temperature of 90°C, after that heating was stopped. To obtain colloidal solutions of nanoparticles the ultrasonic bath (Sapfir, Russia) and submersible ultrasonic disperser (USG-13-0,1/22, Russia) have been used. Magnetic nanoparticles were functionalized by polyelectrolyte shell (polydiallyldimethylammonium chloride–PDDA).

X-ray patterns of powdered samples were recorded on a diffractometer DRON-2.0 (Co K $\alpha$ -radiation) in the range  $2\Theta = 20\text{--}90^\circ$ . The size and morphology of particles were examined using scanning and transmission electron microscopy by LEO 906E, JOEL EM100 CX and LEO 1420 microscopes. Measurements of magnetic characteristics of MNPs were performed using Cryogen Free Measurement System by Cryogenic Ltd. ( $T = (7\text{--}300)$  K,  $B_{\max} = 18$  T).

The NMR measurements were made using NMR relaxometer (Spin Track, Russia) with the magnitude of the magnetic field of 0.33 T. The resonance frequency for protons - 14 MHz. To measure  $T_1$  spin-lattice relaxation time the "inversion-recovery"  $180^\circ\text{-}\tau\text{-}90^\circ$  pulse sequence was used (the duration of  $90^\circ$  pulse - 2.6  $\mu$ s; the duration of the  $180^\circ$  pulse - 5.2  $\mu$ s). To measure  $T_2$  spin-spin relaxation time the Carr-Purcell-Meiboom-Gill (CPMG) pulse sequence was used (the duration of the  $90^\circ$  pulse - 2.6  $\mu$ s; the duration of the  $180^\circ$  pulse - 5.2  $\mu$ s).

## III. RESULTS AND DISCUSSION

The results of x-ray phase analysis (XRA) confirm the formation of single-phase crystalline compounds with a spinel structure when alkaline or carbonate co-precipitation methods were used. According to electron microscopy data, the average size of the nanoparticles is ~ 10 nm for hydroxide precipitant, and ~20 nm for sodium carbonate precipitant. All investigated composite MNPs show superparamagnetic behavior with no coercivity and no remanent magnetization at room temperature.

An aqueous suspensions of unmodified nanoparticles are characterized by multimodal size distribution with a high polydispersity index ( $PDI > 0.4$ ) and sediment instability. A stable suspensions with a narrow size distribution ( $PDI < 0.250$ ) were obtained by powders dispersing of ferrites solid solutions with PDDA. The size of particles covered with a layer of PDDA in distilled water practically does not change within 45 days.

According to the results of NMR relaxation measurements dependencies of longitudinal  $R_1$  and transverse  $R_2$  nuclear magnetic relaxation rates of water protons on the concentration of composite MNPs were obtained. For the most of samples the concentration dependencies of the relaxation rates correspond to a linear dependence of the general form

$R_i = r_i \cdot C + A$ , where  $C$  is the concentration of MNPs, expressed in mmol,  $A$  is a constant determined by the relaxation rate of water protons in the absence of MNPs,  $r_i$  is the relaxivity (relaxation efficiency coefficient). The analysis of concentration dependencies allows to determine the relaxation efficiency coefficient  $r_i$  as the derivative of  $R_i = f(C)$  function at this point and in the case of linear dependence to calculate the angular coefficient as the ratio:  $r_i = (1/C \cdot T_i) (\text{mmol} \cdot \text{s/l})^{-1}$ . The analysis of relaxation efficiency of the studied samples shows that:

- $r_1$  and  $r_2$  relaxation efficiency coefficients for the MNP samples, obtained by co-precipitation with carbonate, higher than the relaxation efficiency coefficients for MNP samples, obtained by co-precipitation with alkali (without heating);
- $r_2$  relaxation efficiency coefficient is much higher than the  $r_1$  relaxation efficiency coefficient for all MNP samples, regardless of synthesis, which confirms the fact that the investigated MNPs are negative contrast agents in MRI [2] ;
- $r_2$  relaxation efficiency coefficient for the samples obtained by co-precipitation with carbonate is lower for the composite MNPs with Zn in the structure.

Concentration dependencies of the  $R_2$  transverse nuclear magnetic relaxation rates of water protons for some MNP samples have been nonlinear. The analysis of these dependencies shows a decrease in the relaxation efficiency by increasing the MNP concentration in the solution. It indicates instability of these MNPs in aqueous solutions and their aggregation ability to form clusters when the concentration of MNPs in the solution increases. This effect of MNP clustering was observed in these samples visually and increased with increasing residence time of the sample in the magnetic field of the NMR relaxometer. Similar results were obtained earlier in the NMR relaxation study of protons in aqueous solutions of  $\text{Fe}_3\text{O}_4/\text{SiO}_2$  nanoparticles [4].

#### IV. CONCLUSIONS

The research of the protons NMR relaxation in aqueous solutions of iron oxide composite MNPs show that their  $r_2$  relaxation efficiency is much higher than  $r_1$  relaxation efficiency and depends on the composition, method of MNP synthesis. It allows to use this parameter to assess the stability of MNPs in aqueous solutions and estimate their aggregation behavior.

#### REFERENCES

- [1] Jinhao Gao, Hongwey Gu, Bing Hu. Multifunctional Magnetic Nanoparticles: Design, Synthesis, and Biomedical Applications. // Accounts of Chemical Research, 2009, vol.42, No.8, p.1097-1107.
- [2] R.Thomas, In-Kyu Park, Yong YeonJeong. Magnetic Iron Oxide Nanoparticles for Multimodal Imaging and Therapy of Cancer. // Int.J.Mol.Sci., 2013, vol.14, p.15910-15930.
- [3] Shao H., C Min, Issadore D., Min C., Liang M., Chung J., Weissleder R., Lee H. Magnetic Nanoparticles and microNMR for Diagnostic Applications. //Theranostics, 2012, vol. 2(1), p.55-65.
- [4] Yu.V.Bogachev, Ju.S.Chernenko, K.G.Gareev, I.E.Kononova, L.B.Matyushkin ,V.A.Moshnikov, S.S.Nalimova. The Study of Aggregation Processes in Solutions of Magnetite-Silica Nanoparticles by NMR Relaxometry, AFM and UV-Vis-Spectroscopy. // Appl. Magn. Reson., 2014, vol.45, p. 329-337.

# On the Use of Wireless Sensors Within a Traffic Monitoring System

Hannes Toepfer<sup>1,2</sup>, Marco Goetze<sup>2</sup>, Elena Chervakova<sup>2</sup>, Tino Hutschenreuther<sup>2</sup>

<sup>1</sup>Institute for Information Technology, Technische Universität Ilmenau, Germany

hannes.toepfer@tu-ilmenau.de

<sup>2</sup>Institut für Mikroelektronik- und Mechatronik-Systeme gemeinnützige GmbH, IMMS

Ehrenbergstraße 27, Ilmenau, Germany

{hannes.toepfer,marco.goetze,elena.chervakova,tino.hutschenreuther}@imms.de

**Abstract**— The work describes a sensor system for monitoring traffic-related data such as the number, type and speed of vehicles on a road. Essential components such as networked intelligent embedded systems for sensor data acquisition and its collection are described. First results of the application are illustrated.

**Keywords**— *electromobility, event detection, smart mobility, tactile road, traffic monitoring, wireless sensor network (WSN)*

## I. INTRODUCTION

Traffic monitoring is considered an essential enabler for introducing concepts of electromobility. As the range of electric vehicles is still shorter as compared to conventional vehicles, navigation strategies with a focus on trip time and distance travelled gain importance. However, these attributes strongly rely on up-to-date traffic information such as, e.g., details of traffic jams, and reachability of the destination. On this background, research is carried out aiming at a solution to bring such information together so that electromobility is enabled or even significantly improved. In particular, research activities are focused on replacing cable systems for acquisition of data on road users by wireless sensor solutions that can be deployed very easily and at lower cost. The sensor unit contains a magnetic field sensor so that passing vehicles can be detected. Besides detection, classification of the vehicles is of interest.

In Section II, the system concept of the traffic monitoring system is described. Section III focuses on the features of the Wireless Sensor Network (WSN).

## II. SYSTEM OVERVIEW

### A. System Design

The described solution is designed for being implemented and operated in the model town Erfurt in central Germany, where they complement approx. 1,150 existing induction loop detectors. As traffic sensors within the road must be rugged in order to be weatherproof, their deployment is challenging. Therefore, wireless communication is a promising solution and has been the network technology of choice for the approx. 170 magnetic field sensors. This way, a “tactile road” is formed. It enables monitoring of the traffic flow, to collect

data, to transmit it wirelessly to a nearby gateway, and then to send it to a data concentrator in the traffic control centre. As a result, the new wireless sensor network complements the data capture methods already in place. Traffic data can be registered in finer detail than before. On this basis, it is possible to create more comprehensive and accurate traffic models for controlling the traffic in real time and making forecasts. Besides the monitoring components, the system comprises a data concentrator in a central control facility with data interfaces to a central computer and a web front-end for status visualization and configuration

### B. Principles of Wireless Sensor Networks

Generally, a Wireless Sensor Networks (WSN) comprises a hierarchy of nodes. Terminal nodes contain the sensors and capture the date. They are sent to other nodes in a way that is specified by a chosen network topology. In the case described, a star topology turned out to be favorable and has been implemented. The individual nodes send data to a gateway which connects the WSN to higher-tier IT infrastructure, usually via Ethernet or the Internet. WSN nodes are embedded systems, usually utilizing an embedded operation system providing elementary features such as implementations of wireless communication standards. A popular variety of WSN is based on the IEEE 802.15.4 standard, which defines the physical layer. Our implementation is based on TinyOS[1], an open-source WSN operating system offering many degrees of freedom for customization. This enabled that the WSN nodes communicate via IPv6 (6LoWPAN), facilitating the integration in networks is easy. Fig. 1 schematically shows the structure of the used WSN.

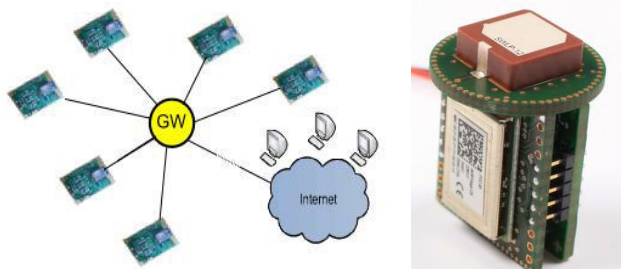


Fig. 1. Left: schematic representation of a Wireless Sensor Network with a star topology [2]. Sensor nodes communicate

with a gateway (GW) which maintains connection to the IT environment. Right: Hardware realization of the WSN node.

### C. Design Requirements

The design constraints arose from the particular installation conditions. The traffic sensors are installed within the road surface, with a certain freedom of choice with respect of the lateral position. The gateways were to be installed on traffic lights or lamp posts, i.e. at fixed positions. An example of such a gateway mounted on a traffic lights post as well as of the sensor node packaged for outdoor installation is shown in Fig. 2.



Fig. 2. Left: Gateway installation at a crossroads, here mounted on a traffic lights post. The red circle indicates the position at an elevation of 4 meters. Right: Housing of the traffic sensor, a plastic shell for deployment in the road.

The described WSN enhancement of the traffic monitoring system is currently being evaluated in continuation of a field trial in the German city of Erfurt, Thuringia [3]. Installations at 17 intersections acquire traffic data from 172 detectors and feed these into a city-wide traffic management platform. With the developed system, near-real-time monitoring of traffic volumes by vehicle class (car/truck), detector occupancy, and – by using paired detectors – speeds is possible. These measured data of the “tactile road” are wirelessly transmitted to the gateway. The gateways then transmit the traffic data and status information to a data concentrator and on to the central traffic management platform.

A web frontend has been realized, allowing for configuring the system and displaying status information for all components. A typical example of visualization of measured data, delivered from a single detector node to the traffic management system, is shown in Fig.3.



Fig. 3. Visualization of results, delivered by a single traffic detector node, in the web frontend. The information contains traffic volume, occupancy and the average speed of vehicles. The trace in the lower part visualizes the traffic volume at this measuring site during the last 24 hours.

### ACKNOWLEDGMENT

This research has been funded by the German Federal Ministry for Economic Affairs and Energy under the reference 01ME12076. Only the authors are responsible for the content of this publication.

### REFERENCES

- [1] P. Levis, S. Madden, J. Polastre, R. Szewczyk, A. Woo, D. Gay, J. Hill, M. Welsh, E. Brewer, and D. Culler, “TinyOS: An operating system for sensor net works,” in *Ambient Intelligence*, Springer Verlag, 2004
- [2] E. Chervakova, W. Kattanek: “QoS-driven Design and Operation of Adaptive, Self-organizing Wireless Sensor Systems”, Proc. 39<sup>th</sup> Annual Conference of the IEEE Industrial Electronics Society IECON, Vienna, November 2013, pp. 7720-7725.
- [3] H. Toepfer, E. Chervakova, M. Goetze, T. Hutschenreuther, B. Nikolić, and B. Dimitrijević, “Application of wireless sensors within a traffic monitoring system”, in Proceedings of the 23<sup>rd</sup> Telecommunications Forum (TELFOR), (Belgrade, Serbia), Nov. 24–26 2015, pp. 236-241.

# On the Role of Wireless Sensor Networks for Intelligent Transportation Systems

Silvia Krug\*, Elena Chervakova#, Hannes Töpfer#, and Jochen Seitz\*

\*Communication Networks Group, Technische Universität Ilmenau, Germany

{silvia.krug, jochen.seitz}@tu-ilmenau.de

#IMMS Institute for Microelectronic and Mechatronic Systems not-for-profit GmbH

Ehrenbergstraße 27, Ilmenau, Germany

{elena.chervakova, hannes.toepfer}@imms.de

**Abstract**—The current trend is to build Intelligent Transportation Systems (ITS) based on modern wireless networks among all participants in traffic scenarios as well as road side infra-structure. Different networking technologies such as 802.11p for Car2X communications need to be integrated into the system in order to enable the full potential of ITS. However, the most important components are sensor systems that are able to collect information on the current traffic or environmental conditions and thus enable the control and management of the traffic. Wireless sensor networks become popular in this area as well. This contribution will present four use cases for sensor networks in ITS context and identify common problems and open challenges.

**Keywords**—Wireless Sensor Networks; Intelligent Transportation Systems; Use Cases.

## I. INTRODUCTION

To build Intelligent Transportation Systems (ITS), different networking technologies need to be integrated in order to enable the full potential of ITS. 802.11p for Car2X communications allows the communication between the vehicles and between vehicles and road side units, such as traffic lights or dedicated communication infrastructure. A similar goal is achieved by using cellular mobile communication networks. Besides that, this technology allows to offload some traffic from the inter-vehicle network by bridging the communication to the infrastructure or other backend components. Finally, public hot spots providing access to the Internet via traditional Wifi-based networks can aid the connectivity further. Each different approach adds another aspect to the overall capabilities of an ITS.

However, these technologies do not address one essential thing directly: the monitoring and surveillance of the actual traffic. This has to be provided by sensors. Sensors tracking different parameters are the essential component of an ITS in addition to the inter-vehicle communication [1]. Traditional sensor systems related to road traffic monitoring and control are cameras or induction loops as well as configurable traffic signs or traffic lights. These systems are usually not connected among each other or in a limited geographical extent for example to cover one intersection. Besides that, the connectivity is achieved based on fixed installations and wired connections. In future systems, the different sensor systems should be connected with each other and the remaining infrastructure as well as the vehicles to form an ITS. This

requires an integration of various different technologies and their co-existence.

In this contribution, we will review existing options to integrate wireless sensor networks (WSNs) into the ITS concept. We give an overview on potential use cases and review example approaches regarding their capabilities and the role of different sensor network approaches in intelligent transportation systems. Based on our initial presentation, we then identify common and general research questions shared among multiple scenarios. Finally, we discuss solution options for selected problems with a focus on co-existence of different technologies as well as robust communication under harsh environmental conditions and design choices.

## II. ITS USE CASES

There are four major use cases regarding the integration of sensor networks into the ITS concept: applying wireless sensors to monitor the traffic, using vehicles as mobile sink in sensor networks monitoring environmental conditions, adding the vehicles as powerful sensor devices to the network and integrating the sensor network into the vehicle itself to enhance its capabilities to sense its surroundings.

### A. Traffic Monitoring WSNs

In the first case, WSN nodes replace or complement the existing traditional sensor systems. While the traditional systems are able to monitor the traffic from an isolated local point of view, WSN-based systems promise to extend this view to a larger scale by deploying suitable cheap sensor nodes throughout the area in question. This will extend the sensing coverage of the ITS and thus allow more informed adaptive reactions to the given traffic conditions [2], [3]. The major challenges in this use case are:

Difficult *Propagation characteristics* due to the nodes actual position result in communication problems due to urban surroundings and potentially obstructed communication paths. *Harsh environmental conditions* result from outdoor deployments with unfavorable weather conditions including rain, frost, or snow as well as de-icing salts. Finally, the *co-existence* with other technologies in the 868MHz (Europe) or 2.4 GHz bands is challenging, especially in dense urban deployments.

All these challenges result in a potentially reduced reliability of the data collected by the network, as error-free

packet reception under all circumstances becomes difficult. Especially, since WSN nodes are traditionally battery-powered but require a long maintenance-free node life time. To achieve this, energy should be conserved but that limits the options for re-transmissions in order to deliver data that could not be received without errors on the first attempt. This requires an ITS to handle missing individual data packets and still provide reliable monitoring conclusions.

#### B. Vehicular Sink Nodes

The second case applies to systems, where vehicles act as data mules for data values collected by distributed sensor nodes that might not be able to establish a connection to the base station or sink node. While this might not be directly related to ITS management at a first glance, for example the current trend to restrict traffic in some areas in case of high air pollution adds new use cases. In such a scenario, the air quality sensors can be distributed in given grids to ensure a required coverage and use vehicles to gather and forward the sensor values. Besides the challenges discussed for the first use case, two special aspects have to be considered here:

*Data storage* is required to ensure that values are not lost while there are no suitable sink nodes available. But if the system has to react adaptively on detected changes in time, *delay constraints* apply.

#### C. Vehicular Sensor Nodes

In the third case, the vehicles act as a sensor themselves using either the on-board sensors of the vehicle or additional sensors such as smartphones of passengers, or specifically designed sensors to capture the desired phenomena [4].

The desired *sensing coverage* is the major challenge in this use case, because to achieve a requested sensing precision of a query in one particular area several nodes are required.

#### D. Intra-Vehicle Sensor Networks

Finally, the vehicle can be equipped with an additional internal sensor network [5] and thus is able to share the collected data. If the sensor data is shared among vehicles or road side infrastructure, the vehicles can benefit from their own sensors but also from data collected by others in their surroundings. This is especially true if autonomous driving is one goal [6]. Another example for this use case is the detection of objects in otherwise blind spots [7].

In this use case, *data aggregation* is required to obtain a combined sensor value based on data from multiple sources. Besides that, a maximum *geographic range* to distribute the data of interest has to be defined if sensor data is shared among different vehicles.

### III. COMMON CHALLENGES

Based on the review in the previous section, it is obvious that robust communication is required for an ITS. The robustness has to handle fluctuating connectivity due to node mobility and difficult propagation characteristics as well as interference from nodes using the same technology or others operating in the same ISM frequency band in order to provide

reliable data transfer. Besides that, gateways are required to interconnect the different networking technologies in order to exchange data via multiple transmission paths again requiring error-free co-existence of the different technologies. To solve these issues, additional work on wireless co-existence and mitigation strategies to build robust communication protocols is required. The evaluation of such protocols should be based on appropriate interference models capturing real-world characteristics based on measurements. Current approaches mainly focus on a single technology only.

Due to these communication-related challenges and potentially limited sensing coverage, the system has to handle missing data values. The loss of packets cannot be avoided completely no matter how robust the communication scheme is, especially if it results from missing communication opportunities. In this case, protocols allowing data to be stored could help. Several further application-related challenges apply, to achieve the desired granularity of the sensor values in both time (e.g. to sample how often) and geographic coverage (where to sample). In these cases, storage might not help as data could be too old when it is finally delivered. This requires other options to estimate the missing values.

### IV. CONCLUSIONS

This paper presented four different use cases for wireless sensor networks in the context of intelligent transportation systems. For each use case, we presented some examples and showed the major challenges. Based on these results, we then identified two common major challenges that have to be solved in order to enable the full potential of ITS use cases. These challenges are related to both communication and application specific aspects and should gain further research attention.

### REFERENCES

- [1] K. Nellore and G. P. Hancke, "A survey on urban traffic management system using wireless sensor networks," *Sensors*, vol. 16, no. 2, p. 157, 2016.
- [2] A. Pascale, M. Nicoli, F. Deflorio, B. Dalla Chiara, and U. Spagnolini, "Wireless sensor networks for traffic management and road safety," *IET Intelligent Transport Systems*, vol. 6, no. 1, pp. 67–77, 2012.
- [3] E. Chervakova, S. Engelhardt, M. Goetze, M. Rink, and A. Schreiber, "Wireless Sensor Networks for Traffic Applications: Challenges and Solutions," in Conference on Design and Architectures for Signal and Image Processing (DASIP). Krakow, Poland: ECSI, Sep. 2015, Demo.
- [4] R. Du, C. Chen, B. Yang, N. Lu, X. Guan, and X. Shen, "Effective urban traffic monitoring by vehicular sensor networks," *Transactions on Vehicular Technology*, vol. 64, no. 1, pp. 273–286, 2015..
- [5] S. Krug, E. Chervakova, H. Toepfer, and J. Seitz, "Integration of 802.15.4 based wireless sensor networks into existing intra-vehicle networks," in 2nd International Scientific Symposium "Sense. Enable. SPITSE. St. Petersburg, Russia, Jun. 2015, pp. 168–171.
- [6] H. Wymeersch, G. R. de Campos, P. Falcone, L. Svensson, and E. G. Ström, "Challenges for Cooperative ITS: Improving Road Safety Through the Integration of Wireless Communications, Control, and Positioning," in International Conference on Computing, Networking and Communications (ICNC). Anaheim, CA, USA: IEEE, Feb. 2015, pp. 573–578.
- [7] J.-R. Lin, T. Talty, and O. K. Tonguz, "A blind zone alert system based on intra-vehicular wireless sensor networks," *Transactions on Industrial Informatics*, vol. 11, no. 2, pp. 476–484, 2015.

# An Approach to Extract Significant Features for Vehicle Classification Based on Magnetic Field Sensor Data

Vladimir Shkoda, Sylvia Brauenig, Hannes Toepper

Institute for Information Technology  
Technische Universität Ilmenau  
Ilmenau, Germany

Marco Goetze

Institut für Mikroelektronik- und Mechatronik-Systeme  
gemeinnützige GmbH  
IMMS  
Ehrenbergstraße 27, Ilmenau, Germany

**Abstract**—This paper describes an approach to extract significant features from raw magnetic field sensor data in order to classify vehicles in the context of traffic monitoring. Also, it discusses the implementation of different machine learning algorithms, and performs a comparative analysis of their performance.

**Keywords**—traffic monitoring; vehicle detection; vehicle classification; event detection; feature extraction; machine learning; electromobility; wireless sensor network (WSN)

## I. INTRODUCTION

An automatic vehicle classification system provides a number of useful applications, such as traffic monitoring, road construction and maintenance, and toll booth collection. The system requires a wireless sensor network (WSN). A big amount of researches among a number of sensors have proved, that the magnetic sensor is the most effective and suitable to apply with WSN due to its low cost, small size, and power efficiency. For now, the sensor network was developed [1] and successfully deployed on the roads of Erfurt in central Germany. It implements two functions: detection and measurement, and communication. The next step is to process a vehicle's magnetic signature in order to identify its class (Fig. 1). For this purpose, we need to extract features from the signal, implement and compare different algorithms of machine learning, and find out which one is the most appropriate.

## II. FEATURES DESCRIPTION

In this section, we perform preprocessing and extracting characteristic values from data. It can be divided in several domains.

### A. Time Domain

The calculation of parameters in the time domain is carried out directly with the signal data. According to [2], there were extracted following values: maximum and minimum values, oscillation range, rectified value, root mean square, shape factor.

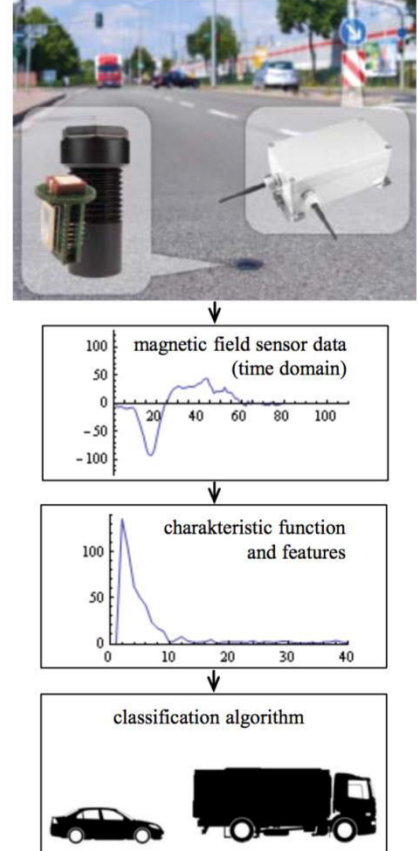


Fig. 8. Schematic representation of the signal processing with an example of the actual sensor of WSN node [1]

### B. Amplitude Density Distribution

From the domain of amplitude density distribution can be the parameters calculated, with which it is possible to make statements about the probability distribution. In comparison with the characteristics of interference-free signal, the characteristics of damaged signal have deviations from the normal distribution. With this purpose, the skewness and the excess kurtosis are computed.

### C. Fourier Transform

More characteristic values can be obtained with pre-processing sensor data. We applied discrete Fourier transform (Fig. 2) and extracted the skewness and the excess kurtosis from this domain.

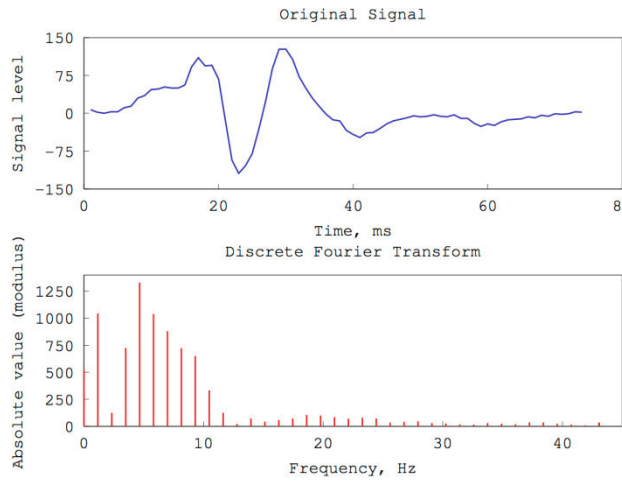


Fig. 9. Processing original signal with DFT

### D. Hill Pattern

Hill pattern is used [3] and the first time was proposed in [4]. The rate of change of consecutive samples is compared with a threshold and declared to be +1 (-1) if it is positive and larger than (negative with magnitude larger than) the threshold, or 0 if the magnitude of the rate is smaller than the threshold (Fig. 3). As a result, we get two features: number of 'peaks' and 'valleys'.

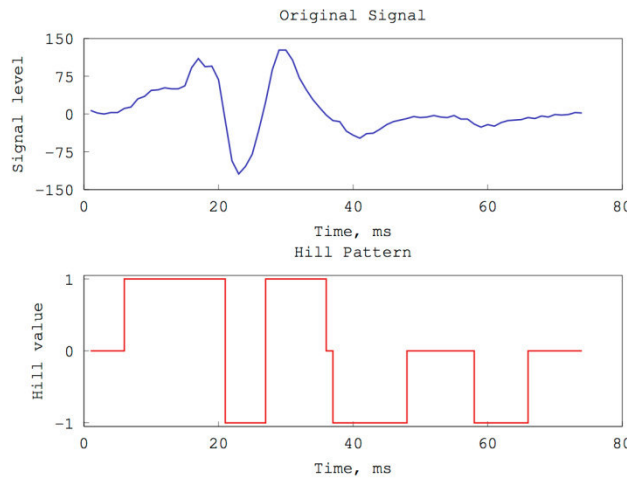


Fig. 10. Transforming original signal to the hill pattern

## III. CLASSIFICATION ALGORITHMS

In order to compare significance of different feature sets, there were implemented four classifiers: minimum distance, k-

Means, naive Bayes, and neural network. The first classifier is based on the unsophisticated idea; the three other ones are described in [5].

The idea of minimum distance classifier is very simple: for each class in the training set, compute the mean point (center), and then assign unlabeled patterns to the nearest center in the feature space. For calculating distance between two points, we used Euclidean metric and Mahalanobis distance.

In the k-Means algorithm, initial  $k$  cluster centers are randomly chosen from the data set. Then they are been moving to the mean points of the  $k$  subsets with each iteration.

The aim of the naive Bayes classifier is the assignment of an object to the most probable class, based on applying Bayes' theorem. Since features of a sample are independent, the assignment of the class takes place by the voting.

The neural network consists of an input layer, one hidden layer with five neurons, and an output layer, interconnected by modifiable weights, represented by links between layers. In addition, there is a single bias unit on every layer that is connected to each unit on the next layer. The weights are calculated with the backpropagation algorithm.

## IV. RESULTS

The experimental results are obtained on a training set consisting of 180 vehicles: 90 trucks and 90 cars. The mean signal value was set to 127, the threshold used in the hill pattern – 10.

Among the four algorithms, the best prediction level was achieved by the naive Bayes classifier and the neural network. Features extracted from the Fourier transform and hill pattern turned out as the most significant (Tab. 1).

The neural network yields on the Fourier transform with hill pattern feature set lower classification rate than the naive Bayes only on the Fourier transform, but with gaining more training data, it can be the other way around due to complexity of the network neurons.

TABLE I  
CLASSIFICATION ACCURACY ON THE DIFFERENT FEATURE SETS, %

Classifier	DFT + Hill Pattern	DFT
Naïve Bayes	98.89	100.00
Neural network	93.98	93.33

## REFERENCES

- [1] H. Toepfer, E. Chervakova, M. Goetze, T. Hutschenthaler, B. Nikolic, and B. Dimitijevic, "Application of wireless sensors within a traffic monitoring system," *Telecommunications Forum Telfor (TELFOR)*, 2015 23rd, pp. 236–241, 2015.
- [2] M. Mekonnen, "Zur Anwendung der Signalanalyse und Mustererkennung in der Geräuschiagnose am Beispiel von elektro-mechanischen Systemen," Ph.D. dissertation, Technischen Hochschule Ilmenau, Fakultät für Technische Wissenschaften, 1991.
- [3] S. Keawkamnerd, J. Chinrungruen, and C. Jaruchart, "Vehicle classification with low computation magnetic sensor," in *2008 8th International Conference on ITS Telecommunications (ITST)*, 2008, pp. 164–169.
- [4] S.Y.Cheung,S.Coleri,B.Dundar,S.Ganesh,C.-W.Tan, and P.Varaiya, "Traffic measurement and vehicle classification with a single magnetic sensor," *California PATH Working Paper*, September 2004.
- [5] R. O. Duda, P. E. Hart, and D. G. Stork, *Pattern Classification*, 2nd ed. John Wiley & Sons, 2001.

# Comparative analysis of digital frequency measurement methods

Andrey Serov  
Information-Measurement Technologies department  
NRU «Moscow Power Engineering Institute»  
Moscow, Russian Federation  
serov.an.iit@yandex.ru

**Abstract**—Currently, the frequency measurement is one of the most essential tasks of measurement technology. There are many digital methods of measuring frequency, with very different static and dynamic methodological errors of measurement and complexity of the final implementation. In the article the comparative analysis of metrological characteristics of the most popular digital methods of frequency measurement for the case of sinusoidal input of polyharmonic signals and in the presence of random noise and flicker. The results obtained by mathematical simulation performed in the software package Matlab.

**Keywords**—frequency deviation; digital signal processing; measurement error, simulation modeling.

## I. INTRODUCTION

Measuring the frequency of the mains supply is one of the most important tasks of measuring equipment. Frequency measurement accuracy indirectly determines the accuracy of the signal parameters such as voltage and current RMS, active, reactive, apparent power, and others. Metrological characteristics of spectrum analyzers also depend on the frequency of measurement error. In modern measuring power quality instruments, the requirements for accuracy of frequency measurement are on the first cast. For this reason the task of accuracy of measuring the frequency of the mains supply is of current interest.

Limited size of the article does not permit to give a detailed description of all the methods listed in the classification. Their detailed description can be found in the publications [1-11].

## II. FINDING DERIVATIVE TECHNIQUE

Finding derivative technique is to measure the frequency of the signal on the basis of information on the rate of change over time. The relation is correct for the sine wave:

$$u''(n) = -(2\pi f)^2 u(n), \quad (1)$$

where  $u(n)$  – is the input signal (sinusoidal);  $u''(n)$  – is the second derivative of the input signal;  $n$  – is the number of the current sampling signal, then the frequency can be determined as follows:

$$f = \frac{1}{2\pi} \sqrt{\frac{-u''(n)}{u(n)}}, \quad (2)$$

To find the second derivative of the input signal the author of the article [2] proposes to approximate the original digital signal by interpolating Taylor polynomials. In the case of use

of the polynomial expression of the second order, the second derivative is given by:

$$u''(n) = \frac{(u(n+1) - 2u(n) + u(n-1))}{T_s^2}, \quad (3)$$

where  $T_s$  – is the sampling period.

Obviously, in case there are additional harmonics in the signal spectrum, equation (1) is not fulfilled, which leads to errors.

## III. ZERO-CROSSING TECHNIQUE

Between the methods of frequency measuring the most widely used method is based on determining the time intervals between the input signal transitions through zero [5-7]. According to this method, the value of the input signal period can be calculated using the following formula:

$$T = \frac{i_{cz,2} - i_{cz,1}}{N_{cz}} T_s, \quad (7)$$

where  $i_{cz,1}$  – the sample number of the first (during the measurement) zero crossing input on the rising (falling) age;  $i_{cz,2}$  – the number of the last sample (during measurement) zero crossing input on the rising (falling) age;  $N_{cz}$  – the number of zero crossings along the rising (falling) age for the period measurement;  $T_s$  – the sampling period.

The main advantage of this method is the ease of implementation and a weak dependence on flicker input. Disadvantages include low accuracy and strong dependence on the harmonics and noise input signal. There are some modifications [3] in order to reduce the above-mentioned disadvantages.

Zero-crossing point in time can be found by solving the equation:

$$a_m (\Delta i_{cz})^m + a_{m-1} (\Delta i_{cz})^{m-1} + \dots + a_0 = 0. \quad (10)$$

In the case of use of the approximating polynomials of the first and second order, there is a simple analytical solution of the equation. Since the sine wave near the zero crossing is close to linear, the use of approximating polynomials more than the second order is unjustified.

In the case of use of the approximating polynomial of the first order, the zero-crossing point input signal is given by:

$$\Delta i_{cz,x} = \frac{u(i_{cz,x} + 1)}{u(i_{cz,x} + 1) - u(i_{cz,x})} T_s. \quad (11)$$

where  $i_{cz,x}$  - is the sample number that is the closest to the intersection of the zero by the input signal.

Concerning the expression (5), the expression becomes:

$$T = (i_{cz,2} - i_{cz,1} + \Delta i_{cz,2} - \Delta i_{cz,1}) T_s / N_{cz}. \quad (12)$$

The task of suppressing the signal distortion can be solved by the use of low-pass or band-pass filtration. The pass-band of the filter is determined by a range of changes in the input signal frequency. In the case of a band-pass filter, the lower stop-band is needed to suppress the flicker, and the top stop-band - to suppress input harmonics and noise.

#### IV. DFT TECHNIQUE

The frequency of the voltage corresponds to the fundamental harmonic. Since the fundamental harmonic is the highest in amplitude, then, knowing the amplitude spectrum of the signal value, the frequency can be determined using the following expression:

$$f_1 = \frac{i_1 f_s}{M}, \quad (20)$$

where  $f_s$  - is the sampling frequency;  $i_1$  - is the number of harmonic with the highest amplitude (fundamental harmonic);  $M$  - is the number of discrete implementation.

It can be seen that the error of the measurement depends on the duration of the measurement is not dependent on the sampling frequency. Sampling rate determines the range of frequencies received, according to the Nyquist theorem its value must be set not under the double upper limit of the input signal spectrum.

To clarify the position of the fundamental harmonic on frequency axis, the authors of the article [10] proposed a method by which the amplitude spectrum of the signal is presented in an analytical form. In the case when we receive the amplitude spectrum using a rectangular window and approximation of the spectrum at two points, the value of the fundamental frequency harmonic is given by:

$$f_1 = \frac{i_1 f_s}{M} + \frac{\text{sign}(H(i_1+1) - H(i_1-1))H(i_{1x})}{|H(i_1)| + |H(i_{1x})|}. \quad (22)$$

where  $H(i_1)$  - is the value of the largest harmonic amplitude spectrum.

This method is suitable for measuring frequency of sinusoidal and also polyharmonic signals. However, in the latter case, the duration of the realization (in terms of maintaining the multiplicity of the signal period) must exceed the period of the signal.

The main advantage of this method is its relative simplicity: in order to perform frequency measurement is necessary to do one DFT of the original implementation. In the case of the FFT algorithm with the number of samples of an input signal power of two, you need to do  $M \log_2(M)$  pair of operations "multiplication - addition."

#### V. CONCLUSION

The results of the study showed that not all the methods of measurement frequencies have high metrological

characteristics in today's power grids. Usage of the finding derivative technique and adaptive filtration technique is very difficult because of their high accuracy measurement in the presence of the input signal harmonics and noise. The flicker has a strong influence on the measurement error for the preliminary integration technique, which also makes it difficult to use.

The method, based on spectral analysis of the input signal (DFT) with subsequent analytical redefining of the fundamental frequency, has a simple implementation (especially for the devices, which include the facilities implemented by the spectral analysis), but it also has a low metrological characteristics. Its advantage is its low sensitivity to the considered type of distortion of input signal (flicker, harmonics and noise).

The modified preliminary integration technique and the zero-crossing technique have high metrological characteristics. However, the first one is preferably to use in a small flicker, and the second one - to complement the low-pass filter in order to reduce the error.

#### REFERENCES

- [1] Wu Jie-kang, HE Ben-teng "An algorithm for frequency estimation of signals composed of multiple single-tones", Journal of Zhejiang University, Science A, vol. 7(2), 2006, pp. 179-184.
- [2] Wu Jie-kang "Wide range parameter measurement of sinusoidal signals", Journal of electrical engineering, vol. 57, NO. 2, 2006, pp. 111-115.
- [3] D. Ould Abdeslam, P. Wira, J. Mercklé, and D. Flieller, "A neural learning approach for time-varying frequency estimation of distorted harmonic signals in power systems", 1st International ICSC Symposium on Industrial Application of Soft Computing (IASC 2005), Istanbul, Turkey, Dec. 15-17, 2005.
- [4] D. Halbwachs, P. Wira, and J. Mercklé, "Adaline-based approaches for time-varying frequency estimation in power systems", 2nd IFAC International Conference on Intelligent Control Systems and Signal Processing (ICONS 2009), Istanbul, Turkey, September 21-23, 2009.
- [5] Miroslav M. Begovic, Petar M. Djuric, Sean Dunlap, Arun G. Phadke. "Frequency Tracking in Power Networks in the Presence of Harmonics", IEEE Transactions on Power Delivery, Vol. 8, No. 2, April 1993, pp. 480-486.
- [6] P J Moore, R D Carranza, A T Johns, "Model System Tests on a New Numeric Method of Power System Frequency Measurement", IEEE Transactions on Power Delivery, Vol. 11, No. 2, April 1996, pp. 696-701.
- [7] Sidhu T. "Accurate measurement of power system frequency using a digital signal processing technique", IEEE Trans. on Instr. and Meas., vol. 48, no. 1, February 1999, pp. 75-81.
- [8] V. S. Popov, E. V. Shumarov "method for measuring the period of electrical signals with a DC component and a non-sinusoidal waveform", Measurement techniques, 1998, No. 7, 34-39.
- [9] V. S. Popov, E. V. Shumarov "period Measurement of the electric signals presented in digital form", Measurement technology, 1995, No. 1, 50-54.
- [10] Dušan Agrež "Fast measurement of power system frequency in the frequency domain", XVIII IMEKO world congress Metrology for a Sustainable Development September, 17 – 22, 2006, Rio de Janeiro, Brazil.
- [11] T. Lobos and J. Rezmer, "Real-Time Determination of Power System Frequency", IEEE Trans. on Instr. Meas., Vol. 46, No. 4, pp. 877-881, August 1997.

# Application of the Semi-Implicit Numerical Integration Methods for the Simulation of Memristor-Based Circuits

Valerii Y. Ostrovskii, Denis N. Butusov

Department of Computer-Aided Design

Saint-Petersburg Electrotechnical University (ETU "LETI")

Saint-Petersburg, Russia

ostrovskiyv@gmail.com

Hannes Toepfer

Advanced Electromagnetics Group

Technische Universität Ilmenau (TU Ilmenau)

Ilmenau, Germany

hannes.toepfer@tu-ilmenau.de

**Abstract**—This paper discusses the application problems of semi-implicit numerical integration methods in computer simulation of nonlinear dynamical systems modelling memristor-based circuits. The algorithm of the proposed method and a series of computational experiments in Wolfram Mathematica and NI LabVIEW programs are presented. An evaluation of computational efficiency of the method modifications compared with the built-in classical methods is provided.

**Keywords**—memristor; nonlinear dynamical system; differential equations; numerical integration; ODE solver; simulation

## I. INTRODUCTION

Due to the development of the titanium dioxide memristor by Hewlett Packard Labs in 2008 [1], the interest in memristors [2] and memristive systems [3] has revived. One of the main tasks to be solved in the computer simulation of electrical circuits based on such devices is a computation of numerical solutions of the differential equations. In this paper we consider the numerical integration methods in terms of their computational efficiency, describe the techniques of increasing their order, and propose relatively new semi-implicit scheme which has significant potential in solving the problems of the topic.

## II. MEMRISTOR-BASED CIRCUIT

We begin with the definition of the dynamical system for the test. The paper [4] presents an autonomous circuit which gives a rise to chaotic attractor and has only three circuit elements shown in Fig.1: a linear passive inductor  $L$ , a linear passive capacitor  $C$  and a nonlinear active memristor  $M$ .

As an example, we will use the memristor model based on fourth order polynomial nonlinearity, provided for this circuit later in [5]:

$$\begin{aligned} u_M &= (d_4q^4 - d_2q^2 - d_0)i_M \\ \frac{dq}{dt} &= i_M - aq + gi_M^2 q. \end{aligned} \quad (1)$$

### A. Circuit Equations

To describe the circuit dynamics the following state variables were defined:

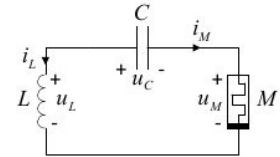


Fig. 1. Schematic of three-element chaotic circuit [4]

- $u_C$  - voltage across the capacitor  $C$  ;
- $i_L$  - current through the inductor  $L$  ;
- $q$  - charge as a control value of the memristor  $M$  .

With the application of Kirchhoff's laws  $i_L = i_C = -i_M$  ,  $u_L + u_C = u_M$  , and taking into account  $i_C = Cdu_C/dt$  ,  $u_L = Ldi_L/dt$  , the system of circuit equations can be obtained:

$$\begin{cases} \frac{du_C}{dt} = \frac{1}{C}i_L \\ \frac{di_L}{dt} = -\frac{1}{L}(u_C + b(d_4q^4 - d_2q^2 - d_0)i_L) \\ \frac{dq}{dt} = -i_L - aq + gi_M^2 q. \end{cases} \quad (2)$$

### B. Normalized System Equations

Let us introduce new reference values to transform circuit equations:

- $x_1 = u_C/U_0 \longrightarrow u_C = U_0x_1$  ;
- $x_2 = i_L/I_0 \longrightarrow i_L = I_0x_2$  ;
- $x_3 = q/Q_0 \longrightarrow q = Q_0x_3$  ;
- $\tau = t/T_0 \longrightarrow t = T_0\tau$  .

Assuming  $T_0 = CU_0/I_0$  ,  $U_0 = Q_0/C$  and introducing  $\delta = (U_0T_0)/(I_0L)$  ,  $\beta_3 = I_0d_4Q_0^4/U_0$  ,  $\beta_2 = I_0d_2Q_0^2/U_0$  ,  $\beta_1 = I_0d_0/U_0$  ,  $\alpha = aT_0$  and  $\gamma = gI_0^2T_0$  , the sought set of system equations can be obtained in the form of:

$$\begin{cases} \frac{dx_1}{d\tau} = x_2 \\ \frac{dx_2}{d\tau} = -\delta(x_1 + (\beta_3 x_3^4 - \beta_2 x_3^2 - \beta_1)x_2) \\ \frac{dx_3}{d\tau} = -x_2 - \alpha x_3 + \gamma x_2^2 x_3. \end{cases} \quad (3)$$

According to the paper [5] the system exhibits chaotic behavior if the following parameters are used:  $\beta_3 = 0.5$ ;  $\beta_2 = 1.5$ ;  $\gamma = 1$ ;  $\delta = 1/3$ ;  $\alpha$  and  $\beta_1$  can be variable.

### III. SEMI-IMPLICIT NUMERICAL METHOD

Research of processes occurring in chaotic systems, to which the system under the test belongs, puts high demands on the efficiency of applied numerical methods. The famous Runge-Kutta methods (e.g. the Dormand-Prince method) do not fully satisfy the requirements because of their limited order, further increase of which is a non-trivial task in itself [6].

One of the known approaches to improve accuracy order for solving ordinary differential equations is the use of extrapolation integration schemes. The most popular extrapolation method in a variety of mathematical packages is the Gragg-Bulirsch-Stoer (GBS) algorithm (see ExplicitModifiedMidpoint [7]). This method differs with relatively low computational costs, but suffers from low numerical stability, that means it is not adapted for solving stiff problems. Implicit schemes applied for such problems in opposite have high computational costs. Some studies has shown that semi-implicit methods [8] are an effective trade-off between implicit and explicit algorithms.

Let us present an algorithm of the semi-implicit method in the analytical form. The increment function for the dynamical system Eq. (3) is defined by:

$$\begin{aligned} x_1[n+1/2] &= x_1[n] + h_l x_2[n] \\ x_2[n+1/2] &= \frac{x_2[n] - h_l \dot{x}_1[n+1/2]}{1 + h_l \delta(\beta_3 x_3^4[n] - \beta_2 x_3^2[n] - \beta_1)} \\ x_3[n+1/2] &= \frac{x_3[n] - h_l x_2[n+1/2]}{1 + h_l (\alpha - x_2^2[n+1/2])} \end{aligned} \quad (4)$$

and

$$\begin{aligned} x_3[n+1] &= x_3[n+1/2] + h_l (-x_2[n+1/2] - \\ &\quad (\alpha + x_2^2[n+1/2]) x_3[n+1/2]) \\ x_2[n+1] &= x_2[n+1/2] + h_l \delta(x_1[n+1/2] + \\ &\quad (\beta_3 x_3^4[n+1] - \beta_2 x_3^2[n+1] - \beta_1) x_2[n+1/2]) \\ x_1[n+1] &= x_1[n+1/2] + h_l x_2[n+1], \end{aligned} \quad (5)$$

where  $x_i[n+k]$  is the value of the state variable in the point  $n+k$  and  $h_l$  is a half of the current step-size  $h$ .

Formally, the first part Eq. (4) of the method is the diagonally implicit first-order method  $\Phi^*$ , the second part Eq. (5) calculated explicitly and "backwards" is the adjoint method

$\Phi$ . Consequent composition of these two methods represented by Eq. (4) and (5) is the second-order symmetric method

$$\Psi_h = \Phi_{h/2}^* \circ \Phi_{h/2}. \quad (6)$$

The property of symmetry significantly increases the efficiency of the presented method by using it as a base for extrapolation schemes [6]. Since the method is partially implicit, in the presence of complex non-linearity it is necessary to perform iterations of Newton's method. However, from the point of view of computational optimization, it is more profitable than time-consuming operations like calculation of the full Jacobian and solution of matrix equations in case of implicit methods.

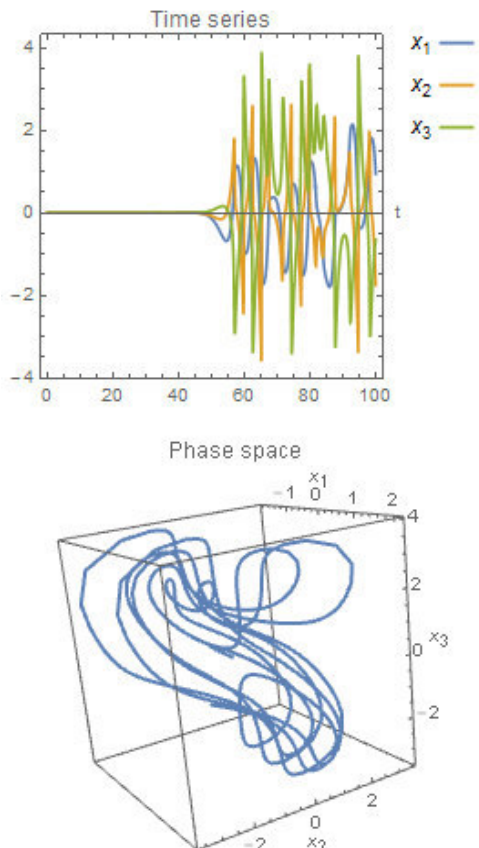


Fig. 2. Graph of the state variables behavior (top) and phase space (bottom) for dynamical system

#### IV. SIMULATION

Rapid prototyping of the extrapolation integrator based on semi-implicit method was carried out in Wolfram Mathematica 10 environment with the use of NDSolve Method Plugin Framework through the built-in template for extrapolation methods. The results of the experiments have allowed to verify the properties of the method and confirm its viability. Fig.2 represents the solution of the initial value problem for Eq. (3) with the following system parameters:  $\alpha = 9/10$ ;  $\beta_3 = 1/2$ ;  $\beta_2 = 3/2$ ;  $\beta_1 = 3$ ;  $\gamma = 1$  and  $\delta = 1/3$ . The simulation parameters are:  $x_1[0] = 10^{-12}$ ;  $x_2[0] = 0$ ;  $x_3[0] = 0$  and  $t = 100$ .

#### V. CONCLUSIONS

This paper demonstrates the high potential of the semi-implicit solvers on the example of the simulation of memristor-based circuit. As further work we note the research and development of new step-size and order controllers, investigation of alternative ways to increase the methods order, for instance, the application of composition methods [9].

#### REFERENCES

- [1] D. B. Strukov, G. S. Snider, D. R. Stewart, and R. S. Williams, "The missing memristor found," *Nature*, vol. 453, pp. 80–83, May 2008.
- [2] L. O. Chua, "Memristor-the missing circuit element," *IEEE Transactions*

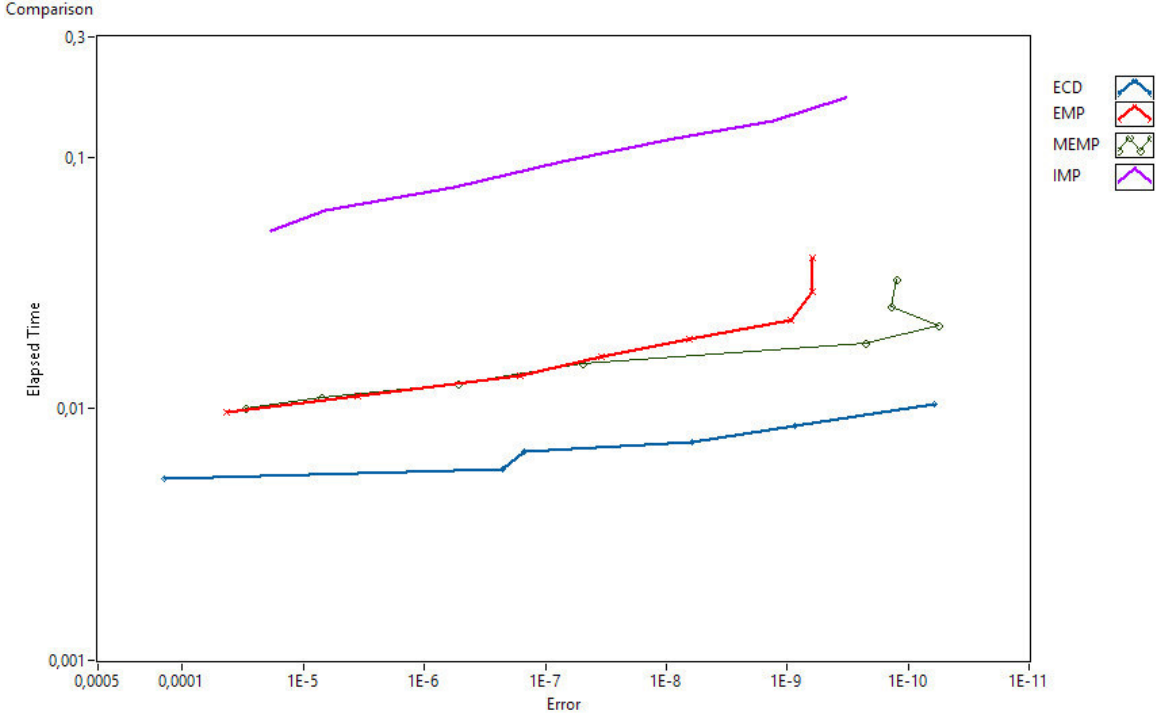


Fig. 3. Performance of investigated methods

Despite the simplicity of the extrapolation method definition in the Mathematica program, fair estimation of the method efficiency compared with built-in kernel methods at this stage is significantly complicated by the use of the framework for user-specified algorithms. Further comparison of the methods was made in the LabVIEW 2015 environment on the desktop-PC (Intel Core i7-6700, 8GB RAM).

Fig.3 displays the benchmark results of the investigated methods for the same parameters of modelling, but applying constant (eighth) order with keeping variable step-size.

As a comparison criterion serves the measurement of CPU time costs (vertical coordinate) with respect to required accuracy (horizontal coordinate). From the graphs in Fig.3 it is obvious to see the superiority of extrapolation scheme based on the proposed semi-implicit algorithm (ECD) over the well-known methods: Explicit Midpoint (EMP), Modified Explicit Midpoint (MEMP) and Implicit Midpoint (IMP).

- on Circuit Theory, vol. CT-18, no. 5, pp. 507–519, September 1971.
- [3] L. O. Chua and S. M. Kang, "Memristive devices and systems," *Proceedings of the IEEE*, vol. 64, no. 2, pp. 209–223, February 1976.
- [4] B. Muthuswamy and L. O. Chua, "Simplest chaotic circuit," *International Journal of Bifurcation and Chaos*, vol. 20, no. 5, pp. 1567–1580, 2010.
- [5] M. H. McCullough, H. H. C. Iu, and B. Muthuswamy, "Chaotic behaviour in a three element memristor based circuit using fourth order polynomial and PWL nonlinearity," in *International symposium on Circuits and Systems (ISCAS)*, Beijing, China, May 2013.
- [6] E. Hairer, S. P. Norsett, and G. Wanner, *Solving ordinary differential equations I: Nonstiff problems*. Berlin: Springer-Verlag, 1996.
- [7] M. Sofroniou and G. Spaletta, "Extrapolation methods in Mathematica," *JNAIAM*, vol. 3, no. 1-2, pp. 105–121, 2008.
- [8] D. N. Butusov, T. I. Karimov, and V. Y. Ostrovskii, "Semi-implicit ODE solver for matrix Riccati equation," in *2016 IEEE NW Russia Young Researchers in Electrical and Electronic Engineering Conference (EICoRusNW)*, Saint Petersburg, Russia, February 2016, pp. 168–172.
- [9] H. Yoshida, "Construction of higher order symplectic integrators," *Physics Letters A*, vol. 150, no. 5-7, pp. 262–268, November 1990.

# Design of Fuzzy System for Control of Water Level in a Boiler Drum

Anisimov D.N., Mai The Anh  
Dept. of Control and Informatics  
Moscow Power Engineering Institute  
Moscow, Russia

**Abstract**—An intelligent system to control the water level in boiler drum is developed in this paper. Drum level control systems are used extensively in heat power engineering. The purpose of the drum level controller is to bring the drum up to level at boiler start-up and maintain the level at constant steam load. In general case three parameters must be controlled for the proper functioning of the boiler: steam flow, water level in the drum and feed water flow. The subsystem of control of water level in the drum using fuzzy-PD controller is presented in this paper.

**Keywords:** *fuzzy control system, relational model, boiler drum, water level control.*

## I. INTRODUCTION

Fuzzy logic controllers (FLC) find a wide application in automatic control systems [1]. However, one of serious problems is FLC tuning ensuring required quality metrics of control. Subject to selected FLC structure and the algorithm of fuzzy inference various factors exert influence on quality of control.

Particularly one can specify following basic factors having an effect on FLC based on relational models functioning:

- i. number of terms of input and output variables;
- ii. form of membership functions describing term-sets of linguistic variables;
- iii. definitional domain of linguistic variables;
- iv. character of fuzzy relation between antecedent and consequent spaces (rule base);
- v. method of defuzzification;
- vi. choice of one or another logical basis (T-norms);
- vii. measures of significance of sub-conditions in fuzzy rules.

Thus the number of degrees of freedom when making of fuzzy control system is sufficiently large. On the one hand this property ensures flexibility of FLC tuning. On the other hand large quantity of factor combinations complicates search of rational decision of controller tuning problem. So, it seems to be important to carry out comprehensive research of dependencies between parameters of FLC and dynamic characteristics of control system.

The analysis of above mentioned factors showed that form

This paper was prepared with the financial support of Russian Foundation for Basic Research (Project № 16-01-0054).

of membership functions, definitional domain of linguistic variables and measures of significance of sub-conditions are the factors those exert monotone influence on control system dynamic properties. So, these three factors are easy-to-use in solving the task of FLC tuning.

## II. PROBLEM STATEMENT

The approach to fuzzy control systems design based on the analysis of dynamic characteristics was considered in [2, 3]. It was demonstrated on the example of the second-order object of control that this approach made it possible to tune the fuzzy controller more efficiently to ensure the required quality metrics. In present research we extend this approach to a more complex object such as the boiler drum. This object contains nonminimum-phase element and can be described by the transfer function [4]:

$$W_0(s) = \frac{0.25 - 0.25s}{0.3s^3 + 2.15s^2 + s}. \quad (1)$$

The fuzzy controller is designed to have two inputs and one output, where the inputs are the error and the error rate and the output is the control signal. The controllers of such a structure are usually called “fuzzy-PD controllers”.

The input ranges from -1 to +1, and each of the linguistic variables is characterized by three terms: “Negative”, “About Zero” and “Positive” respectively designated as N, Z and P.

When building a fuzzy control system we used Mamdani algorithm [5] modified by relational models [6].

The structure of the fuzzy-PD system is shown in Fig 1.

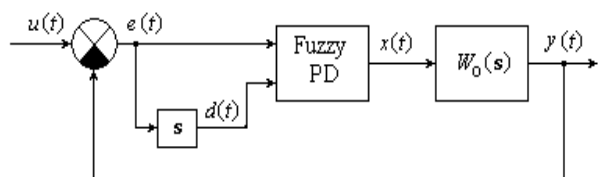


Fig 1. Structure of control system with fuzzy-PD controller

The membership functions used by fuzzy-PD controller are defined in polynomial form:

$$\begin{aligned}
\text{"N"} - \mu_A(h) &= \begin{cases} 1, & h < -H \\ \left(-\frac{h}{H}\right)^{\gamma}, & -H \leq h \leq 0 \\ 0, & h > 0 \end{cases} \\
\text{"Z"} - \mu_A(h) &= \begin{cases} 0, & h < -H \\ \left(\frac{h}{H} + 1\right)^{1/\gamma}, & -H \leq h \leq 0 \\ \left(-\frac{h}{H} + 1\right)^{1/\gamma}, & 0 \leq h \leq H \\ 0, & h > H \end{cases} \\
\text{"P"} - \mu_A(h) &= \begin{cases} 0, & h < 0 \\ \left(\frac{h}{H}\right)^{\gamma}, & 0 \leq h \leq H \\ 1, & h > H \end{cases}
\end{aligned} \quad (2)$$

where  $h$  can possess the values  $e, d$  or  $x$ .

The control rules are designed to achieve the best performance of the fuzzy controller. These are given by the relation matrix  $R$  [6]:

$$R = ZZ \begin{bmatrix} N & Z & P \\ NN & 0.8 & 0.2 & 0 \\ NZ & 0.5 & 0.5 & 0 \\ NP & 0.4 & 0.6 & 0.4 \\ ZN & 0.5 & 0.5 & 0 \\ ZP & 0.3 & 0.7 & 0.3 \\ PN & 0 & 0.5 & 0.5 \\ PZ & 0.4 & 0.6 & 0.4 \\ PP & 0 & 0.2 & 0.8 \end{bmatrix}. \quad (3)$$

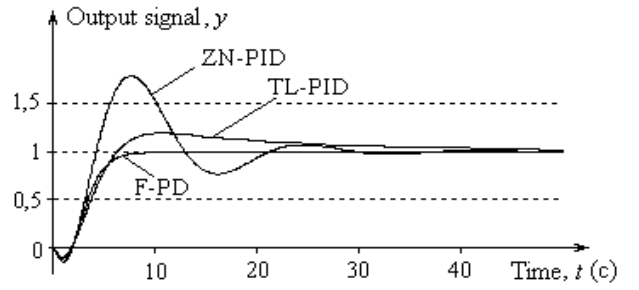
### III.

### MAIN RESULTS

The simulation data of the developed fuzzy systems were compared with the results given in [4] where the control system with linear PID controllers had been considered.

The normalized transient processes in three systems which use the linear PID controllers tuned with Ziegler-Nicols (ZN-PID) and Tyreens-Luyben (TL-PID) methods and with the

fuzzy-PD controller (F-PD) are shown in Fig. 2. Quality metrics of transient processes are presented in Table 1.



FFig 2. Transient processes in three systems

TABLE I. QUALITY METRICS OF TRANSIENT PROCESSES

Controller	Parameter			
	Rise time [c]	Peak time [c]	Peak overshoot [%]	Settling time [c]
ZN-PID	4.22	7.62	77.89	26.67
TL-PID	6.31	10.54	19.24	33.57
F-PD	7.66	—	0	6.88

As follows from Fig. 2 and Table 1, quality metrics of transient processes in the system with the fuzzy-PD controller are quite acceptable. Thus, one can draw a conclusion that the developed approach to the tuning of the fuzzy-PD controller is suitable for the control of complex objects.

### REFERENCES

- [1] Jager R. (1995). Fuzzy logic in control / Ren'e Jager. - [S.l. : s.n.]. - Ill.Thesis Technische Universiteit Delft, 1995. - With index, ref. -With summary in Dutch.
- [2] Anisimov D.N., Drozdova E.D., Novikov V.N. (2014). Construction of Fuzzy Regulator Approximating Model Based on Identification by the Method of Exponential Modulation. Mekhatronika, avtomatizatsiya, upravlenie, № 9, pp. 6-12.
- [3] Anisimov D.N., Mai The Anh (2016). The algorithm for tuning of fuzzy logic controller based on a research of its dynamic properties. Proceedings of XVI International Conference "Informatics: problems, methodology, technologies". Voronezh, Russia, pp. 20-25.
- [4] K. Ghousiya Begum, D. Mercy, H. Kiren Vedi, M. Ramathilagam (2013). An Intelligent Model Based Level Control of Boiler Drum. International Journal of Emerging Technology and Advanced Engineering, Volume 3, Issue 1, January 2013.
- [5] E.H. Mamdani and S. Assilian (1975). An experiment in linguistic synthesis with a fuzzy logic controller. International Journal of Man-Machine Studies, 7(1):1-13.
- [6] Pedrycz W. (1993). Fuzzy Control and Fuzzy Systems. New York: John Wiley and Sons. 1989.

# Increasing the efficiency of the solution of aerodynamic problems using cluster architectures

Sergey A. Burenkov

Applied Mathematics Department  
National Research University "MPEI"  
Moscow, Russia  
burenkovsa@mpei.ru

Olga Yu. Shamayeva

Applied Mathematics Department  
National Research University "MPEI"  
Moscow, Russia  
shamayevaoy@mpei.ru

**Abstract**—Software means of increase of efficiency of the solution of aerodynamic tasks in the form of a complex of functional modules are proposed. The problem of an aerodynamic flow of a profile and its decision by method of the generalized minimum residual (GMRES) is considered. Parallel modification of a method is offered, results of research of characteristics of parallelism at realization of a method in a computing cluster are given.

**Keywords**—computing aerodynamics; GMRES; MPI; cluster architectures

## I. INTRODUCTION

Basic problem of computing aerodynamics is development of modern numerical simulation techniques for the calculation of high-speed flows of continuous medium, the rarefied gas and low-temperature plasma. To solve the task it is expedient in several ways, namely:

- to develop numerical schemes and models of different types of flows;
- to improve the efficiency of methods for solving systems of Euler and Navier-Stokes equations;
- to construct parallel algorithms modifications and to create parallel software applications for effectively problem solution of computational aerodynamics on modern high-performance architectures

It is possible to define aerodynamic characteristics of the stream blowing in any object during natural experiment, which is made in a special wind tunnel. The realization of natural experiment – is a time-consuming, expensive and inaccurate procedure. Nevertheless, by end of the last century aerodynamic tests were carried out only by means of full-scale experiment [1].

Now the solution of the aerodynamic flow problem can be received with use of methods of mathematical modeling. Such approach allows determining all the necessary characteristics with high degree of accuracy without the use of bulky stands and costly trials. However, the modeling of aerodynamic processes belongs to a class of challenges due to the high labor intensity, large amounts of required memory, as well as the presence of specific properties [2]. Therefore, it requires the use of high-performance computing, parallel programming techniques and special solution methods.

In this paper, authors provide a set of software modules that allow:

- to facilitate greatly the development of scalable software packages 3D modeling of aerodynamic processes;
- the most efficient use of available memory;
- to take into account the specifics of aerodynamic problems during solution process;
- to reduce the solution time in proportional to the productivity of the used computer equipment.

Besides the listed advantages software allow to reduce time expenditure by carrying out computing experiments by means of high-performance computer facilities, and also a possibility of the solution of such tasks which didn't manage to be solved because of the requirement of large volumes of memory earlier. It is possible to use the proposed software means to solve problems related to aerodynamics classes, for example, hydrodynamic.

In addition to these benefits it is expected the reduction of the time spent on carrying out computational experiments by means of high-performance computing, as well as the ability to solve such problems, which previously could not be solved due to the requirement of large amounts of memory.

Also, it is possible to use the proposed software means to solve problems related to aerodynamics classes, for example, hydrodynamic.

## II. PROFILE FLOW PROBLEM

The two-dimensional problem of flow profile RAE2822 shown in Fig. 1 is analyzed. Around the profile the computational domain (Fig. 2) is based. Then it is divided by the computational grid (Fig. 3). Required to determine the physical characteristics of the blowing airflow profile, namely speed, pressure, Mach number.

The numerical solution of a task leads to system of the differential Navier-Stokes equations

$$\rho \frac{d\mathbf{W}}{dt} = \mathbf{R} - \text{grad}(p) + \mu \Delta \mathbf{W} + \frac{1}{3} \mu \text{grad}(\text{div}(\mathbf{W})) \quad (1)$$

Because of produced sampling system of differential Navier-Stokes equations (1), the linear system of large dimension is obtained. The coefficient matrix of obtained

system has the properties of sparsity, the lack of property diagonal dominance and symmetry and irregularity portrait.



Fig. 1. Profile RAE2822

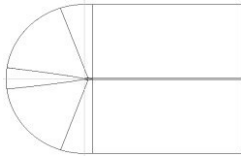


Fig. 2. Computational domain for profile RAE2822

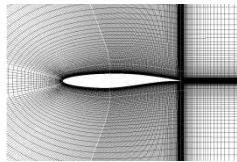


Fig. 3. Computational grid for profile RAE2822

All methods for solving linear systems can be divided into 2 groups: the direct methods (Gauss, Cholesky, etc.) and the iterative methods (Jacobi, Seidel, projection, etc.).

Based on the methods analysis of solutions of linear systems and taken in consideration the mentioned above properties, preference was given to the projection method of General Minimal Residual (GMRES).

### III. PARALLEL IMPLEMENTATION

Concurrent modification GMRES method has been implemented in C++ using the Message Passing Interface (MPI). Computing experiment was made on the cluster consisting of 36 AMD Opteron 6272 processors with a clock frequency of 2.1 GHz; the Gigabit Ethernet network under control of the Linux Kernel operating system 3.12.13.

Storing a sparse matrix produced in the Compressed Sparse Row (CSR) format [3]. This way of sparse matrix presenting is complete (full entire matrix is represented) and orderly, because the elements of each row are stored in accordance with the increase of column indexes.

For matrix processing used bands distribution of data over processors, an example of which is shown in Fig. 4.

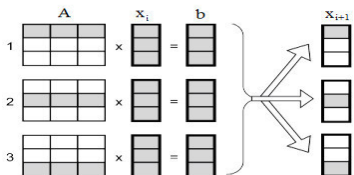


Fig. 4. Distribution of data on processors

The parallel modification of the GMRES method has been developed, implemented and analyzed on high-performance cluster. The graphs are shown accelerating depending on the resources: for systems of different dimensions (Fig. 5), and for systems with different densities of non-zero elements (Fig. 6).

It is possible to note that, than higher the size of system and, than more difficult the structure of a matrix of subjects acceleration of calculations on cluster is higher in comparison with consecutive realization on one processor. The general conclusion is as follows: the higher dimension of a task is, the

bigger effect can be gained from application of parallel technologies for decision.

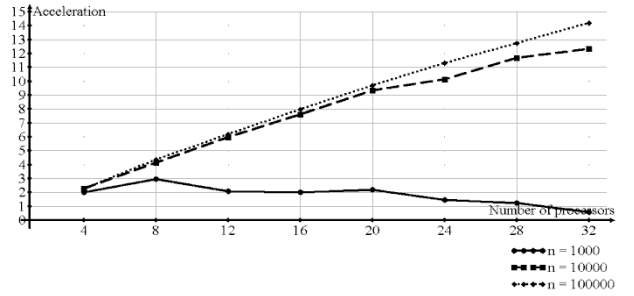


Fig. 5. Dependence of acceleration on resources for different dimensions of system of the equations

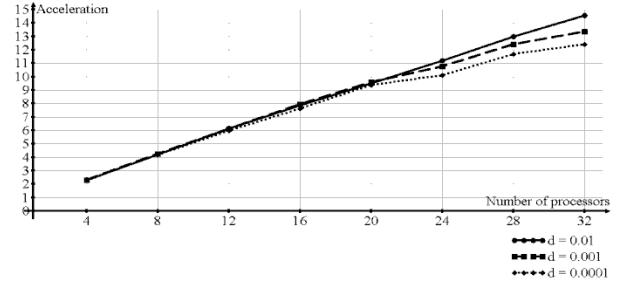


Fig. 6. Dependence of acceleration on resources for different degrees of a sparseness of system of the equations

Results of the solution of a problem of a flow can be presented graphically in the form of distributions of aerodynamic characteristics around the blown profile.

The offered and realized software are focused on developers of large domestic systems of modeling of aerodynamic processes, such as CIAM of P.I. Baranov (Cobra), TESIS (FlowVision), etc.

In the near future the experiments with use of the CUDA technology for graphic processors are planned.

### IV. CONCLUSIONS

Computational aerodynamics problems refer to a class of computational complexity. Therefore, for their solution means of high-performance computing and special numerical methods should be used. The use of a special method, which takes into account the specifics of linear systems, has led to an increase in the rate of convergence; using of parallel technology on high-performance architectures reduced the solution time, and the choice of a special storage format sparse matrix significantly reduced the cost of memory.

### REFERENCES

- [1] K.S. Reent, A.V. Gracheva, V.A. Shorstov, V.E. Makarov "Comparative analysis of counter-rotating propfans noise assessment methods in the case of open rotor with narrow cylindrical shield," CEAA, September 24-27, 2014, Svetlogorsk, Russia
- [2] Spalart P.R. Strategies for turbulence modeling and simulations. Int. J. Heat Fluid Flow, 2000, v. 21, pp. 252-263
- [3] M.Yu. Balandin, E.P. Shurina, "Methods for solving linear systems of large dimension," Novosibirsk, 2000

# Mathematical Methods For Synthesis Of Non-Gaussian Noise Nonlinear Filters

Elena Solovyeva

Theoretical Electrical Engineering Department  
Saint-Petersburg Electrotechnical University "LETI"  
Saint-Petersburg, Russia  
selenab@hotbox.ru

**Abstract**—There are many situations in which linear filters perform poorly, as in the presence of signal-dependent or multiplicative noises or processing of signals having non-Gaussian statistics. In these cases it is evident to apply nonlinear filters. The author focuses on the mathematical models of non-Gaussian nonlinear filters.

**Keywords**—nonlinear system; non-Gaussian noise; nonlinear filter; nonlinear model

## I. INTRODUCTION

Linear filters are widely used in signal processing because of their well-known properties and the inherent simplicity which can in fact guarantee satisfactory performance in a number of applications. There are, however, some situations in which linear filters perform poorly, for example, in the presence of signal-dependent or multiplicative noises and non-Gaussian statistics for the signals. In system modeling applications, for example, it may be necessary to deal with the nonlinearities which characterize real-world systems. In an image processing environment, it is known that linear filters are not able to remove the noise, in particular the impulsive one superimposed on a picture, without blurring the edges. Moreover, it is often necessary to take into account the intrinsic nonlinear behavior of the human visual system or of the optical imaging systems, resulting from the nonlinear relation between the optical intensity and the optical field. For all these reasons, nonlinear filtering has been applied for many years to a number of different applications [1]–[7].

## II. CLASSES OF NONLINEAR SYSTEMS

The most important nonlinear filters families [1] include

- homomorphic filters, relying on a generalized superposition principle;
- morphological filters based on geometrical rather than analytical properties;
- nonlinear mean filters, using nonlinear definitions of means;
- order statistics filters based on ordering properties of the input samples, for instance, median filter;
- polynomial filters, for instance, the truncated Volterra filter;
- neural networks, which attempt to model nonlinear systems using interconnections of simple nonlinear devices called artificial neurons.

## III. EXAMPLES IN APPLICATIONS OF NONLINEAR FILTERS

Several applications of nonlinear filters can be found in the literature, involving discrete signals and systems in one or

more dimensions [1]–[7]. An overview of some of them is demonstrated below.

### A. Nonlinear System Modeling

Modeling of nonlinear systems is one of the first practical applications of the discrete Volterra series. In some cases, depending on the nature of the nonlinearities, high-order kernels and/or odd kernels can be necessary [1]. This happens, for example, in the communication field when modeling highly distorted reference channels, nonlinear transmit amplifiers and nonlinear bandpass channels in digital transmission systems.

In satellite communication systems, the amplifiers located in the satellites usually operate at or near the saturation region in order to conserve energy. The saturation nonlinearities of the amplifiers introduce nonlinear distortions in the signals they process. The satellite channel is typically modeled using three distinct components. The path from the earth to the satellite as well as from the satellite to the earth may be modeled as linear dispersive systems. The amplifier characteristics are modeled usually using memoryless nonlinearities. The equalizers at the receiver must be able to compensate for the nonlinear distortions so that the full capacity of the channel can be utilized [5], [6].

### B. Echo Cancellation

In modern digital subscriber loop modems, echo cancellation techniques ensure full duplex transmission with adequate channel separation. The purpose of the canceller is to remove the near-end cross talk, or "echo" signal, interfering with the signal coming from the distant transmitter. Since the last signal may be highly attenuated (40–50 dB) and the attenuation of the hybrid can be as low as about 10 dB, the required attenuation of the echo signal is of the order of 50–60 dB to achieve an acceptable signal-to-echo interference ratio [1], [2], [5].

In order to guarantee this level of echo attenuation it is very often necessary to take into account nonlinear distortions deriving in practical systems from transmitted pulse asymmetries, saturation effects in transformers and nonlinearities of data converters. A method for expanding an arbitrary nonlinear function of a number of bits in a series is similar to the Volterra expansion. This expansion involves only a finite number of terms including products of couples of bits which correspond to the nonlinear operator [2]–[5].

The echo canceller is implemented as an adaptive filter whose output must compensate for the actual echo by adding to the transversal realization some nonlinear taps [2]–[5].

### C. Noise Cancellation

Nonlinear noise cancellation or compensation of nonlinear distortions is another possible field of application of nonlinear filtering. In digital communication systems, for example, the channel nonlinearities can very often be modeled as memoryless. Since these effects take place in a network where linear filtering operations are used, the overall effect of the channel on the input signal is a nonlinear mapping with memory which is effectively described by a discrete Volterra series. The Volterra series technique has been, in fact, applied for adaptive equalization of channel nonlinearities and nonlinear intersymbol cancellation [2]–[5].

The nonlinear canceller adaptively synthesizes a model of the nonlinear interference impulse response which is used to compensate for the channel nonlinearity [2], [5].

### D. Predistortion

The harmonic distortions introduced by loudspeakers into the audio signals are caused by nonlinearities in the loudspeaker characteristics. The main causes of the nonlinearities are the nonuniform flux of the permanent magnet and the nonlinear response of the suspensions. Several methods have been devised to characterize and compensate for such distortions. One commonly employed model for loudspeakers yields low-order nonlinearity in the form of a truncated Volterra system model. Compensation for the nonlinear distortions is typically achieved by predistorting the audio signals prior to introducing them to the loudspeakers [6].

Predistortion is a kind of the power amplifier linearization technique which modifies the input to a power amplifier such that it is complementary to the distortion characteristics of the power amplifier in communication channels. The cascaded response of complementary predistortion and amplifier distortion should therefore result in a linear response. The technique is generally applied at radio frequency, intermediate frequency or baseband. The digital predistortion is generally performed at baseband. Predistorter parameters are stored in a look-up table or register table which can be updated with adaptive feedback [6].

### E. Image Processing

*Image edge detection* is a basic tool in nonlinear two-dimensional signal processing having many uses in robotic vision, automatic inspection, image coding and so on [7].

The problem of *eliminating noise in an image* without damaging the edges is one of the typical issues which can be faced by nonlinear techniques. In particular, the case of a picture which has been taken in bad illumination conditions and thus has compressed gray level dynamics and is rather noisy has been considered.

Another possible application of nonlinear filters is in image preprocessing for *texture discrimination*. Following the

design procedure, an operator able to discriminate textures having patterns formed by adjacent or separate impulses, according to the given specifications [7].

Differential pulse code modulation and hybrid transform coding are effective methods for reduction of the bit rate in digital transmission of images. Both methods use a predictor and subsequent coding of the prediction error. However, the efficiency of fixed linear predictors is quite limited, as the image signal is far from stationary. To overcome this problem, switched or adaptive linear predictors have been proposed, but their ability to track abrupt spatial and temporal variations remain limited, because of their inherent low-pass characteristics. A *nonlinear predictor*, gathering information from high-order statistical moments and able to possess a sort of high-pass effect, will be more efficient [7].

Skipping frames at the transmitter and interpolating the skipped frames at the receiver is an attractive method of coding image sequences at low bit rates. Since linear interpolation by temporal filtering performs poorly in moving areas, the interpolation algorithm must compensate for the motion of the object in the scene. An alternative approach is based on the use of a *nonlinear interpolation filter*. The arguments to validate are the same used for the prediction case; in fact the problem has been considered as that on finding the frame interpolator as the optimal predictor on a block-by-block basis [7].

## CONCLUSION

The concept of optimum linear filtering has had enormous impact on the recent development of the various techniques to estimate and process stationary time series. The obvious advantage of a linear filter is its simplicity in design and implementation. However, with the minimum mean-square error criterion, the ultimate solution to the optimum filter is in finding the conditional mean which is, in general, a nonlinear function of observed data. In some cases, the performance of a linear filter may be unacceptable. Another important factor in favor of nonlinear filters is the vast capability of modern computers which enables us to overcome the complexity of the nonlinear filtering problem.

## REFERENCES

- [1] V. J. Mathews, G. Sicuranza, Polynomial signal processing. John Wiley and Sons, 2000.
- [2] S. V. Vaseghi, Advanced digital signal processing and noise reduction. /Fourth Editing, John Wiley & Sons, 2008.
- [3] A. Uncini, Fundamentals of Adaptive Signal Processing. Springer International Publishing Switzerland, 2015.
- [4] A. H. Sayed, Adaptive filters. John Wiley & Sons, Inc., 2008.
- [5] S. Haykin Digital communication systems. John Wiley & Sons Inc., 2013.
- [6] Digital Front-End in Wireless Communications and Broadcasting: circuits and Signal Processing / Editor Luo F.-L. Cambridge University Press, 2011.
- [7] R. C. Gonzalez, R. E. Woods, Digital image processing. New Jersey, Prentice Hall, 2001.

# Meters Data Ellipsoidal Approximations for the Power Consumption Control

V. Shikhin

Dept. of Control and Informatics  
Moscow Power Engineering Institute  
Moscow, Russia  
ShikhinVA@mpei.ru

**Abstract**— Introduced in the paper new restrictions and functional transformations lead to the original mathematical formulation of the maximum volume ellipsoid approximation problem. Proposed logarithmic functional transformation allows to convert the approximation via maximum volume ellipsoid problem to the convex nonlinear mathematical programming. The efficiency of the computational procedures is tested with the example of the distribution substation measurements data fusion.

**Keywords**— data fusion; data analysis; convex nonlinear programming; ellipsoidal approximation; smart grid

## I. INTRODUCTION

Proven technology, focused innovation and unmatched expertise in order to optimize end-to-end electrical grid efficiency, reliability and flexibility closely related with the efficiency of the tools applied for measurement data mining and treatment. Our days we have got strong intensions and will to reach the new stage of the electrical grids development called Smart Grid [1]. Smart Grid is the integration of information technologies with the electrical infrastructure that delivers energy efficiency and productivity. In many cases either transmission or distribution networks and substations the ask from utility personnel, dispatchers and network operators for clear and ready for use forms of measurement data information representation is great. In many cases the operational subsystem is associated with real-time and near-real time activities, otherwise known as operational activities. Supervisory Control and Data Acquisition (SCADA) systems are a collection of real-time applications that monitor key grid data at the substation level and not only. Collected data are utilized not only for online control but also can be used for the working capacity indices estimation and analysis. This is supposed to be one of the responsible stages of the substations automated systems design and tuning.

The method for the areas of required criteria level in the form of the maximum volume ellipsoid is represented in this paper and called the Balancing Ellipsoid Method. Method follows the well-known mathematical approach to approximate the areas by the second order geometrical figures [2-5].

## II. FORMULATION

**Definition.** Let the Region of Required Level (RRL) is considered to be the area  $S$  in  $\Omega_x$ , where the appropriate target criterion  $J(X)$  satisfies the given restrictions:

$$S := \{x \in \Omega_x \mid J(X) \leq c\}, \quad (1)$$

while outside the region  $S$ :

$$J(X) > c, \quad (2)$$

where  $c$  is any pre-assigned positive constant,  $X = [x_1, x_2, \dots, x_p]^T$  is the vector of system measured parameters with components

A. Shikhina

Dept. of Research and Development  
RT-Soft LLC  
Moscow, Russia  
Shikhina\_AV@rtsoft.msk.ru

from the space  $\Omega_x := \{x \in R^m\}$  on the variety of real numbers  $R^m$ . Consider criterion  $J(X)$  to be numerically valued.

Accepted restrictions:

*Restriction a).* Consider criterion  $J(X)$  to be numerically valued and continuous, which is supposed to be bounded and positively-defined. This restriction is very strong but acceptable for the most applications in power engineering and electrical grids.

*Restriction b).* RRL-region  $S$  supposed to be convex and constrained. If the premise that RRQ-region has a convex configuration then accept it in the form of ellipsoid.

*Restriction c).* Let the absence for the sub-regions with undefined or nonmeasurable parameters.

The paper follows the mathematical approaches related with ellipsoidal approximations [2-5]. In our case it leads to further operations with static models of the measurement data in the algebraic form which in obvious and compact form represent technological processes.

Let with respect to (1) и (2) exists nonempty set  $S^*$  consisted of linear-independent experimental points of number  $N^* + N^o = N$ :

$$S^* = \{\vec{x}_i^* \in R^m \mid J(\vec{x}_i^*) \leq c\}, i = \overline{1, N^*}, \quad (3)$$

and also exists nonempty set:

$$S^o = \{\vec{x}_i^o \in R^m \mid J(\vec{x}_i^o) > c\}, i = \overline{1, N^o}. \quad (4)$$

Thus, RRL creation problem in the form of the maximum volume ellipsoid can be formulated as construction of ellipsoid  $E^*$  which includes the most elements from the set  $S^*$  and strictly no one from the set  $S^o$ .

The last requirement induces the new mathematical formulation for the minimum volume ellipsoid search [6].

## III. MAIN RESULT

Suppose that some with center in  $\vec{x}_o^* = \sum_{i=1}^{N^*} \vec{x}_i^* / N^*$  appropriates to symmetric positively-defined matrix  $W$ ,  $[m \times m]$  with elements  $w_{i,j}, i, j = \overline{1, m}$ :

$$E = \{\vec{x} : (\vec{x} - \vec{x}_o)^T W (\vec{x} - \vec{x}_o) \leq 1\} \quad (5)$$

For clarity put ellipsoid  $E$  center into origin  $\vec{x}_o = \vec{O}$ . Well-known formula for ellipsoid volume:

$$V_E = \frac{V_s}{\sqrt{\det W}} \quad (6)$$

where the volume of the  $m$ -dimensional hyper-sphere  $V_s$  of radius  $R$  is calculated through gamma-function  $\Gamma(m/2+1)$ :

$$V_s = \pi^{m/2} \Gamma^{-1} \left( \frac{m}{2} + 1 \right) R^m \quad (7)$$

From (6),(7) is clear, that the volume of the ellipsoid  $V_E$  varies while varies the determinant of  $W$ , and hence the formulation will be:

$$V_E \xrightarrow{\hat{w}_{ij}} \max \Rightarrow \det W \xrightarrow{\substack{w_{ij}=w_{ji}, \\ \hat{x}^T W \hat{x} \leq 1, \\ g_j(W) > 0, \\ x \notin S^0}} \min i, j = \overline{1, m}, \quad (8)$$

were  $g_j(W)$  denotes the main co-factors of the matrix  $W$  calculation operation. Indicated in (8) restriction related with the requirement for matrix  $W$  to be positively defined. The restriction on matrix symmetry ( $w_{ij}=w_{ji}$ ) adopts the requirement for  $\lambda_i$  to be s real which appropriate to the half-axe  $\rho_i$  of the ellipsoid  $E$ .

The problem (8) can be converted to the problem of mathematical programming. It can be done through transformation the restrictions on matrix symmetry and positive definition to the form of functional limitations. The restriction related with the requirement for matrix  $W$  to be positively defined can utilize the orthogonal transformation about matrix  $W$  to the diagonal form:

$$\|W\| = \|FWF^T\| = \|\text{diag}(\lambda_1, \lambda_2, \dots, \lambda_m)\| = \sqrt{\lambda_1^2 + \lambda_2^2 + \dots + \lambda_m^2}, \quad (9)$$

where  $F$ - the orthogonal transformation matrix,  $F^TF=FF^T=I_m$ ;  $\lambda_i, i = \overline{1, m}$  are matrix  $W$  eigenvalues;  $\|W\|$  represents matrix norm:

$$\|W\| = \sqrt{\sum_{i=1}^m \sum_{j=1}^m w_{ij}^2} = \sqrt{\text{tr} W^T W} \quad . \quad (10)$$

The transfer from (9) to (10) leads to make visible the desired ellipsoid via half-axe direct relationship with eigenvalues  $\rho_i = \frac{1}{\lambda_i}, i = \overline{1, m}$ . Since it is known that for positive definite matrix  $W$  all eigenvalues  $\lambda_i, i = \overline{1, m}$  should be positive to form the spectrum of the matrix, hence always it can be can be chosen to be sufficiently large number  $\Lambda$ , such that  $\Lambda \geq \lambda_i, i = \overline{1, m}$ . Thus:

$$\|W\| \leq \Lambda \sqrt{m}. \quad (11)$$

Note that for the desired ellipsoid  $E$  the value for  $\Lambda$  defines the length of minimal half-axe as  $\rho_{\min} = \frac{1}{\sqrt{\Lambda}}$ . In the case if can be chosen a sufficiently small number  $\lambda$ :

$$0 < \lambda \leq \lambda_i, i = \overline{1, m}, \quad (12)$$

then the value for  $\rho_{\max} = \frac{1}{\sqrt{\lambda}}$  will define the length of ellipsoid maximum half-axe. Formula (12) corresponds to the limited range of the matrix  $W$  spectrum:

$$0 < \lambda \leq \lambda_{\min}, \dots, \lambda_i, \dots, \lambda_{\max} \leq \Lambda < \infty. \quad (13)$$

Thus, problem (8) is converted to nonlinear programming problem formulation:

$$V_E \xrightarrow{\hat{w}_{ij}} \max \Rightarrow \text{tr} W \xrightarrow{\substack{w_{ij}=w_{ji}, \\ \|W\| \leq \Lambda \sqrt{m}, \\ x \notin S^0}} \min i, j = \overline{1, m} \quad (14)$$

Also, problem (8) can be transferred to the convex nonlinear mathematical programming that makes much easier to find the extremum. We propose to use the following functional transformation:

$$f(W) = 2 \ln \frac{V_E}{V_S} = -\ln(\det W) \quad (15)$$

where function  $f(W)$  is supposed to be obviously convex on the set of positive definite matrix  $W$ . In this case the task of building the border as an ellipsoid of maximum volume (14) converts to the next formulation:

$$V_E \xrightarrow{\hat{w}_{ij}} \max \Rightarrow f(W) = -\ln(\det W) \xrightarrow{\substack{w_{ij}=w_{ji}, \\ g_j(W) > 0, \\ x \notin S^0}} \max i, j = \overline{1, m}, \quad , \quad (16)$$

or after adoption in (16) the result (11):

$$V_E \xrightarrow{\hat{w}_{ij}} \max \Rightarrow f(W) = -\ln(\det W) \xrightarrow{\substack{w_{ij}=w_{ji}, \\ \|W\| \leq \Lambda \sqrt{m}, \\ x \notin S^0}} \max i, j = \overline{1, m} \quad . \quad (17)$$

Formulation (17) contains the restriction on the length of minimal half-axe and does not contain the restriction of the maximum half-axe. In this regard, it is proposed to change the expression to limitations in the formulation (17) with considering the value of the regularization parameter  $\delta$  by Tikhonov:

$$\|W\| \leq \Lambda \sqrt{m} + \delta \quad \text{where} \quad \delta < \lambda \leq \lambda_i, i = \overline{1, m} \quad . \quad (18)$$

The proposed introduction to the algorithm regularization parameter by Tikhonov corresponds to the classical understanding of the regularization parameter, namely, guarantees the convergence and the degeneracy of the computational procedure of the method. Thus, the final formulation of the problem to construct maximum volume will be in the following form:

$$V_E \xrightarrow{\hat{w}_{ij}} \max \Rightarrow f(W) = -\ln(\det W) \xrightarrow{\substack{w_{ij}=w_{ji}, \\ \|W\| \leq \Lambda \sqrt{m} + \delta, \\ x \notin S^0}} \max i, j = \overline{1, m} \quad (19)$$

The appropriate method is called The Method of Balancing Ellipsoid because of continuous manipulations with the ellipsoid axes.

#### IV. NUMERICAL EXAMPLE

The results of the computational procedures testing will be attached to the paper.

#### V. CONCLUSION

Some new restrictions and functional transformations introduced in the paper lead to the original mathematical formulation of the maximum volume ellipsoid approximation problem.

Proposed logarithmic functional transformation allows to convert the approximation via maximum volume ellipsoid problem to the convex nonlinear mathematical programming.

Different start scenarios are studied: procedure starts from excess ellipsoid or from hyper-sphere of minimal radius.

The efficiency of the computational procedures is tested with the example of the synchronous generator multi-channel excitation system tuning.

#### REFERENCES

- [1] Rozanov, Y. K., Burman, A. P., Shakaryan Yu. G. Managing flows of electricity and improving the efficiency of electric power systems, Moscow, MPEL, 2012, 336 p. (in Russian). – заменить на Дьякова.
- [2] Cassagrande D., Sassano M., Astolfi A. Hammilnon-Based clustering. Algorithms for static and dynamic clustering in data mining and image processing. IEEE Control Systems Magazine, 2012, No.8, pp.74-91.
- [3] Dabbene F., Gayb P., Polyak B. Recursive algorithms for inner ellipsoidal approximation of convex polytopes. Automatica, 2003, Vol.39, pp.1773-1781
- [4] Goli M., Najafi A. N. Ellipsoidal approximation of the topographical effects in the Earth's gravity field modeling. Journal of the Earth and Space physics, 2014, Vol.40, pp. 113-124
- [5] Zhou B., Duan G.R. On analytical approximation of the maximal invariant ellipsoids for linear systems with bounded controls. IEEE TAC, 2009, Vol. 54, No. 2, pp.346-353.
- [6] Tarasov S.P., Khachian L.G., Ehrlich I.I. Method of inscribed ellipsoids, Reports of the USSR Academy of Sciences, Moscow, 1988, Vol. 298, No.5, pp. 1081-1085 (in Russian).

# DDoS Attacks Detection in Cloud Computing Using Data Mining Techniques

K. Borisenko<sup>#1</sup>, A. Rukavitsyn<sup>#2</sup>, A. Shorov<sup>#3</sup>

<sup>#</sup>Faculty of Computer Science and Technology, Saint Petersburg Electrotechnical University "LETI",

Professor Popov str. 5, St.Petersburg, 197376, RUSSIA

<sup>1</sup>borisenko@leti@mail.ru, <sup>2</sup>rkvtsn@gmail.com, <sup>3</sup>ashxz@mail.ru

**Abstract**— Cloud computing platforms are developing fast nowadays. Due to their increasing complexity, hackers have more and more opportunities to attack them successfully. In this paper, we present an approach for detection internal and external DDoS attacks in cloud computing using data mining techniques. The main features of the cloud security component that implements suggested approach is an ability to detect both types of DDoS attacks and usage of data mining techniques. The component prototype is implemented in OpenStack cloud computing platform. The paper presents the results of the experiments with different types of DDoS attacks.

**Keywords**— *Cloud Security; Cloud Computing; Cloud Security Architecture; Data Mining; DDoS attack*

## I. INTRODUCTION

Cloud computing systems are developing fast nowadays. There were no such systems 30 years ago; however, according to the report [1] in 2013 47 billion dollars were spent on cloud services all over the world. Moreover, the sum is expected to be doubled by 2017 as companies invest in cloud services for creating new competitive offerings. When starting usage of the cloud technologies in business processes, one should be aware that availability of cloud services depends on the work of cloud platform (infrastructure). It is extremely important for every company to have a cloud platform working up to 24/7. But sometimes that does not happen because hackers are trying to get unauthorized access or just trying to damage the services for different benefits.

The international scientific group in the cloud computing security area published threats report in 2013 [2]. According to it the cloud infrastructure attacks were placed to the 5<sup>th</sup> position in the list of the actual threats to clouds. Moreover, such infrastructure attacks as “distributed denial of service” (DDoS attacks) represent a huge threat for every element of the cloud computing service standard. Distributed Denial of Service attacks are especially harmful to the companies providing services for the customers. It is essential for the companies providing cloud services to be protected against DDoS attacks, because successful attacks can lead to a big loss of money [3].

In this paper, the authors present a novel approach for protection cloud computing against DDoS attacks. We suggest to distinguish external and internal DDoS attacks depending on the location of the attack source relative cloud infrastructure. Such attack classification allows selecting correct counteraction measures. For example, blocking all network traffic from internal virtual node of cloud system can affect the efficiency of all business processes the suspicious node

participates in. In this case, when the detection module detects that the attack originates from the cloud, the counteraction module will try to block network traffic coming from the specific ports of the suspicious node only. We also propose an architecture of security component that is able to detect both kinds of the attack. The architecture does not assume installation of any sensors on client-side and thus all processes in the cloud are kept confidential. At the same time it analyzes not only incoming external traffic like it is done in some commercial tools [4]

Our contribution is also in developing detection techniques based on data mining and machine learning techniques, including self-learning models. We use supervised models in order to classify network traffic. Experiments showed that the developed algorithms are working fast and malicious traffic is caught within 5 second after the attack starts. We collect attributes for models using Netflow protocol. In addition, usage of self-learning algorithms make it easier to maintain cloud security, because models are learning on new types and scenarios of DDoS attacks.

All modules of the security component are flexible and can be deployed on nodes where cloud platform is installed, or on separate ones. The component prototype was implemented in OpenStack cloud computing platform.

## II. CLOUD SECURITY COMPONENT ARCHITECTURE

This section describes component architecture of proposed security system. The key modules of the security component are *gate sensor*, *security controller* that consists of *collector*, *analyzer* and *counteraction module*. They are shown on the Fig. 1. All traffic coming from outside the Cloud Network and inside it goes through the gate. This means that every instance communicates with another inside the cloud network using gate.

The *gate* has sensor that monitors traffic flows passing through the gate and sends data about them to security controller. The *security controller* is a module that processes incoming flow data by defining type of network traffic – benign or malicious - and blocks potentially malicious traffic by sending commands to firewall. The *collector* stores the received data. The *analyzer* prepares input data for the prediction module. The *prediction module* uses data mining classification models. The output of the module is the type of traffic flow. This result goes to the *counteraction module* that in its turn sends commands to firewall according to the received information.

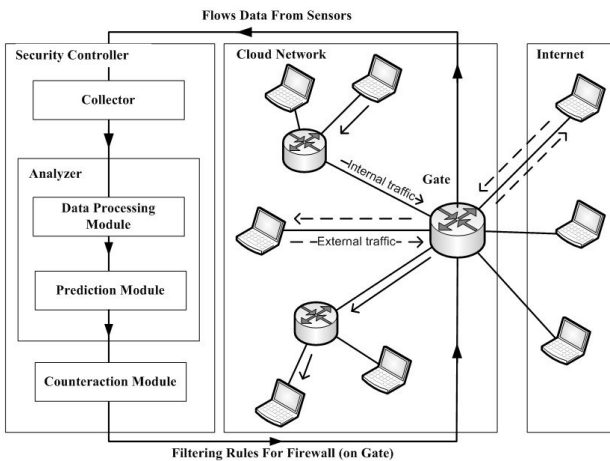


Fig. 11. Security component architecture for cloud networks

The proposed architecture allows creating an analyzer component without analyzing payload of the packets in order to meet requirements of the company's security policy.

The gate sensor and the controller have to operate fast to produce monitoring in real time. The response time of the controller on monitored traffic should be less than 10 seconds to mitigate attacks timely.

The analyzer of the security controller is the part of data mining process. Firstly, the analyzer prepares data vectors from collector's data. Currently, the period of capturing traffic parameters is set to five seconds. Experiments showed that such time slot is enough to obtain high prediction accuracy and produce responses on the malicious traffic flows quickly. The input vector is generated from collector's data every five seconds and is sent to the prediction module. The model produces a prediction on type of monitored traffic and if at some moment it detects incoming traffic as malicious the analyzer sends information about the attack type to the counteraction module. The counteraction module decides how to mitigate this attack and sends command to the gate's firewall. This is how traffic is filtered.

The proposed architecture of the security component was tested using the OpenStack cloud computing system.

### III. THE EXPERIMENT RESULTS

For making experiments, we developed two frameworks. One for evaluating external attacks [5], other — for internal attacks. Both frameworks makes it able to easily setup scenario settings for attacking nodes.

We use different classification models to make decisions on the incoming network traffic. We use supervised learning in order to learn and test data mining models. Currently in the analysis process, we do not determine the location of the attack source. In the future, we will focus on the second detection layer determine the attack source.

This paper consider results of testing data mining models on internal attacks. We implemented series of experiments using different attack scenarios to test classification models against internal attacks. We have made experiments with different attack types: HTTP Flooding, SYN Flooding, UDP Flooding and with benign traffic scenario. To analyze effectiveness of each classification algorithm we calculated false positive and false negative rates (FP and FN), recall, precision and F-measure. HTTP Flooding and benign traffic scenario results are provided in table 1.

TABLE I. RESULTS OF EXPERIMENTS WITH INTERNAL HTTP ATTACK

	Metrics				
	FP rate	FN rate	Recall	Precision	F-measure
kNN	0.33	0.25	98.5	99.9	99.1
Decision Tree	0.05	0.246	99.8	99.8	99.8
SVM	4.1	2.7	96.2	97.9	97.0
Naïve Bayes	15.74	75.1	0.7	25	1.4

Decision Tree model was the best classification model again. False positive rate is 0.05% of all. So 99.95% of legitimate traffic is not rejected. 99.75% of malicious traffic is rejected. Practically that means that only 250 Mb/sec goes through attack detection system when 100 Gb/sec attack power will be on the cloud network. Naïve Bayes showed the worst results with very high false negative rate.

The results of the tested models show high accuracy and small false positive and false negative rate with high F-measure. The future research will be devoted to the enhancement of the prediction module and development of the self-training models. This can help to react correctly on changes in traffic power or in the amount of public services. Next papers will be focused on the DDoS attacks mitigation based on information gained by the improved prediction module, described in this paper. In addition, we plan to improve legitimate traffic model and implement experiments involving many instances facing DDoS attacks.

### REFERENCES

- [1] Salesforce.com,: What is Cloud Computing? - Salesforce UK, <http://www.salesforce.com/uk/cloudcomputing/#where>.
- [2] Cloudsecurityalliance.org,: Top Threats : Cloud Security Alliance, <https://cloudsecurityalliance.org/research/top-threats>.
- [3] Editor, L.: Cyberattacks and Distributed Denial of Service (DDoS) threats on financial firms produce big pay offs - Beyond Bandwidth, <http://blog.level3.com/finance/cyberattacks-and-distributed-denial-of-service-ddos-threats-on-financial-firms-produce-big-pay-offs/>.
- [4] Kaspersky DDoS Protection,: Kaspersky Lab, <http://media.kaspersky.com/kaspersky-ddos-protection-data-sheet.pdf>.
- [5] Bekeneva, Y., Borisenko, K., Shorov, A., Kotenko, I.: Investigation of DDoS Attacks by Hybrid Simulation. Information and Communication Technology Lecture Notes in Computer Science. 179–189 (2015).

# Eddy current sensing for conductive deposit evaluation on the outer surface of the tubes steam generator

Valery Lunin, Vladislava Vystavkina

National Research University Moscow Power Engineering Institute

Department of Electrical Engineering and Introscopy,  
Moscow, Russia

Valery.Lunin@mtu-net.ru

Anton Stoliarov, Natalia Kodak

National Research University Moscow Power Engineering Institute

Department of Electrical Engineering and Introscopy,  
Moscow, Russia

neron-neronov@mail.ru

**Abstract**— This article presents the results of a research of conductive deposits formed on the outer surface of heat exchanger tubes (HET). Research conducted at the Department of Electrical Engineering and Introscopy in Moscow Power Engineering Institute. Main purpose of the work is building a calibration curve to determine the volume of electrically conductive deposits.

**Keywords**— *heat exchanger tubes; steam generator; conductive deposit*

## I. INTRODUCTION

Steam generator heat exchanger tubes (HET) are the subject of high risk in a nuclear power plant. Personnel safety and performance of nuclear power plant depends from condition of heat exchanger tubes. Through-passage eddy-current sensor use internally to test condition of the HET. From four to six absolute and differential channels are obtained depending of the testing system.

Conductive deposits formed on the outer surface of HET adduct a serious threat because there is a breach of heat exchange, it is difficult to determine defect under deposit on HET signal.

## II. RESEARCH PROCEDURE

To identify indication of conductive deposits HET signal was processed in data analysis program PIRATE, developed at MPEI. Processing includes some steps: preprocessing, calibration, setting limits. Preprocessing is used to eliminate the dc component in the signal. Calibration is used to do phase of through defect on calibration tube -40 degrees and amplitude of through defect 1 Volt. Setting limits used to detect conductive deposits.

The channel to detect conductive deposits is absolute channel with lowest frequency (it is 60 kHz for system AIDA). For indication of conductive deposits is typically used increasing of imaginary component of signal. Therefore, the conductive deposits are determined by the imaginary signal component, without using the real signal component. If the

amplitude of indication set above the threshold this indication value is recorded as the deposit.

## III. MAIN RESULT

The conductive deposit signals are similar to the signals caused by the structural elements (structural grids). Grid indications have length 50mm and arrange in certain locations. Therefore, it is needed to know the map of steam generator to determine conductive deposits having a length close to length of structural grids.

Experiments were conducted to identify the chemical composition of conductive deposits for constructing the calibration curve to determine the deposit volume. Chemical compounds have been used, which could give a signal similar to the signal caused by conductive deposits.

Copper powder does not have sufficient conductivity to create amplitude similar to the amplitude of the deposit. The reason is the high resistance between the powder particles.

Iron oxide powder (magnetic) does not have sufficient conductivity to create signal amplitude similar to the signal amplitude of the deposit. The inclination angle of hodograph is opposite for the angle from deposit.

Signals caused by salt solutions with different concentrations (up to saturation) do not have amplitude bursts on profile of conductive deposit signals.

Indications caused by metallic samples lead to hodograph angle deviation toward a hodograph angle deviation from conductive deposit. Signals caused by metal samples have the amplitude larger than the signals caused by salt solutions. The signal form is very close to the form of signal caused by conductive deposits. The best similarity has been achieved when steel foil has been used.

In this moment, as a material for constructing calibration characteristics was used stainless steel and copper. Minimum thickness of conductive layer for the calibration curve was 0.2mm, maximum thickness is 1.2mm. The signal amplitude caused by deposit varies linearly to thickness.

To construct the calibration characteristics from known values of the of artificial conductive deposits volume, were calculated the energy parameter:

$$e = \sum_{i=1}^n (X_i^2 + Y_i^2) \quad (1)$$

where e - energy parameter, x - amplitude of real signal component, y - the imaginary signal components, i - counter number.

The thickness of deposit layer is determined from the fact that the deposits formed on the upper surface of the heat exchange tube, where deposits retained on the surface under gravity (half of the cross sectional area is used in the calculations).

#### IV. MATHEMATICAL MODELING

To determine the processes that take place when the through-passage eddy-current sensor passes the conductive deposits, it was decided to carry out numerical simulation of control procedures in the software product. The reason for choosing software product was the ability to send the results obtained in the software in MATLAB software for further analysis and creation of software code, applicable to a variety of models that simulate conductive deposits. The ability to perform calculations defined in the MATLAB has influenced at the speed of the monitoring process.

Three-dimensional model was used to carry out calculations. The reason: in a two-dimensional model is not possible to set parameters of conductive deposits upper surface of the heat exchange tube. The study of the electromagnetic field has been selected.

The model was made using three-dimensional elements. The basis was taken fragment of a HET 250 mm long, 1.5 mm wall thickness, outer radius 8mm. The magnetic permeability of the material of the tube was taken equal to 1.2, conductivity 1.34 million Cm/m. The material of the tube is a stainless steel. Control procedure is modeled as follows: sensors have moved with relation to the heat exchange tubes.

The following procedure has been set for the automation and optimization of the modeling process:

1. Creating a three-dimensional model of the HET without conductive deposits. This step is used for preprocessing.
2. Creating a three-dimensional model of the HET with conductive deposits.
3. Creating a three-dimensional model of the HET with through defect. This step is used for calibration.
4. The preprocessing procedure was held.

5. The calibration procedure was held.

6. Analysis of the results.

Boundary conditions and parameters (conductivity, magnetic permeability, current densities) of the system elements was defined for steps 1, 2, 3.

Further energy parameter was calculated. The results were similar to the experimental:

1. The channel to detect conductive deposits is absolute channel with lowest frequency.
2. Signals caused by salt solutions and oxide do not have amplitude bursts on profile of conductive deposit signals.
3. Signals caused by high conductivity have amplitude bursts on profile of conductive deposit signals.
4. If we know the length of the conductive deposit we can determine cross-sectional area of the deposit.

#### V. CONCLUSION

As a result of this work the problem of finding and determination of parameters of conductive deposits on the outer surface of the heat exchanger tubes nuclear steam generator was studied. Calibration tube, numerical model of eddy current HET control were designed. Comparing the data of mathematical modeling and prototyping experiments was done.

In the future study have been planned the experiments and data analysis to calculate the calibration dependence for determining the volume of conductive deposits in automatic signal processing mode.

#### REFERENCES

- [1] Min-Kyoung Kim, Chang-Jae Yim, Eui-Lae Kim, Chang-Joon Lee and Joong-Ahm Park "Eddy current signal analysis from non-homogeneous sludge pile", 12th A-PCNDT 2006 – Asia-Pacific Conference on NDT, Auckland, 5th – 10th Nov 2006.
- [2] Tarja Jäppinen, Kari Lahdenperä и Sanna Ala-Kleme "Locating Magnetite on the steam generator tubes with eddy current", 18th World Conference on Nondestructive Testing, 16-20 April 2012, Durban, South Africa.
- [3] Joseph R. Wyatt, John Griffith, Victor Newman, Jeffrey M. Fleck "Steam generator mapping with reflections of eddy current signal", US patent no.: US7405558 B2, 2008.
- [4] Min-Kyoung Kim, Chang-Jae Yim, Eui-Lae Kim, Chang-Joon Lee and Joong-Ahm Park "Development of scale measurement technologies for steam generator tubing", Singapore International NDT Conference & Exhibition , 3-4 November 2011.
- [5] M. Piriou, S.W. Glass "Steam generator secondary side deposit – NDE method for supporting plate clogging", Yokohama, 2009.

# Investigation of Shielding Factor for Information Protection Problem

A. Naumova, I. Bogomolov, V. Lunin

Dept. of Electrical Engineering and Introspection

National Research University “Moscow Power Engineering Institute”  
Moscow, Russia  
annete.naumova@yandex.ru

H. Brauer

Dept. Advanced Electromagnetics  
Technische Universität Ilmenau  
Ilmenau, Germany  
hartmut.brauer@tu-ilmenau.de

**Abstract** — a new factor of information security threats is the possibility of intentional magnetic influence on the critical objects by magnetic effects. Protection from magnetic fields can be done using magnetic shielding. In this paper, passive magnetic shielding effect was investigated, applying multi-layered shields of different materials and with different geometrical parameters. This investigation was conducted analytically as well as numerically using finite element simulations. Thus, the magnetic fields inside and outside of the samples were calculated and were compared with measurements.

**Keywords**— *information protection, multi-layered magnetic shielding, shielding factor.*

## I. INTRODUCTION

Potential vulnerability of information systems in relation to casual and premeditated negative influences requires adoption of adequate protective measures. The implementation of the threat of intentional magnetic influence is the destruction, distortion and blocking of information resulting from magnetic attacks on key elements of the vital objects. The use of quality screens allows to solve tasks such as the protection of information in premises and technical channels, protection against intentional magnetic influence on the airwaves.

Magnetic shielding is a process of reducing the magnetic flux between two locations. This can be done either by separating this locations with magnetic shield materials (passive shielding) or generating field of the same value but at opposite polarization (active shielding).

In the paper will be considered passive magnetic shielding. Passive magnetic shielding is based on putting an enclosure made out of metal around the region of interest. The shielding effectiveness depends on the shell material. The permeability of the material affects the part of the magnetic flux going through the metal. With high-permeable metal, it is possible to push major parts of magnetic flux into this metallic shields and therefore reducing the field in the region of interest.

## II. CALCULATIONS

To describe the magnetic shielding capability of the material, its shielding factor (SF) can be defined as:

$$SF = \frac{H_0}{H} \quad \text{or} \quad SF = \frac{B_0}{B} \quad (1)$$

where  $H_0$  and  $B_0$  – magnetic field strength and flux density without the shielding,  $H$  and  $B$  - magnetic field strength and flux density inside the shielding.

The magnetic field produced by a Helmholtz coil (Fig. 1) can be calculated by the formula [1, 2]:

$$B_0 = \frac{\mu_0 \cdot i \cdot N}{2 \cdot l \cdot (r_2 - r_1)} \left[ x_2 \cdot \ln \left( \frac{\sqrt{r_2^2 + x_2^2} + r_2}{\sqrt{r_1^2 + x_2^2} + r_1} \right) - x_1 \cdot \ln \left( \frac{\sqrt{r_2^2 + x_1^2} + r_2}{\sqrt{r_1^2 + x_1^2} + r_1} \right) \right] \quad (2)$$

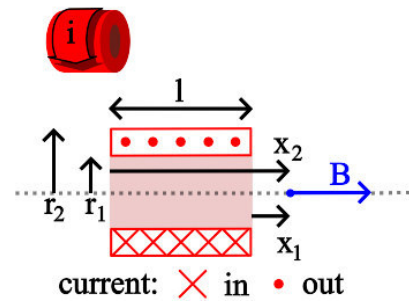


Fig. 1 Helmholtz coil with  $N$  turns,  $l$  – the width of coil,  $r_1$  – the inner coil radius,  $r_2$  – the outer coil radius,  $x_1$  – the distance from the inner side of Helmholtz coils to the center between them,  $x_2$  – the distance from the outer side of Helmholtz coils to the center between them

## III. SHIELDING CONCLUSION

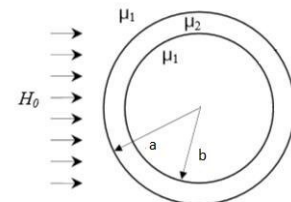


Fig. 2 Shield cross-section in a homogeneous field

In this paper shielding properties of different cylindrical samples were considered. As shields hollow cylindrical tubes have been used, with different diameters and shell thicknesses. The length of the samples was 150 mm and 300 mm. The geometry is shown in Fig. 2.

The flux density inside the magnetic shield can be calculated by the formula [3]:

$$B = \frac{4 \cdot B_0 \cdot \mu \cdot a^2}{a^2 \cdot (1+\mu)^2 - b^2 \cdot (1-\mu)^2} \quad (3)$$

The shields were made of following materials: steel, stainless steel, copper, mu-metal and brass.

Each sample was placed into a DC magnetic field in two different ways (parallel and perpendicular to the field lines) and the magnetic field was measured inside tubes. These results were compared to analytical calculations and FEM simulations using COMSOL. Measurements have been done at the Advanced Electromagnetics Group of Technische Universitaet Ilmenau, Germany [6]. The SF values for some samples are listed in Table 1.

One of the most important conditions of magnetic shielding is the shell thickness. The greater the thickness the better the shielding factor.

TABLE I. SHIELDING FACTORS DETERMINED FOR DIFFERENT SHIELD MATERIALS

Material	Marking of shieldings	SF
Copper	60x63, 150 mm	1.0
	35x30, 150 mm	1.0
Steel	60x53, 150 mm	14.0
	60x53, 300 mm	13.9
	37x33, 150 mm	12.9
	37x33, 300 mm	13.1
Stainless steel	40x37, 150 mm	1.0
	40x37, 300 mm	1.0
Brass	54x50, 300 mm	1.0
	32x26, 150 mm	1.0
Mu-metal	51x50, 150 mm	15.5
	52x51, 150 mm	15.0

On the other hand this means that the more amount of metal should be used for production of shield, the price will be higher as well.

The next step is the extension to multi-layered magnetic shielding. They have the same cylindrical shape but consist of two or more layers [4]. Layers can be made of the same material, having between them an air layer, or each layer is made of a different material and they fit very close to each other [5]. The geometry is shown in Fig. 3.

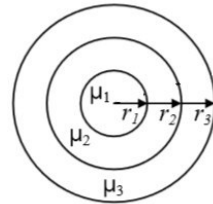


Fig. 3 Cross-section of the multi-layered shield

#### IV. CONCLUSION

The aim of this work was to investigate different composition of multi-layered magnetic shielding.

The follow conclusions have been done during the work:

- The high-permeable shields have better shielding factors than others;
- The thickness plays important role for shielding with the high- permeable shields;
- It was defined that if the shield is placed perpendicular to the magnetic field, its shielding factor will be higher than placed along the field;
- The shielding factor depends little on the shield length if the shield is placed perpendicularly, and much more if it is placed parallelly to the field.

#### REFERENCES

- [1] A.N. Gormakov, I.A. Ulyanov, "Calculation and modeling of magnetic fields generated by the system "Helmholtz ring-solenoid" (in Russian), Fundamental Research – Modern Problems of Science and Education, №3, 2015, pp. 40-45
- [2] Jupyter nbviewer, URL: <http://nbviewer.jupyter.org/github/tiggerntatie/emagnety/blob/master/soloids/solenoid.ipynb> (accessed date: December 16, 2015)
- [3] E.S. Smith, "Calculations of magnetic shield effectiveness for long μ-metal cylinders", Report, University of Regina, Canada, 2007
- [4] C.P. Bidinosti, J.W. Martin, "Passive magnetic shielding in static gradient fields", AIP ADVANCES 4, 047135 (2014)
- [5] B. Kuzmanovic, K. Hot, D. Zigman, "Multi-layered spherical magnetic shielding", Annala of the University of Craiova, Electrical Engineering series, No. 30, 2006.
- [6] A. Naumova, I. Bogomolov, H. Brauer, H. Toepper, "Magnetic Shielding", Internal Report, Advanced Electromagnetics Group, Technische Universitaet Ilmenau, Germany, Dec. 2015.
- [7] Transl. J. Magn. Japan, vol. 2, pp. 740-741, August 1987 [Digests 9th Annual Conf. Magnetics Japan, p. 301, 1982].
- [8] M. Young, "The Technical Writer's Handbook", Mill Valley, CA: University Science, 1989.

# Development Of An Integrated Environment For Intelligent Decision Support Systems Based On Forecasting And Reinforcement Learning

Eremeev A.P.

Institute of Automatics and Computer Engineering  
Moscow Power Engineering Institute  
Moscow, Russia  
eremeev@appmat.ru

**Abstract**—In the report considers the possibility of creating a tool environment, based on the integration of forecasting methods and reinforcement learning for intelligent systems (IS) of semiotic type, focused on the functioning of the open and dynamic problem areas and are capable of modification and adaptation.

**Keywords**—artificial intelligence, intelligent system, real time, decision support, forecasting, reinforcement learning

## I. INTRODUCTION

Typical representative of IS systems of semiotic type are real-time intelligent decision support systems (RT IDSS) [1, 2], designed to help the dispatching staff (decision makers) in the management of complex technical, logistical, and organizational systems. During development IS of semiotic types, an important attention should be given to the instruments of forecasting (the development of the situation at the facility, the consequences of decisions, etc.) [2] and learning tools that required to modify and adapt to changes in the RT IDSS at the object and environment [3, 4].

## II. FORECASTING METHODS

Following methods of forecasting based on statistics and expert evaluations were analyzed and implemented, in terms of use in RT IDSS: extrapolation on the moving average, a double exponential smoothing, Bayesian approach, ranking method and the method of direct evaluation.

Based on the above methods, combined (integrated) prediction method was suggested [2]. Combined method composed of averaging the results obtained by the extrapolation on the moving average method, and Bayesian approach, based on weighting coefficients. The resulting forecast adjusted with considering the values of the sequence, acquired by the method of exponential smoothing. After that, forecast adjusted by results of the expert methods: ranking and direct evaluations. The probability of each outcome acquired by statistical methods, increased or decreased depending on the expert assessment values for these outcomes.

Comparative analysis methods of reinforcement learning was made for the future realization in RT IDSS.

## III. REINFORCEMENT LEARNING METHODS

*Monte Carlo (MC) methods.* These methods require only the presence of experimental data - sequences of samples states, actions and rewards, obtained by direct or simulated interaction with the environment [3]. MC methods allow solving problems of RL-learning, based on profit, averaged on some selection. Simple MC method for the nonstationary environment:

$$V_{st} \leftarrow V(S_t) + \alpha[R_t - V(S_t)] \quad (1)$$

Kozhukhov A.A.

Institute of Automatics and Computer Engineering  
Moscow Power Engineering Institute  
Moscow, Russia  
saaanchezzz@yandex.ru

*Methods based on temporary differences (Temporal-Difference Learning).* The TD-methods based directly on obtained experience without the prior knowledge of the environmental behavior of the environment model. TD-methods update estimates, based partly on other estimates received, without waiting for the final result. Simple TD-method TD(0):

$$V_{st} \leftarrow V(S_t) + \alpha[r_{t+1} + \gamma V(S_{t+1}) - V(S_t)] \quad (2)$$

The advantage of TD-methods over MC methods is that they are inherently interactive, incremental methods. In the case of MC methods, each time necessary to wait the completion of the episode, where advantage becomes known, whereas TD methods must await the next time step only [5]. Using in RT IDSS this feature is often crucial. In some situations, episodes could be so lengthy that the delay of learning process, related to the necessity to complete the episode, will be too large. [4]

## IV. SUBSYSTEM DEVELOPMENT

Developed subsystem consists of prediction module based on statistical methods (extrapolation methods for moving average, exponential smoothing, and the Bayesian approach) and on forecasting expert methods (methods of ranking and direct evaluations) [2].

Subsystem make forecasting evaluation of the situation on the complex technical objects, performed on the task of the expert diagnosis of complex technical object. Subsystem emulator developed for testing. Based on the test results, conclusions about the applicability of the developed system to solve the problem of forecasting were made.

Also the future prospects of the work has been given, such as creation an integrated environment based on the methods of forecasting and reinforcement learning for RT IDSS of semiotic type.

## REFERENCES

- [1] Vagin V.N., Eremeev A.P. Some basic construction principles of real-time intelligent decision support systems // Izv. RAN. Theory and management System. – 2001. – № 6. – pp. 114-123.
- [2] Varshavsky P.R., Kozhukhov A.A. Development of forecasting subsystem using statistical and expert methods // VII International Scientific and Practical Conference "Integrated models and soft computing in artificial intelligence".– M.: Fizmatlit, 2015. – pp. 174-180.
- [3] Sutton R.S., Barto A.G. Reinforcement learning. – London, The MIT Press, 2012, - 320 p.
- [4] Eremeev A.P., Podogov I.U. Reinforcement learning methods for real-time intelligent decision support systems // Vestnik MPEI. – 2009. - № 2. - pp. 153-161.
- [5] Schwartz H. Multi-agent machine learning : a reinforcement approach. – Hoboken, NJ : John Wiley & Sons, 2015. – 256 p/

# Application of CBR Module for Solving Problems of Expert Diagnostics

Pavel Varshavskiy<sup>1</sup>, Roman Alekhin<sup>2</sup>, Ar Kar Myo<sup>3</sup>

Applied Mathematics Department  
National Research University “MPEI  
Moscow, Russia

<sup>1</sup>VarshavskyPR@mpei.ru, <sup>2</sup>r.alekhin@gmail.com, <sup>3</sup>arkar2011@gmail.com

**Abstract**— In this paper the problem of the application of case-based reasoning for solving problems of expert diagnostics is considered. The hybrid method of case-based reasoning for the solution of problems of diagnostics and forecasting is described. This paper demonstrates how the case-based reasoning module can be used in intelligent decision support systems.

**Keywords**—analogous reasoning; case-based reasoning

## I. INTRODUCTION

One approach to solving the problem of modeling commonsense reasoning in artificial intelligence (AI) systems and especially in intelligent decision support systems (IDSSs) is to use inductive reasoning, temporal reasoning, fuzzy logic as well as methods of reasoning based on analogies and precedents (cases) [1,2].

Case-based reasoning (CBR) can be used in various applications of AI and for solving various problems, e.g., for diagnostics and forecasting or for machine learning.

## II. CASE-BASED REASONING

CBR based on the accumulation of experience and the subsequent adaptation of previously successful solutions to similar new problems. This approach allows to simplify the decision-making process in condition of time limits and in the case of unexpected (abnormal) situations that may occur in the presence of various kinds of factors (incompleteness, inconsistency, uncertainty, etc.) In the input data and expert knowledge. The precedent is defined as a case that took place earlier and serving as an example or justification for future cases of this kind [3].

## III. METHOD OF CASE RETRIEVAL

### A. Well-known methods for case retrieval

There are large number of case retrieval methods and their modifications, for example, the nearest neighbor (NN) method, induction method (based on decision trees), methods using neural network models and others. Well-known methods for case retrieval (NN, induction et al.) can be used alone or combined into hybrid retrieval strategies.

The choice of case retrieval method is directly depends on the organization of CL and method of case representation. The

NN algorithm and its modifications are used for the definition of a similarity for most common and simple parametrical case representation. For more complex case representations, like temporal or structural cases, the methods of case retrieval on the basis of structural analogy (e.g. structure-mapping theory (SMT) are used [4].

### B. Structure-Mapping theory

SMT allows formalize the set of implicit constraints, which are used by man who operates with concepts such as analogy or similarity. This theory uses the fact that an analogy is a mapping of knowledge of one domain (base) in another domain (target) based on the system of relations between objects of the base domain, as well as the target domain. The main principle of SMT is a principle of systematicity [4], that reflects the fact that humans (DMP) prefer to deal with a system of connected relations, not just with a set of facts or relations.

### C. Hybrid method for case retrieval

This paper proposes a hybrid approach to finding solutions based on CBR. Case retrieval and determination of similarity of case and current situation is proposed to implement in two stages [4,5]:

- determination of similarity of case and current situation on the basis of problem domain ontology and formation of pair matchings by an algorithm based on the SMT;
- determination of similarity of case and current situation by the nearest neighbor method taking into account the obtained pair matchings.

The result is a set of precedents, each of which corresponds with two estimates of similarity to the current situation, which can be expressed as a percentage:

- estimate on the basis of problem domain ontology:  $S_{STRUCT} = \sum_{i=1}^k LS_i / SES_{MAX}$ ,  $k$  – number of correspondences,  $LS_i$  – plausibility estimation of  $i$  correspondence,  $SES_{MAX}$  – estimation for the case where a base is selected as the target;
- estimate by nearest neighbor method:  $Sim(C, Q) = 1 - d_{CQ} / d_{MAX}$ ,  $d_{CQ}$  – distance between the current situation and case,  $d_{MAX}$  – maximum distance in the selected metric.

This work was supported by RFBR projects 15-07-04574, 14-01-00427, 16-51-00058.

Based on these two estimates, the DMP can choose the most appropriate precedent and get a solution to the current situation.

#### IV. IMPLEMENTATION OF CBR MODULE FOR IDSS

The proposed approach has been implemented in a CBR module prototype. Figure 1 shows the architecture of developed module.

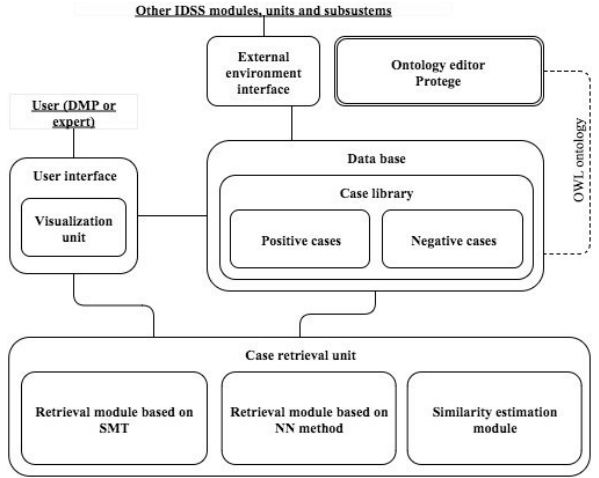


Fig. 1. Architecture of CBR module

Implemented CBR module prototype was examined by an example of solving a problem of complex object state diagnostics and detection of controlling impacts on the example of the automatic cooling system of pressurized water reactor of nuclear power plant [5]. On the basis of technological rules and operational guidelines ten initial cases were established. We give a semantic interpretation of one of them (Fig. 2) and new problem situation on object (Fig. 3): it is recommended to inject TH11D01 with boric concentrate 40 g/kg caused by switching off ACS 1 (automatic cooling system) due to closing the gates TH11S24 and TH11S25; ACS is switched off due to the closed gates TH11S24 and TH11S25; the upper setting T517B01 (pressure in the container of ACS 1) is equal to 63; the lower setting T517B01 (pressure in the container of ACS 1) is equal to 56; the upper setting TH11T500 (temperature in the frame of ACS 1) is equal to 60; the lower setting TH11T500 (temperature in the frame of ACS 1) is equal to 20.

As a results of CBR module (Fig. 4) – DMP has the ability to choose the most appropriate case based on two similarity estimates: structural estimation based on the SMT; estimation based on the nearest neighbor method.

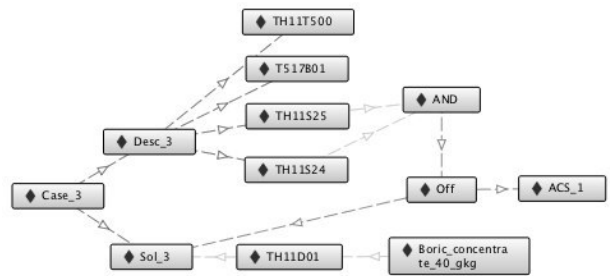


Fig. 2. Case representation

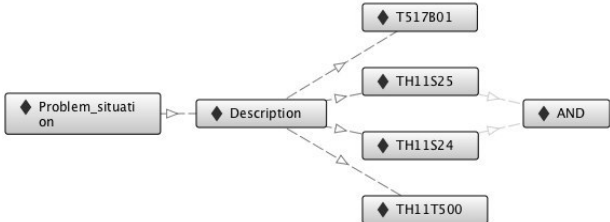


Fig. 3. Problem situation representation

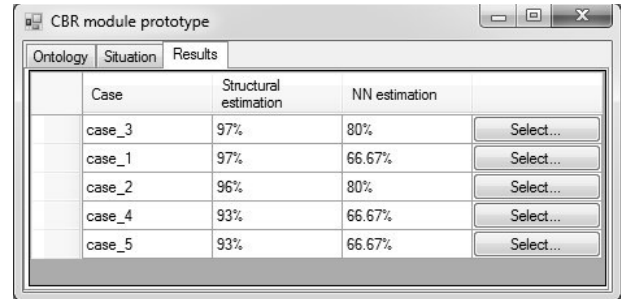


Fig. 4. Results of CBR module

#### REFERENCES

- [1] P. Varshavskii, A. Eremeev “Modeling of case-based reasoning in intelligent decision support systems,” Scientific and Technical Information Processing, 37 (5), 2010, pp 336–345.
- [2] David C. Wilson, David B. Leakes “Maintaining Case-Based Reasoners: Dimensions and Directions,” Computational Intelligence, Volume 17, Number 2, 2001, pp 196–213.
- [3] A. Aamodt, E. Plaza “Case-Based Reasoning: Foundational Issues, Methodological Variations, and System Approaches,” AI Communications, IOS Press, Vol. 7(1), 1994, pp 39–59.
- [4] A. Eremeev., I. Kurilenko, P. Varshavskiy “Temporal Case-Based Reasoning System for Automatic Parking Complex,” World Academy of Science, Engineering and Technology, International Science Index 101, International Journal of Computer, Electrical, Automation, Control and Information Engineering, Vol:9, No:5, 2015, pp 1232–1238.
- [5] A. Eremeev., P. Varshavskiy, R. Alekhin “Case-Based Reasoning Module for Intelligent Decision Support Systems,” Proceedings of the First International Scientific Conference “Intelligent Information Technologies for Industry” (IITI’16), Vol. 1, 2016, pp 207–216.

# Argumentation and machine learning

Morosin O.L.

Institute of Automatics and Computer Engineering  
Moscow Power Engineering Institute  
Moscow, Russia  
oleg@morosin.ru

Derevyanko A.V.

Institute of Automatics and Computer Engineering  
Moscow Power Engineering Institute  
Moscow, Russia  
777alterego777@gmail.com

*Abstract—This paper contains a description of methods and algorithms for solving the generalization problem in intelligent decision support systems. For this purpose the argumentation approach for inductive concept formation is used. The methods for finding the conflicts and the generalization algorithm based on the rough set theory are proposed. It is suggested to use the argumentation, based on defeasible reasoning with justification degrees, to improve the quality of the classification models obtained by the generalization algorithm. Noise models in the generalization algorithm are viewed. Experimental results are introduced.*

**Keywords:** Argumentation, justification degrees, inductive concept formation, noise, generalization.

## I. INTRODUCTION

At present, more and more attention is paid to the development of Intelligent Decision Support Systems (IDSSs) and expert systems [1]. Application of plausible methods of inference, such as argumentation and induction, can significantly increase the potential (abilities) of these systems. Using the non classical logics was caused, first of all, by the presence of uncertainties, fuzziness, ambiguities and contradictions in data, on the basis of which is required to assess a situation and offer recommendations on possible control actions. When looking for solutions in the IDSS, it is necessary to use inference methods that allow to find some reasonable, though perhaps not the optimal, solution. Inductive components in IDSSs and expert systems are intended to improve the decision accuracy, i.e. to increase the number of situations in which an intelligent system is capable to offer a solution (to give a recommendation) as close to the human expert solution as possible. Such decisions can be useful in areas such as economics, medicine, technical diagnostics and so on.

In this paper we propose to consider a combination of methods and algorithms for machine learning and argumentation techniques to improve the efficiency of decision-making in the IDSSs.

Argumentation gives us much more instruments for modelling plausible reasoning. From well known formalisms of the argumentation theory, we use the theory of defeasible reasoning proposed by J. Pollock [2] and apply the first order logic. In the classical argumentation theory only qualitative answer "pro et con" is possible, i.e. whether the argument is acceptable or not. For solving this problem, it is proposed to use the mechanism of justification degrees [3]. A justification degree is a numerical assessment of argument plausibility.

As the practical application of the argumentation theory, the modified algorithm for calculating justification degrees to improve the quality of classification models, obtained by generalization algorithms, is proposed [4]. There is a number of machine learning algorithms that are able to solve the problem of inductive concept formation on the basis of analyses of real data presented in the form of database tables. Thereby the machine learning algorithms based on learning sets build classification rules that can be further used to identify a class to which an object belongs.

Let  $O=\{o_1, o_2, \dots, o_N\}$  be a set of  $N$  objects that can be represented in an IDSS. Each object is characterized by  $K$  attributes:  $A=\{a_1, a_2, \dots, a_K\}$ . Quantitative, qualitative, or scaled attributes can be used[1]. Among a set  $O$  of all objects represented in a certain IDSS, separate a set  $V$  of positive objects related to some concept (a class) and  $W$  is a set of negative objects not concerned with this concept (a class). Let a learning set  $U=\{x_1, x_2, \dots, x_n\}$  be a non-empty subset of objects  $O$  such that for each object from  $U$  it is reliably known to which class ( $V$  or  $W$ ) it belongs.

Thus, the concept was formed if one manages to build a decision rule that for any example from a learning set  $U$  indicates whether this example belongs to the concept or not. The algorithms that we study form a decision in the form of production rules. The decision rule is correct if, in further operation, it successfully recognizes the objects that originally did not belong to a learning set. The generalization algorithms build a generalized concept as a set of decision rules  $\mathbb{R}$ . It is known that the main criterion of the quality for a built generalized concept (i.e. a decision rule set  $\mathbb{R}$ ) is a successful classification of a test set of examples (examples not entering into a learning set  $U$ ) by the given decision rules.

It is proposed to use the argumentation methods for obtaining an improved set  $\mathbb{R}^*$ , that is able to classify test examples with a greater accuracy than the original set  $\mathbb{R}$ .

The quality of a decision rule set  $\mathbb{R}$  depends, primarily, on the representativeness and consistency of a learning set  $U$ . The basic idea is to divide the learning set of examples  $U$  into two subsets  $U_1$  and  $U_2$ , such that  $U_1 \cup U_2 = U$ ,  $U_1 \cap U_2 = \emptyset$ , and to produce separate learning on each of these subsets using any generalization algorithm that generates classification rules of the form of production rules. It is proposed to use the methods of argumentation for obtaining an improved classification model, combining the results of a separate learning on  $U_1$  and  $U_2$ . Let decision rule sets  $\mathbb{R}_1$  and  $\mathbb{R}_2$  using

some generalization algorithm (in particular, algorithms C.4.5(Quinlan) [5], CN2(Clark and Boswell) [6] and GIRS(Vagin, Fomina and Kulikov) [7] can be used) be built for learning sets  $U_1$  and  $U_2$ . Our task is to form a consistent set  $\mathbb{R}^*$  that combines rules from both sets  $\mathbb{R}_1$  and  $\mathbb{R}_2$ . The method of combining multiple sets of decision rules in a conflict-free set of rules by defining justification degrees for all defeasible rules in such a way that all conflicts arising in a learning set becomes solvable was proposed. This method using the C4.5 and GIRS algorithm as a basic generalization algorithm was successfully implemented and tested on some standard Problems from UCI Repository of Machine Learning Datasets (Information and Computer Science University of California)[8].

The results of the experiment are presented in fig. 1-3.

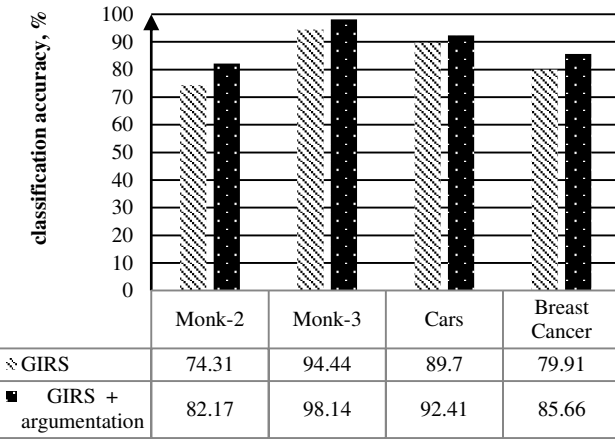


Fig. 1. Classification accuracy of different test problems with algoritm GIRS

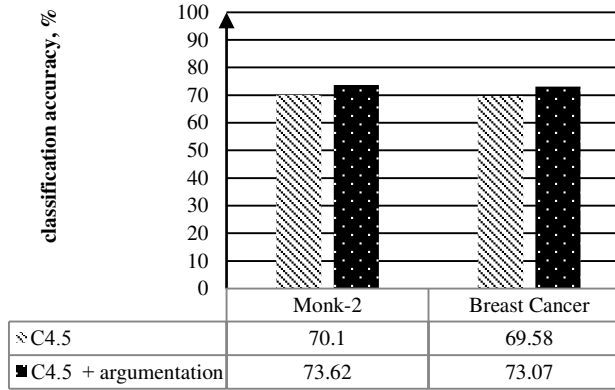


Fig. 2. Classification accuracy of different test problems with algoritm C4.5

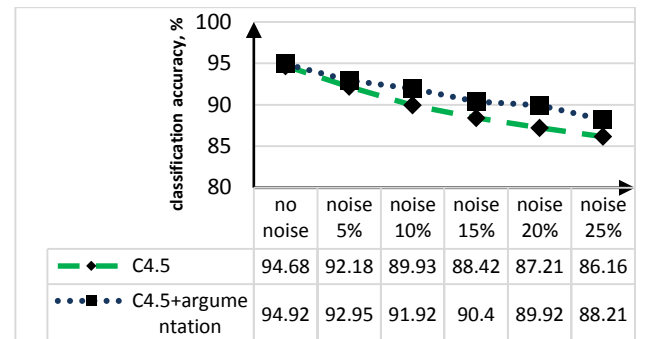


Fig. 3. Classification accuracy of MONK-3 problem with algoritm c4.5 and different noise levels

Application of argumentation methods for the generalization problem allowed to enhance the classification accuracy for test problems. Furthermore, it was analyzed the influence of noise on the classification accuracy. The use of argumentation for noisy data as well significantly improved classification results.

## REFERENCES

- [1] V. Vagin, E. Golovina, A. Zagoryanskaya and M. Fomina, "Exact and Plausible Inference in Intelligent Systems", FizMatLit, Moscow, p. 714, 2014 (in Russian).
- [2] J. Pollock, "Oscar – a General Purpose Defeasible Reasoner", Journal of Nonclassical Logics, vol.~6, 1996, pp.~89--113.
- [3] Item J. Pollock, "Defeasible reasoning with variable degrees of justification", Artificial Intelligence, vol.~133, 2001, pp.~233--282.
- [4] V.N. Vagin, O.L. Morosin, "Modeling defeasible reasoning for argumentation", Proceedings of BRICS-CCI'2013 – 1st BRICS Countries Congress on Computational Intelligence and CBIC'2013 – 11th Brazilian Congress on Computational Intelligence}, Recife, Brasil, 2013, pp.~304--309.
- [5] J.R. Quinlan (em C4.5: Programs for Machine Learning), Morgan Kaufmann Publishers Inc., San Francisco.,p. 302, 1993.
- [6] P. Clark and R. Boswell., "Rule Induction with CN2: Some Recent Improvements", Machine Learning - Proceedings of the Fifth European Conference (ESWL-91)}, Springer-Verlag, Berlin, 1991, pp.~151--163.
- [7] V. Vagin, M. Fomina and A. Kulikov, "The Problem of Object Recognition in the Presence of Noise in Original Data", 10th Scandinavian Conference on Artificial Intelligence SCAI}, 2008, pp.~60--67.
- [8] C. Merz, "UCI Repository of Machine Learning Datasets.", Information and Computer Science University of California}, [Online]. Available: <http://archive.ics.uci.edu/ml/>.

# An Approach to Model-Based Modification of Embedded Systems for a Specialized Soft Microprocessor

Elena Rozova

Software Architectures and Product Lines Group  
 Ilmenau University of Technology  
 98684 Ilmenau, Germany  
 elena.rozova@tu-ilmenau.de

Bernd Däne

Computer Architecture and Embedded Systems Group  
 Ilmenau University of Technology  
 98684 Ilmenau, Germany  
 bernd.daene@tu-ilmenau.de

**Abstract**—This paper reports on an ongoing case study that deals with model based design of soft microprocessor applications for FPGA implementation. It focuses at a model based enhancement and implementation of additional features in the computational core and of functions for generating and optimizing binary program code for single-core and multi-core configurations.

**Keywords**—*embedded systems; soft microprocessor; model based design*.

## I. INTRODUCTION

The goal of this case study is to investigate how to realize a softcore processor, how to optimize binary program code, including pipeline optimization and multicore parallelization at instruction level, and how such systems can be modified in a model based manner by using a graphical modeling environment. The case study deals with the soft microprocessor LiSARD (LabVIEW integrated Softcore Architecture for Reconfigurable Devices) that is under development in this project and has been discussed previously in [1], [2], [3] and [5].

## II. DEFINING MAIN PARTS

The project LiSARD deals with a model based design approach and is made of a *Configurable Processor, Code Converter and Testbench*.

Our processor uses the Harvard architecture with a five-staged pipeline (see fig. 1). Pipeline control is simplified by omitting branch instructions. The arithmetical-logical unit (ALU) features fully pipelined implementations of several floating-point operations (so-called operators) that accept one pair of operands and deliver one result per clock cycle, with an individual but fixed delay. Generation and optimization of binary program code (from source code that has been designed in earlier steps), also other functions (e.g. allocation of variables in data memory and management of some processor configuration features) is performed by the Code Converter. [1] It produces memory images for both program and data memory that will be used by the special component for automatically producing memory initialization routines. The data memory architecture is flattened by merging data memory and the register set into one structure. [2] Soft microprocessor LiSARD

supports multi-core structures (setups with more than one processing core), and thus, raising the potential of micro parallelism.

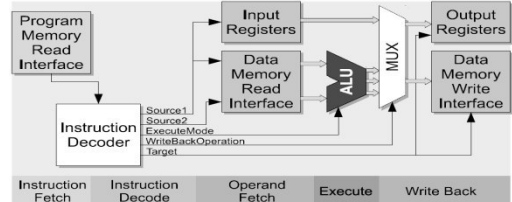


Fig. 1. Pipeline architecture [1]

The resulting configured processor component is connected to a testbench that provides interfacing and debugging functionality.

## III. EXTENSION

### A. Core

In our case it was important to extend the functionality of the processor, adding special (so called MLookup-Table-) operations in one of the cores, which read a value from special memory (lookup table) and execute addition, subtraction or multiplication operations with this value. Figure 2 shows a part of one core, where the conversion block “Dbl2I16”, a Lookup-Table and an ALU with MLuTo were realized.

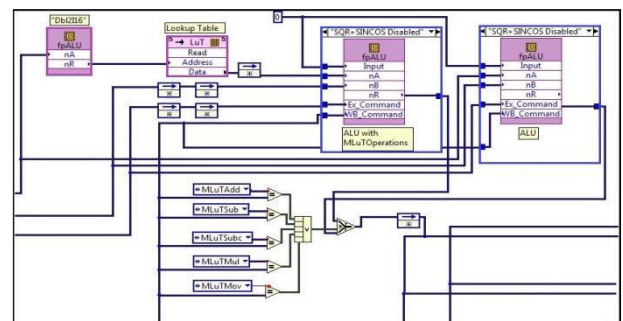


Fig. 2. ALU's in core

In MLuT-operations the first operand holds an address of a constant in the LuT. The second operand is an arbitrary value and the third is the output operand. Any access to the lookup table requires address conversion. The “Dbl2I16” block is responsible for such conversions. After access to lookup table and additional delay, which is needed for coordination, both operands and the execution command will be passed to the ALU with MLuTo. Both ALUs (common and new) execute operations and the results will be MUXed, using the writeback command.

### B. Code Converter

Pipeline optimization basically means raising utilization of calculation resources by overlapping. [4] Obviously this can lead to changes in the sequence of instructions. [5] But operand dependencies have to be taken into account, therefore a special block (subcomponent) for this task in the code converter was implemented.

Figure 3 shows a part of the model that implements address comparison as a central point of checking RaW (Read after Write) dependencies. Source operand addresses (Execution Address) of one instruction are compared to the destination address (Write Back Address) of another instruction. Prior to comparison all addresses are filtered in order to cover multiple instances of the same variables. The structure resides inside two nested loops (not shown) both running for all instructions of the program, in this way performing comparisons between all source and all destination operands.

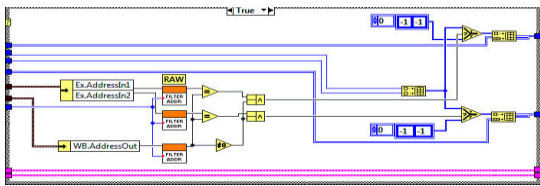


Fig. 3. Check dependencies model

In another part of this subcomponent the address of one of the source operands is modified if a data dependency that spans across multiple program runs requires using another instance of the same variable.

### IV. TESTING AND RESULTS

The extension of parts of the project LiSARD has been validated by conducting experiments using several programs.

Table 1 provides results for both pipeline optimization efficiency and multi-core instruction scheduling efficiency, expressed by speedups achieved. Columns three and four show speedup of pipeline-optimized versus non-optimized programs, both being measured with single-core setups. The remaining columns at the right side of the table present speedup of *n*-core configurations versus single-core configuration, but always with pipeline optimization being turned on. As expected, results greatly depend on characteristics of the programs, concerning the availability of independent operations. Our 6-Axes program, implementing an adaptive six-channel control algorithm [2], offers plenty of independent operations, leading to efficient multi-core implementations.

TABLE I. SPEEDUP OF OPTIMIZED PROGRAMS

Program	Indicators					
	Instr. count	Non- optim.	Pipeline- optim.	I- core	2- core	4- core
FIR-64	196	1.00	4.81	1.00	1.88	2.60
Kalman-2	350	1.00	5.75	1.00	1.63	2.40
6-Axes	866	1.00	4.97	1.00	1.72	3.09
Ellipse	364	1.00	2.40	1.00	1.11	1.13
Ellipse-4	1456	1.00	5.16	1.00	1.51	1.84

In contrast the Ellipse algorithms (ellipse-shaped regression) provide a lower degree of independency that can be used by pipeline optimization while efficiency of multi-core implementations is limited.

Tests for validation of modified core-part were also executed, using several different versions of PID-controller programs, where different ways for access to lookup table (constants, which contain addresses for LuT access; one calculated variable; several calculated variables) were used. It was shown that use of predefined addresses in constants is more effectively than several calculated variables (benefit 12.9 %) and much more effectively than one calculated variable (benefit 61.3 %).

### V. CONCLUSION AND FURTHER WORK

Results from a case study on model based modification and implementation of additional features in the core have been presented. This research is intended as a step towards an enhancement of a more comprehensive model based design processes. The future steps in this research work aim towards technical improvements of the processor design and optimization strategies as well as further research about model based design processes.

### ACKNOWLEDGMENT

This work is funded by Deutsche Forschungsgemeinschaft (German Research Foundation) under grant SFB622 at the Ilmenau University of Technology, Ilmenau, Germany.

### REFERENCES

- [1] A. Pacholik, J. Klöckner, M. Müller, I. Gushchina, and W. Fengler, “LiSARD: LabVIEW integrated softcore architecture for reconfigurable devices,” IEEE Computer Society CPS, International Conference on Reconfigurable Computing and FPGAs, Cancun, Mexico, 2011, pp. 442–447.
- [2] B. Däne, A. Pacholik, S. Zschäck, W. Fengler, C. Ament, and T. Braune, “Designing a control application by using a specialized multi-core soft microprocessor,” Z. Slanina, editor, 12th IFAC Conference on Programmable Devices and Embedded Systems, Velke Karlovice, Czech Republic, 2013, pp. 221–226.
- [3] B. Däne, “Tool-supported Design of an Application-specific Soft Microprocessor,” H. Unger, and W. A. Halang, editors, Autonomous Systems 2014, VDI Series 10 No. 835, VDI Verlag Düsseldorf, Proceeding of the 7 GI Workshop, Cala Millor, Spain, 2014, pp. 90–101.
- [4] K. Cooper, and L. Torczon, “Engineering a Compiler, Second Edition,” Elsevier Morgan Kaufmann, Burlington, USA, 2011.
- [5] E. Rozova, “Modifikation und Weiterentwicklung des Softcore-Prozessors LiSARD,” Master Thesis, TU Ilmenau, Department IA, 2013.

# Workflow management system for academic collaboration

Vasilii Ganishev, Olga Fengler and Wolfgang Fengler

Computer Science and Embedded Systems Group

Ilmenau University of Technology

Ilmenau, Germany 98693

Email: {vasily.ganishev, olga.fengler, wolfgang.fengler}@tu-ilmenau.de

**Abstract**—Nowadays the development of communication facilities have led the rise of academic collaboration. Unlike in times of “Big Science” these collaborations have flexible structures and are being characterized by severe geographical diversity of collaborators. Some communities that work on the same project unite scientists from various countries and research centres. In this case there is a need in tools to simplify a teamwork and to clarify whole collaboration. However, it should not be understood as another scientific workflow management system which support calculations for research project. This system should configure, control and optimize collaborative work of individual scientists in a group. Therefore, a high degree of adaptivity is required for handling and structuring the processes beforehand. One of the practical necessities for developing such systems is their use in settling the workflow of the scientific projects which are known to be highly dynamic and long-term processes.

**Keywords**—*Workflow Management Systems, Collaboration Systems, Scientific Project Collaboration, Adaptive Case Management*

## I. INTRODUCTION

For a long time there is a discussion about lack of flexibility in workflow systems. Classical Business Process Management (rigid BPM) that suits for “tayloristic” work support does not provide necessary process evolution and/or exception handling mechanisms. If one takes into consideration all possible changes in the process, it makes process presentation unreadable and sophisticated that eliminates all advantages of such an approach [1].

Some researchers propose to use high-level change operations to provide structural flexibility such as “Insert Process Fragment” [2] or with change primitives of higher degree of granularity like “Add Node” and “Add Arc” in recovery nets [3]. These approaches require the use of change correctness and change control systems (e.g. Opera [4]). Despite several advantages, these concepts require complex process support.

In our opinion the problem lies in the basic concept of BPM, which is too restrictive and has problems dealing with change [1]. Complex projects, not only limited to scientific projects, require collaboration of knowledge workers, whose work may not fit predefined process model due to changing circumstances (new information, feedback from already done

steps, exceptions, etc.). The BPM, more suitable for short routine operations, does not provide possibilities to handle this, because it is too much “process-centric”.

Advanced (or adaptive) case management (ACM) is concept to configure knowledge work processes. It is more “goal-centric” and defines the approach as “what could be done”, rather than “how should it be done” [5]. This concept provides more flexible process description, however it has almost lost the connection with BPM and acts completely separate. Therefore, we propose that the ACM together with the BMP could make a great contribute to adaptive workflow systems. In this work we will mainly address to this problem, filling the gap between the flexibility of the ACM and the accuracy of the BPM.

## II. SYSTEM CONCEPT

The proposed system supports the scientific project execution, helps to identify the best practices or avoid faults that occurred in the past. This involves the separation of actors or participants by following roles:

- *Manager (Process Owner)*. A Manager is the main actor in the system. This actor is responsible for determination of scientific project primary goal, setting the initial project schedule and budget. Manager also approves important decisions as the transition between design-time and run-time stages or primary goal changes.
- *Designer*. As the name implies, a Designer plays a crucial role at the design-time phase. The main task of the designer is to determine a set of Plan Items and dependencies among them required to achieve the project primary goal. The project’s plan in the form of CMMN diagram should be approved by a Manager and then present itself as instructions for project execution. When major changes in the project accrue, the designer could be called to review the project plan.
- *Principal Investigator*. This role represents “mid-level manager” of the project. Its mission is to distribute tasks among scientific groups, to monitor compliance with the schedule, to manage provided resources in the project and to take operational decisions (e.g. inclusion

of new additional subgoals and defining of their priorities).

- *Resource Manager.* The role of Resource Manager is optional (in sense that it can be automated) and may be associated with multiple projects. Its main responsibilities are: coordination of utilization schedules of material resources (such as experimental facilities) and human resources (scientific groups and/or single scientists) among several projects.
- *Scientific Group.* This role is a main working unit of the project. Scientific groups report to the system on the work done, so these data form an operation log required for further analysis. Users in this group decide themselves about the order in which tasks are solved, the necessity of predefined discretionary tasks execution and adding new tasks (this possibility can be ruled out by policy adopted on the project).

By proposed separation some roles can be combined for smaller scientific groups.

The analytical part of the system consists of three modules:

- *Process discovery subsystem* allows to convert the log of activities to the business process model, which is required for further analysis. The simplest method to obtain process model from the operation log is the  $\alpha$ -algorithm [6]. In the original  $\alpha$ -algorithm the model is a Workflow net, however it can be easily translated to YAWL (Yet Another Workflow Language) or BPMN (Business Process Model and Notation) nets.
- *Subsystem of simulation and analytics* generates possible execution scenarios and analyses them according to certain criteria.
- *Process data warehouse* is necessary to keep the information about previous projects and analyse similarity of current project to them. This can be useful to avoid previous faults as well as adhere to established practices. In our work we propose to use  $m^3$  similarity measure. Because satisfies the property of triangle inequality, it is possible to bound the similarity of two models with already computed distances:

$$dist(B_0, B_2) \leq |dist(B_0, B_1) + dist(B_1, B_2)|$$

$$dist(B_0, B_2) \geq |dist(B_0, B_1) - dist(B_1, B_2)|$$

This reduces the computation by rejecting in advance not prospective models.

### III. SUMMARY AND CONCLUSION

In this paper the system concept for scientific project collaboration is presented. It supports the scientific project execution, helps to identify the best practices and avoid faults occurred in the past.

In future work we will address the mechanism of obtaining a log of work as well as criteria for selecting the most appropriate process of the generated ones. Also further investigations in the consideration of human resources performance with fuzzy logic or the use of defeasible logic in describing the semantic relationships among tasks in the CMMN model are planned.

### REFERENCES

- [1] W. M. P. van der Aalst, M. Weske D. Gruenbauer, Case handling: A new paradigm for business process support // Data and Knowledge Engineering, vol. 53, 2005.
- [2] B. Weber, M. Reichert, S. Rinderle-Ma, Change patterns and change support features enhancing flexibility in process-aware information systems // Data & Knowledge Engineering, vol. 66, no. 3, pp. 438 – 466, 2008.
- [3] R. Hamadi, B. Benatallah, Recovery nets: Towards self-adaptive workflow systems // Web Information Systems – WISE 2004: 5th International Conference on Web Information Systems Engineering, Brisbane, Australia, November 22–24, 2004. Proceedings, X. Zhou, S. Su, M. P. Papazoglou, M. E. Orlowska, and K. Jeffery, Eds. Berlin, Heidelberg: Springer Berlin Heidelberg, 2004, pp. 439–453.
- [4] C. Hagen, G. Alonso, Exception handling in workflow management systems // IEEE Trans. Softw. Eng., vol. 26, no. 10, pp. 943–958, Oct. 2000.
- [5] K. D. Swenson, N. Palmer, B. Silver, Taming the Unpredictable Real World Adaptive Case Management: Case Studies and Practical Guidance // Future Strategies, October 2011.
- [6] W. M. P. van der Aalst, Process Mining: Discovery, Conformance and Enhancement of Business Processes. Springer Berlin Heidelberg, 2011.
- [7] M. Kunze, M. Weidlich, M. Weske,  $m^3$  — a behavioural similarity metric for business processes, Services und ihre Komposition, 2011.

# A method of the X-parameters measurement for high-power S-band power amplifier

O. Adonev, D. Kotov, A. Pluteshko, A. Blinnikov

Dept. of Research and Development  
VNIIRT JSC  
Moscow, Russia  
oadonev@yahoo.com

A. Zaycev, P. Maslov

Dept. of Research and Development  
Akmetron JSC  
Moscow, Russia  
zav@akmetron.ru

**Abstract**—Performed a series of the X-parameters measurements for high-power S-band power amplifier. This method is the foundation to provide similar measurements and as result to obtain the behavioral model of power amplifier to further simulations in ADS. This method describes all the calibration and measurement steps to obtain X-parameters.

**Keywords**—RF power amplifier; X-parameters; behavioral model of RF power amplifier; ADS; PNA-X; non-linear device modeling

## I. INTRODUCTION

Developing of the RF power amplifiers required to take into consideration the different operation modes of the transistor. Behavior of the amplifier in these modes can't be predicted using the analytical models. Keysight Technologies co. in association with Maury Microwave co. suggests to resolve this problem with X-parameters. X-parameters describe properties of the devices operating in non-linear area [1,2]. Measured X-parameters are imported in CAD Keysight Advanced Design System (ADS) to further simulation.

X-parameters describe the behavior of device stimulated by applying the appropriate large-signal. In large-signal mode also measure the responses on harmonics of the signal. To describe the behavior of the model with different input and output impedances, in X-parameters included the transfer ratio for small-signals on carrier frequency and harmonics. These signals named extraction tones, applying together with large-signal at the input and the output of device. The extraction tones have a level -30..-20 dB in relation to large-signal [3].

The behavioral model contains the data array obtained in research of power amplifier. For each device choose the following parameters: frequency range, input power, input and output impedances. This parameters array defines set of points to provide the measurements. The interpolation uses to define the behavior of device in intermediate points.

## II. FORMULATION

Measurements of X-parameters have been performed for the S-band RF power amplifier using LDMOS-transistor NXP-BLS6G2735LS-30. Output power is 40 W in frequency range 2.7-2.9 GHz. The transistor operating in pulsed mode (a duty cycle is 5). To perform the measurements have been used the Network Analyzer PNA-X with NVNA software [4] and impedance tuner Maury Microwave with IVCAD software [5].

The frequency points chose for measurements: from 2.65 GHz to 2.95 GHz step is 50 MHz. Frequency points 2.65 GHz and 2.95 GHz are required to increase the analyzing frequency range. In measurements used the “load-pull” method [6]. Measurements are made up to the third harmonic. Input power range varied from 20 dBm to 33 dBm step is 1 dBm.

Figure 1 shows the simple block-diagram describing the measurement setup to characterize the DUT.

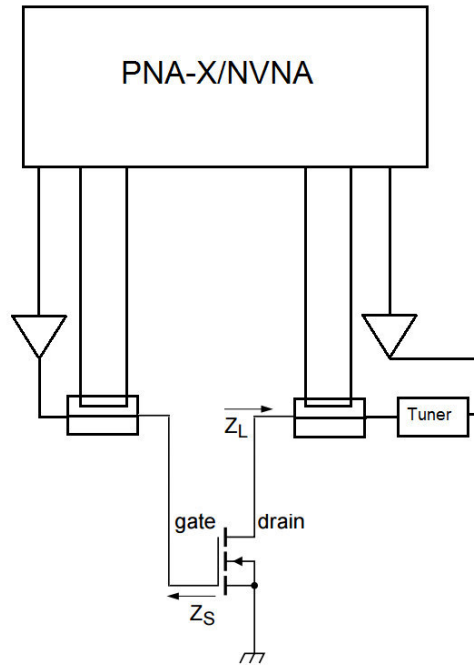


Figure 1. Block diagram of the measurement setup for X-parameters measurement.

## III. MAIN RESULT

The scheme for measurements X-parameters shown on Fig.2:

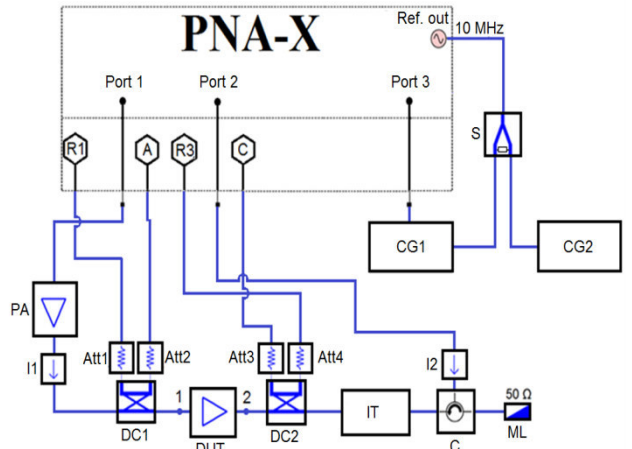


Figure 2. The scheme for measurements X-parameters

The measurement scheme includes:

PA – preamplifier (30 dB)  
I1, I2 – isolators

Att1, Att2, Att3, Att4 – attenuators (20 dB)  
 DC1, DC2 – directional couplers (35 dB)  
 DUT – device under test (S- band power amplifier)  
 IT – impedance tuner Maury Microwave  
 C – circulator  
 ML – matched load (50 Ohm)  
 CG1, CG2 – comb generators  
 S – splitter.

Agilent PNA-X Microwave Network Analyzer acts as the main device [7] of the measurement setup and PNA-X also configured to Non-linear Vector Network Analyzer (NVNA) mode to enable large-signal mode and X-parameters measurements. PNA-X controls all hardware in measurement scheme, X-parameters measurement and extraction process. Extraction tones coming from ports 1,2 and it comes to receivers R1, A, R3, C. Output power in port 1 varied from: -10 dBm to 3 dBm. Two comb generators are used together, CG1 is always connected to port 3 and defines the phase reference, CG2 using in calibration process. Impedance tuner Maury Microwave is controlling by PNA-X/NVNA and performing a load-pull impedance sweep.

The first step is calibration of the IT Maury Microwave using IVCAD. Calibration provides for each frequency point from 2.65 GHz to 2.95 GHz with step 50 MHz. In process of calibration Impedance Tuner provides sort of impedances for each frequency point. Also there is an option to choose the impedance distribution on Smith chart.

The second step is calibration of receivers (R1, A, R3, C) considering the impact of measurement scheme for high-power devices. To provide this procedure using measurement scheme, contains DC1, IT and DC2. Out of the port 1 is connecting to DC1 and out of the port 3 is connecting to the out of DUT. Then required to connect Impedance Tuner, PNA-X and power meter to the IVCAD. Before start the calibration internal generator in PNA-X is set to CW mode and set the signal power level in PNA-X. Then ECal (Electronic calibration module) is connecting to pins 1, 2 and in IVCAD starting the procedure “tuners auto de-embedding”.

The third step is calibration of the full measurement scheme to provide the X-parameters measurements. Preliminary is assembling the scheme shown on Fig.2 with the exception of PA and I1. Then using IVCAD, internal generator in PNA-X is switching to pulsed mode and setting up the parameters of pulses. In NVNA defines frequency range, calibration power level, the switch positions in PNA-X, number of signal harmonics and power levels each of extraction tones, outgoing from port 1 and port 3. The calibration in NVNA includes 3 procedures: vector calibration, phase calibration using CG2 and power calibration. The vector calibration provides using ECal, it's connected to pins 1 and 2 then perform the calibration. Phase calibration provides using CG2 connected to pin 1 while CG1 connected to port 2 and defines the phase reference of signal. Power level calibration provides using power meter connected to pin 1. The results of calibrations are automatically importing to IVCAD.

The fourth step is connecting the DUT between pins 1 and 2. Then connect PA and I1. Setup the number of impedance points for measurements and output power range from port 1. Start the measurements. The measurement results automatically save in file «\*.xnp».

For each of measured points created a X-parameters file. To obtain the full device model all files for each frequency point should be united in one file by editing. The united file using in ADS to further modeling. It contains the parameters of the power amplifier operating in non-linear mode.

Block-scheme of the method describes main steps to provide the measurements shown on Fig.3:

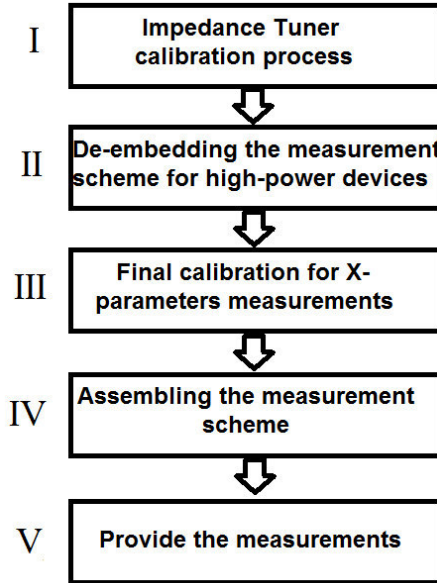


Figure 3. Block-scheme of the measurement process

#### IV. CONCLUSION

This paper shows the method of X-parameters measurements includes all the necessary steps to provide X-parameters measurements. The X-parameters file («\*.xnp») could be used in Keysight ADS to further simulations and enable to develop the models of active devices considering non-linear effects. The created X-parameters model is able to predict the behavior of the power amplifier up to 3<sup>rd</sup> harmonic load-tuning in chosen points in Smith chart. To characterize the behavior of the model in point between measured points, imported model in Advanced Design System (ADS) uses interpolation methods. To extract the transistor model from X-parameters required to perform fixture de-embedding, in PNA-X there is an option AFR (Automatic fixture removal) allows to measure S-parameters of the fixture.

#### REFERENCES

- [1] Root D.E., Horn J., Betts L., Gillease C., Verspecht J. X-parameters: the new paradigm for measurement, modeling, and design of nonlinear RF and microwave components. *Microwave Engineering Europe*, 2008. - pp. 16-21.
- [2] Configuration of PNA-X, NVNA and X-parameters. [web source] URL: [https://www.av.it.pt/X-tutorial/0\\_PNAX\\_intro.pdf](https://www.av.it.pt/X-tutorial/0_PNAX_intro.pdf) (25.01.16)
- [3] High Power Amplifier Measurements Using Agilent's Nonlinear Vector Network Analyzer. [web source] URL: <https://www.av.it.pt/62-PNA-X/X-tutorial.pdf> (25.02.16)
- [4] Software NVNA, [web source] URL: <https://www.keysight.com/find/nvna.html> (18.02.16)
- [5] Software IVCAD, [web source] URL: [https://www.maurymw.com/MW\\_RF/IVCAD\\_Advanced\\_Measurement\\_Modeling\\_Software.php](https://www.maurymw.com/MW_RF/IVCAD_Advanced_Measurement_Modeling_Software.php) (15.02.16)
- [6] IVCAD NVNA and X-parameters - Load Pull. [web source] URL: [https://maury.zendesk.com/hc/en-us/article\\_attachments/202784476/IVCAD\\_MT930C\\_GS\\_NVNA\\_Load\\_Pull.pdf](https://maury.zendesk.com/hc/en-us/article_attachments/202784476/IVCAD_MT930C_GS_NVNA_Load_Pull.pdf) (14.01.2016)
- [7] Modeling a UMS GaN transistor (CHZ015A) with a B1505, a PNA-X and ICCAP. [web source] URL: [http://www.keysight.com/upload/cmc\\_upload/All/gan\\_transistor.pdf](http://www.keysight.com/upload/cmc_upload/All/gan_transistor.pdf) (22.01.2016)

# A Comparison of two Modular Multilevel Cascade Converter Topologies for Motor Drive Applications

Elizaveta K. Samygina, Andrey Dudin, Jürgen Petzoldt

Technische Universität Ilmenau  
Ilmenau, Germany

elizaveta.samygina@tu-ilmenau.de, andrey.dudin@tu-ilmenau.de, juergen.petzoldt@tu-ilmenau.de

**Abstract—** in this work two modular multilevel cascade converter topologies are compared for a motor drive application over complete frequency range: Back-to-Back Double Star Chopper Cell and Double Delta Bridge Cell. Both converters are simulated in MathLab Simulink. The main comparison criteria are the sum of the switches' peak and rms currents, along with the capacitors'rms currents sum and capacity demand for the energy variation.

**Keywords—** Modular multilevel converters, Frequency converters, Motor drive.

## I. INTRODUCTION

In recent years several Topologies of Modular Multilevel Cascade Converters (MMCC)[1][2] were studied and developed for high power and high voltage applications. The MMCC have a high voltage and power capability with low blocking voltage devices and low switching frequency capability in the high-voltage and high-power range. One of the applications for the MMCC family is the power supply of the high power motor drives [3], [4], [5]. For three-phase AC/AC grid coupling applications the Back-to-back (BTB) DSCLC, the Modular Multilevel Matrix Converter (M3C) and the DDBC topologies are suited. The disadvantage of these three Converters is that they need an energy balancing between converter branches. Such balancing is realized by injecting current- and voltage-harmonics that increase the switch current ratings.

The parameters for a design comparison are: branch voltage and current amplitude, RMS currents of the switches and capacitors and the steady-state energy ripple of submodule capacitors. Different MMCC Topologies for the coupling of three-phase systems for motor drive applications were compared in [3][4]. No works comparing MMCC design-relevant parameters are known by far.

In this work the DSCLC and DDBC topologies are compared over the full frequency range.

## II. BTB-DSCLC TOPOLOGY

The BTB-DSCLC topology is shown in Fig.1. The grid and branch voltages and currents are defined as:

$$u_{ay} = \hat{u}_a \cdot \cos(\omega_1 \cdot t + (y-1) \cdot 2\pi/3) \quad (1)$$

$$i_{ay} = i_{py} - i_{ny} = \hat{i}_a \cdot \cos(\omega_1 \cdot t - \phi_1 + (y-1) \cdot 2\pi/3) \quad (2)$$

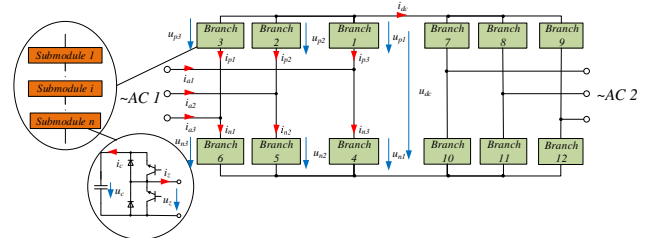


Fig.1 BTB DSCLC topology and chopper cell structure

where  $y$  – is a phase number,  $\hat{u}_a$  – the amplitude of the AC current,  $\omega_1$  – network round frequency and  $\phi_1$  – shift angle between the network voltage and current

Whereby circulating current is:

$$i_{ci} = [(i_{p1}+i_{n1})/2 \quad (i_{p2}+i_{n2})/2 \quad (i_{p3}+i_{n3})/2]^T \quad (3)$$

The control system of the DSCLC is realized as a double-loop structure[4] with an internal current control loop and an external energy loop. The AC current control is realized in rotating (dq) coordinates and circulating current control in  $\alpha\beta$  coordinates. The overall control structure is shown in Fig. 2. Control of two DSCLC-parts in the BTB topology is implemented separately.

## III. DDBC TOPOLOGY

DDBC topology is in the opposite to DSCLC a direct AC/AC converter and it can be considered as three delta-connected branches as shown in Fig. 3.

The network voltages and currents in DDBC can be expressed as:

$$u_{al} = \hat{u}_{al} \cdot \cos(\omega_1 \cdot t + (y-1) \cdot 2\pi/3) \quad (4)$$

$$i_{al} = \hat{i}_{al} \cdot \cos(\omega_1 \cdot t - \phi_1 + (y-1) \cdot 2\pi/3) \quad (5)$$

$$u_{az} = \hat{u}_{az} \cdot \cos(\omega_2 \cdot t + \phi_{12} + (y-1) \cdot 2\pi/3) \quad (6)$$

$$i_{az} = \hat{i}_{az} \cdot \cos(\omega_2 \cdot t + \phi_{12} - \phi_2 + (y-1) \cdot 2\pi/3) \quad (7)$$

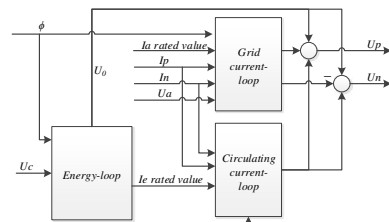


Fig.2 DSCLC control system

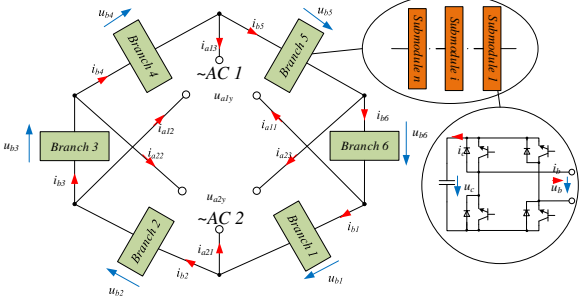


Fig. 3 DDBC topology and the bridge cell structure

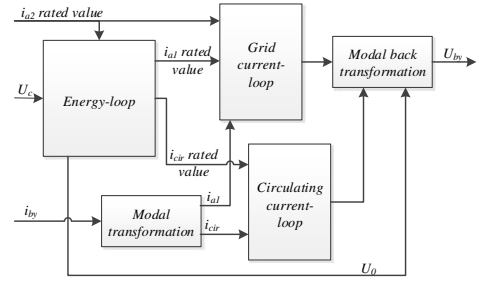


Fig. 4 An overview over the DDBC control system

TABLE I. CAPACITOR CURRENTS

$$u_b = \begin{pmatrix} 1 & 0 & 0 & -1 & 0 & 0 \\ 0 & -1 & 0 & 1 & 0 & 0 \\ 0 & 1 & 0 & 0 & -1 & 0 \\ 0 & 0 & -1 & 0 & 1 & 0 \\ 0 & 0 & 1 & 0 & 0 & -1 \\ -1 & 0 & 0 & 0 & 0 & 0 \end{pmatrix} \cdot \begin{pmatrix} u_{a11} \\ u_{a12} \\ u_{a13} \\ u_{a21} \\ u_{a22} \\ u_{a23} \end{pmatrix} \quad (8)$$

$$i_b = \begin{pmatrix} -\frac{1}{2} & \frac{\sqrt{3}}{6} & \frac{1}{2} & \frac{\sqrt{3}}{6} & 1 \\ -\frac{1}{2} & \frac{\sqrt{3}}{6} & -\frac{1}{2} & \frac{\sqrt{3}}{6} & 1 \\ 0 & -\frac{\sqrt{3}}{3} & -\frac{1}{2} & \frac{\sqrt{3}}{6} & 1 \\ 0 & -\frac{\sqrt{3}}{3} & 0 & -\frac{\sqrt{3}}{3} & 1 \\ \frac{1}{2} & \frac{\sqrt{3}}{6} & 0 & -\frac{\sqrt{3}}{6} & 1 \\ \frac{1}{2} & \frac{\sqrt{3}}{6} & \frac{1}{2} & \frac{\sqrt{3}}{6} & 1 \end{pmatrix} \cdot \begin{pmatrix} i_{a1\alpha} \\ i_{a1\beta} \\ i_{a2\alpha} \\ i_{a2\beta} \\ i_{cir} \end{pmatrix} \quad (9)$$

The structure of DDBC control system is common to DSCL control and includes energy-loop and two current-loops (for network currents and for circular current). DDBC control system [6] is shown in Fig. 4.

#### IV. TOPOLOGY COMPARISON

The application of both described MMCCs for electrical drive supply causes additional requirements to the semiconductors and capacitors as well as to the control structure. The total semiconductor cost correlates to the sum of the peak- and RMS currents of the switches. The total capacitor cost is determined by the sum of the capacitor energy ripples and the sum of the rms capacitor currents at steady-state operation. The energy control dynamics put an additional requirement of the dynamic capacity reserve and is considered as well.

In this paper given comparison is realized for power supply of 17 kW synchronous motor from 0.4 kV AC-grid with 50 Hz frequency. The simulation results for capacitor current comparison are shown in the Table I.

Motor electrical frequency, Hz	rms capacitor currents, A		
	DDBC	BTB-DSCL(DSCL1)	BTB-DSCL(DSCL2)
50	4.31	1.01	4.4
70	4.18	1.42	4.62
100	4.61	2.03	4.92
120	4.48	2.44	5.09
150	4.56	3.05	5.36
170	5.86	3.45	5.4

It is observed that BTB-DSCL capacitors are asymmetrically loaded by high velocity ranges. That allows to compensate costs of submodules, which number is almost twice more than in DDBC.

#### REFERENCES

- [1] H. Akagi, „Classification, terminology, and application of the modular multilevel cascade converter (MMCC),“ IEEE, 2011.
- [2] K. Ilves, L. Bessegato and S. Norrga, „Comparison of Cascaded Multilevel Converter Topologies for AC/ AC Conversion,“ IPE Conference, 2014.
- [3] N. Mukherjee; P. Tricoli, “A new state of charge control of modular multilevel converters with supercapacitors for traction drives. in: 2015 IEEE Energy Conversion Congress and Exposition”, Montreal, QC, Canada, S. 3674–3680.
- [4] K. Thantirige; Rathore, K. Akshay; S. K. Panda; G. Jayasignhe; M. A. Zagrodnik; A. K. Gupta, “Medium voltage multilevel converters for ship electric propulsion drives”, in: 2015 International Conference on Electrical Systems for Aircraft, Railway, Ship Propulsion and Road Vehicles (ESARS), Aachen, Germany, S. 1–7.
- [5] J. Kolb; F. Kammerer; M. Gommeringer; M. Braun (2015), „Cascaded Control System of the Modular Multilevel Converter for Feeding Variable-Speed Drives“, in: *IEEE Trans. Power Electron.* 30 (1), S. 349–357. DOI: 10.1109/TPEL.2014.2299894.
- [6] L. Baruschka and A. Martens, „A new 3-phase direct modular multilevel converter,“ Proc. 14th EPE, 2011.
- [7] J. Kolb, „Optimale Betriebsführung des Modularen Multilevel-Umrichters als Antriebsumrichter für Drehstrommaschinen,“ Karlsruhe: Karlsruher Institut für Technologie, 2013.
- [8] L. Baruschka and A. Martens, „A new three-phase ac/ac modular multilevel converter with six branches in hexagonal configuration,“ Industry Applications, IEEE Transactions, 2013.
- [9] D. Karwatzki, L. Baruschka and A. Martens, “Survey on Hexwetter Topology – A Modular Multilevel Converter,” International Conference on Power Electronics-ECCE, June 2015. 1989.

# Investigation and Analysis of a Passive Filter to Suppress Conducted Electromagnetic Interferences

M. Sc. Wared Mualla

Department of Power Electronics and Control Group  
TU Ilmenau  
Ilmenau, Germany  
wared.mualla@tu-ilmenau.de

Univ.-Prof. Dr.-Ing. habil. Jürgen Petzoldt

Department of Power Electronics and Control Group  
TU Ilmenau  
Ilmenau, Germany  
juergen.petzoldt@tu-ilmenau.de

**Abstract—**Electromagnetic interferences can badly affect the behavior of other electrical and electronical devices in an electric vehicle, e.g. breaking system, navigation system. They may even damage some sensitive components. Thus, these interferences should be suppressed and in ideal case totally eliminated. For this reason there are many choices: filtering, shielding, etc. In this paper, a filter concept has been introduced to be applied in the motor drive circuit. It should give the needed attenuation to keep the electromagnetic emissions lower than the standard levels. A simulation model based on a cascaded circuit has been used.

**Keywords—**EMI filter; differential mode; common mode; electric vehicle; cascaded circuit; CISPR-25

## I. INTRODUCTION

Due to increasing of gas and oil prices and running out of fossil fuel, the interest of using clean renewable energy sources has increased in the last few decades [1][2]. This can partially introduce a solution for the pollution problem as electric vehicles (EVs) continuously become dominant in the industry of transport. Anyway, it does not matter if the EV is purely electric or hybrid, it needs a certain type of converter to drive its motor.

In the conventional converters, the DC voltage is going to be changed from one level to another level depending on the modulation ratio. A pulse width modulation (PWM) has been widely used to control the electronic switches [3]. This active process of switching produces electromagnetic interference (EMI). This EMI depends mainly on the value  $dv/dt$ . To reduce this effect, there can be taken into consideration two possibilities: one is to let the voltage rises up in more time, which can produce extra losses in the electronic switches. The other is to make the voltage less. This can be realized by cascading many steps to form the desirable voltage.

However there will be always unwanted signals which need an additional filter to be eliminated.

## II. THEORETICAL PRINCIPLE

### A. Fourier Transformation

Every periodic signal  $x(t)$  can be written as summation of its mean value, its fundamental signal and an infinite number of harmonics [4]. Mathematically it can be written as (1).

TABLE I. Standard limits defined by CISPR-25 for the band of frequency [150 kHz – 1 MHz] and for the classes 1,2 and 3

Class	Frequency band [0.15 – 0.3] MHz		Frequency band [0.53 – 1.8] MHz	
	$dB\mu V$	$mV$	$dB\mu V$	$mV$
1	110	316	86	20
2	100	100	78	7.9
3	90	31.6	70	3.2

$$x(t) = F_0 + \sum_{n=1}^{\infty} \left[ a_n \cos\left(\frac{2\pi n}{T} t\right) + b_n \sin\left(\frac{2\pi n}{T} t\right) \right] \quad (1)$$

Where  $F_0$  is the mean value of the signal  $x(t)$  over one period  $T$ .

It is meaningful in EMC researches to represent the frequency spectrum of voltage and current signals using the units  $dB\mu V$  and  $dB\mu A$  respectively.

### B. Standard Limits

The international standard limits, which the spectra should not exceed, depend on the frequency range, type of class, the usage of the electrical device, etc. This paper considers that the cascaded circuit is going to be used inside an electric vehicle to drive an electrical motor. Thus, the limits are specified by CISPR-25 [5]. The frequency range [150 kHz – 1 MHz] is going to be considered in this paper. These limits are defined in  $dB\mu V$  and  $mV$  depending on their classes in TABLE I; (A maximal value receiver has been used).

### C. Cascaded Circuits

The harmful effects of using power electronics are highly related to the value  $dv/dt$ , which can be lowered by reducing the voltage jump value in each on/off operation [6]. To keep the device working at the same power level, a cascaded circuit using non-isolated converters was introduced. The Spectrum seems to be more effective than the one with one high voltage jump.

Although a cascaded circuit has been used, the produced spectrum still does not satisfy the standard limits over the frequency range. Therefore, an EMI filter concept is needed.

## III. FILTER DESIGN

In order to suppress the unwanted harmonics of a signal, a passive filter is used. It is a favorable solution to compare it

with the shielding and active filters, which are commercially expensive. For a cascaded circuit, an EMI-filter is needed for each voltage step as Fig. 1 shows. The filter design depends on the position, where it is going to be placed, i.e. what impedance level is on its input and output [7]. TABLE II shows this principle of designing a filter.

The proposed filter consists of two steps each with a connection to ground; the first is connected internal in the cascaded full-bridge DC-DC converter step, and the second is connected external with other second filter steps and then to main earth of the vehicle (chassis or vehicle body), Fig. 1.

Filter parameters are mostly defined by using the *trial and error* method [8]. Bode diagram (Magnitude in dB) of the filter determines the offered attenuation for both differential and common mode (DM and CM) at each frequency. This filter can provide attenuation more than 35 dB and 43 dB for common mode and differential mode interferences respectively, considering the range from 150 kHz.

#### IV. SIMULATION RESULTS

The filter was tested simulative using Matlab/Simulink and Matlab/SimScape on an open load circuit. Different voltage types can be measured. This paper takes the symmetric (DM) and non-symmetric (CM) voltages under consideration.

Conducted CM interferences are going to be tracked using the measurements of non-symmetric voltages at the output of each step of the cascaded circuit i.e. the red lines in Fig. 1. Conducted DM interferences are measured between *Line1* and *Line2* in Fig. 1.

Differential mode interferences after using the proposed filter have been distinctly reduced as Fig. 2 shows. On the other hand, interferences of common mode (which are measured at the first two red conductors of Fig. 1) are shown in Fig. 3.

TABLE II. Main principle of designing a passive EMI-filter

Suitable filter design related to input and output impedances		Suitable filter design related to input and output impedances	
LOW		LOW	HIGH
LOW		HIGH	HIGH

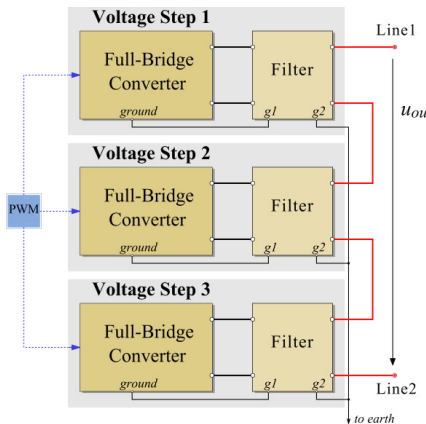


Fig. 1. Cascaded circuit with EMI-filters

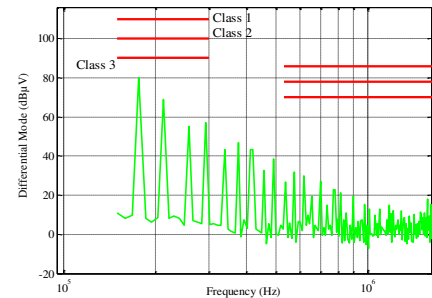


Fig. 2. Differential mode after using the EMI filter

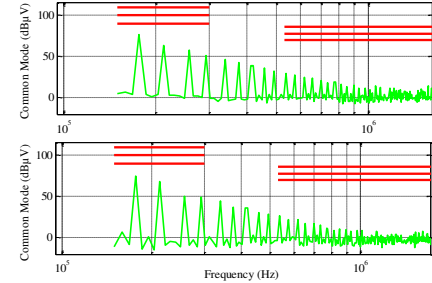


Fig. 3. Common mode measured at the first two conductors after using the EMI filter

#### V. CONCLUSION

For a proper work of an electric vehicle, radiated as well as conducted emissions caused by electronic devices should be in ideal case eliminated. A filter was introduced to suppress conducted interferences. A cascaded circuit with non-isolated full-bridge converters was used. Simulation was made on an infinite load. The results of simulation show that the proposed EMI filter can effectively reduce both common and differential mode interferences in the case of open circuit. The conducted emissions after using the filter satisfy the international standard regulations specified by CISPR-25.

#### REFERENCES

- [1] M. Ehsani, Y. Gao, and A. Emadi, "Modern electric, hybrid electric and fuel cell vehicle fundamentals, theory and design," 2nd ed., New York, NY, USA: CRC Press, 2010.
- [2] A. Nahavandi, M.T. Hagh, M.B.B. Sharifian, and S. Danyali, "A nonisolated multiinput multioutput DC-DC boost converter for electric vehicle applications," IEEE Transactions on Power Electronics, vol. 30, no. 4, pp. 1818-1835, April 2015.
- [3] D.M. Bellur, and M.K. Kazimierczuk, "DC-DC converters for electric vehicle applications," 2007 Electrical Insulation Conference and Electrical Manufacturing Expo, Nashville, TN, 2007, pp. 286-293.
- [4] K.L. Kaiser, "Electromagnetic Compatibility Handbook," Washington: CRC Press, 2004.
- [5] DIN EN 55025 (VDE 0879-2): "Fahrzeuge, Boote und von Verbrennungsmotoren angetriebene Geräte – Funkstörleigenschaften – Grenzwerte und Messverfahren für den Schutz von an Bord befindlichen Empfängern," (IEC/CISPR 25:2008), VDE, 2009.
- [6] W. Mualla, „EMC-Filter analysis for an electrical circuit cascade,” Technical University of Ilmenau, 2015.
- [7] D. Stoll, "EMC: elektromagnetische Verträglichkeit," Berlin: Elitra-Verl., 1976.
- [8] A. Nagel, and R.W. De Doncker, "Systematic design of EMI-filters for power converters," Industry Application Conference, 2000. Conference Record of the 2000 IEEE, Rome, 2000, pp. 2523-2525 vol. 4.

# Interval criterion of the steady-state of the transient in the measuring circuit

Aleksey Lupachev

National Research  
University "MPEI"

Moscow, Russia

LupachevAA@yandex.ru

Igor Sapelkin

National Research  
University "MPEI"

Moscow, Russia

civ9019@mail.ru

**Abstract**—This paper describes the criterion of the end of the transient in the measuring circuit. The circuit model is represented by a dynamic element of the first order. The dependence of the critical value of the maximum time constant of the measuring circuit is found.

**Keywords**—measuring circuit; transient analysis; criterion of the end of the transient; duration of the observation interval; the critical time constant;

## I. INTRODUCTION

The dynamic measurement (DM) of the constant physical value by applying step input to the inertial measuring circuit (MC) at time  $T_0 = 0$  implies a specific criterion of the moment  $T_s$  of the end of the transient and the setting time. In this case steady-state value of the transient yields measuring information. Determining the transient time, i.e., the steady-state is an urgent task for many branches of technology.

## II. MEASURING CIRCUIT MODEL

The measuring object model in the form of the transient response that is represented as the sum of the exponents is very important for DM in practice. The dynamic element of the first order with the largest time constant is dominant among the components of this sum [1].

This property is common in a large number of natural processes. They are based on the fact that the deviation will be reduced, tending to zero or to a new steady-state value during relaxation after the disequilibrium in the system.

The steady-state value  $A_\infty$  of the transient signal isn't known a priori in the measuring task and is determined in the measuring experiment. Therefore it's impossible to determine the current dynamic error  $\Delta_{DYN}(t) = A(t) - A_\infty$  and being calculated only a posteriori. Thus it's impossible to calculate in advance the time  $T_{TR}$  of the end of the transient with a given dynamic error.

## III. INTERVAL CRITERIA OF THE END OF THE TRANSIENT

The standard GOST 3484.1-88 [2] considers the criterion of the end of the transient in the absence of a priori information of the transformer windings time constant and of the steady-state operating current in the measuring circuit: “*The steady-state reading of the instrument should be considered as a reading that varies by no more than 1% of the counted value for at least 30 seconds.*” The time constant of the power transformer

(PT) is changed in the range [10...500] seconds depending on the rated power of PT (from 10 to 100000 KVA) [3].

The approximate thermal time constants of PT heating with natural oil cooling (for transformer rated capacity ranging from 0.001 to 6.3 MVA) are assumed to be equal to 2.5 or 3.5 hours, [4], or from 0.5 to 5 hours [5].

Dry-type power transformers have large thermal time constants – up to 10 hours. The steady-state temperature is achieved for this type of transformers if the temperature change is less than 2K or 2% per hour [6]. Instrument transformers have time constants of from 0.5 to 50 hours. During the heating test temperature reaches a steady state, if its change has fallen below 1K per hour [6].

These criteria that can be defined as the interval ones use information about the allowable value of the transient signal change during a predetermined observation interval. Interval criteria imply that results are independent from the time constant of the MC. The derivative of the transient is assumed to be monotonic and absolute decreasing.

A constant duration of the  $j$ -th observation interval of the transient dynamics is designated as  $\Delta T_O(j)$ , as shown in Fig. 1.

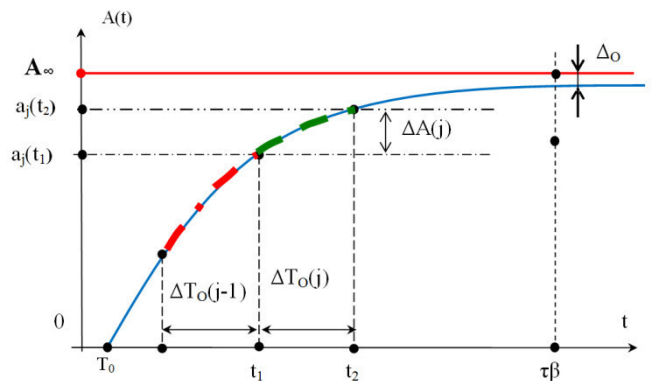


Fig. 1. Position of the observation interval on the transient curve

According to the criterion the allowable change of the signal  $A(t)$  at this interval is  $\Delta A_O(j)$ :

$$\begin{aligned}\Delta T_O(j) &= \Delta T_O = t_2 - t_1, \\ \Delta A_O(j) &= \Delta A_O = B\% \Delta a / 100,\end{aligned}\quad (1)$$

where  $t_1$  – the start of the  $j$ -th observation interval;

$t_2$  – the end of the j-th observation interval;

$\Delta a$  – the absolute value of the maximum deviation; It is taken as a sampled transient signal  $a_j(t_1)$  at the moment  $t_1$ ;

$B\%$  – maximum relative deviation that is appointed by the criterion,  $B\% = 1\%$  [2].

The time of the transient end  $T_{TR,INT}$  that is defined by the interval criterion can be attributed to the beginning  $t_1$  and to the end  $t_2$  of the observation interval  $\Delta T_O$ . The relative increment of the transient signal in the time  $\Delta T_O$  can be determined for both ends of the j-th observation interval as follows:

$$\begin{aligned}\rho_{j1} &= 100[a_j(t_2) - a_j(t_1)]/a_j(t_1) \\ \rho_{j2} &= 100[a_j(t_2) - a_j(t_1)]/a_j(t_2),\end{aligned}\quad (2)$$

thus:  $\rho_{j2} = \rho_{j1}/v_j$ ,  $v_j = a_j(t_2)/a_j(t_1) > 1$ .

The steady-state occurs when the criterion  $B\% \geq \rho_{jk}$  is fulfilled at the j-th interval at the moment  $T_{TR,INT,2}$ , where  $T_{TR,INT,2} = \min\{\arg[B\% \geq \rho_{j2}]\}$ .

Since the observation interval contains  $M$  sampling intervals, the settling interval fits up to  $j^*M$  overlapping observation intervals shifted by  $\Delta T_D$  (for example,  $\Delta T_D = 1\text{s}$ ).

#### IV. INTERVAL CRITERION INTERPRETATION

Reference [15] transforms interval criterion for linear MC: "no more than 1% of the counted value for at least 30 seconds." [2]:

$$B\% \geq 100[a_j(t_1 + \Delta T_O) - a_j(t_1)]/a_j(t_1) \quad (3)$$

Fig. 2 shows transient curves with different values of  $\tau$  and dedicated observation intervals for them, satisfying the interval criterion (3).

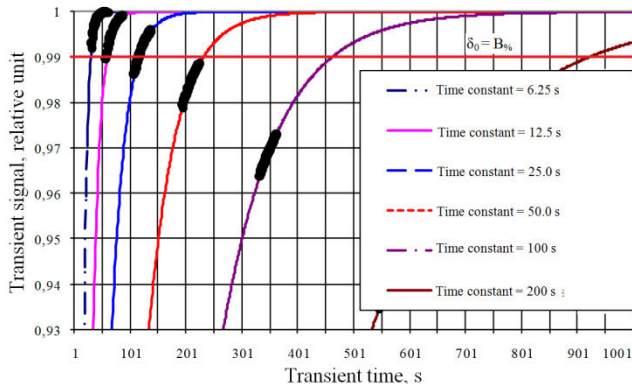


Fig. 2. Observation interval position on the transient curves with different time constants

The position of these intervals beyond allowable dynamic error illustrates the fact that the interval criterion (3) doesn't guarantee the steady-state at this interval with the error  $\delta_0 = B\%$  required by this criterion.

The relative errors are designated a posteriori at the ends of observation interval as: at the beginning –  $\delta_1(\tau, j)$  and at the end –  $\delta_2(\tau, j)$ :

$$\delta_1(\tau, j) = 100[A_\infty - a_j(t_1)]/A_\infty; \quad (4)$$

$$\delta_2(\tau, j) = 100[A_\infty - a_j(t_2)]/A_\infty. \quad (5)$$

Table 1 presents the error  $\delta_2(\tau, j)$  at the end of the observation interval for the analyzed range of  $\tau$  change. It's approximated by a linear dependence with accuracy no more than  $\pm 1\%$  of:

$$\delta_2^*(\tau, j) = \zeta\tau - 0.328, \%, \text{ when } \tau \geq 25 \text{ s}, \quad (6)$$

where  $\zeta = 0.0299 \text{ %/s}$ .

TABLE I. THE ERROR AT THE END OF THE OBSERVATION INTERVAL

$\tau, \text{s}$	6.25	12.5	25	50	100	200
$j(\tau)$	2	3	4	8	12	19
$\delta_2(\tau, j), \%$	0.0067	0.094	0.417	1.16	2.68	5.64
$T_{TR,INT,2}, \text{s}$	60	87	137	233	362	575

#### V. LIMITATIONS OF THE INTERVAL CRITERION

Thus the limitation of the interval criterion was found when MC time constant exceeds a certain critical  $\tau_{CR}$ . This constant can be found from (6) to the first approximation equating  $\delta_2^*(\tau, j)$  to the allowable relative error at the end of the interval, i.e.,  $\delta_2^*(\tau_{CR}, j) = 1\%$ . So  $\tau_{CR} = 44.4 \text{ s}$ . The relation  $\Delta T_O = \lambda \tau_{CR}$  between the observation interval duration and the critical value of the maximum time constant due to the interval criterion can be shown. This ratio is  $\lambda = 30\text{s}/44.4\text{s} \approx 0.68$ .

#### VI. SUMMARY

It was found that the interval criterion that is recommended by the modern standards doesn't define the required moment throughout the range of possible time constant of the MC model.

The relation between the transient observation interval duration and the critical value of the time constant is found, beyond which the reliability of the criterion isn't provided.

#### REFERENCES

- [1] V. Didenko, A. Moskvichev, RF patent № 2491559, "Method for determining the resistance and leakage inductance of the primary winding of the voltage transformer," G 01R27/26, 2013.
- [2] The Transformers. Test methods and measurements, IPK Publishing house of Standards, Moscow, 1996.
- [3] A. Lupachev, I. Sapelkin, N. Serov, Y. Behtin, A. Shostak, "Technology of constant physical quantity measurement," 25-th National Scientific Symposium with international participation "METROLOGY and METROLOGY ASSURANCE 2015", Sozopol, Bulgaria, September 2015, pp. 163-174.
- [4] A.V. Kabyshev. The supply of the objects. Part 1. Calculation of electrical loads, heating conductors and electrical equipment. Tomsk: Publishing house TPU. 2007.
- [5] IEC 60076-2. Power transformers: Temperature rise, February 2011.
- [6] Z. Godec, "Steady-State Temperature Rise Determination," Automatika, 33, 1992, pp. 129-134.

# Measuring module for power quality meters

I.T. Galiev

National Research University “Moscow Power Engineering Institute”  
Moscow, Russian Federation  
galiev.ilyas@gmail.com

**Abstract—**This article is about the module for measurement of power quality (MM PQ). This module can be used for design and development of power quality meters (PQM).

**Keywords—**power quality; measuring module

## I. INTRODUCTION

Currently the solutions of modules for power quality measuring are known. For the first time the MM PQ was developed by department IIT of the «NRU «MPEI» in 2005 as an initiative work of group of experts. The idea was to make invariant the basic hardware and software node of the PQM – to make the finished product for construction of PQM for any purpose.

## II. FIRST MEASURING MODULE

In fact, the MM PQ is the highly intelligent measuring transducer with complicated software. The use of the MM PQ in the power quality meters' design has a number of benefits. For example, it reduces the design time and the cost of the developed PQM, also it's relatively easy to extend the nomenclature of PQM. The main advantages of the MM PQ: low cost in mass production, compact dimensions, high reproducibility of the metrological characteristics, high functionality, minimum consumption. Typical structure of MM PQ is shown in Fig.1.

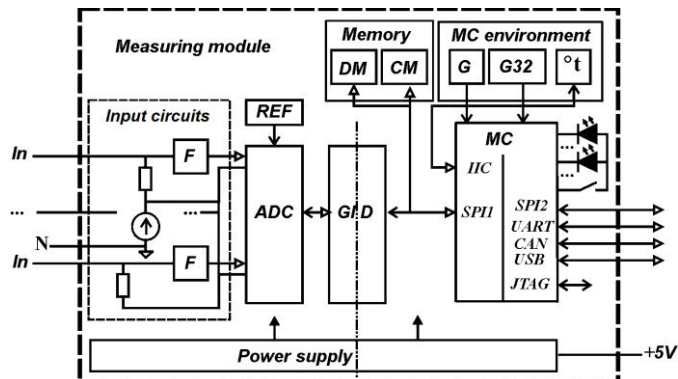


Fig. 1. Typical structure of MM PQ

## III. MEASURING MODULE FOR RESPONSIBLE USE

If we use the MM to build meters designed for use in monitoring mode (long-term continuous measurement), as well as in other critical cases, MM has special demands on reliability. The process of monitoring, as is known, involves the use of low-maintenance equipment. It is important that, in

addition to the functional reliability of the PQM, it is necessary to ensure the reliability of metrology. In other words, the accuracy characteristics of the measurements results must comply with the requirements of existing standards.

The task of increasing functional and metrological reliability in the design of the MM becomes complicated, because of the tough operating conditions of the final product (a wide range of operating temperature, ambient humidity, electromagnetic interference generated by electric power and possibly radio equipment).

A new direction in the development of the MM PQ is to create it for development the most responsible PQM. Functional and metrological reliability of these products, often used in harsh environments, is the main performance indicator.

In order to maintain the necessary metrological characteristics over a wide range of operating, bit capacity (and accuracy) of the ADC should be chosen with the metrological margin (at least 16 effective digits). For current design the ADC of family ADAS302 of Analog Devices company was selected. The selected ADC – is the modern product of AD company. It is intended for use in industrial application conditions. For this purpose, in particular, the ADC has a wide range of measured voltage (10,24 V) and a double protection for overvoltage on the input.

As a microcontroller (MC) there was selected the dual-core MC of TI company: Hercules TMS570 LS3134APGE QQ1. These MC are designed for responsible in terms of reliability, industrial and automotive applications.

## IV. FURTHER WORK

The direction of further work: to research all the sources of unreliability for developed MM PQ, to find the best solutions in circuit design, to find the best electronic components for development. Also technological requirements will be developed. Particular attention will be paid to the software design. There are following requirements for the software: the maintenance of the entire infrastructure of MM PQ; processing input data in real time in order to calculate the PQ values; ensuring required metrological characteristics in operating conditions of environment; high availability and rapid self-healing of failed states.

## REFERENCES

- [1] P.Makarychev - Means of measuring power quality, 2 Russian School-Seminar of Young Scientists and Specialists: Energy Conservation - Theory and Practice, October 2004, MPEI, pp. 47-52.
- [2] A. Shatohin, P.Makarychev - Recoorder of 3-phase AC networks, Electronics News №6 (86), 2010, pp. 16-20

# Novel Shack-Hartmann based surface characterisation with extended spatial range and resolution

M. Walther, K. John, S. Schramm, D. Baumgarten  
Institute for Biomedical Engineering and Informatics  
Technische Universität Ilmenau  
Ilmenau, Germany  
maximilian.walther@tu-ilmenau.de

**Abstract—** This contribution presents a new measurement method that applies a wave front measurement with a Shack-Hartmann sensor for the characterisation of surface roughness and waviness. This new approach offers the opportunity to characterise a flat surface area.

The method includes a variable iris aperture that increases the spatial range and resolution of the spot's intensity profile of the Shack-Hartmann image.

A first demonstrator was built as proof of concept and the first results have shown that the mean intensity of the images increases with increasing aperture size. The slope of the intensity is steeper for surfaces with lower roughness.

**Keywords—** surface characterisation, roughness, waviness, optical sensor, Shack-Hartmann- Sensor

## I. INTRODUCTION

Characterising technical surfaces is crucial for quality assurance in manufacturing in many fields. Surface roughness and waviness are the important parameters for describing shape deviations. The measurement, however, is often cumbersome and does not allow for 100% testing in most production processes. Especially fine grinded and lapped surfaces with a very low roughness and low form deviations require precise testing methods that are not suited for industrial environments.

Optical measurement methods, such as interferometer technologies [1], can gather the exact surface profile to receive the waviness but have too low lateral resolution for roughness measurement. Other optical technologies, like angle-resolved scattering (ARS) or total-integrated scattering (TIS) measurement analyse scattered light [2-4] which can be used to deduce the surface roughness usually at a single surface point. Non-contact methods don't cause damage to the surface, thus they are suitable for 100% testing in manufacturing if they are fast enough to keep up with the production throughput.

## II. METHODS

This contribution presents a new measurement method that applies a Shack-Hartmann (SH) wave front sensor to characterise both, surface roughness and waviness, in a single measurement. The integrated system analyses the wave front that is reflected from a flat surface under test. Thus, it can provide spatially resolved information from an extended sample area in an optical measurement. The fast and non-contact method prevents damage to the sample and can detect local defects on a surface, which makes it well suited for industrial applications. The proposed application is based on a related system published previously by the Institute for Biomedical Engineering and Informatics in Ilmenau [5]. This system characterises stray light from the human eye with a SH sensor.

P. Schikowski, A. Keading  
GMC Systems mbH  
Ilmenau, Germany

Figure 3 illustrates a schematic of the sensor system with the directly reflected light path in red and the scattered light path in green. The illumination is realised by a homogeneous plane wave. A 4f-relay system images the reflected light onto the SH wave front sensor. The analysis of the deviation of the spots from their reference positions yields information about the surface waviness. Simultaneously, the dimension and shape of each spot carries information about the roughness that causes stray light [4] at the respective surface point. A variable iris aperture is placed at the common focal point of both lenses of the relay system in order to increase the resolution of the spots' intensity profile and the measurable field angle. By changing the aperture diameter, the maximum detectable scattering angle can be controlled. For small diameters, only the light of the direct reflection (red path) is allowed to pass. Obtaining SH images with increasing aperture sizes results in a stack of images with increasing scattering light intensity (green path). This allows for reconstruction of the intensity profile of scattering light that is contained in the angular step between the corresponding aperture diameters. Thus, even if the spot diameters exceed their corresponding pixel area on the sensor, the intensity profile can be reconstructed realistically. The angular measurement range is hence extended beyond the spatial limits of the SH sensor.

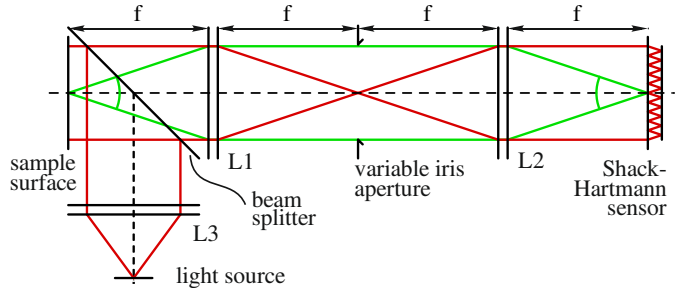


Figure 3. Schematics and ray path of the measurement system. Directly reflected light is shown in red and scattered light in green.

## III. RESULTS

A first demonstrator was built as proof of concept and to further investigate the performance of the measurement method. The setup uses two identical achromatic lenses (L1 and L2) in a 4f layout and a red (660 nm) fibre laser as light source. It can detect scattering light up to a field angle of 17.6°, limited by the numerical aperture. A high-quality mirror with a very low roughness (10.5 Scratch-Dig specification) serves for calibration purposes. Several metallic surfaces with a roughness between  $R_a = 0.0289 \mu\text{m}$  and  $R_a = 0.20805 \mu\text{m}$  were tested.

In the evaluation of the SH point image several parameters proved useful to characterise the sample surface. The overall intensity of the image, for example, is best expressed by

averaging the intensity of every individual SH spot and then taking the average of all spots. The dependence of the resulting value, denoted Tile mean mean, from the aperture diameter is depicted in Figure 4. It increases with increasing aperture size. The slope is steeper for surfaces with a lower roughness. However, the first results have shown that the behaviour of such parameters is diverse for different surface roughness and manufacturing processes.

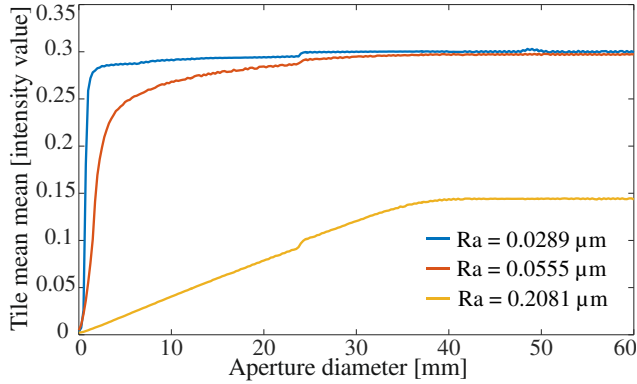


Figure 4. Average intensity of each SH spot averaged over the whole field (tile mean mean) in dependence of the aperture diameter for three sample surfaces with different roughness values.

#### IV. CONCLUSION

The new surface characterisation approach using a SH sensor offers new opportunities in surface analysis. It provides a combination of two different modalities to characterise roughness and waviness within one system for a flat part of a metallic surface. Other optical methods like confocal microscopy, focus variation or angle resolved scattering method

are only capable of pointwise measurements. Contact methods like tactile measurements are slow and limited to measurement of a short line where they can cause damage to the sample surface. The method presented here can overcome these limitations to enable faster tests and higher throughput for industrial quality assurance of surfaces.

In future work, the relation between surface roughness and image parameters will be investigated in more detail. Furthermore, the proposed method will be expanded to the characterization of roughness and waviness of curved surfaces.

#### V. ACKNOWLEDGEMENTS

This research was funded by the German Federal Ministry of Economic Affairs and Energy according to a decision of the German Federal Parliament (ZIM project RauMuS, grant KF2250118UW4).

#### REFERENCES

- [1] Dörband, B., Gross, H., Müller, H.: *Handbook of optical systems: Metrology of optical components and systems*. Weinheim: Wiley-VCH, 2012. – ISBN 3-52740-381-7
- [2] Duparré, A., Ferre-Borrull, J., Gleich, S., Notni, G., Steinert, J., Bennett, J.M.: *Surface characterization techniques for determining the root-mean-square roughness and power spectral densities of optical components*. Applied Optics, 2002, Vol. 41, No. 1, pp. 154-171
- [3] Schröder, S., Duparré, A., Corriand, L., Tünnermann, A., Penalver, D.H., Harvey, J.E.: *Modeling of light scattering in different regimes of surface roughness*. Optics Express, 2011, Vol. 19, No. 10, pp. 9820-9835
- [4] Stover, J.C.: Optical scattering, measurement and analysis. Bellingham, Washington, SPIE Optical Engineering Press, 1994. – ISBN 0-8194-1934-6
- [5] Schramm, S., Seifert, B.-U., Schikowski, P., Prehl, J., Kunert, K.S., Blum, M., Kaeding, A., Haueisen, J.: *A modified Hartmann-Shack aberrometer for measuring stray light in the anterior segment of the human eye*. Graefe's archive for clinical and experimental ophthalmology, 2013, Vol. 251, No. 10, pp. 1967-1977

# Detection of Anomalies In Individual And Group Movement Within Dynamic Environment

E. Novikova, E. Fedotov, I. Murenin

Computer Science Department, Saint Petersburg Electrotechnical University "LETI"

Saint Petersburg, Russian Federation

novikova.evgenia123@gmail.com, fedotov\_e1290@mail.ru, imurenin@gmail.com

**Abstract**—The understanding of the life patterns in trajectories of individuals or groups is necessary for a better management in general and for the mitigation of potential security risks. In this paper we focus on detecting anomalies in trajectories and present the concept of anomalies detection in individual movements based on property of individual path integrity relative controlled zone.

**Keywords**— trajectory analysis, life patterns and features, anomaly detection, path integrity.

The sets of moving point data sets are relatively new type of spatial data source [1]. The amounts of them are constantly increasing due to the availability and, therefore, wide usage of the mobile devices with positioning capabilities. They can be collected by mobile phones, cars, proximity card readers, video cameras at public places, and checkpoints using RFID. The points can be obtained on regular basis or irregularly; they can be acquired by the moving object itself or by an external observing sensor.

Generally, the set of moving points or trajectory consists of sequence of points with coordinates with timestamps: <x,y,t>. In some cases it can be complemented by additional data, for example, user ID, checkpoint status, velocity, temperature, etc. Such trajectories are analyzed to extract life patterns of the studied objects or phenomenon [1,2]. They are also analyzed to reconstruct constraints existing in the underlying environment, for example, rules or security policies, restricting access to the specified zones, or infrastructure available to the individuals, i.e. places of interests, ATMs, etc [1]. Another important application of the trajectory analysis is the generation of the features of the object life pattern to detect possible anomalies in observing data sets [3]. The root of the detected anomalies can be different: they can be rather harmless like a driver encountering problems in the unknown place, or they can be signs of possible crimes, for example an employee not observing company security policies.

In this paper we focus on detecting anomalies in trajectories and present the concept of anomalies detection in individual movements based on property of individual path integrity relative controlled zone. The notion of the path integrity for the individual or group of individuals is described in terms of high-level features extracted from the life patterns and therefore depending on specific subject domain. However in general case this property defines that an object can enter into the monitored zone only from adjacent zones, the zone check in and check out of the individual are ordered in time,

the density of the zone visiting is characteristic to the type of the individual.

In the research we investigate two use cases both dealing with individual movements in public places. In the first use case the dataset describes the movement of the visitors of the typical modest-sized amusement park hosting thousands of visitors each day [4]. The available data has format <timestamp, visitor id, x, y, checkpoint status>. The analysis of the data set showed that the major anomalies were connected to the integrity breach of the pairs of the check in-check out status of the park object and time of visiting of it. Thus in this case the path integrity of the individual relative zone is described in term of the integrity of the check-in and check-out pair, the duration of the visitor's staying and time of the visit. The second use case refers to the movements of the employees of the organization [5]. The company staff members are required to wear proximity cards while in the building. The available data can be transformed to the format <timestamp, employee ID, department, monitored zone>. The primary analysis of this data set showed that according to life patterns the path integrity depends on the zones adjacent to the controlled zone, probability of visiting specified zone by the employee of the given department, density of the visiting by the employee of the given type and duration of the visiting.

Focusing on the state of the controlled zones defined by individual integrity path has certain benefits relative monitoring movements of each object within controlled zone. The first and the most important one is the possibility to reduce data dimension provided to analyst. Instead of monitoring movements of all visitors or employees which quantity can exceed thousands the approach allows focusing on the state of the monitored zones which number is significantly less than number of visitors. This feature also allows designing rather simple visualization models without information overload. Tracking each individual is also very computational consuming task. The detecting anomalies in the suggested approach can be easily distributed.

## REFERENCES

- [1] A.Millonig, G.Maierbrugger. Identifying unusual pedestrian movement behavior in public transport infrastructures. In: Proc. of Movement Pattern Analysis Workshop (MPA2010), Zurich. Pp.106-110. 2010.
- [2] S. H. Chavoshi, et al. Movement Pattern Analysis Based on Sequence Signatures. ISPRS International Journal of Geo-Information 2015. Vol. 4, pp.1605- 1626.
- [3] M. Verschelle, T. Neutens, M. Delafontaine, N. van de Weghe. The use of Bluetooth for analysing spatiotemporal dynamics of human movement at mass events: A case study of the Ghent Festivities. Appl. Geogr. 2012, 32, 208–220.
- [4] 2015 VAST Challenge: MC1, http://vacommunity.org/2015+VAST+Challenge%3A+MC1, retrieved on 13.05.2015
- [5] 2015 VAST Challenge: MC2, http://vacommunity.org/2016+VAST+Challenge%3A+MC2, retrieved on 13.05.2015.

# Optical sensors for spacecraft attitude estimation

I. Kruzhilov

Dept. of Applied Mathematics  
Moscow Power Engineering Institute  
Moscow, Russia  
Ivan.Kruzhilov@daad-alumni.de

A. Chernetsov

Moscow Power Engineering Institute,  
Moscow, Russia  
chernetsovam@mail.ru

**Abstract**—Optical sensors such as star trackers, Earth and Sun sensors are crucial for spacecraft GUIDANCE AND CONTROL. Star trackers provide the most precise attitude estimation. Multiple-head star trackers have an advantage over single-head star trackers because they ensure equal estimation accuracy for all three Euler angles.

**Keywords**—star tracker; quaternion; satellite; orientation;

## I. INTRODUCTION

A spacecraft angular attitude requires continual adjustment to counteract torque moment caused by the Sun light pressure, the Earth magnetic field, gravitation and aerodynamic forces. Various types of momentum wheels and propulsions are used for the correction of the spacecraft torque moment. The estimation of a spacecraft current angular attitude is crucial for its guidance and control. Optical sensors such as star trackers, Earth and Sun sensors provide precise spacecraft attitude estimation with respect to an inertial frame.

## II. EARTH AND SUN SENSORS

Earth sensors measure the direction to the Earth and Sun sensors measure the direction to the Sun respectively. A sun sensor has a wide FOV (field of view) and consists of two orthogonal photodiodes protected by a cover glass. Earth sensors work in the infrared region to be operable in the dark side of the Earth. Both sensors provide 1-2 arcmin accuracy of the direction vector, but have a low accuracy in the torsion angle estimation. Earth and Sun sensors are useful for the missions not requiring precise attitude estimation e.g. the Russian navigation system GLONASS.

## III. STAR TRACKERS

The Star trackers are the most precise sensors providing spacecraft attitude estimation. They are being used for a variety of satellites like cubesats or big satellites for long-life missions.

A star tracker consist of an optical system, a photo receiver (usually CCD or CMOS matrix) and a computing block capable executing advanced algorithms. A typical spectral response of a star tracker lies between 400 and 1000 nm. A baffle protects a star tracker from the sun light and improves its exclusion angle. The star tracker FOV varies from 1° to 30°.

The tracker optical system should be manufactured of radiation-hard glass to prevent a photo receiver from the harsh space environment. Spaceborne electronics is used for the star tracker design for the same reason. The radiation is extremely intense for the high elliptical orbits crossing van Allen radiation belts.

Star trackers determine the attitude of a satellite by analyzing the placement of the surrounding stars. The key

point of the determination is the star identification algorithm seeking for the match for stars in the FOV and the onboard catalog. Spacecraft attitude estimation provided by a star tracker results in Euler angles (roll, pitch, yaw), a rotation matrix or a normalized quaternion.

## IV. MULTIPLE-HEAD STAR TRACKERS

The attitude estimation accuracy of roll angle (rotation around optical axis) exceeds the estimation of pitch and yaw rotation angles. Due to the application of several optical heads mounted in different directions a multiple-head star tracker doesn't possess this drawback. Examples of multiple-head star tracker being operated in space are French Hydra and Russian 348K.

Star tracker 348K [1], developed by JSC NPP Geofizika-Cosmos, is an autonomous multiple-head star tracker with a 19 degree FOV. Each optical head comprises an active pixel sensor (APS)-based camera with a Peltier cooler. Using advanced field and spectral correction and radiation-hard glass, each optical head has three variants of baffles: 40, 30, and 25 degrees. A unique feature of 348K is an internal optical reference mechanism in the optical head. This provides in-orbit self-calibration of bias shift and estimation of object defocus. Using its tracker hardware and software, 348K can reach 11 arcseconds (three sigma) accuracy of attitude determination during its 150,000 hour lifetime.

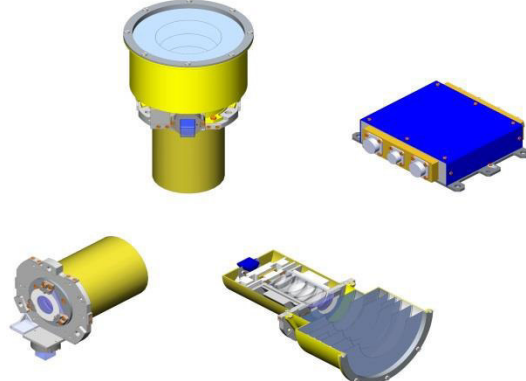


Fig. 1 – 348K star tracker

## V. CONCLUSION

The study have been supported by Russian Foundation for Basic Research RFBR, research project No 16-37-00010.

## REFERENCES

- [1] Kruzhilov, I. Small-angle rotation method for star tracker orientation, J. of Applied Remote Sensing, 2013, V. 7, pp. 073479-1 – 073479-19.
- [2] Kruzhilov, I., Karelina, A., Kniazev, V., et al, Calculating stellar magnitude to enhance guide star catalog, SPIE Newsroom. 2013.

# Signal Classification in Digital Filter Bank Channels in Radio Monitoring and Hydroacoustic Monitoring Tasks

D. Klionskiy, D. Kaplun, A. Golubkov, V.

Gulvanskiy, M. Kupriyanov

Computer Science Department

Saint Petersburg Electrotechnical University "LETI"

Saint Petersburg, Russian Federation

klio2003@list.ru, dikaplun@etu.ru, alexgol92@mail.ru,

slava-a-a@mail.ru, mikhail.kupriyanov@gmail.com

R. Taha Al-Kasasbeh

Faculty of Engineering Technology

Al-balqa Applied University

Amman, Jordan

rjordanjo@mail.ru

**Abstract—** We consider classification of sub-band signals in digital filter bank channels. Application of digital filter banks allows us to compute these characteristics in a parallel way and therefore to significantly increase the classification efficiency.

**Keywords—** signal classification, digital filter bank, radio monitoring, hydroacoustic monitoring

## I. INTRODUCTION

Digital filter banks are an important tool of signal processing and signal analysis in different areas including radio monitoring tasks, hydroacoustic monitoring tasks, vibrational signal processing, etc. [1-4] Signal classification in digital filter bank channels [5-10] is needed due to the following reasons:

- signal demodulation after the reception device – each type of signal requires a demodulator and classifiers help select the appropriate demodulator for a particular type of signals;
- signal recognition - determining the type of signal in radio monitoring applications;
- further signal processing - each type of signal needs particular mathematical processing, which is normally different from that applied to other types of signals.

In order to implement classification algorithms it was decided to take computers with CUDA (Compute Unified Device Architecture) [11] since many algorithms (e.g., in radio monitoring and hydroacoustic monitoring tasks) can be parallelized for the required number of flows. Furthermore, application of the same computational tools for both signal preprocessing (using filter banks) and classification allows us to dramatically reduce the amount of time for computations and data exchange. We can also use the single data format, which reduces significantly the memory size needed for storing intermediate results. Finally, we have the opportunity of saving time for data format conversion.

As a rule, the main ideas behind a classifier are computation, accumulation and identification of signal features (parameters, attributes) using the following characteristics:

- 1) amplitude spectrum;
- 2) power spectral density (PSD);
- 3) autocorrelation function(ACF);
- 4) instantaneous frequency;
- 5) complex cepstrum.

After signal processing by a filter bank we can obtain all the characteristics at the output of each channel. Application of

digital filter banks allows us to compute these characteristics in a parallel way and therefore to significantly increase the classification efficiency. Furthermore, it is possible to increase the number of signals for producing classifiers within one system.

The sampling rate of the signals is 1 MHz. All signal frequencies have been taken in the so-called main frequency band, i.e. within the range [0; 0.5] MHz. Each signal has 1000 samples in order to use the classifier close to real time.

## II. SIGNAL CLASSIFICATION

Classification has been performed on the basis of various signal features:

- 1) samples of the discrete Fourier transform (DFT) computed by the fast Fourier transform (FFT). Due to the DFT symmetry relative to the Nyquist frequency we have taken half of the total number of samples (i.e. 500 samples);
- 2) ACF samples; ACF employs averaging over the realization and is therefore a useful statistical characteristic of random signals.

The training set for the classifier has been taken 90% of the total number of objects (signals) and the testing set – 10 % of the total number of signals. The signals in the training set differ from each other by their carrier frequencies, frequency change rate and change point locations where one pulsing is substituted with another.

The total number of objects (signals) for each class is 250 and 25 of them (10%) have been used as part of a training set. Thus, we have 100 objects for all 4 (four) classes in the training set and 900 objects for the testing set. Classification has been performed on the basis of a binary tree and Adaboost technology with 25 iterations.

The experimental research has been conducted for several different signal-to-noise ratios (SNR): 80 dB, 40 dB, 0 dB, -20 dB. Four combinations of classes have been studied during the computer simulation:

- 4 classes: tone signal; LFM-signal (linear frequency-modulated signal); AM-2 (amplitude-manipulated signal); FM-2 (frequency-manipulated signal);
- 4 classes: tone signal; LFM-signal; AM-2; PM-2 (phase-manipulated signal);
- 3 classes: tone signal; LFM-signal; FM-2;
- 3 classes: tone signal; LFM-signal; PM-2.

The total classification error of 10% was considered acceptable during the experimental research for radio monitoring tasks.

A total classification error of 10% can be reached for signal-to-noise ratios  $SNR \approx 15 dB$  (tone signal; LFM-signal; AM-2; FM-2) and  $SNR \approx 10 dB$  (tone signal; LFM-signal; AM-2; PM-2). When the total number of classes is equal to 3 (three) it becomes possible to obtain the classification error of 10% for  $SNR \approx 7 dB$  (tone signal; LFM-signal; FM-2) and  $SNR \approx 4 dB$  (tone signal; LFM-signal; PM-2). When the signal-to-noise ratio is decreased, the classification error starts to grow. The lowest classification error is reached for LFM-signals; the classification error is growing more rapidly for other signals.

Consider the classification results with ACF samples used as features. In comparison with the previous case the classification error of 10% can be reached for a smaller signal-to-noise ratio, which confirms a better classification on the basis of ACF samples. The classification error of 10% is reached for  $SNR \approx 0 dB$  (tone signal; LFM-signal; AM-2; FM-2) and in  $SNR \approx -2 dB$  (tone signal; LFM-signal; AM-2; PM-2), which means that the level of noise exceeds that of a wanted signal (signal embedded in noise). When considering 3 (three) classes the error of 10% is reached for  $SNR \approx -3 dB$ . The smallest classification errors are also achieved for LFM-signals like in the previous cases.

Thus, the classification results for using the ACF samples exceed those for using DFT-coefficients from the point of view of reaching the classification error of 10% for a smaller signal-to-noise ratio.

Consider the classification results obtained by using the values of the continuous wavelet transform as features. These results yield to those discussed earlier. The total classification error exceeds 10% even for large signal-to-noise ratios (approximately 40 dB) - for the combinations (tone signal; LFM-signal; AM-2; FM-2) and (tone signal; LFM-signal; AM-2; PM-2). In the case of 3 (three) classes the classification error of 10% is achieved for  $SNR \approx 15 dB$  and  $SNR \approx 25 dB$ , respectively.

Consider the classification result for 4 (four) classes using neural networks and ACF samples as features. Selection of ACF samples is due to their best performance for the classifier

based on decision trees. The total classification error reaches 10% for  $SNR \approx 7 dB$ .

An artificial neural network is a set of neurons connected to each other. As a rule, the transfer functions of all neurons in a neural network are fixed and the weights are the changeable parameters of a neural network. Some neuron inputs are marked as external inputs of a neural network and some outputs – as output exits of a neural network. Neural network acts to transform an input vector into an output vector and this transform is determined by the weights of a network.

### III. CONCLUSION

Finally, we can make the following conclusions: the best classification results are achieved for ACF samples used as classification attributes (features); the classification error reaches 10% for  $SNR \approx -2...0 dB$  in the case of 4 (four) classes and ACF samples used as attributes; the classification error reaches 10% for  $SNR \approx -3 dB$  in the case of 3 (three) classes and ACF samples used as attributes; the smallest classification error is normally achieved for LFM signals.

### REFERENCES

- [1] D. Porcino, W. Hirt Ultra-Wideband Radio Technology: Potential and Challenges Ahead // IEEE Communications Magazine. – 2003. - Vol. 41(7). – P. 66–74.
- [2] W. Hirt Ultra-Wideband Radio Technology: Overview and Future Research, Comp. // Computer Communications. – 2003. - Vol. 26(1). – P. 46–52.
- [3] R.P. Hodges Underwater Acoustics: analysis, design, and performance of sonar // UK, Wiley Interscience, 2010, 353 p.
- [4] N. Levanon, E. Mozeson Radar signals // UK, Wiley Interscience, 2004, 411 p.
- [5] A. Antoniou, A. Digital Filters: Analysis, Design, and Applications. – USA: McGraw-Hill, 1993. – 689 p.
- [6] S.K. Mitra Digital Signal Processing: A Computer-Based Approach /. – USA: McGraw-Hill, 1998. – 940 p.
- [7] A. Oppenheim, R. Shafer Digital Signal Processing /. – USA: Prentice Hall, 1975. – 585 p.
- [8] L. R. Rabiner, B. Gold Theory and applications of digital signal processing. – USA: Prentice Hall, 1975. – 762 p.
- [9] A. Piotrowski, M. Parfieniuk Digital filter banks: analysis, synthesis and implementation for multimedia systems - Poland: Wydawnictwo politechniki bialostockiej, 2006. – 389 p.
- [10] R. E. Crochiere, L. R. Rabiner Multirate digital signal processing. – USA: Prentice Hall, 1983. – 411 p.
- [11] D. B. Kirk, Wen-mei W. Hwu Programming Massively Parallel Processors: A Hands-on Approach / USA: Morgan Kaufmann, 2010. – 280 p.

# Non-standardized measurement methods and measuring instruments for parameters and characteristics of laser diodes radiation and their standardization prospects

V. Bliznuk,  
Dept. of Physics,  
National Research University  
"Moscow Power Engineering Institute",  
Moscow, Russia  
40595141@mail.ru

N. Berezovskaya,  
Dept. of Physics,  
National Research University  
"Moscow Power Engineering Institute",  
Moscow, Russia  
Natalia.Berezovskaya@inbox.ru

A. Tarasov,  
Dept. of Physics,  
National Research University  
"Moscow Power Engineering Institute",  
Moscow, Russia  
TarasovAY@gmail.com

V. Parshin,  
Dept. of Physics,  
National Research University  
"Moscow Power Engineering Institute",  
Moscow, Russia  
ParshinVasa@gmail.com

**Abstract** — This article deals with not standardized methods of diagnosis of highly divergent radiation of the laser diodes. Special attention is paid to the methods of measurements of mode structure of such radiation. It is shown that the most promising in terms of standardization is a method of determining the generation of the laser diode at a fundamental mode, based on measurements of angle of divergence in the far field.

**Keywords** — *laser diode; radiation pattern; near field and far field; the angle of divergence*

## I. INTRODUCTION

The widespread introduction of laser diodes (hereinafter, LD) in various fields of science and technology made it necessary the creation of new methods and means of measurements of space-energy and polarization parameters and characteristics of radiation. This is due to the relevance of measurements of radiation parameters of LD in a free space characterized by large (up to  $90^\circ$ ) divergence. At present, measurement of parameters of laser radiation are conducted in accordance with the requirements of more than ten international standards, authentic translations, which as the national standards of the Russian Federation were enacted by the Federal Agency for technical regulation and Metrology from 2008 to 2015.

Methods of measurements of spatial and power parameters of laser radiation are comprehensively considered in [1]. However they are applicable only for highly directional laser beams.

In [2] methods and measuring instruments of polarizing characteristics of radiation of LD are considered. Moreover, in [2] along with diagnosis of beam radiation, a method of measuring the polarization of highly divergent laser beams is described. However, it is based on the use of a collimator and the analysis of the passed through it directional radiation. As

the measurement technique of angular dependences of polarizing parameters of strongly dispersing laser radiation is based on the same principles, as measurement techniques of spatial and power parameters of such radiation, we will limit to the consideration of the latter.

Among LD the lasers generating radiation on fundamental mode take a special place. Violation of the mode of generation on fundamental mode leads to essential deterioration in the LD parameters and sharply reduces efficiency of their use. Therefore the special attention is paid to the analysis of the mode of generation of LD on fundamental mode.

Because of the lack of standards on measurements of spatial and power parameters of strongly dispersing laser radiation now for such measurements not standardized techniques are used. We will consider some of them, and estimate a possibility of their standardization.

## II. NOT STANDARTIZED METHODOLOGY FOR MEASURING THE SPATIAL AND ENERGY PARAMETERS OF THE RADIATION OF THE LASER DIODE

As a rule, these techniques are based on the analysis of the normalized angular dependences  $f^\perp(\theta)$  и  $f^\parallel(\theta)$  of the emission intensity of LD in a plane perpendicular to p-n-transition (hereinafter, vertical direction) and in plane p-n junction (hereinafter, the horizontal plane). If with increasing power of the emission of LD normalized angular dependences of the radiation intensity in the vertical and horizontal plane are not changed and it is possible a good approximation of these dependencies by the Gaussian function, it is assumed that the generation on the fundamental mode take place. However, such a method of analysis of radiation patterns of radiation allows only a qualitative assessment of its modal structure, which eliminates the possibility of standardization.

The strict definition of LD lasing at the fundamental mode is accomplished by measuring the beam dissemination factor  $M^2$ . In the case of highly divergent radiation LD parameter  $M^2$  is determined by the method described in [3]. The authors use a factored representation of the transverse intensity distribution in the laser beam:  $M^2 = M_x M_y$ , where  $M_x$  and  $M_y$  - factors for the vertical and horizontal planes, respectively, and it is believed that the Factor  $M_x$  with a good degree of accuracy is always equal to one.

In this case

$$M^2 = M_y = 2k_0 \sigma_y \sigma_\theta = (2\pi/\lambda_0) \sigma_y \sigma_\theta, \quad (1)$$

where  $k_0$  and  $\lambda_0$  – wave number, and the wavelength in the vacuum;  $\sigma_y$  and  $\sigma_\theta$  – RMS beam size in the horizontal plane in the near and far field.

These dimensions are determined by the equations [3]:

$$\sigma_y = \left[ \frac{\int F(y) y^2 dy}{\int F(y) dy} \right]^{1/2}; \quad \sigma_\theta = \left[ \frac{\int I(\theta) \sin^2 \theta d(\sin \theta)}{\int I(\theta) d(\sin \theta)} \right]^{1/2} \quad (2)$$

where  $F(y)$  and  $I(\theta)$  – distribution of radiation intensity in the near and far field;  $y$  – coordinate of the point on the LD output mirror;  $\theta$  – the angular coordinate of a point located in the far field.

It should be noted that the definition of the type of function  $F(y)$  is associated with a complex processing of measurement results, making it difficult to standardize the described methods.

We have developed a methodology of determining the mode LD on the fundamental mode without measuring the intensity of the LD light distribution in the near field. It is based on the fact that the radiation pattern of radiation with a divergence defined by the diffraction limit is generated when the intensity distribution in the near field is described by a Gaussian function [4]:

$$F^\perp(x) = \exp[-a^2 x^2], \quad (3)$$

found by Fourier transformation (3) normalized angular distribution of radiation intensity in the same plane in the far field is given by:

$$f^\perp(\theta) = G^2(\theta^\perp) \exp(-k_0^2 \sin^2 \theta^\perp / (2a^2)), \quad (4)$$

where  $k_0$  – wave number in vacuum;  $G^2(\theta^\perp)$  – square angular factor Huygens [5]:

$$G^2(\theta^\perp) = \left( \frac{m^2 + \sqrt{n^2 - \sin^2 \theta^\perp}}{m^2 \cos \theta^\perp + \sqrt{n^2 - \sin^2 \theta^\perp}} \right)^2 \cos^2 \theta^\perp, \quad (5)$$

where  $m = 1$  for the TE-modes, or  $m = n$  for TM-modes, and  $n$  – refraction index of the waveguide.

From (4) and (5) it follows that the diagram of the radiation at the fundamental mode is symmetric with respect to the laser beam axis. To analyze of such diagrams the angle  $\theta_{1/2}^\perp$ , defined by the formula is used:

$$\theta_{1/2}^\perp = 0.5 \theta_{1/2}^\perp \text{ trad}, \quad (6)$$

where  $\theta_{1/2}^\perp \text{ trad}$  – the total angle of divergence of the radiation, measured at the level of 1/2 of the maximum intensity of the LD light.

Substituting  $\theta_{1/2}^\perp$  to (4) and using the condition  $f^\perp(\theta_{1/2}^\perp) = 0.5$ , you can find a formula to calculate the index  $a$  appearing in (3):

$$a^2 = k_0^2 \sin^2 \theta_{1/2}^\perp / (2 \ln[2G^2(\theta_{1/2}^\perp)]). \quad (7)$$

Then, without the radiation intensity distribution measurements in the near zone (7) and (4) the type of function that describes the radiation pattern of LD is determined:

$$f^\perp(\theta) = G^2(\theta^\perp) \exp\left(-\frac{\ln[2G^2(\theta_{1/2}^\perp)]}{\sin^2 \theta_{1/2}^\perp} \sin^2 \theta^\perp\right) = G^2(\theta^\perp) \exp(-A^2 z^2). \quad (8)$$

Where

$$A^2 = \ln[2G^2(\theta_{1/2}^\perp)] / \sin^2 \theta_{1/2}^\perp; \quad (9)$$

$$z^2 = \sin^2 \theta^\perp, \quad (10)$$

where  $z$  – abscissa of the point of the curve describing the function  $\exp(-A^2 z^2)$  in the Cartesian coordinate system.

The inflection points of the curve are the coordinates  $\pm 1/(A\sqrt{2})$ ,  $1/\sqrt{e}$  [6]. Let  $\pm z_p$  abscissa these points. Then  $z_p^2 = 1/(2 A^2)$ , and

$$f^\perp(\theta_p^\perp) = G^2(\theta_p^\perp) \exp(-1/2). \quad (11)$$

Using condition  $A^2 z_p^2 = 1/2$ , and (11) and (10) we find design parameter  $\theta_p^\perp$  from the following equation:

$$\sin^2 \theta_p^\perp = \sin^2 \theta_{1/2}^\perp / (2 \ln[2G^2(\theta_{1/2}^\perp)]), \quad (12)$$

according to the formula (5) we count the square of the angular factor  $G^2(\theta_p^\perp)$ . If the experimentally obtained value  $f^\perp(\theta_p^\perp)$  is equal to the right side of (11), there is a generation of LD on the fundamental mode

The measuring instruments of spatial-energy radiation characteristics of LD, providing for the implementation of the proposed method, has a fairly simple structure and the array processing system of numbers obtained by field measurements of directivity pattern of the radiation. The latter circumstance is due to the fact that there is no need of analyzing the whole radiation pattern. This increases the accuracy of measurement of spatial-energy radiation characteristics of LD, and opens the possibility of standardization, such as methods of measurement and means of measurement.

### III. CONCLUSION

When considering methods of measuring space-energy characteristics of highly divergent radiation LD, found that standardization is possible only one of them, in which the function, that describes the radiation pattern is determined without explicitly measuring the intensity distribution in the near field zone. It is through this ensures high precision measurements of space-energy characteristics of the LD light.

### REFERENCES

- [1] GOST R/TR ISO 11146-3-2008. Lasers and laser systems (systems). Methods of measurement of widths, divergence angles and coefficients of propagation of laser beams. Part 3 Stigmatic (homocentric) and poorly astigmatic beams.
- [2] GOST R/TR ISO 12005-2013. Lasers and laser systems (systems).
- [3] Popovichev VV Davydova EI Marmalyuk AA, AV Simakov, MB Uspenskiy, Chelny AA, Bogatov AP Drakin AE With Plisuk A., Strattonnikov AA Powerful cross-single-mode semiconductor lasers with the ridge structure of the optical waveguide // Quantum Electronics. T.32 2002, №12. S. 1099 - 1104.
- [4] Casey H., Panish M. Lasers on heterostructures. M.: Mir. 1981 V.1 - with 299, Vol.2 -. 364.
- [5] Thompson G.H.B. Physics of semiconductor laser devices. N.Y.: J. Wiley and Sons.1980. pp. 185 – 186.
- [6] I.N. Bronstein, K.A. Semenyaev. "Handbook of mathematics." M.: State Publishing House technical and theoretical literature. 1957. 608 p.

# Modernization of the modular helium reactor project with the gas turbine for the hydrogen and electric energy production

Sergey Podgrony

MPEI Volzhsky branch

Volzhsky/ Russian Federation

serkonpod@gmail.com

Vyacheslav Kuzevanov

MPEI Volzhsky branch

Volzhsky/ Russian Federation

kuzevanov@vfmei.ru

**Abstract— Followed research is devoted to solve main problems of the modular helium reactor with the gas turbine for hydrogen and electric power production.**

**Keywords—gas turbine; GT-MHR; modular helium reactor; over heated steam; steam generator**

## I. INTRODUCTION

Nowadays gas-cooled reactors are the most promising type of reactors. Mainly it is caused of a unique ability to reach very high temperature of the heat carrier (~1000 °C) also high level of safety. Gas-cooled reactors can be used in following sectors of industry: electric power generation (the production of electric power at high efficiency), the transport (sea transport and spacecrafts) and the hydrogen production.

The most promising way of using gas-cooled reactors is the hydrogen production. The most common ways of the hydrogen production are the steam methane reforming and the water electrolysis. The methane reforming is not an eco-friendly option due to the carbon dioxide emissions. From the other side, the water electrolysis is an eco-friendly process, but it is a lot more expensive process. If temperature of the water electrolysis will be raised to 900 Celsius degrees it will make the water electrolysis profitable process. The project of the Nuclear power station for the hydrogen production based on the GT-MHR project, which means "gas turbine - modular helium reactor". Except the main modules, such as the nuclear reactor and the gas turbine, the project of the nuclear plant for the hydrogen production includes high temperature heat exchangers, which produces superheated water steam, and high temperature electrolytic device.

As mentioned before, temperature of the electrolysis must be raised to 900 Celsius degrees. It means that hydrogen and oxygen must have temperature about 900 Celsius degrees. The project of the Nuclear power station for the hydrogen production has two main problems. First problem is about usage of the thermal energy of hot hydrogen oxygen. Second problem is about operating mode of the nuclear power plant when the electrolytic device is off.

The thermal energy of hot hydrogen can be used for the production of superheated steam, which will be expanded in steam turbine and thermal energy of hot oxygen can be used to warm up water for electrolysis. Due to using thermal energy of hot hydrogen and oxygen, their temperature will be lowered to the level, which is suitable for consumers. If electrolytic device is off, superheated steam, which produces in high temperature heat exchangers, must be mixed with water, because steam temperature is about 900 celsius degrees. It is necessary because otherwise a steam turbine will be damaged. Steam with lowered temperature will be expanding in the steam turbine.

## II CONCLUSION

Normal operating modes of the nuclear power plant is impossible without solved previously mentioned problems. That's why the modernization of the modular helium reactor project with the gas turbine for the hydrogen and electric energy production is necessary.

## REFERENCES

- [1] Booklet of GT-MGR. JSC OKBM im. Afrikantova [An electronic resource] [http://www.okbm.nnov.ru/images/pdf/gt-mhr\\_ru\\_web.pdf](http://www.okbm.nnov.ru/images/pdf/gt-mhr_ru_web.pdf)

# Investigation process control of system sintering agglomerate

Kuponosova Valentina

MPEI Volzhsky branch

Volzhsky/ Russian Federation

Kuponosovavalentina@mail.ru

Yulia Malygina

MPEI Volzhsky branch

Volzhsky/ Russian Federation

mokicheva@mail.ru

**Abstract—**In this paper analyzed the technological process of sintering. Identified analytical dependence of the temperature of the charge from the temperature in the furnace. On the basis of the study developed a temperature control system of the charge.

**Keywords—**agglomeration; control system; temperature regulation; the temperature of the charge

## I. INTRODUCTION

Agglomeration was first used in non-ferrous metallurgy sintering sulfide ores and copper ores. Agglomeration is the process of obtaining of pieces (agglomerate) by sintering fine ore with a fuel high temperature combustion. The task of the agglomeration process is to prepare high quality raw materials for blast furnace production.

Modern sinter plant is a complex system of different vehicles operating in different modes and perform different functions. The continuous growth of sinter production, increase of requirements to quality created the conditions for widespread introduction of automated control and management. The main aim of this work is to improve the quality of sintering in the furnaces through the use of an automatic control system.

The process of sintering starts with the ignition of the upper layer of the charge. The process occurs in the furnace chamber. The gas supply to the furnace is allowed only with the guarantee of its ignition from the heated surface of the charge. The main parameters that characterize the sintering process is the temperature of the charge. It is physically impossible to control the temperature of the charge. After analyzing the technological process of sintering furnaces have been identified with the analytical dependence of the temperature of the charge from the temperature in the furnace.

The temperature in the furnace depends on the expense of air and of fuel delivered by pipeline. The temperature in the furnace depends on the consumption of air and of fuel

delivered by pipeline. Thus, we can maintain the required temperature, by controlling the consumption of fuel and air. The optimum temperature of the radiating surface of the burner is equal to 800-950° C. To improve the sintering process is proposed single-circuit control system.

The main objective of this work was the temperature control in the furnace. For optimal performance of the control system were calculated controller settings. Equation 1 is the transfer function of the controller.

$$W(p)=0,115 \cdot (1+1/0,415 \cdot p) \quad (1)$$

For optimal sintering regulates the flow of gas and air depending on the temperature in the sintering zone. In this work was a comparative analysis of the transition process at a temperature in the furnace before the regulation and after. Thanks to regulation, necessary temperature in the furnace is established quicker.

## II. CONCLUSION

Thanks to the automation control system of sintering, it is possible to obtain the required temperature of the charge in a shorter time. Automation increases the production of sinter and improves its quality and reduces its costs by more efficient use of fuel resources.

## REFERENCES

- [1] Seleznev A. E. Sintering equipment of factories of ferrous metallurgy.- M.: Metallurgizdat, p.320, 1960
- [2] I.M. Sal'nikov, V. D. Getalo and Getalo A. T. the Practice of improving the automation of the sintering process with the aim of improving the quality of sinter. Steel, 1993.
- [3] Makovsky, V. A., Vlasyuk Y. N., and Chernyshov Yu. V. Optimal control of the sintering process.- K.: Higher school, p .117, 1987.

# Application of fuzzy pyramidal network tools for analyzing the IT-project feasibility

Bulygina Olga Valentinovna

department of management and information  
technologies in economics,  
branch of National Research  
University «MPEI» in Smolensk,  
Smolensk, Russia  
baguzova\_ov@mail.ru

Chernovalova Margarita Vital'evna

department of management and information  
technologies in economics,  
branch of National Research  
University «MPEI» in Smolensk,  
Smolensk, Russia  
0208margarita@bk.ru

**Abstract** — In the article the necessity of investment project realization for development of information and telecommunication infrastructure of industrial enterprise is substantiated and the procedure of development and implementation of such type of IT-projects is a detailed. It's shown that for the preliminary analysis of the complex IT-project prospects it is expedient to use the data mining methods for scanning the enterprise internal and external environment. The authors have developed the procedure of analyzing the investment IT-project prospects based on the application of the proposed growing pyramidal network modification for various project characteristic diagnosis and the fuzzy logic algorithms for their aggregation.

**Keywords** — *information and telecommunications infrastructure, IT-projects, fuzzy logic, fuzzy pyramidal network.*

## I. INTRODUCTION

In the current situation of financial resource austerity development of most organizations is associated with an increase in the efficiency of information and telecommunication infrastructure, which can be achieved by switching to national analogues, using cloud-based and mobile technologies, implementing support systems for managerial decision-making, etc.

Carried out analysis of IT-project realization features has revealed the impossibility of application of existing project management approaches because of their uniqueness. It is caused by the specifics of the company production and management and the presence of the functioning hardware and software system automating the different technological and business processes.

This fact determines the need to create a conceptually new approach to managing the investment processes of modernization and development of the information and telecommunication infrastructure, based on the implementation of latest scientific and technological achievements in the info-communication technology. It is assumed that their usage will increase efficiency of the industrial enterprise as a whole.

## II. IT-PROJECTS DIAGNOSTIC PROCEDURE

Mathematically, the process of IT-project implementing can be presented as follows:

$$G = (D, F, C_O, L), \quad F = (I, R, P, E, J, O),$$

where  $D$  - initial technical specification parameters,  $F$  - array of project stages,  $C_O$  - initial conditions of project realization,  $L$  - vector of stage duration,  $I$  - technical specification of a particular stage,  $R$  - resources allocated to the stage implementation,  $P$  - enterprise potential,  $E$  - external conditions of the stage implementation,  $J$  - set of works required to the stage implementation,  $O$  - stage implementation results.

Development and implementation of complex investment IT-project is aimed at improving the functioning of enterprise information and telecommunication infrastructure. In most cases, such projects are expensive and time-consuming process, requiring detailed study and preliminary examination [1].

During the investment project development a particular attention should be given to the analysis of internal enterprise resources directly engaged in the implementation of stages and works and involved in the automated technological and business processes.

In general, the IT-project prospect assessment is provided to solve the classification problem related to determining the adequacy of available resources, accumulated enterprise potential and favorable environmental conditions for its effective implementation. It is obvious that the unique character of the investment IT-projects restricts the usage of standard analytical procedures due to the lack of sufficient volume of accumulated reliable and comparable statistical data [2, 3].

This fact determines the expediency of intelligent methods capable to generate the informed decisions on the basis of the semi-structured information analysis in uncertainty conditions.

The authors have proposed a modification of the growing pyramidal network apparatus, based on the application of fuzzy logic methods, that has allowed to evaluate the influence of

some factors on the other (the connection power) and the degree of their importance in the search for a single solution (the vertex significance) in the quasi statistics conditions.

Conceptually pyramidal network is an acyclic oriented graph, consisting of the receptors (the characteristics of the internal / external environment component), the conceptors (the intermediate vertices - the states of various component elements) and the outcomes (integrated assessment of the environment component state) [4].

The article [5] describes the algorithms of construction, training and use of fuzzy pyramidal networks to assess the internal and external environment of the organization. The values of analytical indicators characterizing the state of the various elements of internal or external IT-companies environment use as the receptors.

Fuzzy logic inference according to Mamdani algorithm is used for the integrated assessment of the state of the internal / external environment, resulting from the application of fuzzy pyramidal networks.

The authors have developed a special procedure for the analysis of the investment IT-project prospects based on the application of fuzzy pyramidal networks for diagnostics adequacy of internal enterprise resources and favorable environmental conditions and the fuzzy inference algorithms for a comprehensive assessment (Figure 1).

### III. CONCLUSION

The proposed approach to evaluate the prospects of the implementation of investment IT-projects for information and telecommunication infrastructure development, based on the application of fuzzy network pyramidal models, forms the basis for building an effective system of selecting technologically advanced, cost-effective and technically well-developed IT-projects aimed at innovative enterprise development.

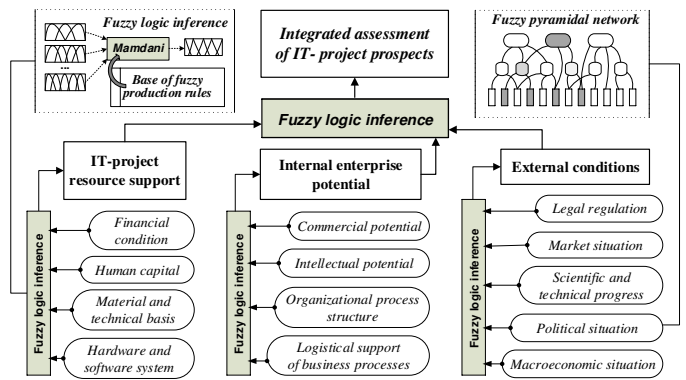


Fig. 1. The procedure of the integrated assessment of the IT-project implementation

### ACKNOWLEDGMENT

The article has financially supported by the grant №16-01-00293-a of Russian Foundation for Basic Research.

### REFERENCES

- [1] Berkhou G., Van Der Duin P. New ways of innovation: an application of the cyclic innovation model to the mobile telecom industry // International journal of technology management. 2007. Vol.40. №4. p. 294-309.
- [2] Sarkisov P.D., Stoyanova O.V., Dli M.I. Principles of project management in the field of nanoindustry // Theoretical Foundations of Chemical Engineering. 2013. T. 47. № 1. C. 31-35.
- [3] Meshalkin V.P., Stoyanova O.V., Dli M.I. Project management in the nanotechnology industry: specifics and possibilities of taking them into account // Theoretical Foundations of Chemical Engineering. 2012. T. 46. № 1. C. 50-54.
- [4] Gladun V., Vashchenko N. Analytical processes in pyramidal networks // International journal on information theories & applications. 2000. Vol.7. p. 103-109.
- [5] Buligina O., Selyavskiy Y., Masutin S. Procedure of the prospects assessing of the implementation of innovative IT-projects in indeterminacy // Transport business in Russia. 2015. Vol. 2(117). P.156-157.

# Fuzzy Kalman filter in electrothermal reactor control system

Puchkov Andrey Yrjevich

department of management and information  
technologies in economics,  
branch of National Research  
University «MPEI» in Smolensk,  
Smolensk, Russia  
putchkov63@mail.ru

Zhigareva Anastasia Alexandrovna

department of management and information  
technologies in economics,  
branch of National Research  
University «MPEI» in Smolensk,  
Smolensk, Russia  
Anastaziru@mail.ru

**Annotation – One of the feasible approaches to get a system model (forming filter), which output signals are subsequently treated by fuzzy Kalman filtration is represented in this article. The authors suggest that a general structure of the forming filter description is known, this makes it possible to undertake the iteration procedure of its parametric adjustment. In the quality of the under study system is an electrothermal reactor, the mathematical model of its, in this approximation of lumped parameters, constitutes the specific system of non-linear ordinary differential equations. The adjustment algorithm includes the system of fuzzy logical output which analyses a output signals discrepancy of the mathematical model and forming filter and realizes the correction calculations. This article represents the results of a numerical experiment in the programming environment MathLAB which implements the suggested method of forming filter adjustment.**

**Key words:** *electrothermal reactor, thermalphysic process, fuzzy logic, Kalman filter.*

## IV. INTRODUCTION

The task of data-measuring and managing systems of ore-smelting electric furnace involves the most definitive information acquisition from indirect measures that characterize proceeding technological processes. It can be provided by measurement information processing intellectual algorithm application, based on mathematical models. Notwithstanding input information for these algorithms, incoming from measuring equipment, involves noises of different nature that influence on produced controlling action. In this connection the task of removal and the impact of these noises on end result of management reduction is actual. The complexity of under consideration technological process and availability of just its approximated mathematical models predetermine the application of fuzzy logic apparatus for data measuring processing which is well proven in such conditions of applying. The application of the suggested method of measurement information processing allows improving the quality of electrothermal reactor management through noise level in proceeded data decrease.

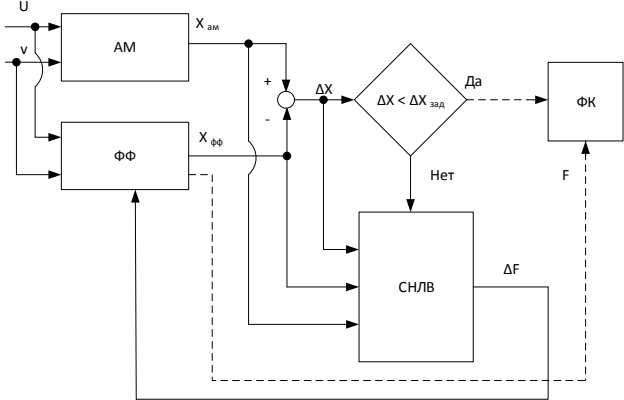
## V. METHODS

The characteristic of a state of an ore-smelting electrothermal phosphoric furnace is based on incoming from measuring equipment information which roughness and noises can come down an accuracy of results, got by the application of the existing mathematical model as well as the quality of managing process [1].

Frequency filters can be used for noise suppression, but if frequency spectrum of noise and useful signal are overlapped, then their application is not reasonable. In these conditions it can be spoken about statistic filtration, one of the methods of it is the Kalman filter (KF). In contrast to frequency filters, it doesn't demand additional hardware for its realization, it is enough to update the existing procedure of data measurement processing. This fact and facilities of filtration process organization in the form of recurrent expression at a digital computer makes the task of based on FK data processing algorithm development efficient. This filter in combination with intellectual methods has good perspectives in application for different natured objects and formulations of the state evaluating tasks [2-4].

To start the computational process, realizing the FK, the starting data  $\bar{X}_0$  and a model of the observing process in the kind of differential equation should be assigned. This model is called a forming filter (FF), that means a system, forming a correlated random process on the base of input white noise. Methods of the FF finding usually are conjugated with complex computation even for stationary processes. For example, one of the methods is based on the frequency spectrum of stationary random signal X factorization and physically realizing accentuation. More generally, when a random process has an arbitrary continuous correlating function, the task of the FF definition can be solved.

In this situation the methods used at regulators with parameters trimming are suggested. The general structure of the suggested method of parametric adjustment of the FF is demonstrated on the picture 1.



Picture 1 – The scheme of forming filter adjustment algorithm

The algorithm works as follows. Models of control action signal  $u$  and input random process  $v$  are given to the input of the existing analytic model AM. These signals go to the entry of the FF. The difference between output signals  $\Delta X$  of the analytic model  $X_{AM}$  and the FF  $X_{FF}$  go to the entry of the system of the fuzzy logistic inference (SFLI), with on the basis of the existing knowledge base forms a signal of the correction  $\Delta F$  and then changes of the matrix  $F$  elements are made of the description of the FF. If the difference of signals doesn't exceed the set value  $\Delta X_{exc}$  the trimming process stops and the matrix  $F$  is used in the FK.

It should be noted that the same transmissibility FF can match different structures of its model that differs with an modeling error sensibility [5]. Obviously, it is reasonable to apply in the programming realization the suggested approach a model, which has such an property when a dispersion of the state vector component  $X$  stays constant and the error dispersion doesn't grow indefinitely in terms of a variation of constant time system. Considering further the two-component state vector (otherwise a separated filter for a controlled parameter of the process should be applied) such structures allow simplifying the FF adjustment process, because with the use of this structure unknown is only one of the matrix  $A$

element of the indefinite system which definition helps to find the required matrix  $F$  for the discrete description:  $F_k = e^{-AkT}$ , where  $T$  – is a digitization interval.

The carried out numeric experiments in the programming environment MatLAB revealed that after the transient the forming filter becomes adjusted and its output signal becomes close to the signal, produced by the analytic model.

## VI. CONCLUSION

The suggested method of forming filter parameters definition in the structure of the fuzzy Kalman estimation the electrothermal reactor, has proved it's workability and can be used in terms of the corresponding mathematical model existing, for other objects and technological processes which output parameters are subjected to measurement and are noised.

## ACKNOWLEDGMENT

The work is written with the support of the grant of RFBR № 16-07-00491 A.

## REFERENCES

- [1] Panchenko S.V., Meshalkin V.P., Dli M. I., Borisov V. V. Computer and visual model of heatphysical processes in the electrothermal reactor//Non-ferrous metals. 2015, No. 4, S.55-60.
- [2] Bunches A.YU., Pavlov D. A. Options of creation of algorithm of search of the solution of the return tasks with application of neural networks. Software products and systems. No. 2 (98), 2012 of Page 149 – 153.
- [3] Puchkov A.Y. , Pavlov D.A. Kalman filter in structure of the solution of the return tasks/ Materials of the iii international research and practice conference "Science, Technology and igher Education". Vol. II. Westwood, Canada, P. 481-482
- [4] Sage E. P. Whyte Ch. of Page III. Optimum control of systems: The lane with English / Under the editorship of B. R. Levin. – M.: Radio and communication, 1982. – 392 pages.
- [5] Lagovsky A. F., Mysherin A. V., Shagimuratov I. I. The analysis of computing difficulties at realization of the filter of Kallman for an assessment of full electronic contents ionosfery./the Bulletin of the Baltic federal university of I. Kant. No. 10, 2007. Page 22-27.

# Determining the Stages of the Composite Vessel Destruction on the Basis of the Acoustic Emission Testing Results

Chernov D.V., Barat V.A.  
National Research University MPEI  
Moscow, Russia  
chernovdv@inbox.ru

Elizarov S.V.  
LLC INTERUNIS-IT  
Moscow, Russia  
serg@interunis-it.ru

**Abstract** — composite materials are very widespread in aerospace, reinfinary and chemical industries. The nondestructive evaluation of the composite materials is an actual and complicate problem. Traditional ultrasonic, thermal and electromagnetic NDT methods have a limited application which is explained by anisopropic properties of the composite materials. This study focuses on the problems of acoustic emission arising during the composite materials testing.

**Keywords**— composite materials, acoustic emission, data processing.

## I. INTRODUCTION

Composite materials are widely used in many industries, such as aircraft, oil – refining, chemical and other ones due to their high strength level and low relative density. Development of testing methods for objects made of composite materials is actual as such objects are widespread ones. Object state estimation is performed by conventional methods of non-destructive testing (NDT), and one of this methods is acoustic emission (AE) testing method.

In the case of composite materials testing AE – method has a set of advantages over other NDT methods. It is a passive method that is based on registration of acoustic waves generated by structural alternations of material such as plastic strain, defects generation and growth. AE method has a high sensitivity and does not demand full surface scanning. Besides this method is universal enough to be applied for either metallic or non-metallic objects. Moreover multilayer complex structure of material under test influences on results of control less then in case of ultrasonic or thermal testing.

AE method provides remote acting control in the area from several to hundred meters [1]. It worth mentioning that AE method determines hazard rating of defect but not the size of defect which is determined by conventional NDT methods (ultrasonic, magnetic, radiation). The further exploitation or shutdown of the object is concluded on the basis of determined hazard rating [2].

The main problem for AE testing of composite materials is inapplicability of conventional criteria which were developed

for metallic structures. Thus the goal of research is development of criteria for state estimation of either composite or metallic composite structures.

## II. OBJECT DESCRIPTION

The object under research is a metallic composite vessel that is composed from titanium lining tube and composite shell (fig. 1). During pneumatic test object was carried to failure. The goal of testing is research of vessel destruction stages, development of diagnostic model on the basis of AE signal parameters and criteria for object state estimation.



Fig. 1. Object under test

Fig.1 pictures object under test with AE transducers mounted on its surface, Fig.2 plots load curve during test. Object was loaded incrementally with delay after linear buildup of pressure. Base pressure values on the load curve are 50, 80, 110, 130, 150, 180, 200, 300 kgf/cm<sup>2</sup>.

AE signals were obtained by industrial system A-Line32D and by unit of continuous data recording L-Card. A-Line32D system was registering parameters of AE signals. L-Card unit was acquiring AE data flow on the basis of which AE signals waveforms and spectra alterations were revealed on different stages of destruction.

The object destruction is composed from two stages – strain of titanium lining tube and destruction of composite shell. Strain of lining tube starts at load 1 and continues till full

destruction of the vessel. Titanium would be fully under plastic strain when pressure value is 30 . After pressure value reaches point 30 strain intensity decreases as titanium turns into plastic mass.

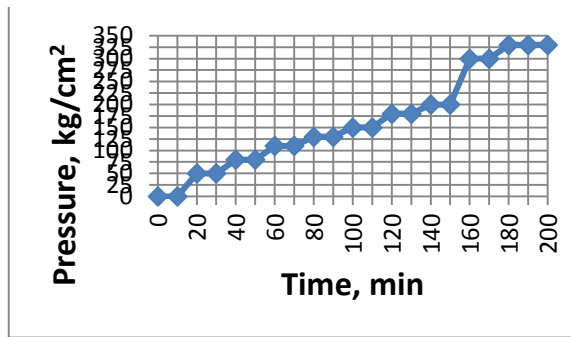


Fig. 2. Load curve

Composite material destruction starts when pressure value is about 50 . As theory states composite material destruction has 3 stages which goes sequentially as load increases [3, 4].

Matrix cracking is the first stage. Cracking process is negligible for structural load factor and it continues till full object destruction. The second stage which arises with further load increment is delamination.

Delamination is the process of destruction of adhesive bond as matrix is destructing and fibers are moving. This process significantly reduces stress limit of the material. The third stage is fibers destruction. This process arises just before stress limit is reached. It should be mentioned that on the stage of fibers destruction processes of matrix cracking and delamination are still active.

### III. ANALYSIS OF AE DATA OBTAINED DURING TESTING

The first step of research is matching of the vessel destruction stages with AE data in order to reveal the general dependencies which are characteristic for destruction stages.

When load starts to increment lining tube strain arises. Strain with wall thickness decrease occurs at the poles zone and material stretch happens from pole to equator. Plastic strain of lining tube goes with continuous emission and this is additional problem for data analysis. Spectra of such a signal has special properties which allows to detect plastic strain against noise background.

While load increases composite shell starts to strain. Composite strain starts with the processes of matrix cracking and delamination. This processes has a specific trend of amplitudes growing (Fig. 3).

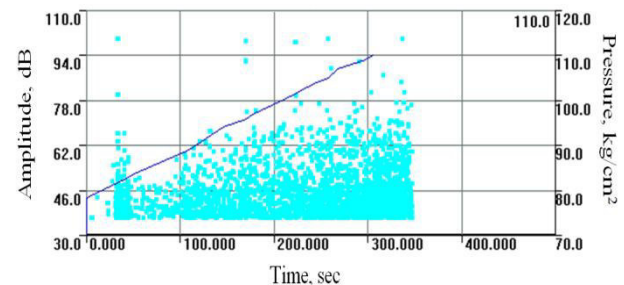


Fig. 3. Time dependence of AE impulses amplitudes with load curve for loads below 110

Amplitudes trend to increasing characterizes the process of damage accumulation in composite matrix [5], and a transition to the next stage of the object strain (Fig. 4).

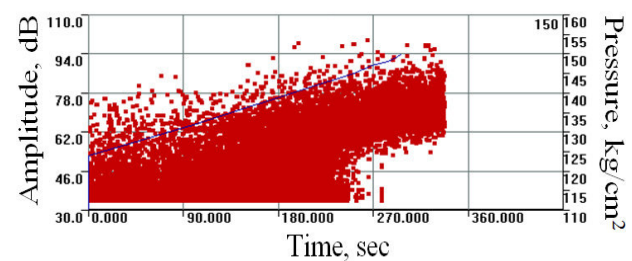


Fig. 4. Time dependence of AE impulses amplitudes with load curve for loads below 150

Fig. 4 shows time dependence of AE impulses amplitudes while pressure increases to 150 dB. On this stage there is an indicative time interval without small amplitudes (less than 50dB). This time interval reveals the start of the stage of fibers destruction.

### REFERENCES

- [1] Ivanov V.I., Vlasov I.E. Acoustic emission testing method. Nondestructive testing: Handbook; volume 7, editor Kluev V.V.: Mashinostroenie. 2005, – 340 pp.
- [2] PB 03-593-03. Rules of organizing and conducting acoustic emission testing of vessels, vehicles, boilers and process piping
- [3] Fracture Mechanics of Composite Materials. Moscow, Mir 1982, 232 p.
- [4] Cherepanov GP Fracture mechanics of composite materials. - M : Science, Home edition of Physical and Mathematical Literature, 1983. - 296 p.
- [5] DV Chernov, VA Barat and Vasiliev IE The development of methodology for assessing the stages of destruction of multilayer composite materials according to the parameters of acoustic emission signals, Electronics, Electrical Engineering and Energy: Twenty-first int. scientific and engineering. Conf. undergraduate and graduate students, Moscow: Tez.dokl. Publishing House MEI

# Assessment of Fracture Toughness of Hardening Coatings by Instrumented Indentation and Acoustic Emission Parameters

V.M. Matyunin, V.A. Barat  
National Research University «MPEI»  
Moscow, Russia  
BaratVA@mpei.ru

V.V. Bardakov, A.Yu. Marchenkov  
National Research University «MPEI»  
Moscow, Russia  
MarchenkovAYu@mpei.ru

**Abstract**—The possibility of effective application of instrumented indentation method together with Acoustic Emission (AE) method for evaluation of fracture toughness of hardening coatings is described in the article. It has been established that the presence of one of the fractures on the instrumented indentation diagram line on the axes “load – indent displacement - time” can be explained by appearance of the first crack in the coating and it almost coincides in time with appearance of acoustic emission impulse with the increasing of energy rate.

**Keywords**— *acoustic emission, instrumented indentation, hardening coatings, fracture toughness*

## I. INTRODUCTION

It is known that AE method is based on registration of acoustic waves generated by strain and defects formation. It has been established that AE method is capable to detect the moment of strain conversion from elastic type to elastoplastic type during material indentation by hardness testing ball [1]. The papers [2] state an applicability of AE method in the field of experimental material engineering, including plastic properties estimation of coatings.

While indentation by hardness testing ball the first plastic strain occurs beneath the dent at the depth of about half the ball radius. In this area while further generation and growing of hydrostatic core the first medial crack is generated. While unloading of the dent the medial crack usually closes due to contractive forces of the elastically deformed material. However on the surface strains reverse sign what leads to occurrence of radial and circular cracks, which grow while unloading. After full unloading near deformation zone substantial tensile stresses arise and this broadens cracks zone [3].

## II. EXPERIMENT

The next experiments with AE and indentation were performed for development of the method of first crack detection while it occurs on the coating surface with registration of corresponding load and indentation depth.

Universal direct stress machine Instron 5982 was used in the compressive loading mode for indentation. Vickers indent and diamond spherocapillary penetrator (Rockwell indent with radius of 0.2 mm) were rigidly fixed by tailor-made tool which allowed to apply load perpendicular to coating surface. The load measurement accuracy was  $\pm 0.1$  N, and the accuracy of the indent displacement measurement was  $\pm 0.25$   $\mu\text{m}$ . Deformation rate during indentation was 0.025 mm/min. For reliable measurement of indent displacement  $t$  elastic compliance of stress machine was taken into account.

While indentation two test diagrams - «load  $F$  – indent displacement  $t$ » and «load  $F$  – time  $\tau$ » were registered simultaneously. AE signals were obtained by sensor mounted on the side face of specimen on which coupling fluid was applied. The sensor was resonant transducer GT200 with resonance frequency equal to 150 kHz. Signal from sensor was sent to amplifier with gain of 34 dB and 1...500 kHz pass band filter. As AE data registration system 2-channel device UNISCOPE was used. Signals were sampled at 2.5 MSPS rate which is matched with measuring channel band.

## III. RESULTS AND DISCUSSION

Fig. 1 depicts testing results for TiN - based coating with thickness of  $\approx 25 \mu\text{m}$ . Fig. 1a is a test diagram «load  $F$  – indent displacement  $t$ » for spherical indent ( $R = 0.2 \text{ mm}$ ), Fig. 1b is a test diagram «load  $F$  – time  $\tau$ » joint with RMS of AE signals.

AE signal RMS( $\tau$ ) marks the displacement of the object surface  $S$  in time  $\tau$  by the action of acoustic wave. Fig. 1B presents RMS value of the signal RMS( $\tau$ ) that is counted in running window with the length  $l\tau = 0.4 \text{ ms}$ .

AE signal contains impulse components. Each impulse corresponds to event of material structure change or plastic flow or defects birth. AE signal contains about 100 AE impulses which are registered both during loading and during unloading of the coating under test.

Analysis of diagrams shown at Fig. 1a and 1b stated 3 main local zones: zone 1 is strain conversion from elastic type to elastoplastic type, zone 2 is first crack occurrence and zone 3 is indent penetration into the base of coating. This local zones

correspond to discontinuities 1, 2 and 3 on the diagram «F - t» (Fig. 1a) and to AE impulses 1, 2 and 3 on the diagram «RMS - τ» (Fig. 4b). First AE impulses were obtained while strain conversion from elastic type to elastoplastic type at the load  $F \approx 4$  N. They are composed as a sequence of low amplitude impulses which arises at frequency about 4...5 impulses per second (Fig. 1c). This impulses were registered in the time interval 3...9 s from the test start what is adequate to the duration of the coating strain from elastic type to elastoplastic type.

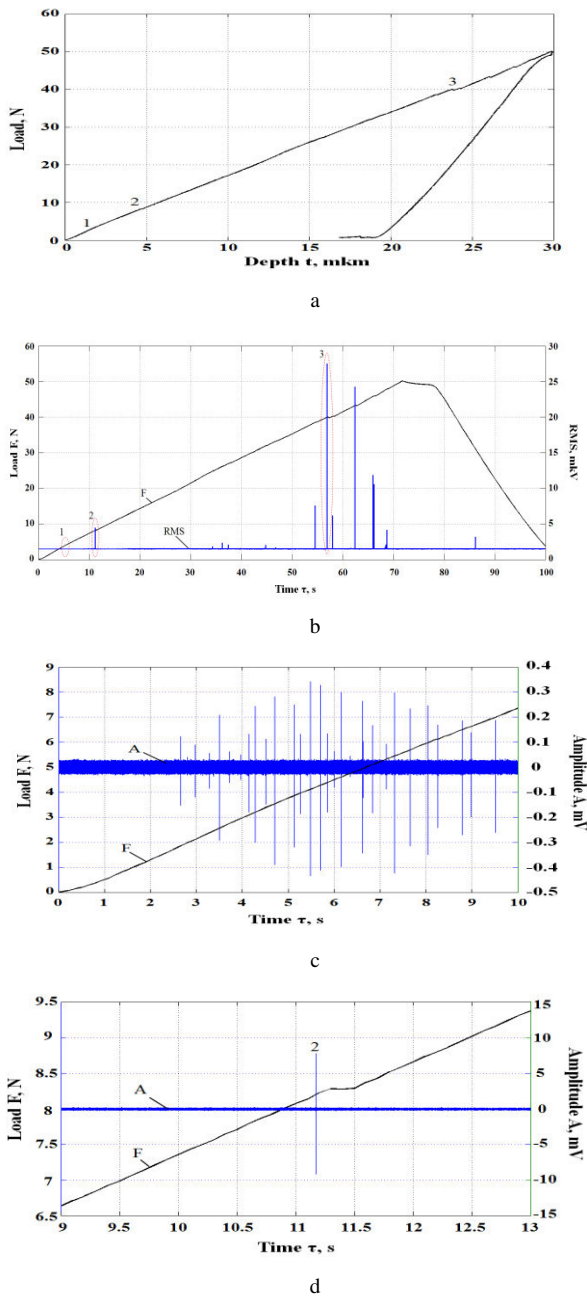


Fig. 1. Test diagram «load F – indent displacement t» for spherical indent ( $R = 0.2$  mm) (a), test diagram «load F – time  $\tau$ » joint with RMS of AE

signals (b); 3 main local zones on the diagrams: (c) – strain conversion from elastic type to elastoplastic type; (d) – first crack occurrence on the coating surface

At the zones 2 and 3 AE impulses have high amplitude and energy values. Zone 2 corresponds to first crack occurrence and is revealed at the load  $F \approx 8$  N. This could be checked by performing of another indentation of the coating till the load  $F = 8$  N, with further full unloading and microphotographing of the dent (Fig. 2).

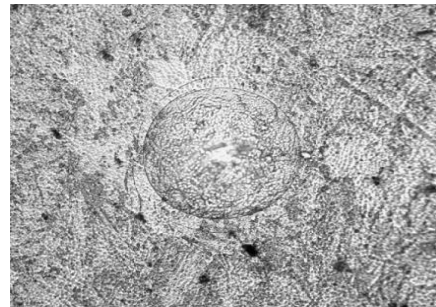


Fig. 2. Microphotographing of the dent ( $F = 8$  N)

Zone 3 - indent penetration into the base of coating – is revealed at the load  $F \approx 40$  N. At this point indentation depth is 23  $\mu\text{m}$ , which is equal to coating thickness (22...25  $\mu\text{m}$ ). Diagram line discontinuity in the zone 3 is explained by base hardness which is less than a coating one. Moments when discontinuities 1, 2 and 3 arise on diagram «F — t» almost the same as ones of AE impulses in the zones 1, 2 and 3. Fig. 1 d shows discontinuity 2 on the diagram «F — τ» with AE signals amplitudes in expanded scale.

The same tests were performed with Vickers diamond pyramid. Diagram «F - t» had the same discontinuities in the points 1, 2, 3, that correspond to loads and dent depths of strain conversion from elastic type to elastoplastic type, first crack occurrence and indent penetration into the base of coating. AE impulses in the points 1, 2, 3 were simultaneous with moments of discontinuities on the diagram.

Repeated tests of coatings with indentation by spherical and pyramid indents and with registration of «F - t» diagrams proved repeatability of results for determination of loads, depths and hardnesses in the discontinuities points.

#### ACKNOWLEDGMENT

The work was carried out in Moscow Power Engineering Institute (Moscow, Russia) with financial support from Russian Science Foundation (project code 15-19-00166).

#### REFERENCES

- [1] Kachanov V.K., Kartashov V.G., Sokolov I.V. Mechanical of contact destruction, Moscow, MPEI, 2008, 278 p. (in Russia).
- [2] Semashko N.A., Shport V.I., Marin B.M. Acoustic Emission in experimental material engineering, Moscow, Mashinostroenie, 2002, 240 p. (in Russia).
- [3] Kolesnikov U.V., Morozov E.M. Ultrasound jam resistant non-destructive testing, Moscow, Nauka, 1989, 220 p. (in Russian).

# Adaptive prediction of complex projects dynamics

Stoianova O.V.

department of management and information technologies in economy

department of MPEI National Research university in Smolensk

Smolensk, Russia

ovstoyanova@list.ru

**Abstract**—This paper describes a procedure of complex projects dynamics prediction that based on a project goals model. The proposed model represents logical and temporal relations between project goals, external events and management decisions. Expert estimations of events impacts on the project at different moments of time are used for adaptive prediction of project goals attainability. The results of prediction can be used for analysis of management decisions under uncertainty.

**Keywords**—adaptive prediction; complex project dynamics; uncertainty; expert-analytical method; model of goals

## I. INTRODUCTION

Among different types of project formal models [1] network models represented a structure of project works are the most popular. An essential disadvantage of such models is a difficulty in prediction complex project dynamics under the influence of external factors [4]. Very often there is a necessity to modify the structure of project works to decrease negative impact.

The proposed model of a complex project as a network model of project goals does not demand to modify the model main structure in turbulent environment. In the model expert estimations of strength (level) of external factors impact on each project goal are used. These estimations may have various values on the project timeline. The described approach allows predicting complex project dynamics taking into account combined impact on the project of different factors, levels of impact and temporal changes of these levels.

## II. THE COMPLEX PROJECT MODEL OF GOALS

The proposed model of a complex project can be described in the following way

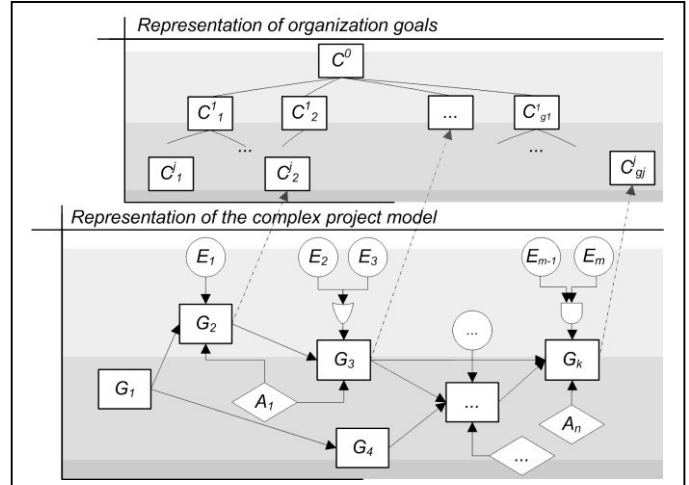
$$M = \langle G, G_r, E, E_r, EG_r, A, A_r \rangle, \quad (1)$$

$G$  – the set of project goals,  $G_r$  – the set of logic-temporal relations between the goals,  $E$  – the set of events represented the impact on the project of external factors,  $E_r$  – the set of logic relations between the goals,  $EG_r$  - the set of logic relations between the goals and the events,  $A$  - the set of actions for negative impact decrease,  $A_r$  - the set of relations between the goals and the actions.

Fig. 1. Relations between the complex project and goals of the organization

Fig. 1 shows a graphical representation of the model (1)

The work is supported by the Russian Foundation for Basic Research (project no. 15-07-02935-a).



and its links with the hierarchical model of organization goals.

Each project goal is characterized with indicators. Project goals are related with organization goals through the common indicators. We distinguish three types of indicators: point-quantitative, interval and qualitative. The indicators are used for estimation of feasibility of the project goals [3]. The feasibility is the attainability of planned results by planned date. An expression for an actual value of the feasibility of the project goal  $G_i$  is the following

$$V_i|_t = \frac{\alpha_{qn}}{n_{qn}} \cdot \sum_{\eta=1}^{n_{qn}} \frac{2 \cdot K_{\eta}^{qn}|_t - K_{\eta}^{qn}}{K_{\eta}^{qn}} + \frac{\alpha_{int}}{n_{int}} \cdot \sum_{\lambda=1}^{n_{int}} \frac{2 \cdot K_{\lambda}^{int}|_t - K_{\lambda_{min}}^{int}}{K_{\lambda_{max}}^{int} - K_{\lambda_{min}}^{int}} + \frac{\alpha_{qv}}{n_{qv}} \cdot \bigotimes_{\omega=1}^{n_{qv}} (K_{\omega}^{qv}|_t), \quad (2)$$

$K_{\eta}^{qn}|_t$ ,  $K_{\lambda}^{int}|_t$ ,  $K_{\omega}^{qv}|_t$  - actual values of point-quantitative indicators  $K_{\eta}$  ( $\eta=1..n_{qn}$ ), interval indicators  $K_{\lambda}$  ( $\lambda=1..n_{int}$ ), qualitative indicators  $K_{\omega}$  ( $\omega=1..n_{qv}$ );  $\alpha_{qn}$ ,  $\alpha_{int}$ ,  $\alpha_{qv}$  - significance levels for each type of indicators,  $(K_{\eta}^{qn})^n$  - target values of indicators  $K_{\eta}$ ,  $[K_{\lambda_{min}}^{int}; K_{\lambda_{max}}^{int}]$  - target intervals of indicators  $K_{\lambda}$ ,  $\otimes$  - convolution operation on the set of qualitative indicators.

A model construction procedure is described in [6]. This procedure is based on transformation the model of project states into the model of project goals. Such approach provides the consistent description of various project characteristics in the process of model creation.

## III. ADAPTIVE PREDICTION OF PROJECT DYNAMICS USING THE MODEL OF GOALS

System dynamics is reflected in the proposed project model through the set of events. This model, unlike the other models,

e.g. described in [2], represents logical relations between events (see fig.1). Temporal relations are encapsulated into the structure of connections between project goals.

The problem of project dynamics prediction can be reduced to the evaluation of events impact on the feasibility of project goals. This problem is complicated by the existence of uncertainty of different types [5]. The claimed approach to solving the problem accounts the following types of uncertainty: incompleteness of input data and inaccuracy of the model. It combines the ideas of Bayesian networks [8] and confidence factors theory [7].

Input data:  $V_i|E_g$  – expert estimation of the confidence that project goal  $G_i$  will be achieved, if the event  $E_g$  happened;  $V_{il}$  – actual value of the goal  $G_i$  feasibility according to (2). Output data:  $V_i$  – the predicted value of the goal  $G_i$  feasibility.

Taking into account types of logical relations between the events find the measures of belief ( $MB$ ) and disbelief ( $MD$ ) and the predicted value for each project goal that is under the influence of these events

$$V_i = \max(-1, [\min(1, (V_i + MB(G_i, \{E_g\})) - MD(G_i, \{E_g\}))], (3)$$

Expressions for  $MB$  and  $MD$  depend of quantity of events and types of relation. The idea is illustrated by the following example.

The measure of belief

$$MB(G_i, \{E_g\}) = MB(G_i, E_1 \wedge E_2 \vee E_3)$$

can be calculated as

$$MB(G_i, E_1 \wedge E_2 \vee E_3) = \max(MB(G_i, E_1 \wedge E_2), MB(G_i, E_3)). \quad (4)$$

For events linked by “and” logical relation  $MB$  evaluated as

$$MB(G_i, E_1 \wedge E_2) = \frac{\sum_{g=1}^2 \max(V_i|E_g, V_i) - \prod_{g=1}^2 \max(V_i|E_g, V_i) - 1}{1 - V_i^2} - 1. \quad (5)$$

For single event impact estimation the next expression is used

$$MB(G_i, E_3) = \begin{cases} 1, & V_i = 1 \\ \frac{\max(V_i|E_3, V_i) - V_i}{1 - V_i}, & V_i \neq 1 \end{cases} \quad (6)$$

Expressions for the measure of disbelief

$$MD(G_i, \{E_g\}) = MD(G_i, E_1 \wedge E_2 \vee E_3)$$

are outlined below.

$$MD(G_i, E_1 \wedge E_2 \vee E_3) = \min(MD(G_i, E_1 \wedge E_2), MD(G_i, E_3)), \quad (7)$$

$$MD(G_i, E_1 \wedge E_2) = 1 - \frac{\prod_{g=1}^2 \min(V_i|E_g, V_i) - 1}{V_i^2} \quad (8)$$

$$MD(G_i, E_3) = \begin{cases} 1, & V_i = 0 \\ \frac{V_i - \min(V_i|E_3, V_i)}{V_i}, & V_i \neq 0 \end{cases} \quad (9)$$

To get estimations of  $MB$  and  $MD$  for other combinations of event relations one should use iterative procedure with the help of expressions (4)-(6) and (7)-(9).

#### IV. CONCLUSIONS

Predicted values of the project goals feasibility can be used for critical goals search. Critical goals are those for which event influence leads to maximum increase of the measure of disbelief. Such goals demand careful planning and the complex project model should be decomposed in nodes of these goals.

The proposed procedures provides adaptive prediction because at any moment of time values of the project goals feasibility can be estimated taking into account new information about project environment or actual information about project state. In both cases the main structure of the project model remains stable.

#### REFERENCES

- [1] A Guide to the Project Management Body of Knowledge: fifth Edition. Pennsylvania USA : Project Management Institute, Inc, 2013.
- [2] B. K. Choi, D. Kang, Modeling and simulation of discrete-event systems. John Wiley & Sons, Inc., 2013.
- [3] M.I. Dli, O.V. Stoyanova, A.U. Belozersky, The trajectory estimation model for project management in creation and organization of high-technology industrial products production. Prikladnaya Informatika [Journal of Applied Informatics], vol. 10, no. 6 (60), 2015, pp. 105-117.
- [4] G. A. Korn, Advanced Dynamic-System Simulation: Model Replication and Monte Carlo Studies, 2d ed., Wiley, 2013.
- [5] A.S.Narin'yani, Nedoopredelenost' v sistemakh predstavleniya i obrabotki znanii [Indeterminacy in knowledge representation and processing systems]. Izvestiya AN SSSR. Tekhnicheskaya kibernetika, no. 5, 1986, pp. 3-28.
- [6] V.P. Meshalkin, O.V. Stoyanova, Procedure for Constructing Model of Innovative Projects in the Field of Nanoindustry. Theoretical Foundations of Chemical Engineering, vol. 48, no. 1, 2014, pp. 82-89.
- [7] Rule-Based Expert Systems: The MYCIN Experiments of the Stanford Heuristic Programming Project / edited by B. G. Buchanan and E. H. Shortliffe. Massachusetts: Addison-Wesley Publishing Company, 1984.
- [8] A.L. Tulupiyev, S.I. Nikolenko, A.V. Sirotkin, Bayesian Networks: A Probabilistic Logic Approach. St. Petersburg: Nauka, 2006.

# Forecasting of power efficiency of the electro network enterprise on the basis of regression methods

Sultanov M.M.

MPEI Volzhsky branch  
Volzhsky/ Russian Federation  
vfmei@vfmei.ru

Anohina E.P.

MPEI Volzhsky branch  
Volzhsky/ Russian Federation  
vfmei@vfmei.ru

**Abstract**—This article is about the analysis of undersupply of energy, the number of technological violations in work of electric equipment of the electroneutral enterprise and financing of the repair program.

**Keywords**—technological violations, costs of repair, undersupply of energy, interpolating, approximation, forecastin.

## I. INTRODUCTION

The analysis of undersupply of energy, the number of technological violations in work of electric equipment of the electro network enterprise and financing of the repair program on the example of work of PJSC IDGC of the South branch of "Volgogradenergo" is carried out. The purpose of the analysis was the detection of functional dependence between the considered data and definition of approach to forecasting of refusals and undersupply with use of methods of the regression analysis.

The basis of power efficiency of the modern power enterprise is a reduction of number of refusals of electric equipment and reliable power supply of consumers.

## II. CREATION OF REGRESSION DEPENDCES

The analysis of data allows finding functional dependence by the number of annual technological violations and refusals and annual financing of the repair program.

Basic data are presented in the form of arrays

$$t = \begin{bmatrix} t_1 \\ t_2 \\ \dots \\ t_n \end{bmatrix}, \quad O_t = \begin{bmatrix} O_{t_1} \\ O_{t_2} \\ \dots \\ O_{t_n} \end{bmatrix}, \quad Z_t = \begin{bmatrix} Z_{t_1} \\ Z_{t_2} \\ \dots \\ Z_{t_n} \end{bmatrix}, \quad Nd = \begin{bmatrix} Nd_1 \\ Nd_2 \\ \dots \\ Nd_n \end{bmatrix} \quad (1)$$

where  $t_i$  – time periods;  $O_{ti}$  – the refusals and technological violations given to time periods;  $Z_{ti}$  – the financing of repair work given to time periods;  $Nd_i$  – undersupply of energy, brought to time periods.

Settlement formula

$$F(t) = \sum_{i=0}^n O_{ti} f_i(t), \quad (2)$$

where  $f_i(t)$  – basic polynomials,  $O_{ti}$  and  $t$  – massifs of knots of interpolating.

For definition of interrelation between elements the approximating functions allowing predicting the number of failures of the equipment of the electro network enterprise and undersupply of energy with costs of repair activity [1] have been constructed.

Similar dependence has been received in the analysis of the  $Z_t$  and  $Nd$  arrays.

According to the analyzed data of massifs of expenses and refusals has been constructed linear ( $f_1(k)$ ), square ( $f_2(k)$ ) and cubic ( $f_3(k)$ ) the approximating functions.

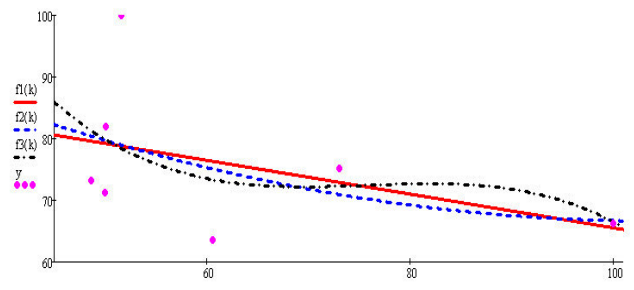


Fig. 1. Approximation of basic data on refusals and costs of repair

According to the analyzed data of massifs of expenses and the undersupply of electricity has been constructed linear cubic ( $f_3(k)$ ) the approximating functions.

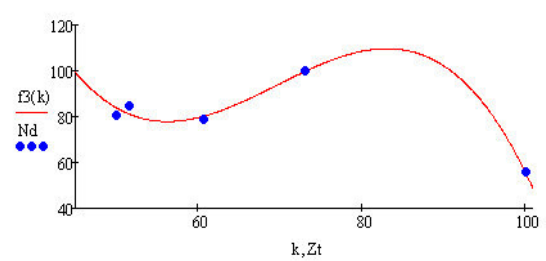


Fig. 2. Approximation of basic data undersupply of energy and expenses

## III. VERIFICATION OF RESULTS

Verification of the obtained data, for the choice of a type of the approximating function yielding the most reliable result on

the forecast of number of refusals at change of financing towards increase has been carried out. The most reliable result on the forecast has been received when using a cubic polynomial.

The approximating functions were based by results of work in 2008-2015 and in earlier years. The best result has been received at approximation by cubic function.

#### IV. CONCLUSIONS

By results of researches the technique is developed and approach to forecasting of number of refusals and

technological violations, and also sizes of undersupply of energy in work of the electro network enterprise from the size of investments on implementation of the repair program is defined, and also it is received. The offered method can well be modeled at change of input parameters and doesn't demand labor-consuming calculations.

#### REFERENCES

- [1] Sultanov M.M., Anokhina E.P. "Use of methods of Interpolating in forecasting of number of technological violations in electroneetwork economy". – Reliability of power No. 6, 2016

## The new Item for IEC

V.N. Kuryanov  
MPEI Volzhsky branch  
Volzhsky/ Russian Federation  
vek077yandex.ru

**Abstract** — The indicator of efficiency of electric energy use unambiguously is the level of technical losses at its transportation and use, and decrease in losses and increase of efficiency is a task of the today's operating organizations.

**Keywords** — efficiency; technical losses; electric energy; IEC; wires.

#### I. INTRODUCTION

The main elements and methods of dropper the overhead contact line system of railways presented in figure 1.

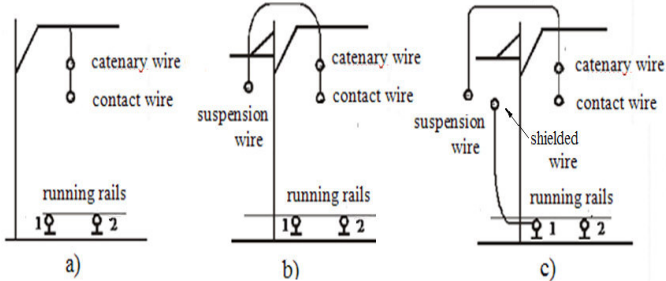


Fig. 1. Description of overhead contact line system of railways

- The catenary (messenger) wire, the contact wire, running rails;
- The same but with the reinforcing wire;
- Catenary wire, the contact wire, the reinforcing wire - (reverse) wire, connected in parallel with the rails.

The catenary wire is not a less important element of the overhead catenary system of railways than the contact wire, both from the point of view of reliability, and from the point of view of energy efficiency.

Existing standards for overhead catenary system of railways:

- Russian. There are standards that apply to all areas of the industry, and not only on the railways;
- International. International standard "Railroad carrier cables of contact network GOST 32697-2014" and experience requirements for the justification of catenary wires used in Armenia, Belarus, Kyrgyzstan, Russia, Tajikistan and Ukraine from June 1, 2015.
- Foreign. These are not detected.

The lack of standards of the contact railway network cables in the majority of countries around the world is pushing for the necessity of international data structuring in European, Asian and other countries to a single IEC. Comparative characteristics of some of the catenary wires used in the Russian Federation presented at table 1.

Wires are classified by types of construction (table 2):

- Containing central wire. The inside weaving has 6 wires, outside – 12 wires (turning of weaving must have opposite direction, and outside weaving must have the right direction of turning);
- Containing central wire. The first inside weaving has 7 wires. The second inside weaving alternate 7 wires of one diameter and 7 wires of another. The third outside weaving has 14 wires (all three weavings have the same step of turning and also the same direction. They have liner touch of wires. The wires of inside weavings have the round cross section form. The wires of outside weavings are compacted).

The wire must not have any crossing, protrusion, gap, fracture, and connection of separate wires.

The construction length of the wire is settled by customer and manufacturer.

Weaving step multiplicity must be 10 – 18 for inside and 10 – 15 for outside weavings (but not more than inside weaving step multiplicity).

The technology of wire manufacturing must provide its construction length no less than 2000 m.

Also, all the requirements for mechanical and electric parameters, marking, packing, methods of control, and so on are pointed out in the international standards for participating countries.

II. The presence of experienced experts in the Russian Federation for writing a supranational standard of the railway ropes contact network

Option structure of the new IEC standard for supporting catenary wires railroads:

- Introduction and general provisions;
- Terms and Definitions;
- General requirements;
- System engineering and project management;
- Requirements for ropes;
- Verification of conformity;
- The use of wires for communication between power substations;
- The use of wires for data transmission.

### III. SUMMARY

- Necessity to systematize the best international practices in terms of standardization of the local catenary wires, followed by putting them into a joint standard IEC;
- The proposal to base on international standard «railroad carrier cables of contact network GOST 32697-2014 », and

experience the justification of the systematization of catenary wire. As well as similar local regulations at option of experts and to start the development of a joint unitary standard IEC catenary wires for overhead catenary system of railways.

TABLE I. COMPARATIVE CHARACTERISTICS OF SOME OF THE Catenary WIRES USED IN THE RUSSIAN FEDERATION

Indicator	Catenary wires		
	C-I20	C-I50	CC-I20
Nominal diameter, mm	14,0	15,8	14,0
Nomenal cross section, mm <sup>2</sup>	120	150	120
Counted squire of the cross section of all the wires in the cable, mm <sup>2</sup>	117,0	148,0	140,06
counted weight of 1 000 m cable, kg	1 058	1 338	1 300
Specific electric resistance at 20°C, Om/km	0,1580	0,1238	0,1383

TABLE II. TECHNICAL REQUIREMENTS FOR WIRES

Nominal diameter, mm	Extreme deviation of fact diameter from the nominal one, %. But no more	Nominal cross section, mm <sup>2</sup>	The fact cross section, mm <sup>2</sup> . But no less		The fact weight of 1km, kg. But not more	
			Round	Compacted	Round	Compacted
10.70	from -2,0 to +6,0	70.0	67.7	83.4	612	803
12.60		95,0	94.0	119,2	850	1146
14.00		120.0	117.0	137,3	1058	1320
15.80		150.0	148.0	181.8	1338	1748

# Resonant coupling of 3 DC-circuits

Marvin Jandesek, Christian Sauerbrey, Daniel Hißbach

Fachgebiet Leistungselektronik  
Technische Universität Ilmenau  
Ilmenau, Germany

**Abstract**— This paper will show a topology of how to couple three DC-circuits by resonance with one another and will point out one of the problems regarding that topology, which lead to the questioning of my bachelor thesis. An approach of how to solve this problem will be discussed.

**Keywords** — resonant coupling of 3 DC-circuits

## I. INTRODUCTION

This Paper presents a certain topology to couple 3 DC-circuits by resonance with one another and some of the problems that go along with that topology. To generate high efficiency for the transfer of electric power, LC circuits are a viable option, because of the possibility of zero current switching (ZCS) and zero voltage switching (ZVS). Especially to realize the idea of a distributed power supply, with a high frequency AC-bus, the use and viability of resonant inverters are discussed more often nowadays [1-3]. Even more advantages of a series resonant inverter can be named as followed. The input voltage can be regulated by the transformers transmission ratio. Furthermore are inputs and outputs potential isolated and the power flow can be bidirectional.

## II. THEORY

To accomplish a state of ZCS, a square-wave voltage signal  $U_1$ , provided by a Full-Bridges converter, of a certain frequency  $\omega_s$  is needed. At best, this frequency would equal the resonant frequency  $\omega_r$ . In this specific case the current of the resonant tank is would be at the zero crossing event, right when the square-wave voltage is toggled (compare Fig.2 b)). While the electrical power would equal zero at this moment, the Full-Bridge switches would go without losses. While this is the state of resonance the blind current, resonating between the capacity and the inductivity, would also equal zero at this point.

## III. APPROACH

Fig.1 shows the topology presented in this paper. The three resonant circuits are coupled by three separate high-frequency transformers. The Full-Bridges, to insert the square-wave voltage to the resonant tanks, are all driven by the same frequency. Like the different numbering on the capacities and the inductivities indicates, in reality there will be small differences between each of the resonant-circuits, which leads to different resonant frequencies.

$$f_{res} = \frac{1}{2\pi\sqrt{L \times C}} \quad (1)$$

The problem faced regarding this issue, would be to decide on a frequency to trigger the MOSFET's in a way that the losses

in the whole system would be minimal, since for sub- or super-resonant behavior ZCS cannot be ensured anymore (compare Fig.2 a,c)). The approach here would be to calculate the blind current of each LC-circuit. This values will be summed up and will be regulated to find a frequency in which the blind current in the system will be minimal.

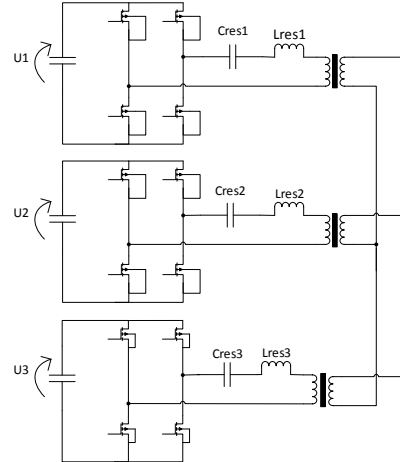


Fig.1. Topology

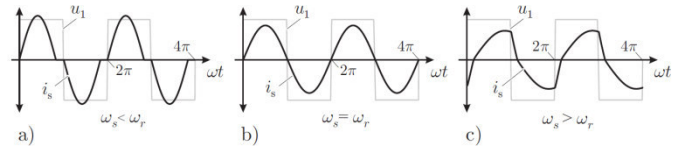


Fig.2. a) Sub-resonant: switching frequency lower than resonant frequency  
b) Resonant  
c) Super-resonant: switching frequency higher than resonant frequency

## REFERENCES

- [1] Z. M. Ye, P. K. Jain, and P. C. Sen, "Analysis and Design of Full Bridge Resonant Inverter for High Frequency AC Distributed Power System Application", 31<sup>st</sup> Annual Conference of IEEE Industrial Electronics Society, 2005. IECON 2005.
- [2] J. A. Sabate; M. M. Jovanovic; F. C. Lee; R. T. Gean, "Analysis and Design-Optimization of LCC Resonant Inverter for High-Frequency AC Distributed Power System", IEEE Transactions on Industrial Electronics
- [3] Kunrong Wang; Yimin Jiang; S. Dubovsky; Guichao Hua; D. Boroyevich; F. C. Lee , "Novel DC-rail soft-switched three-phase voltage-source inverters", Industry Applications Conference, 1995. Thirtieth IAS Annual Meeting, IAS '95., Conference Record of the 1995 IEEE

# A Stricter Heap Separating Points-To Logic

René Haberland, Kirill Krinkin  
Saint Petersburg Electrotechnical University "LETI"  
Saint Petersburg, Russia

**Abstract.**—Dynamic memory issues are hard to locate and may cost much of a development project’s efforts as it was found e.g. in [5] and was repeatedly reported similarly afterwards independently by different persons. Verification as one formal method may proof a given program’s heap matches a specified dynamic behaviour. Dynamic (or heap) memory, is the region within main memory that is manipulated by program statements like alloc, free and pointer manipulation during program execution. Usually, heap memory is allocated for problems where the amount of used memory is unknown prior to execution. Regions within the heap may be related “somehow” with each other, often, but not always, by pointers containing absolute addresses of related heap cells [1]. The data structure described by all valid pointer variables manifests heap graphs.

**Keywords**—separation logic, dynamic memory verification, points-to memory model, partial heap specification, ambiguous heap assertions.

A heap graph is a directed connected simple graph within the dynamic memory which may contain cycles, and where each vertex represents an unique memory address and every edge links two heap vertices. The heap graph must be pointed by at least one variable from the local stack or a chain of other heap graphs which is finally pointed by at least one stacked variable. Heap vertices may not overlap. A heap formula expresses the assertion on dynamic memory and can either be a heaplet, or a recursively defined heap-spatial or logical formula.

One of many different ways to specify the heap graph is by a points-to model as it was proposed by Burstall [2] and Reynolds [3]. Essentially, both specify pairs  $loc \rightarrow val$  of a location and its pointed by value, they differ in whether an address or an immediate value is used. The advantage of a points-to model over e.g. a shape region is *locality*, which causes only local changes to the heap graph specification on changes due to its edge-centric view, and provides an intuitive style of how program statements correspond to heap graph. Burstall and Reynolds introduce a non-repetitive *Separation Logic*, which weakens, for instance, constants which become in fact functions. The underpinning theoretically apparatus is a *Substructural Logic* [4].

Initially, Reynolds proposed to use the “,”-operator in order to describe heap graphs, which works fine for linked-lists or cactus-shaped heap graph, but which would imply a search for perfect matchings, if proceeded for heap graphs in general. Reynolds defines the set of heap graphs, but not a single heap graph which can only be defined approximately from his written objections as either a conjunction of existing heaps or a disjunction of (possibly connected) heaps.

Our Class-instantiated objects are considered as pointer generalisations, though an object pointer may point at the same time to more than one object. Motivated mainly by our believe in many cases arbitrary heap access by immediate addresses can and should be restricted by different modelling, it is first of all not primarily an expressibility issue for that particular case. Motivated by Prolog predicates may be introduced to specify heap, which are naturally relational and are not classical functions. Since its semantic is relational, it makes them flexible, for instance when it comes to express general heap graphs. We call parameterized predicates *abstract*.

The main new idea behind this approach is to distinguish strictly in syntax and semantics between heap conjunction and disjunction. Therefore, algebraic rules are agreed which may eventually be used to define equalities, which then might be used to toggle a SMT-solver reducing simplifications more efficiently and consequently reduce bloated verification rules. It may be considered as a side-effect verification rulesets could be checked for completeness according to specified heap terms. The motivation behind making operators stricter is to undermine exceptional cases, which eventually will make calculations simpler.

Locations may be local variables, objects, and object fields. All locations in a heap graph must be unique. With the heap terms defined the next pointer-pointed quantities may be associated: 1:1, m:m, and m:1. However, 1:m is prohibited, except we understand as an object with all outgoing pointers as “one”. W.l.o.g. inner objects must always be modelled as exterior objects. Heap conjunction binds stronger than disjunction. Late binding is currently ignored. Pointers of pointers are also not further considered, although not prohibited, for the reason that they do not change anything essentially to a heap graph one could not do without further indirection. *true* interprets true for any matching heap (*false* in analogy), *emp* interprets only true if the matching heap is empty – those are used for partial heap specifications.

The proposed heap conjunction says that two heaps are connectible, where the right heap must be a points-to expression, iff there exists exactly one joining point otherwise it interprets as false. False, after all is not undefined, and therefore conjunction on unconnectible heaps is total. Alternatively, the conjunction may be refined further which part is going to be source and which is going to be target. The above heap conjunction can be generalised according to the extended heap terms. By convention it is agreed that for  $H1$  being a heap  $H1 \circ \underline{emp} = \underline{emp} \circ H1 = H1$  holds. When dealing with object fields, we agree further object accessors are left-associative  $object1.field1.field2.field3 = ((object1.field1).field2).field3$ , so

left parts of paths may be assigned by symbols: this is most important when using abstract predicates, because only fields for an unspecified object are usually provided.

All “◦”-connected heaps generate a commutative group with several arrangements: closure follows from totality of “◦”, identity is *emp*, associativity holds only for connectible elements – if heaps are not connectible, then *false* is returned except it will be connected until last element of “◦” is consumed. It always holds that unrelated heaps may not be “◦”-conjunction, so  $a \rightarrow b \circ a \rightarrow d = \text{false}$  regardless if  $b = d$  holds or not. It does not matter in which order the (connectible) heaps are connected, important is that they are all connected, this establishes confluence of “◦”-joined heaps. Without any extra costs in Prolog, locations may be symbols. Due to associativity and closure the problem of abstract predicates may be interpreted as Word-problem. Furthermore, existence of an inverse heap w.r.t. “◦” always exists due to the generalised heap inversion  $G \circ G^{-1} = \text{emp}$ , which can be shown over the heap term inductively. The possibility to refer to an inverse may be useful when a proof refutes in order to digest expected from actual heaps, and of course, it is as for instance Galois field extensions, a convenient technique in order to calculate in terms of algebraic equations. Intuitively inversion may be interpreted as heap negation plus some extra clean-up heap vertices, if those are no more needed. Let the convention be  $\text{emp}^{-1} = \text{emp}$ . It was found, that required precautions on calculations with inverses can easily be linearly adapted after each calculation step over heap conjunction and disjunction. First, this is the case whenever source/target are still in use, then they may not be substituted by disjunction. Second, when a bridging edge between graphs is removed, then a heap conjunction needs to be turned into a disjunction.  $(G_1 \circ G_2)^{-1} \equiv GI^{-1} \circ G2^{-1}$  holds for any heaps  $G_1$  and  $G_2$ .

Heap disjunction becomes very straight and intuitive, because there are no more exclusive cases to be taken into consideration when defining verification rules: Two heaps  $H1$  and  $H2$  are indeed independent, iff  $H1||H2$ . Similar to heap conjunction, but under different circumstances, heap disjunction and heap partitions form a group. In analogy to point-wise heap conjunction, the disjunction of heaps may be point-wise, too – both operations are dual.

Now heaps may be built upon consistent and strict operations. Besides these operations, heaps may also be used to define partially ordered sets with an infimum element *emp*, a totally connected graph as supremum, and “◦”-operator as joining operator.

Local variables as points-to expressions, may be grouped together among “◦”-conjunctioned heaps to invariant parts when procedures or methods are called, however it needs to be taken into consideration heap inversion may invalidate the heap frame rule which may need make procedure calls specially aware on unaffected changes. Object fields are “◦”-conjunctioned too, and so the same constant formulae are applicable to objects just to distinguish all locals from all fields from a particular

object, constant formulae, like *true*, are parameterized for objects.

So,  $a.f\ 1 \rightarrow x \circ \underline{\text{true}}(a)$  may denote property  $f$  1 of object  $a$  on the lefthand-side of “◦” where  $\underline{\text{true}}(a)$  may denote all remaining fields from  $a$  (except  $f1$ ). This is why, in  $\underline{\text{true}}(a) \circ \underline{\text{true}}(a)$  the lefthand side accumulates all properties where the second  $\underline{\text{true}}(a)$  actually accumulates none which makes it equals to *emp*. The bottom line is, the object fields need to be traced while verification, so partial specification may fill in all non-specified fields automatically, which eases specification a lot without making the specification imprecise by default. From the point of view of *Separation of Concern* it is highly recommended abstract predicates specify as much as possible of an object’s behaviour rather than spreading object behaviour all over different abstract predicate definitions – also but not only because the stack-based approach, would be limited to abstract predicates calls in depth rather than in width.

The Object Constraint Language (OCL) [6] is a specification language for class-instantiated objects in companion to the Unified Modeling Language. It implements a considerable part of first-order predicate logic, furthermore it has got quantification, supports collection types and ad-hoc polymorphism by sub-classing. There is a way to specify an object’s life-cycle and class methods. However, OCL does not know of pointers nor aliases. In combination with abstract predicates the new logic presented may be used as recommendation for an update of the recent OCL definition w.r.t. the intrinsic points-to model, which would benefit in better modularity and improved Separation of Concerns.

#### ACKNOWLEDGMENT

Parts of this paper are prepared as a contribution to the state project of the Board of the Ministry of Education of the Russian Federation (task # 2.136.2014/K).

#### REFERENCES

- [1] R. Jones, A. Hosking, and E. Moss, *The Garbage Collection Handbook: The Art of Automatic Memory Management*. Chapman & Hall/CRC, 2nd ed., 2011.
- [2] R. M. Burstall, “Some techniques for proving correctness of programs which alter data structures,” in *Machine Intelligence* (B. Meltzer and D. Michie, eds.), vol. 7, pp. 23–50, Scotland: Edinburgh University Press, 1972.
- [3] J. C. Reynolds, “Separation logic: A logic for shared mutable data structures,” in *Proceedings of the 17th Annual IEEE Symp. on Logic in Computer Science*, (Washington DC), pp. 55–74, IEEE Computer Society, 2002.
- [4] G. Restall, *Introduction to Substructural Logic*. Routledge, 2000. ISBN 041521534X.
- [5] B. P. Miller, L. Fredriksen, and B. So, “An Empirical Study of the Reliability of UNIX Utilities,” in *Proc. of the Workshop of Parallel and Distributed Debugging*, pp. 1-22, Digital Equipment Corp., 1990.
- [6] Object Management Group: Object constraint language v. 2.2, from 15th Feb 2010 available at <http://www.omg.org/spec/ocl/2.2>.

**NESEFF**

**“Network for energy supply and energy efficiency”**



## **International Scientific Conference “NESEFF – 2016”**

**"Network for energy supply and energy efficiency"- "NESEFF"**

was created in September, 2015 in Baku to provide a sustainable development of continuous scientific communication and cooperation of its members in the field of power supply and energy efficiency.

The members of NESEFF are:

- ❖ Technical University of Liberec (Liberec, Czech Republic)
- ❖ Wrocław University of Technology (Wroclaw, Poland)
- ❖ Azerbaijan Technical University (Baku, Azerbaijan)
- ❖ National Mining University (Dnepropetrovsk, Ukraine)
- ❖ Brandenburg University of Technology Cottbus - Senftenberg (Cottbus, Germany)
- ❖ National Research University "Moscow Power Engineering Institute" (Moscow, Russia)

The NESEFF founder and chairman is  
Prof. Dr.-Ing. habil. Sylvio Simon.

# Über Normativen und den Einfluss der städtischen Bebauung auf den Wärmebedarf von Gebäuden

G. Afonina, V. Glazov

Fakultät für Wärme- und Stoffübertragung Prozesse und Anlagen  
Moskauer Energetische Universität  
Moskau, Russland

[AfoninaGN@mpei.ru](mailto:AfoninaGN@mpei.ru), [GlazovVS@mpei.ru](mailto:GlazovVS@mpei.ru)

**Abstract** - the article presents the results of the research work that prove the necessity of a technique creation that capable to quantify the impact of topology changes of the urban environment in conditions of external heat exchange, changing the required heat consumption value in the premises of the existing buildings.

**Keywords:** mathematical simulation of heat exchange, temperature distribution unevenness, topology of urban development

## I. EINLEITUNG

Die Grundlage für die Durchführung der vorliegenden Arbeit wurden die Daten des Analytischen Zentrums bei der Regierung der Russischen Föderation [1], nach denen Der Wärmeenergieverbrauch ist äußerst ungleichmäßig in Wohnhäuser, die sogar der gleichen Bautyp haben, und kann von mehr als vier Mal variieren. Das ist ein ernstes Problem, denn der Anteil des Energieverbrauchs nur die Bevölkerung und die Unternehmen der Wohnungs- und Kommunalwirtschaft ist ziemlich groß in Moskau und beträgt 52 %.

Die unterschiedliche Effektivität von Gebäuden eine Serie ist durch die folgenden Gründe bedingt:

- Die unterschiedliche Haupthimmelsrichtung des Gebäudes;
- Unterschiedliche Windrose, verzerrte Stadtentwicklung (benachbarte Gebäude).
- Menschlicher Faktor (materielle Zustand der Bewohner und deren subjektive Gefühl von Komfort bei einer unterschiedlichen Kombination von Temperatur, Windgeschwindigkeit und Luftfeuchtigkeit innen).
- Technologischer Faktor (Zeit, Weg und Wetter-Bedingungen für die Errichtung des Gebäudes, sondern auch die Qualität der Baumaterialien).

## II. AUFGABEN DER ARBEIT

- Die Berechnung und die vergleichende Analyse des Wärmeenergieverbrauchs und das Heizungskosten des Mittelraums und des Eckraums;
- Die Durchführung der mathematischen Modellierung der Wärmeübertragung zwischen dem Gebäude und der äußeren Umgebung in städtischen Gebieten;
- Vergleichende Analyse der Ergebnisse der mathematischen Modellierung.

## III. ERGEBNISSE

Die Ergebnisse der Berechnungen, die nach der normativen Methode [2-4], für Gebäude, die sich in Moskau befinden, zeigen, dass das Heizungskosten des Eckraums kann um 1,5-2-faches das Heizungskosten des Mittelraums übertreffen (Abb.1).

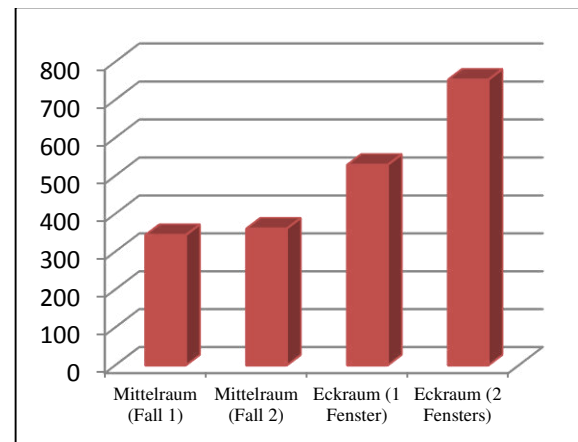


Abbildung 1 – Die Kosten für die Heizung pro Monat, RUR.

In Mangel an den einstellbaren thermischen Zählern müssen einige Leute unterbezahlen, andere überbezahlen für die Heizung die Service-Organisation, für die ist wichtig eine endliche Summe, und nicht, wie es verteilt sich zwischen den Bewohnern.

2. Da die aktuellen Vorschriften nicht berücksichtigt die Auswirkungen der Topologie der städtischen Bebauung auf Temperatur- und High-Speed-Leistung und die Luftverschmutzung bei Gebäuden, die durchgeführt wurde, mathematische Modellierung in einer PHOENICS-Umgebung unter Berücksichtigung dieses Faktors (Abb.2-3).

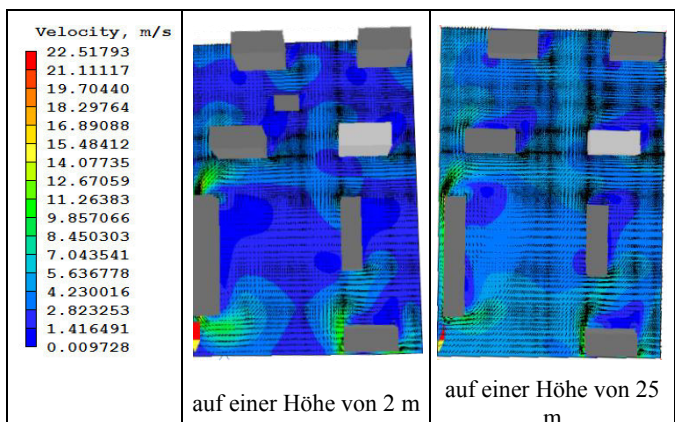


Abbildung 2 – Das Geschwindigkeitsfeld für das Gebäude №1

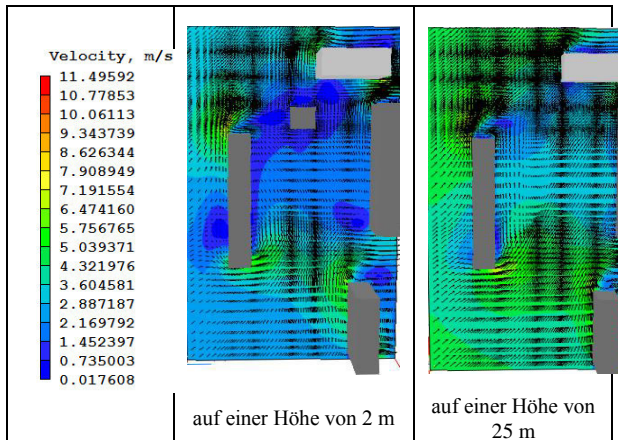


Abbildung 3 – Das Geschwindigkeitsfeld für das Gebäude №2

3. Vergleichende Analyse der Ergebnisse der numerischen Simulation erhaltenen Gebäuden einer Serie, die sich in verschiedenen Bezirken Moskaus, zeigte, dass der größte ungleiche Verteilung der Temperatur und des Wärmedurchgangskoeffizienten auf der äußeren Oberfläche des noch-Hochhäuser beobachtet in horizontaler Richtung (Abb.4-5).

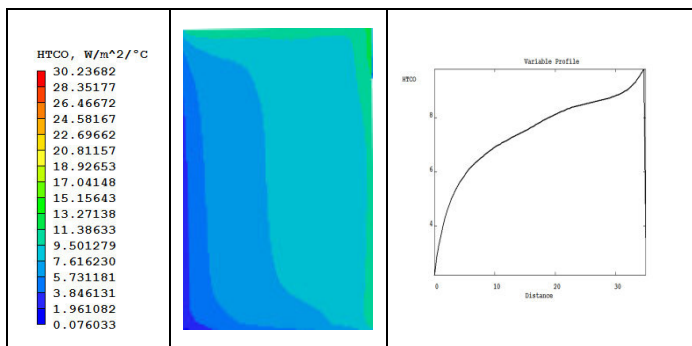


Abbildung 4 – Die Verteilung des Wärmedurchgangskoeffizienten an Südseiten des Gebäudes №1

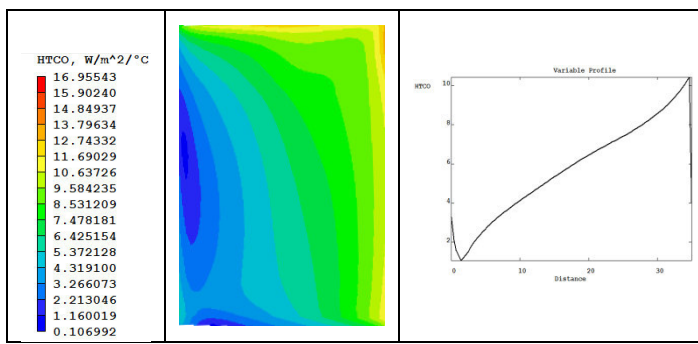


Abbildung 5 – Die Verteilung des Wärmedurchgangskoeffizienten an Südseiten des Gebäudes №2

Das bedeutet, dass für optimalen Komfort in Räumen, die sich auf der gleichen Etage befinden, benötigen Sie eine unterschiedliche Anzahl von Wärme.

D.h. die Kosten für den Aufenthalt in den Wohnungen wird bestimmt nicht nur die Kosten für Wärmeenergie, und der Topologie der städtischen Bebauung.

#### IV. SCHLUSSEN UND PROBLEMMEN

*1. Schluss:* Die Verfügbarkeit der Zähler beseitigt ein Problem mit der Überbezahlung /Unterbezahlung für die Heizung und die Hauptsache - die hilft die Problembereiche in Wärmeschutzhülle des Gebäudes zu lokalisieren, und dann die Wärmebilduntersuchung bestimmter Räume mit mehr als einer detaillierten Bestimmung von Schwachstellen in der äußeren Zaun zu führen.

*Problem:* Die Notwendigkeit der Bestimmung und Lokalisierung von energiesparenden Maßnahmen zur Beseitigung der Mängel und zur Verbesserung Wärmeschutz Eigenschaften der Gebäudehülle.

*2. Schluss:* Die Wohnungserfassung des Wärmeenergieverbrauchs im Gebäude hilft der Unterschied in der Bezahlung für die Heizung identische Räume, deren Außenwände sind unter verschiedenen Umweltwirkungen, identifizieren.

*Problem:* Die Notwendigkeit der Abstimmung mit den Gebäudebesitzern Maßnahmen, die ist mit der Errichtung neuer oder dem Abbruch der alten Gebäude verbinden. Wenn diese Gebäude können die Bedingungen der Wärmeaustausch in einer städtischen Umgebung ändern und auf das Heizungskosten einwirken.

#### V. VERALLGEMEINERUNG

Die Qualitative Analyse der Ergebnisse der vorliegenden Arbeit führt zu dem Schluss, über die Notwendigkeit, eine Methodik zu erstellen, die kann die Quantifizierung der Auswirkungen von Änderungen in der Topologie der städtischen Umwelt auf die Bedingungen der äußeren Wärmeübertragung schätzen.

#### REFERENZEN

- [1] Gascho E. Analyse der Wirksamkeit der Instrumente des Konsums der thermischen Energie auf die Ziele Energiesparen Heizung – Theorie und Praxis: Proceedings des siebten Internationalen Schule-ein Seminar der Jungen Wissenschaftler und Fachleute. In 2 Bänden. – M.: Verlag Mei, 2014.
- [2] SNiP 23-01-99\*. Bauklimatik. Moskau, 2006.
- [3] SNiP 23-02-2003. Der Wärmeschutz der Gebäuden. Moskau, 2004.
- [4] SNiP 41-01-2003. Heizung, Lüftung und Klimaanlage. Moskau, 2004.

# Example of Improving the Energy Efficiency of Industrial Enterprise by using Absorption Chillers in the Refining Industry

S. Prishchepova, A. Fedyukhin, I. Sultanguzin  
Dept. of Industrial Heat Power Engineering Systems  
Moscow Power Engineering Institute  
Moscow, Russia

**Abstract —** In the paper it is described the use of absorption chiller in the isomerization workshop of refinery for utilization of steam condensate and refrigeration the top product of deisohexanizer. The work performed energy audit of isomerization unit and proposed a method of improving its energy efficiency, calculated cycle of absorption chiller, and presented the final results of the calculation. All calculations are based on the data from the isomerization unit at the refinery.

**Keywords—** absorption chillers; refining industry; waste heat; secondary energy resources; energy efficiency.

## I. INTRODUCTION

Identification and use of secondary energy resources (SER) - one of the most important ways of increasing the efficiency of industrial equipment in the energy-intensive industries. By utilizing SER, some enterprises can fully meet its own needs for heat, cold and partly in electrical energy. Environmental aspects of the use of SER are not less important, as the reduction of unused energy resources reduces the costs of their disposal and decreases pollution.

The importance of the use of secondary energy resources is still in the fact that investment in measures to save fuel and energy resources (FER) is much more favorable than the increase of production the latter. The existence of significant amounts of SER in the energy-consuming enterprises, as well as a large number of possible methods of disposal provides the economic feasibility of the implementation of measures for the use of SER.

One of the effective directions of SER utilization is the production of cold for the processes of the enterprise where it is required [1]. Solving the issues of rational and efficient use of secondary energy resources, we should pay attention to the fact that along with getting cold the processes of transformation of heat from low temperature level to a higher, and vice versa could be implemented with the use of lithium bromide absorption heat transformers (LAHT).

For the LAHT work, depending on their purpose, we must have a heating source temperature 80-120 °C (in single-stage steam generation in a generator) or 160-170 °C (in a two-stage steam generation in the generator). When LAHT is working to generate cold, it requires environmental source of cooling (air or water) and cooled source.

In this paper you can see a variant of absorption chiller application in the refinery.

## II. DESCRIPTION OF THE ISOMERISATION UNIT

The main objective of this work is the use of absorption chiller in the isomerization workshop of refinery for utilization of steam condensate and refrigeration the top product of deisohexanizer.

Due to the fact that Russia planned transition to "Euro-5" grade gasoline sales in 2016, many refineries needed to introduce an isomerization unit for deeper processing of raw materials. The aim of this installation process is to increase the octane number of a light naphtha (commercial gasoline component) to 90.3 points on the research method.

In light naphtha isomerization unit to conduct the process a significant amount of steam with different process parameters is using. The steam of various parameters is preparing directly in front of technological devices by throttling after it is done at the the boiler. The biggest consumer of the steam in the installation is deisohexanizer column (DIG).

Deisohexanizer column consists of 102 plates and it is designed for separation of stable isomerizate to the top product, upper and lower side products, bottom product of the column. The vapor from the top of the column goes to a condenser of the deisohexanizer, it is condensed there and further goes to the receiver of the column. The condenser is an air cooler, equipped with supply chemically treated water to increase the efficiency of cooling in summer.

Depending on the ambient air temperature to maintain the desired temperature of the top product in the control zone the amount of fans varies remotely and fed chemically treated water.

## III. PROBLEMS IN THE ISOMERISATION UNIT AND ITS SOLUTION

After the energy audit was carried out, it was concluded that additional cooling capacities are needed. This conclusion was made as the air coolers could not cope with cooling of the top product of the column. According to the regulations the top product temperature after air coolers should be 40-45 °C, but in summer it is not cooled below 45-48 °C.

This problem can be solved in several ways: to put an extra row of air coolers, to put a vapor compression chiller or an absorption chiller. An additional number of air coolers takes too much area, which the plant doesn't have on its territory. Vapor compression machine requires a large amount of electric

power, which is undoubtedly undesirable for the plant. The variant of absorption chiller use is suitable for solving this problem, because it does not require large areas, large energy costs, besides there is a sufficiently large number of secondary energy resources in the form of condensate after the reboiler of DIG column with a temperature of 115 °C.

## I. EQUIPMENT PARAMETERS CALCULATION

In order to choose the right equipment, it is necessary to study the method of calculating the absorption chiller cycle [2].

Temperature conditions of operation are determined by parameters of three independent sources of external heat. For example, in the modes of cool generation they are temperature of the heating source Th, cooling water temperature Tw1 and cooled source temperature Ts2.

Calculation of any thermodynamic cycle of absorption chiller is based on the adopted temperature differences between the substances in the installation.

According to the adopted temperature differences some parameters are defined: higher temperature of the solution at the end of the boiling process in a generator, a lower temperature at the end of the absorption process in the absorber. According to the adopted temperature difference in a solution heat exchanger the temperature at the outlet of the unit is determined. Then in the  $\xi$ - $i$ -diagram (concentration and enthalpy) for the selected solution the position of the nodal points of the thermodynamic cycle of the absorption chiller is determined and calculations are carried out.

Further, from the heat balance of the installation heating,

TABLE I  
TECHNICAL CHARACTERISTICS

Parameter	Conditions of the customer	
	AC-600W	AC-1000W
Cooling capacity, kW	700	800
Cooled water		
Volume flow rate m <sup>3</sup> /h	120	137
Temperature (input/output), 0C	12/7	12/7
Cooling water		
Volume flow rate m <sup>3</sup> /h	179	205
Temperature (input/output), 0C	27/35	27/35
Heating water		
Volume flow rate m <sup>3</sup> /h	70	70
Temperature (input/output), 0C	120/108	108/94

AC- Absorption chiller

cooling and cooled water flow rates are found.

As there is a sufficiently large amount of condensate (~ 70 m<sup>3</sup> / h) at a temperature of 115-120 °C after the reboiler of

DIG column, the amount of energy that can be obtained by cooling of condensate to 100 °C will be 1628 KW. This amount of energy can be used to generate cold in the absorption chillers. According to the amount of heating source the calculations were done (Table 1). Nominal technical characteristics which satisfy the conditions of the customer are given in the table 1 .

## II. CONCLUSION

To improve the energy efficiency of the isomerization unit was made an offer to put the cooling system, consisting of 2 single effect absorption lithium bromide refrigerating machines with series connection for heating water and parallel connection of cooled and cooling water. The first in the course of the heating water is -Abs.Ch-600, second is Abs.Ch.-1000, both machines constructed by the company "OKB Teplosibmash".

The installation of this equipment will allow to use the condensation heat and cool the top product of deisohexanizer

to provide its full condensation. Full condensation of the top product of deisohexanizer will allow to reach its design capacity (600 thousand tons / year). At the moment, its capacity is 360 thousand tons / year.

## REFERENCES

- [1] Herold K.E., Radermacher R., Klein S.. Absorption chillers and heat pumps. Boca Raton (FL): CRC Press;1996
- [2] Baranenko A.V., Timofeevskiy L.S., Dolotov A.G., Popov A.V. Absorption heat converters: St.Petersburg,2005. – 338 p.

# Effectiveness Evaluation of Blower and Expansion Appliances as Part of Equipment and System

N.Kalinin, Y. Zhigulina, V. Kulichihin  
Dept. of Industrial Heat Power Engineering Systems  
Moscow Power Engineering Institute  
Moscow, Russia

**Abstract**— the article considers advantages of exergy method of effectiveness evaluation of blower and expansion appliances in comparison with other efficiency indicators. It is shown that in some cases the effect obtained from power installation can be determined only by means of the exergy efficiency.

**Keywords**— adiabatic efficiency factor, exergy method, blower and expansion appliances, turbine, compressor.

## I. INTRODUCTION

The determination of the effect generated by the blower and expansion machines and the effectiveness assessment of machines, plants and systems to which they belong – are the most difficult questions in engineering.

This is explained by several factors. First, the efficiency of the processes occurring in the blower and expansion machines are often assessed in relative terms by comparing the ideal processes with valid ones. These indicators illustrate the perfection degree of processes and devices, but do not always characterize the effect created by this device. However, it is the correct definition of the process, or device, or installation effect that allows to estimate the produced result from technical and economic point of view.

## II. EXERGY METHOD

In our opinion, the most correct way of the blower and expansion machines efficiency  $\eta$  determination is to use the ratio of the obtained effect  $E$  to the cost  $C$ , expressed in comparable units of energy:

$$\eta = \frac{E}{C} \quad (1)$$

It is logical that such efficiency  $\eta$  must satisfy the inequality  $0 < \eta < 1$ . However, in a number of widely known technical examples of formal use of this ratio is  $\eta > 1$ , that is just puzzled and criticism.

For example, the heat pump efficiency is usually measured by:

$$\varphi = \frac{Q_t}{N}, \quad (2)$$

called the transformation ratio. Here  $Q_t$  - the generated heat,  $N$  – the compressor power consumption. This ratio is always greater than one, and in the initial period of heat pumps application this caused the just baffled in the technique. Even greater difficulties arise in the performance assessing of the combined plant for the heat and cold joint production. It is a widely spread situation when the combined plant total effect determination is obtained via summation of non-additive value of heat production -  $Q_h$  and cold production-  $Q_c$ . At the same time large values of this indicator do not characterize the quality of heat and cold production.

The solution of this problem was found when the exergy method was developed [1].

The exergy concept lies in the basis of this approach as a measure of entire converting in other forms of energy. This implies that energy is divided into two category: one that can be completely converted in any other form of energy and the other that cannot.

power installations efficiency

The most common and simple example of expansion machinery performance assessment is to use the relative efficiency factor often called an adiabatic or isoentropic efficiency factor  $\eta_s$ :

$$\eta_s = \frac{\Delta h}{\Delta h_s}, \quad (3)$$

where  $\Delta h$  and  $\Delta h_s$  are the enthalpy differences in the real and ideal isentropic processes of expansion, respectively. This indicator characterizes the perfection of the expansion process and takes into account only one effect: for power machines –it is the received work, and for expanders - the working medium cooling.

In fact, in any expansion process there is always a second effect, that can be used.

In the case of power machines (steam or gas turbines) it is the temperature (enthalpy) at the outlet and it differs from environmental parameters.

The most vivid examples: counter-pressure steam turbines and combustion turbines with sufficiently high temperature of flue gas (e.g. 450÷500 °C)

In General case exergy efficiency for any turbine can be evaluated via the following formula:

$$\eta_e = \frac{N_t + E_2}{E_{wm} + E_q}, \quad (4)$$

where  $N_t$  - available turbine capacity, that is given to a generator or a compressor or a pump,  $E_2$ - exergy of working medium at the turbine output if the generated heat or cold is beneficial used,  $E_{wm}$ – working medium exergy at the turbine inlet,  $E_q$ – exergy of heat or cold supplied at the turbine inlet.

In the case of cogeneration exergy efficiency will be:

$$\eta_{eco} = \frac{N_t + E_{qt}}{E_{wm} + E_q},$$

where  $E_{qt}$  is the exergy of consumed heat at temperature level of  $t$ .

There are many other examples in engineering when the effect obtained from the power installation can be determined only by means of the exergy efficiency.

## REFERENCES

- [1] Brodyansky, V. M., Exergy method of thermodynamic analysis.- M., Energy.1973-296 S.

# Определение Потребления Энергии для Отопления с Использованием Удельной Характеристики Здания

В.Г. Гагарин<sup>1</sup>, В.В.Козлов, В.Н. Гагарина, Чжоу Чжибо<sup>2</sup>

Научно – исследовательский институт строительной физики (НИИСФ РААСН), Москва, Россия

Московский государственный строительный университет, Москва, Россия<sup>2</sup>

[gagarinvg@yandex.ru](mailto:gagarinvg@yandex.ru)<sup>1</sup>, [tchzhou.tchzhibo@yandex.ru](mailto:tchzhou.tchzhibo@yandex.ru)<sup>2</sup>

**Аннотация —** Рассмотрены основы расчета потребления энергии зданием. Потребление энергии на отопление здания пропорционально объему здания, градусо-суткам отопительного периода и удельной характеристике здания. Рассмотрен расчет трансмиссионных теплопотерь при помощи удельной теплозащитной характеристики. Рассмотрен расчет тепловых потерь на основе удельных характеристик, представленный в СП «Тепловая защита зданий»

**Ключевые слова —** удельная характеристика здания; потребление энергии на отопление здания; трансмиссионные теплопотери; тепловая защита зданий.

## I. ВВЕДЕНИЕ

При постановке задач расчета потребления энергии на отопление зданий содержится много неопределенностей. Очевидно, что влияет климат региона строительства, архитектурно-планировочные решения здания, теплозащитные характеристики ограждающих конструкций, особенности эксплуатации здания, в том числе зависящие от субъективных причин, и др. [1]. При рассмотрении повышения энергоэффективности строительства зданий чаще всего рассматривают увеличение сопротивления теплопередаче ограждающих конструкций [2]. Это чрезвычайно однобокий подход. Он вызван тем, что инициируют и поддерживают кампанию по энергосбережению в строительстве производители теплоизоляционных материалов. Поэтому проблема сводится к возможно большему использованию теплоизоляционных материалов [3]. В настоящей статье рассмотрен подход к тепловым потерям при отоплении здания, которыйложен в основу в нормативном документе СП «Тепловая защита здания» [4].

## II. УРАВНЕНИЕ ТЕПЛОВЫХ ПОТЕРЬ ЗДАНИЯ

Если предположить, что здание представляет собой тело с температурой, равной температуре внутреннего воздуха  $t_e$  при температуре наружного воздуха  $t_n$  то из закона Ньютона следует, что при отоплении здания потери теплоты в единицу времени,  $q$ , Вт, будут пропорциональны разности температур:

$$q = C(t_e - t_n), \quad (1)$$

где  $C$  – коэффициент пропорциональности, Вт/°C.

Потери теплоты,  $Q$ , Дж, за время  $z$  будут выражаться уравнением:

$$Q = \int_0^z q d\tau = \int_0^z C(t_e - t_n) d\tau = C \int_0^z (t_e - t_n) d\tau \quad (2)$$

Коэффициент  $C$  в уравнении (2) является характеристикой здания и не зависит от климатических параметров. Можно положить, что этот коэффициент пропорционален отапливаемому объему здания  $V$ :

$$C = kV \quad (3)$$

Коэффициент  $k$  измеряется Вт/(м<sup>3</sup> °C) и известен как удельная характеристика. В зависимости от того, какие тепловые потери здания рассматриваются, к названию удельная характеристика добавляется определяющий термин. Смысл этой характеристики – количество энергии теряемой единицей объема здания в единицу времени при перепаде температуры в один °C.

Интеграл  $\int_0^z (t_e - t_n) d\tau$  является параметром климата при отоплении здания. Он называется числом градусо-суток. Если  $z_{on}$  – продолжительность периода отопления в течение года, то интеграл носит название градусо-сутки отопительного периода (ГСОП):

$$ГСОП = \int_0^{z_{on}} (t_e - t_n) d\tau \quad (4)$$

В [4] для нормирования используются удельные характеристики. Этой особенностью СП 50.13330.2012 выгодно отличается от нормативных документов многих других стран. При сравнении потребления энергии зданием необходимо проводить расчеты значений  $k$  и отапливаемых объемов по одним и тем же методикам.

## III. УДЕЛЬНАЯ ТЕПЛОЗАЩИТНАЯ ХАРАКТЕРИСТИКА

Удельная характеристика вычисляется из рассмотрения тепловых потерь здания. Например, если рассматриваются только трансмиссионные тепловые потери через оболочку здания, то они описываются при небольшом упрощении формулой:

$$Q = \left( \sum \frac{A_i}{R_{o,i}^{np}} \right) \cdot ГСОП \cdot 24 / 1000 \quad (5)$$

где  $Q$  - потери теплоты зданием за отопительный период, кВт·ч/год;

$A_i$  - площади наружных ограждений, м<sup>2</sup>;

$R_{o,i}^{np}$  – приведенные сопротивления теплопередаче соответствующих наружных ограждений, м<sup>2</sup> °C/Вт;

ГСОП – градусо-сутки отопительного периода, °C сут./год;

$V$  – отапливаемый объем здания, ограниченный рассматриваемой совокупностью ограждающих конструкций, м<sup>3</sup>;

$A_h^{sum}$  - суммарная площадь всех наружных ограждающих конструкций, м<sup>2</sup>.

Преобразование уравнения (5) дает:

$$\begin{aligned} Q &= 0,024 \cdot ГСОП \cdot \left( \sum \frac{A_i}{R_{o,i}^{np}} \right) = \\ &= 0,024 \cdot ГСОП \cdot V \cdot \frac{A_h^{sum}}{V} \cdot \left( \sum \frac{A_i}{R_{o,i}^{np}} \right) / A_h^{sum} = \\ &= 0,024 \cdot ГСОП \cdot V \cdot k_{ob} \end{aligned} \quad (6)$$

Из (6) и (3) следует, что удельная характеристика в рассматриваемом случае равна:

$$k_{ob} = K_{комп} \cdot K_{обиц} \quad (7)$$

где

$$K_{комп} = \frac{A_h^{sum}}{V} \quad K_{обиц} = \left( \sum \frac{A_i}{R_{o,i}^{np}} \right) / A_h^{sum} \quad (8)$$

Величина  $k_{ob}$  называется «теплозащитной удельной характеристикой», Вт/(м<sup>3</sup> °C). Из (8) следует, что чем больше объем здания, тем меньше коэффициент компактности здания и тем меньше удельная теплозащитная характеристика здания. Из (7) и (8), следует, что величина  $k_{ob}$  не зависит от климатических характеристик района строительства и определяется свойствами здания и его ограждающих конструкций. Однако сопротивления теплопередаче ограждающих конструкций здания принимаются в зависимости от ГСОП района строительства. Поэтому нормативные значения удельной теплозащитной характеристики выбираются в зависимости от ГСОП района строительства. В [4] требования к удельной теплозащитной характеристике заданы в виде  $k_{ob} \leq k_{ob}^{mp}$ . Требуемые значения  $k_{ob}^{mp}$  заданы в виде таблицы 1.

Таблица 1

Нормируемые значения удельной теплозащитной характеристики здания [4].

Отапливаемый объем здания, V, м <sup>3</sup>	Значения $k_{ob}^{mp}$ , Вт/(м <sup>3</sup> °C), при значениях ГСОП, °C сут/год				
	1000	3000	5000	8000	12000
300	0,957	0,708	0,562	0,429	0,326
600	0,759	0,562	0,446	0,341	0,259
1200	0,606	0,449	0,356	0,272	0,207
2500	0,486	0,360	0,286	0,218	0,166
6000	0,391	0,289	0,229	0,175	0,133
15000	0,327	0,242	0,192	0,146	0,111
50000	0,277	0,205	0,162	0,124	0,094
200000	0,269	0,182	0,145	0,111	0,084

#### IV. УДЕЛЬНАЯ ХАРАКТЕРИСТИКА ПОТРЕБЛЕНИЯ ЭНЕРГИИ НА ОТОПЛЕНИЕ И ВЕНТИЛЯЦИЮ ЗДАНИЯ

В [4] рассчитывается также и удельная характеристика потребления энергии на отопление и вентиляцию здания,  $q_{om}^p$ :

$$q_{om}^p = [k_{ob} + k_{вент} - (k_{быт} + k_{рад}) \cdot v \cdot \zeta] \cdot (1 - \xi) \cdot \beta_h \quad (9)$$

где:

$k_{ob}$  – удельная теплозащитная характеристика здания, Вт/(м<sup>3</sup> °C), определяемая по формулам (7) и (8);

$k_{вент}$  – удельная вентиляционная характеристика здания, Вт/(м<sup>3</sup> °C) [5];

$k_{быт}$  – удельная характеристика бытовых тепловыделений здания, Вт/(м<sup>3</sup> °C);

$k_{рад}$  – удельная характеристика теплопоступлений в здание от солнечной радиации, Вт/(м<sup>3</sup> °C) [6].

Значения  $k_{вент}$ ,  $k_{быт}$ ,  $k_{рад}$  и коэффициенты  $\beta_h$ ,  $v$ ,  $\zeta$  определяются по методикам, содержащимся в [4]. Нормируется удельная характеристика потребления энергии на отопление и вентиляцию здания,  $q_{om}^p$  обычным образом:  $q_{om}^p \leq q_{om}^{mp}$ . Однако требуемая величина зависит только от объема здания, выраженного его этажностью.

Если умножить удельную теплозащитную характеристику на ГСОП и на размерный коэффициент 0,024, то получится количество тепловой энергии в кВт ч, которое теряется через оболочку здания одним м<sup>3</sup> отапливаемого объема за отопительный период, если это количество разделить на высоту этажа, то получится «удельный расход тепловой энергии на отопление здания», обусловленный теплопотерями через оболочку здания, измеряемый в кВт ч/(м<sup>2</sup> год).

#### V. ЗАКЛЮЧЕНИЕ

Использование для нормирования потребления энергии зданиями удельных характеристик позволяет записать общие требования для зданий на всей территории России и, соответственно, сравнивать здания с точки зрения их энергосбережения.

#### ЛИТЕРАТУРА

- [1] Гагарин В.Г., Чжоу Ч. О нормировании тепловой защиты зданий в Китае // Жилищное строительство. 2015. № 7. С. 18-22.
- [2] Пастушков П.П., Павленко Н.В., Коркина Е.В. Использование расчетного определения эксплуатационной влажности теплоизолационных материалов. // Строительство и реконструкция. 2015. № 4 (60). С. 168-172.
- [3] Пастушков П.П., Жеребцов А.В. Об эффективности применения экструдированного пенополистирола в ограждающих конструкциях первых и цокольных этажей. // Строительные материалы. 2015. № 7. С. 68-71.
- [4] СП 50.13330.2012 «Тепловая защита зданий». Актуализированная редакция СНиП 23-02-2003. – М.: Минрегион России, 2012. – 96 с.
- [5] Гагарин В.Г., Неклюдов А.Ю. Использование матричного метода для определения вентиляционной составляющей тепловой нагрузки на систему отопления здания. // Промышленное и гражданское строительство. 2014. № 7. С. 21-25.
- [6] Коркина Е.В. Комплексное сравнение оконных блоков по светотехническим и теплотехническим параметрам. // Жилищное строительство. 2015. № 6. С. 60-62.

# Status and Prospects of Use of Nonconventional Renewed Energy Sources

F.G.Amirov; A.S.Mammadov,  
Azerbaijan Technical University  
Baku, Azerbaij

**Abstract—** Analysed status and prospects of use of nonconventional renewed energy sources. Technical and economic indicators of creation of sea wind park on stationary platforms in the Azerbaijan sector of Caspian sea are demonstrated. The model for the description of a wind mode in this region is offered.

**Keywords—** nonconventional renewed energy source, wind generators, wind turbines, solar, hydraulic power

The problem of introduction of nonconventional renewed energy sources (NRES) is now one of the most actual problems in the world. Abroad, especially in industrially developed countries, considerable experience on design excellence of electro generators for wind-driver power stations, which can be used at creation of generators by capacity to 1000 kW, capable to work with variable frequency of rotation [2] is stored.

Seven principal views of energy are known: solar, hydraulic power, wind, burning of gas, oil, coal and nuclear. Results of poll in the countries of Europe have shown that solar energy use, on the second place - hydraulic power, then wind, burning of gas, oil, coal and nuclear are the most preferable.

It is necessary to notice that in the world the established capacity of WEI with 6172 MB in 1966 has increased to 12000 MB in 1999 , and the forecast for 2010 constitutes approximately 36000 MB .

The main manufactures of WEI in Europe - are Denmark, Great Britain, Germany and Belgium. Now 3,75 % of requirement of the industry in the electric power has become covered at the expense of wind power. In the north of Germany numerous coastal installations are expanded to 25 % using energy in spite of the fact that Germany on a geographical position represents a zone with light breezes.

In Azerbaijan with a considerable quantity of slopes from high-mountainous areas to Caspian sea and strong stable air currents, there exist perfect conditions for use of wind energy.

With a view of carrying out of reliable power and technical and economic calculations on wind power use, operation modes of WEI and their productivity data on repeatability of speeds of a wind in a considered zone, their chronological course and a number of other characteristics are necessary. Such data are resulted in wind power cadastre.

In a cadastre, data on a wind is represented usually in the form of statistical regularities, in the tabular or graphic form, using materials of long-term supervision on meteorological stations, and also the given special intelligence.

As it is known, one of the most power-intensive branches of economy of Azerbaijan is the oil and gas extraction branch which annually consumes over 1 billion kWh electric power. The State Oil company of the Azerbaijan Republic (SOCAR) is interested in application of WEI as the source, allowing to save a considerable part of energy, and from positions of ecological cleanliness of manufacture (absence of harmful emissions) and continuous maintenance with the electric power of the extracting enterprises in the emergency situations connected with failure in power supply.

Wind generators can break only local ecological equilibrium. Such generators are not in a status to influence ecology in broad range. Turbine noise, vibration, electromagnetic waves can negatively affect migration of birds around 100-200 metres. At worst, living creatures can leave this zone. Nevertheless, this situation is more localised.

Now, villages around Surabad, in such areas as Sulutepe and Gobustan some wind turbines by the general capacity 16 MB are established. Thus, creation of sea wind park on stationary platforms in the Azerbaijani sector of Caspian sea represents the big economic interest and allows to receive non-polluting, reliable and economically effective power system.

## REFERENCES

- [1] A.H. Janahmedov, etc. / The wind power installations – Baku: Chashiogli,2009. page 164.
- [2] Amirov F.G., Analysis of transitional processes in the work of wind power installations with application // The Mechanical Engineering ,2010, №1.
- [3] Amirov F.G., Influence of circulation of a wind round blades of wind tribune on its aerodynamics // The Mechanical Engineering, 2009, №10.
- [4] www. clean-wind. ru
- [5] Popel O.S., Tumanov V.L., Renewed energy sources: a status and development of prospects // Alternative power and ecology, 2007, №22 (46).
- [6] Shefter J.I., The use of wind power. –M:Energoatomisdat, 1983. page 200.
- [7] Sibikin J.D. & Sibikin M.J., Nonconventional renewed energy sources. – M: Radio Software, 2009. page 232.

# Применение Микроканального Теплообменника в Схеме Теплового Насоса

А.Б. Гаряев, Н.М. Савченкова, Д.Р. Колдашева

Department of Heat-and-Mass Exchange Processes and Installations

National Research University MPEI

Moscow, Russia

[gab874@yandex.ru](mailto:gab874@yandex.ru), [Savchenkovam@mpei.ru](mailto:Savchenkovam@mpei.ru), [koldasheva\\_dr@mail.ru](mailto:koldasheva_dr@mail.ru)

**Abstract** —The article discloses the use of microchannel heat exchanger as a heat pump condenser. This increases the cost of the apparatus but this reduces the cost of installation and operating costs of the apparatus. The payback period of such replacement is one - three years.

**Keywords** —*microchannel heat exchanger, waste heating, low-grade heat, heat pump, energy efficiency.*

## I. ВВЕДЕНИЕ

На современном этапе все чаще поднимаются вопросы об эффективном использовании энергетических ресурсов, о снижении энергозатрат в промышленности и коммунальном хозяйстве, ведутся непрерывные разработки «альтернативных», «нетрадиционных» источников энергии. В тоже время, большинство технологических процессов, работа многих механизмов и устройств сопровождается выделением большого количества тепла, которое никак не используется, а рассеивается в окружающем пространстве, т.е. попросту сбрасывается. Сбросное тепло является низкопотенциальным с температурой незначительно (от 10-30 °C) большей температуры окружающей среды, поэтому его использование обычным путём затруднено. Низкопотенциальное тепло обладает колossalной энергией, поэтому его утилизация, то есть преобразование «бесплатной», выбрасываемой тепловой энергии в полезную энергию является важной научно-технической задачей.

## II. РЕЗУЛЬТАТЫ

Одним из механизмов, использующих низкопотенциальное тепло, является тепловой насос. Использование тепловых насосов в Европе с каждым годом возрастает, однако в России тепловые насосы получили меньшее распространение. Причиной этому является стоимость ТН, которая составляет более миллиона рублей, не считая буровые работы для аппарата с геотермальным низкопотенциальным источником.

Одним из вариантов снижения стоимости аппарата является замена трубчатого конденсатора на микроканальный. В отличие от применяемых сейчас теплообменных аппаратов с каналами, имеющими размеры порядка нескольких десятков миллиметров, эквивалентный диаметр каналов микроканального теплообменника составляет сотни или даже десятки микрометров. Это позволяет не только увеличить площадь теплообменной поверхности аппарата в единице его объема (компактность), но и заметно повысить интенсивность теплообмена.

Традиционный путь повышения эффективности теплообмена в микроканальных теплообменниках состоит в уменьшении размеров теплообменных каналов при увеличении их числа и создания микрорельефа на

поверхности каналов. Это увеличивает материалоемкость и стоимость теплообменников.

Предлагаемый теплообменник отличается от существующих микроканальных теплообменников тем, что в нем обеспечивается преимущественно противоточная схема движения теплоносителей за счет возможности подвода и отвода потока теплоносителя с разных сторон, которая более эффективна, чем схема «перекрестного тока», а также тем, что за счет малой длины каналов достигается малое гидравлическое сопротивление проточной части, и за счет обеспечения высокой компактности и высокого значения коэффициента теплопередачи достигается высокая тепловая эффективность аппарата. Тонкие теплопроводные пластины теплообменника спаиваются между собой с помощью тонкой проволоки, образуя микроканалы, что обеспечивает жесткость конструкции и фиксированное расстояние между пластинами от 100 до 2000 микрон.

Предлагаемый теплообменник обеспечивает также снижение потребления дорогостоящей электрической энергии на прокачку теплоносителя, увеличение срока эксплуатации насосного оборудования, уменьшение материоемкости.

## I. ВЫВОДЫ

Задача повышения эффективности микроканальных теплообменников, снижения потребления дорогостоящей электрической энергии на прокачку теплоносителя, увеличения срока эксплуатации оборудования, уменьшении материалоемкости, снижении стоимости теплообменных аппаратов и эксплуатационных затрат решается путем организации преимущественно противоточной схемы относительного движения теплоносителей, уменьшении гидравлического диаметра и снижении гидравлического сопротивления проточной части за счет снижения длины основных каналов микроканальных теплообменников.

## ЛИТЕРАТУРА

- [1] Бараненко А.В., Цветков О.Б., Лаптев Ю.А., Ховалыг Д.М.Ю. «Миниканальный теплообменник в холодильной технике». Научный журнал НИУ ИТМО. Серия «Холодильная техника и кондиционирование» № 3, (2014).
- [2] Popescu T., Marinescu M., Pop H., Popescu G., Feidt M., Microchannel Heat Exchangers – Present And Perspectives U.P.B. Sci. Bull., Series D, Vol. 74, Iss. 3,(2012), Page 55 – 70.
- [3] S.G. Kandlikar, W.J. Grande, “Evolution of microchannel flow passages-thermohydraulic performance and fabrication technology”, Heat Transfer Eng., 24 (1), 2003, pp. 3-17
- [4] J.J. Brandner, K. Schubert, Fabrication and testing of microstructure heat exchangers for thermal applications, in: Proceedings of ICMM2005, 3rd International Conference on Microchannels and Minichannels, June 13–15, 2005, Toronto, Ontario, Canada, ASME, 2005, pp. (no pagination)/paper number ICMM2005-75071, published as CD-ROM.

# Deep Heat of the Earth – Energy Source for Remote Consumers

S. Grigoriev

Dept. of Industrial Heat Power Engineering Systems  
Moscow Power Engineering Institute  
Moscow, Russia  
grigoriev.srcw@gmail.com

**Abstract** —The work is devoted to a study of temperature reduction during thermal energy extraction from deep Earth's rocks. Known experimental results from not deep wells are given. Computational analysis results have shown, that it is possible to extract deep Earth's thermal energy for 25 years and more.

**Keywords**— *enhanced geothermal systems, temperature reduction, deep geothermal single well system, deep heat of the Earth*

Today the efficient use of energy resources is one of the global problems all over the World. Its successful solution will be important not only for the further development of the international community, but also it will preserve its habitat. It is possible to note the following basic problems in electric and thermal energy generation:

- limited oil and gas resources;
- the high cost of mineral energy resources production and transportation;
- low environmental safety during the production of electric and thermal energy;
- difficult fuel transporting to remote consumers of electric and thermal energy.

The depletion of fossil fuels and the environmental consequences of its burning will significantly increase the interest in alternative and renewable energy sources. The need for renewable energy is noted in various government programs and by different political figures.

Today there are two main ways to implement a geothermal circulation system: an "open" system and "closed" system. The "open" method of extracting the deep Earth's thermal energy is the following: with the help of hydraulic fracturing a deep reservoir is made. This reservoir connects to two or more wells: injection and extraction wells. The disadvantage of the "open" method is the possibility of impurity and mineralization of heat transfer fluid due to its contact with the reservoir surface (in fact with Earth's rocks), the volume of which can be up to 2 cube kilometers.

A less common "closed" system needs only one well in which a deep "tube in tube" heat exchanger is placed. A heat transfer fluid circulation is carried out in a closed circuit inside the heat exchanger. Using this method, we can significantly reduce the energy source cost. There is no need to drill several wells and create deep collector by hydraulic fracturing. Besides there is no contact between heat transfer fluid and hot rocks, so the transfer fluid stays clean.

Thermal energy can be produced by deep geothermal single well (DGSW) system at different extraction rates. Excessive production can bring economic benefits, like earlier return of investment, but can also lead to hot dry rocks full temperature reduction around the heat exchanger and to high hydraulic losses in the system.

V. Bekker

Dept. of Industrial Heat Power Engineering Systems  
Moscow Power Engineering Institute  
Moscow, Russia  
becker14@mail.ru

Minimal hydraulic losses can be achieved when the velocity of heat transfer fluid in single borehole heat exchanger varies from 0.5 to 0.8 m/s [1]. There is also an optimal flow rate of heat transfer fluid which can be determined by different locational characteristics. In this case long and sustainable production can be achieved. But any way at the start of thermal energy extraction temperature reduction occurs.

Initially, temperature of heat exchanger surface is the same as hot dry rocks temperature. But during DGSW operation rocks temperature reduces and temperature reduction distributes in the borehole subsurface volume [2].

According to the preliminary experimental data provided by Switzerland scientists, the temperature reduction process around the well is not infinite [3]. But after a while the system starts to operate in steady mode with a new temperature behind the wellbore. They studied 105 meters depth borehole heat exchangers with heat pump system. During the first 5 years the temperature of the soil around the borehole heat exchanger reduced by 1-2 °C. During the next 10 years subsurface temperature had varied for only 0.5 °C. At some distance from the borehole rock's temperature rate was close to the natural initial value.

This experimental data was obtained for borehole heat exchanger with small diameter end depth (only 105 m). Bigger diameters and depths (up to 7000 m) provide a larger amount of thermal energy, but temperature reduction can distribute to dozens of meters around the borehole. This case has been studied using computational analysis. A single borehole heat exchanger ("tube in tube") of 7000 m length, placed in the territory with temperature gradient 3 °C/100 m was studied. Results show, that temperature reduction distributes to distances from 14 to 36 meters and this process takes about 25 years.

The work was undertaken with the financial aid by the Ministry of Education and Science of the Russian Federation (Order about the appointment of the President's scholarships to young scientists and graduate students engaged in research and development in priority areas of modernization of the Russian economy in 2015-2017 years, from March 10, 2015, № 184).

## REFERENCES

- [1] Ryzhenkov V.A. et al Temperature reduction in deep Earth's rocks during thermal energy extraction.. Natural and technical sciences, 2012. Vol.3, pp. 321-326 (in russian)
- [2] Ladislaus Rybach Geothermal Sustainability. GEO-HEAT CENTER QUARTERLY BULLETIN, 2007. Vol. 28, №3, pp. 2-7
- [3] Rybach L., Eugster W. Sustainability aspects of geothermal heat pump operation, with experience from Switzerland. Geothermics, 2010. Vol. 39, Issue 4, pp. 365-369

# Investigation of the Cogeneration System Based on Secondary Energy Resources

A.Ya. Shelginsky, A.S. Malenkov<sup>1</sup>  
Dept. of Industrial Heat Power Engineering Systems  
Moscow Power Engineering Institute  
Moscow, Russia  
malenkov.as.ya.ru@yandex.ru<sup>1</sup>

**Abstract —** The research examines the problem of supply by heat and cold ventilation and heating systems through the effective use of renewable energy resources (RES) on manufacture.

**Keywords —** absorption chiller, renewable energy resources, energy consumption, energy efficiency

## I. INTRODUCTION

This research is focused on the study of heating and cooling systems based on absorption chillers. We are considering the problem of supply ventilation and heating systems by heat and cold through the effective use of secondary energy resources on the example of the production plant of ammonium phosphate. The administrative building on the production was selected as the object in question. As the technical solution to produce cold has been considered the use of absorption chillers. Comparison of the two basic types of absorption chillers (water-ammonia and lithium bromide chillers) was carried out.

## II. FORMULATION

Annual and estimated demand of heat for ventilation and heating systems during the cold season, the estimated and annual demand in the cold during the warm season for ventilation systems for the considered object were shown.

Preliminary calculations and production circuit analysis show that the basic needs of heat and cold can be achieved through the use of heat of secondary energy resources such as secondary vapor and exhaust gases. Among the variety of choices of working substances for absorption chillers water solution of lithium bromide or ammonia are considered as conventional [1], and for this type of machines calculations were carried out.

The basis of mathematical models to calculate the cycles of absorption chillers is on the equations for calculating the thermodynamic properties of the respective solutions. The coefficient of performance of one-stage absorption chillers for different temperatures in generator and for different heat regeneration degree inside the cycle were obtained.

Heat regeneration degree inside the cycle is:

$$\chi = \frac{T_4 - T_8}{T_4 - T_2} \quad (1)$$

where  $T_4$  – the solution temperature at the outlet of the generator °C,  $T_2$  – the solution temperature at the outlet of the

absorber °C,  $T_8$  – the solution temperature at the inlet of the absorber °C.

Rate of coverage required indoor conditions using heat RES has been calculated. Data processing and analysis of real climatic data for the summer period for the Moscow region have been carried out. Number of hours standing outside temperatures has been defined. Cooling load dependence on the number of hours standing outside temperatures has been obtained. The importance of selecting the estimated cooling load due to climatic data to provide the operation of the cooling system with a given rate of coverage has been shown. The technical solution to produce heat and cold is «heat-cold station» [2]. This is a heat station scheme with integrated absorption chiller. Generator of absorption machine is connected to the pipe of supply water and pipe of back water. Absorber and condenser is connected to the cooling tower and they can be cooled either sequentially or in parallel. In addition, it is suggested the use of the heat of adsorption and condensation to heat hot water.

## III. CONCLUSION

Evaluation value of total cooling capacity, which may receive as a result of utilization of RES for cases of use different types absorption chillers has been performed. The main provisions used to create mathematical models of water-ammonia and lithium bromide absorption chillers have been presented.

A comparison of operating costs of energy when using different types absorption chillers and in comparison with the use of vapor compression chillers has been performed. Specific electricity consumption for the production of 1 kW·h of cold for absorption chillers and compression chillers has been given. Annual energy savings in tons of equivalent fuel by utilizing RES has been calculated. Effectiveness of the proposed solution has been shown. General economic indicators and heat balances in the case of the proposed solutions is calculated. Discounted payback period is acceptable and it is approximately 7 years.

## REFERENCES

- [1] Galimova L.V. Absorption chillers and heat pumps: Textbook for specials. Technique and physics of low temperature. - Astrakhan: Publishing House of the Astrakhan State Technical University, 1997. - 226 p. (in Russian)
- [2] Shelginsky A.Ya., Malenkov A.S. Cogeneration systems based on renewable energy resources in the production of mineral fertilizers. Industrial Power Engineering. 2014, Vol.7, pp. 32-37. (in Russian)

# Energetische Sanierung von Fachwerkwänden mit ½ - Stein starker Vormauerung

Bewertung des hygrothermischen Verhaltens der Holzkonstruktion

Torsten Bark

Brandenburg University of Technology  
Cottbus-Senftenberg,  
Cottbus, Germany  
Torsten.Bark@b-tu.de

Prof. Dr. sc. techn. Horst Stopp

Brandenburg University of Technology  
Cottbus-Senftenberg  
Cottbus, Germany  
Horst.Stopp@b-tu.de

**Abstract**— Die Anwendung von Innendämmssystemen bietet bei der energetischen Sanierung gute Lösungsansätze. Für Konstruktionen aus Mauerwerk mit einbindendem Holztragwerk ist das hygrothermische Verhalten bei veränderten Nutzungsbedingungen und baulicher Maßnahmen hinsichtlich der Schadenfreiheit neu zu bewerten. Für eine spezielle Wandkonstruktion, dem Fachwerk mit ½ Stein starker Vormauerung, wird das Schadenspotential bei Applikation verschiedenartiger Innendämmungen untersucht. Die Thermographie zur Lokalisierung des Holztragwerks, Methoden zur Bewertung des gekoppelten Stoff- und Energietransports und die Erkenntnisse aus einem Mess- und Laborraum in Barockschloss werden vorgestellt.

**Keywords** — *Fachwerk mit Vormauerung; Innendämmung; Thermographie; Wärme- und Feuchteschutz, Numerische Simulation*

## I. EINLEITUNG

Eine Fassade mit originalen Befunden zu erhalten und die bauzeitliche Bausubstanz schonend zu ertüchtigen, sind Herausforderungen bei der Sanierung historischer Gebäude, die eine genaue Kenntnis der verwendeten Baukonstruktion erfordern. Anforderungen an ein behagliches Raumklima und das Reduzieren des Aufwands für die Gebäudekonditionierung gewinnen dabei immer mehr an Bedeutung und sind als ganzheitliche Fragestellung bei der Sanierungsaufgabe zu behandeln. Die Anwendungen von Innendämmungen sind bei dieser Aufgabe häufig ein alternativloser Ansatz.

Charakteristisch für die untersuchte Konstruktion ist, wie in Abbildung 1 dargestellt, dass ein innenliegendes Fachwerk mit einer ½ Stein starken Vormauerung ausgeführt ist und die schlanken Wände mit prachtvollem Stuck das ein oder andere Mal über die eigentlich sparsame Konstruktion hinwegtäuscht. Der sparsame Materialeinsatz und die Verbesserung der bauphysikalischen Eigenschaften sind Motivation, diese Bauweise im 18. und 19. Jahrhundert unter anderem bei Schlössern, Kirchen und Gutshäusern anzuwenden. Bei dieser Baustoffkombination besteht für das Holztragwerk offensichtlich das größere Schadenspotential.

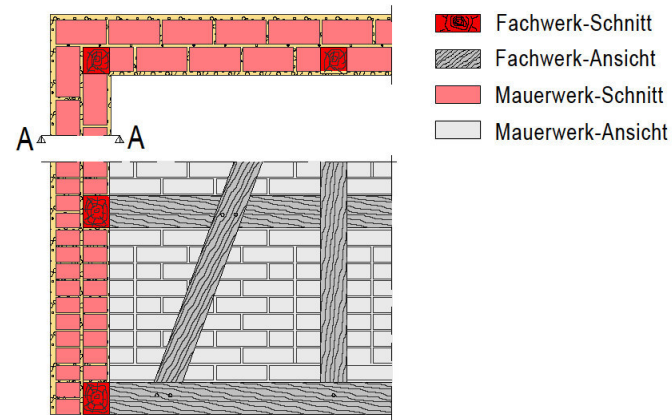


Fig. 2.  
Abb. 1: Fachwerk mit ½-Stein starker Vormauerung, oben: Horizontalschnitt, unten: Ansicht

Ursächlich ist die Zerstörung durch Pilze und Insekten. Eine Schädigung ist möglich, wenn Temperatur und Feuchte zeitgleich über einen angemessenen Zeitraum in einem lebensfreundlichen Bereich vorherrschen. Allgemein wird eine Holzfeuchte unter 20% als unkritisch angesehen [1]. Mit der Applikation einer Innendämmung wird die hygrothermische Situation verändert und das Schadenspotential aus den Vorgängen des gekoppelten Stoff- und Energietransports ist neu zu bewerten.

## II. METHODEN

### A. Lokalisierung des Fachwerks

Fig. 3. Für eine erfolgreiche Sanierung ist die Kenntnis über die verwendeten Baustoffe und die ausgeführte Konstruktion unabdingbar. Bei dem Fachwerk mit Vormauerung ist aufgrund der Lage innerhalb der verputzten Wand eine visuelle Bestandsaufnahme nicht möglich. Zur Klärung der Frage, ob ein Fachwerk verwendet ist, kann mit der Thermographie, wie in Abbildung 2 zu sehen, eine zerstörungsfreie Lokalisierung problemlos erfolgen. Aussagen zum Zustand des Holztragwerks können damit jedoch nicht gewonnen werden, so dass eine traditionelle Untersuchung durch Öffnen der Wand für die Bewertung notwendig ist.

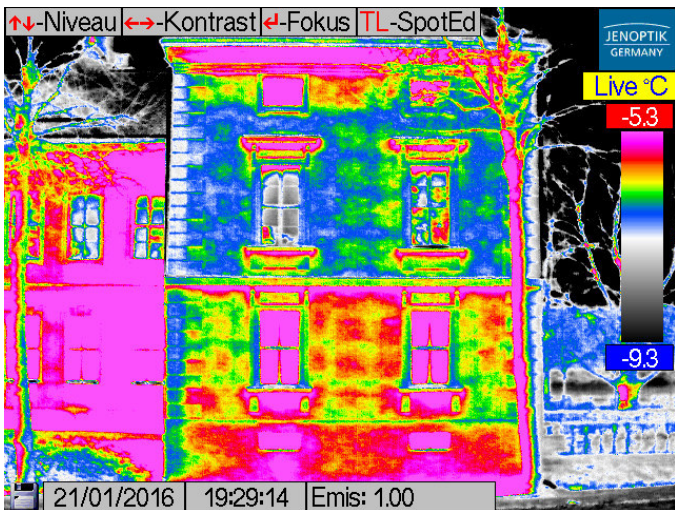


Abb. 2 Thermographie mit Darstellung des Fachwerks, Schloss Rheinsberg

### B. Numerische Simulation

Die numerische Simulation der hygrothermischen Verhältnisse ist ein anerkanntes Instrument bei der Bearbeitung zahlreicher Bauaufgaben [2]. Eine wirklichkeitsnahe Abbildung des Temperatur- und Feuchteverlaufs wird bei homogenen Wandaufbauten mit Programmen wie Delphin und Wufi erzielbar, wenn die Randbedingungen, wie Innen- und Außenklima und die Materialkennwerte der verwendeten Baustoffe bekannt sind. Für das im Mauerwerk eingebundene Fachwerk ist momentan lediglich eine zweidimensionale Berechnung praktikabel. Dazu wird der Fachwerkstiel bei der Beurteilung des Schadenpotentials betrachtet und mit der Software Delphin für verschiedene Randbedingungen untersucht. Die Ergebnisse erreichen eine Holzfeuchte in Abhängigkeit von den Randbedingungen von ca. 20%.

### C. Messungen in einem Barocksenschloss

Die aktuell zur Verfügung stehenden rechnerischen Methoden sind noch nicht in der Lage, zuverlässig den realen Feuchteverlauf sämtlicher Konstruktionen abzubilden. Daher sind messtechnische Untersuchungen für den wissenschaftlichen Erkenntnisgewinn nach wie vor unerlässlich. In einem Barocksenschloss, dass gegenwärtig umgebaut wird, sind Teile der Fachwerkkonstruktion in der Außenwand erhalten geblieben. Das Mauerwerk hat eine Stärke von ca. 32 cm und erfüllt damit nicht die Anforderungen an den baulichen Mindestwärmeschutz. Mit der Applikation einer Innendämmung soll eine Reduzierung des Heizenergiebedarfs, die Vermeidung des Schimmelpilzrisikos und eine behagliche Oberflächentemperatur erreicht werden. Nach der Sanierung des Mauerwerks, sind 3 Systeme mit einer Konstruktionsstärke von 120 mm angewendet worden. Damit wird der U-Wert der Wand mit Innendämmung von 1,72 W/m<sup>2</sup>K auf im Mittel 0,47 W/m<sup>2</sup>K verbessert. Die Systeme mit Plattenmaterial aus XPS und Kalziumsilikat sind auf einem Egalisierungsputz aufgebracht. Ohne Egalisierungsputz ist als 3. Variante eine Zelluloseschüttung zwischen Mauerwerk und einer 20 mm starken Holzfaserplatte ausgeführt. Alle Varianten haben als Schlussbeschichtung raumseitig einen mineralischen Glattputz. Mit der Anordnung von Sensorik in situ wird experimentell das Holztragwerk bei Applikation von Innendämmssystemen mit verschiedenartigen hygrothermischen

Eigenschaften auf Schlagregensicherheit und ein sich veränderndes Innenklima von 30% bis 60% relative Luftfeuchte bei ca. 20°C Raumtemperatur untersucht.

In Abbildung 3 ist der Verlauf der Porenluftfeuchte für einen Fachwerkstiel mit 2 Feuchte- und Temperatursensoren für jedes Innendämmssystem dargestellt. Der erste Messpunkt befindet sich oberflächennah hinter der Innendämmung und der zweite unmittelbar vor einem Luftraum zur Vormauerung. Anhand der Sorptionsisotherme, die aus dem Bohrmehl jedes einzelnen Messpunktes bestimmt wurde, erfolgt die Umrechnung der gemessenen relativen Porenluftfeuchte in Holzfeuchte. Betrachtet werden Tagesmittelwerte der Holzfeuchte im Zeitraum November 2014 bis März 2016. Die Abbildung zeigt den Verlauf der Holzfeuchte für alle 3 Varianten mit Werten nahe aber unter 20% Holzfeuchte.

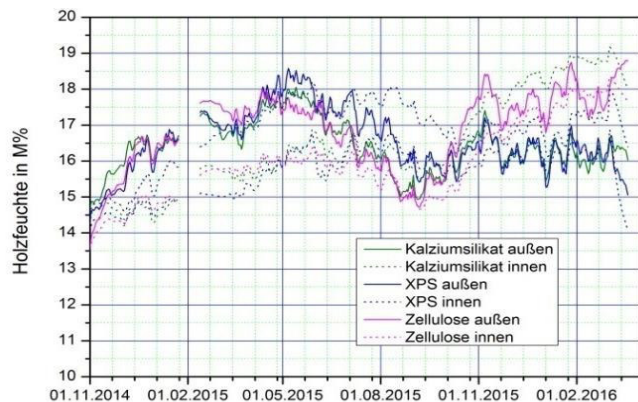


Abb. 3: Holzfeuchte als Tagesmittelwerte in einem Fachwerkstiel bei Applikation von Innendämmssystemen

### III Fazit

Die Thermographie ist eine geeignete Methode, Fachwerkstrukturen trotz Vormauerung zu lokalisieren; sie kann jedoch eine traditionelle Bewertung der Tragfähigkeit nicht ersetzen. Eine Abschätzung des Schadenpotentials mit numerischen Simulationen ist für Konstruktionen, bei denen zweidimensionale Stoff- und Energietransporte stattfinden, die Rand- und Nebenbedingungen bekannt sind, mit ausreichender Genauigkeit möglich. Problematisch ist das Ermitteln der erforderlichen Werte für die praktische Anwendung. Maßnahmen zur energetischen Ertüchtigung von Fachwerkstrukturen mit Vormauerung, zeigen anhand der Untersuchungen im Barocksenschloss Drebkau, dass die 3 Innendämmssysteme geeignet sind, die energetische Qualität zu verbessern. Die Holzfeuchte liegt mit 19% unterhalb der Grenze von 20% in einem unbedenklichen Bereich.

### LITERATUR

- [1] DIN 68 800-1: Holzschutz – Teil 1: Allgemeines, Beuth Verlag Berlin, Oktober 2011
- [2] Staar A., Strangfeld P., Bark T. 2016: Numerische Simulation am Praxisbeispiel der Hygrothermie von Holzbalkenköpfen. Beitrag zur BauSIM 2016, TU Dresden

# Efficiency Analysis of Residential Areas Cold Supply Systems

D. Romanov

Dept. of Industrial Heat Power Engineering Systems  
Moscow Power Engineering Institute  
Moscow, Russia  
dimrom09@yandex.ru

Y. Yavorovsky

Dept. of Industrial Heat Power Engineering Systems  
Moscow Power Engineering Institute  
Moscow, Russia  
YavorovskyYV@mpei.ru

**Abstract** — problems of choice between centralized and decentralized cold supply systems are considered in the paper; the idea of cold load density is introduced and its range of possible values for climate conditions of Moscow is defined; calculating program for approximate estimation of cold supply system efficiency is developed.

**Keywords**— cold supply system, efficiency, cold load density, discounted payback period.

The determination of whether the centralized or decentralized cold supply system feasibility is a complicated problem. Technical, economic, ecological, social factors have influence on the final decision in favour of one system or another. In the paper cold load density is considered as a factor influencing on such decision. Cold load density is defined as ratio of total cold load to area of residential district. Also economic factors of cold supply systems are considered.

In the paper cold load calculation of residential areas with similar buildings was performed. Five abstract residential districts were chosen for calculation:

1. District with only 5 storey buildings;
2. District with only 9 storey buildings;
3. District with only 12 storey buildings;
4. District with only 16 storey buildings;
5. District with only 25 storey buildings.

According to [1] estimate enthalpy of outdoor air is 56,8 kJ/kg. To define enthalpy of incoming air heat balance equation of building for summer season was written on the analogy of winter season. Structural heat gains, inflow seepage gains, solar heat gains, internal heat gains were taken into account. In a result to maintain inside temperature at 25 °C it is necessary to blow incoming air with following parameters:

1.  $t = 18^\circ\text{C}$ ,  $\varphi = 25\%$ ,  $h = 26,2 \text{ kJ/kg}$  (for unfavourable climate conditions in Moscow)
2.  $t = 24^\circ\text{C}$ ,  $\varphi = 30\%$ ,  $h = 38,3 \text{ kJ/kg}$  (for favourable climate conditions in Moscow).

After that minimum and maximum thresholds of cold load density of the abstract districts were defined. Values varies from 0,067 to 0,108 MW/ha and from 0,111 to 0,179 MW/ha accordingly (fig. 1).

For plotting cold load duration curve the information about temperature and relative humidity of outdoor air is necessary. According to the data from Moscow meteorological station near VDNH district [2] hourly values of temperature and relative humidity for 2012 and 2013 were received. After processing the data stand of temperature hours curves for warm season ( $t > 8^\circ\text{C}$ ) of 2012 and 2013 were plotted. In a

similar way stand of enthalpy hours curves ( $h > 35 \text{ kJ/kg}$ ) were plotted. The last curves were plotted on one of two conditions:

1. Outside temperature is more than  $25^\circ\text{C}$ ;
2. Simultaneously outside temperature is more than  $20^\circ\text{C}$  and relative humidity is more than 60 %.

So cold load duration curves for district with 5 storey buildings for 2012 and 2013 were plotted and analyzed.

Also calculating program for economic estimation of cold supply systems was developed. The program allows to compare cold supply system with vapor compression refrigerating machine and cold supply system with absorption refrigerating machine [3;4]. For systems with absorption refrigerating machine user can choose the source of heat:

1. Local source of heat (boiler house);
2. Heat supply company;
3. Technology process at the factory evolving waste heat.

The program allows taking into account a change of prices on energy carriers and wage indexation during the first eight years of exploitation. Also the program allows changing currency rate and cost of imported equipment. In a result it is possible to define simple payback period, discounted payback period and net present value [5]. Based on these factors reasonable choice of cold supply system can be made. The program is designed for fast and simple techno-economic analysis of cold supply system. The program may be helpful on initial stage of cold supply system designing and developing residential areas.

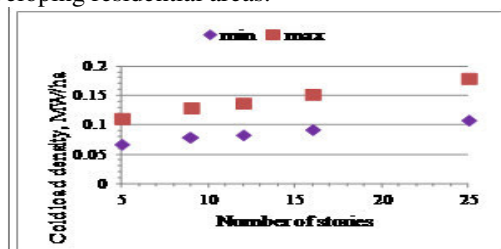


Figure 1. Cold load density dependence on number of stories in building.

## REFERENCES

- [1] SP 131.13330.2012. Building climatology, Gosstroy of Russia, 2012. (in Russian)
- [2] Weather archive of Moscow. – [www.rp5.ru](http://www.rp5.ru)
- [3] Sokolov E. Y., Brodyansky V. M. Energy basis of heat transformation and cooling processes, Energoizdat, 1981, pp 48-66. (in Russian)
- [4] Koshkin N. N., Sakun I. A. Refrigerating machines, Mashinostroenie, 1985, pp 416-460. (in Russian)
- [5] Rogalev N. D., Zubkova A. G., Masterova, I. V. Energy economics, MPEI, 2008. (in Russian)

# The Closed Thermosyphon Application for the Flue GasHeat Recovery

Savchenkova N.M., Kravtsov D.A

Department of Heat-and-Mass Exchange Processes and Devices

National Research University MPEI

Moscow, Russia

[savchenkovam@mpei.ru](mailto:savchenkovam@mpei.ru), [kdzhurml@mail.ru](mailto:kdzhurml@mail.ru)

**Abstract -** The installation has been designed to increase index of energy efficiency of technological processes due to its own advantages. The boiler developed in NRU MPEI at the Department of Heat And Mass Transfer Processes And Devices.

**Keywords -** heat pipe, thermosyphon, heat transfer, waste boiler, energy saving.

The waste heat boiler with thermosyphon was designed and compared with other boilers, commonly used in heating systems.

The boiler consists of a thermosyphon, upper flange, lower flange, condensate return tube, cover, support element, walls, thermal insulation material, steel plates and air duct.

This is the boiler unit uses the heat of exhaust gases [1]. Closed thermosyphon is heat transfer device that provides heat transfer from the flue gases to the cold water as a result of evaporation-condensation cycle [2].

The apparatus consists of a unique pipe or thermosyphon tube bundle. This part is the main element in which heat is transferred from flue gas to the liquid through the wall, therefore in tubes there is a boiling process.

Vapor is supplied into the cover that contains a tube bundle. In these tubes water is heated up to the programmed temperature by vapor coming from the thermosyphon. The number of tubes depends on the power of the boiler [3].

The tubes are made with ribbed pins to intensify the process of heat exchange with the walls of the thermosyphon. These pins have staggered arrangement. Their length is 10 mm/per each unit, and the diameter is 5 mm/per each unit. Thermosyphon tube fixed in the upper and lower flue sheets via flanges.

Tube sheets have form of steel plates of 20 mm thickness because of the pressure increase in the thermosyphon. These tube sheets also contain two condensate return tubes, which at the same time serve as support elements. The condensate inflows into the lower reservoir and returns into the tube thermosyphon (due to the pressure difference).

Heating chamber in which the heat transfers from the flue gas to liquid bounded on both sides of the wall. Heating chamber walls are made with the thermal insulation material to avoid heat leakage. Admission and removal gases in the chamber works with air duct.

The calculation is divided into two parts. One of them is the calculation of the thermosyphon, the other is the calculation of the tube bundle, located above it. Thermosyphon was calculated as an evaporator, wherein the cold coolant is boiling water and the hot is flue gases. The second part was designed as a regenerative tube heat exchanger. The hot coolant is the saturated vapor and the cold coolant is water that flows through several tubes. Saturated vapor heats the water in the tubes, condenses and returns into the thermosyphon. The whole system is used to supply hot water and heating both industrial and domestic premises.

Application of finned at the motion of flue gases allows to increase the heat transfer coefficient and the heat transmission coefficient, respectively. Evaporation and condensation processes are the most effective at the transfer of heat from the hot flue gases to the cold water for heating and hot water supply [4, 5].

## II. CONCLUSION

It is necessary to understand an importance of using the heat energy of all levels and reduce the heat loss by any means. This device can be used in various heating systems.

The recovery boiler will help increase the energy efficiency of technological processes due to its advantages: simplicity of design; low price: the possibility of manufacturing of some elements with wastes of production; efficiency increase of secondary energy resources; reduced hydraulic resistance through the use of ribbed pins; high heat conductivity of the thermosyphon; reduction of electricity consumption.

## REFERENCES

- [1] L.N. Sidelkovsky, V.N. Yurenev, Boilers industrial enterprises, Energoatomizdat, 1988.
- [2] A.A. Borodkin, V.D. Portnov, A.Y. Shashin, V.N. Fedorov. Calculation heat-and-mass transfer devices, Publishing House MPEI, 1997.
- [3] A.M. Baklastov, V.A. Gorbenko, O.L. Danilov, Heat-and-mass transfer industrial processes and plants, Energoatomizdat, 1986.
- [4] F.F Tsvetkov, R.V. Kerimov, V.I. Velichko, Book of problems in heat-and-mass transfer, Publishing House MPEI, 2008.
- [5] A.L. Efimov, A.V. Danilina, Calculation and intensification of heat transfer in industrial heat exchangers, Publishing House MPEI, 2009.

# Hygrothermisches Verhalten von Holzbalkenköpfen in innengedämmtem Außenmauerwerk

Messungen und numerische Simulation des gekoppelten Wärme- und Feuchttetransports

Andrea Staar

Brandenburg University of Technology  
Cottbus-Senftenberg,  
Cottbus, Germany  
Andrea.Staar@b-tu.de

Prof. Dr. sc. techn. Horst Stopp

Brandenburg University of Technology  
Cottbus-Senftenberg  
Cottbus, Germany  
Horst.Stopp@b-tu.de

**Abstract**— Innendämmssysteme werden zur energetischen Sanierung von Außenwänden in historischen Gebäuden mit erhaltenswerten Fassaden eingesetzt. Die Planung dieser Maßnahme erfordert hygrothermische Berechnungen zur Beurteilung des Feuchteschutzes. Besonders in Holzbalkenauflagern in Außenwänden muss ein Schadenrisiko aufgrund eines kritischen Feuchteanstiegs vermieden werden. Hygrothermische Simulationen und Messungen an Balkenköpfen in Testhäusern zeigen die Veränderungen des bauphysikalischen Verhaltens.

**Keywords**—component; Innendämmung, Wärme- und Feuchteschutz, Holzbalkenköpfe, Numerische Simulation

## I. EINFÜHRUNG

In der Praxis haben sich Innendämmssysteme zur energetischen Sanierung von erhaltenswerten Fassaden bewährt. Voraussetzung für einen schadenfreien Einsatz ist die Beurteilung des hygrothermischen Verhaltens der Konstruktion als Nachweis des Feuchteschutzes [1]. Als Planungswerkzeug dienen numerische Simulationen des gekoppelten Wärme- und Feuchttetransports. Bei der Berechnung findet eine Vielzahl von Randbedingungen Berücksichtigung:

- Geometrie der Konstruktion
- Materialeigenschaften der Baustoffe (z.B.: Wasseraufnahmekoeffizient und Wasserdampfdiffusionswiderstandszahl)
- Außenklimabedingungen (z.B.: der instationäre Verlauf der Außenluftfeuchte und Temperatur, der Sonnenstrahlung; die Wirkung von Schlagregen als Resultat aus Regenmenge, Wind und Windrichtung)
- Innenklimabedingungen (z.B.: der instationäre Verlauf der Raumluftfeuchte und –temperatur)
- Wärmeenergieeinträge (z.B.: aus Flächenheizungen)
- Baufeuchte aus Sanierungsmaßnahmen

Die Anwendung der Simulationssoftware bei zweidimensionalen Konstruktionen, wie ebenen Wänden, ist validiert und liefert hinreichend genaue Ergebnisse. Eine exakte Berechnung dreidimensionaler Konstruktionen, wie im Außenmauerwerk eingebundene Balkenauflager, ist mit der verfügbaren Software nicht möglich. Die Weiterentwicklung

der Software für dreidimensionale Fragestellungen wird in einem Verbundforschungsprojekt bearbeitet, das sich ebenfalls mit einem Wachstumsprognosemodell für holzzerstörende Pilze befasst [2]. Darüber hinaus werden hygrothermische Messungen in Testhäusern, Laboruntersuchungen und Experimente durchgeführt.

## II. METHODEN

Untersuchungen des hygrothermischen Verhaltens an Balkenköpfen in Testhäusern sind ein unverzichtbarer Erkenntnisgewinn für die Validierung der Software. Gegenüberstellungen von Messergebnissen mit Berechnungsergebnissen zeigen, dass eine Beurteilung des Schadenrisikos anhand des berechneten Feuchteverlaufs möglich ist [3].

### A. Numerische Simulation

Abbildung 1 zeigt das Porenluftfeuchtfeld eines Balkenauflagers im innengedämmten Außenmauerwerk, berechnet mit der Software DELPHIN [4]. Es ist der Zustand an einem Novembertag dargestellt. Unmittelbar hinter der Innendämmung und im Außenputz tritt die höchste Feuchte auf. Im Bereich des Balkenauflagers dieses Deckenbalkens ist die Feuchte im unkritischen Bereich.

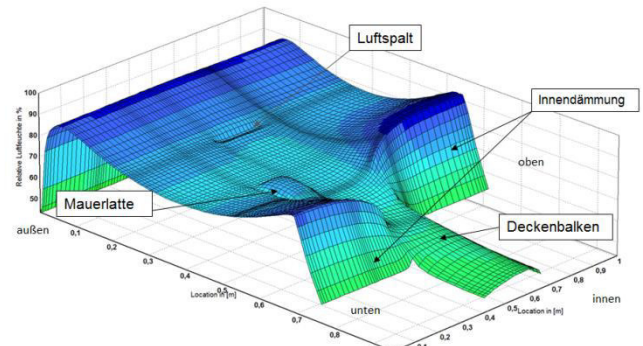


Fig. 4. Abb. 1: Relative Porenluftfeuchte im Vertikalschnitt eines Balkenauflagers / Ergebnis der numerischen Simulation mit der Software DELPHIN

Fig. 5. Numerische Simulationen setzen eine möglichst genaue Kenntnis der Konstruktion und der Materialeigenschaften der verwendeten Baustoffe voraus. Das Außenklima steht als

Klimadatensätze verschiedener Standorte als Testreferenzjahr für die Berechnungen zur Verfügung. Die Software ermöglicht darüber hinaus die Verwendung eigener Klimadatensätze.

### B. Hygrothermische Messungen in Testhäusern

Messungen in unterschiedlichen Testhäusern zeigen, dass die Ausführung der Innendämmung bauphysikalisch schadensfrei ist und nicht nachteilig auf die im Mauerwerk eingebundenen Holzbalkenköpfe wirkt [5]. Auch nach der Applikation eines Innendämmssystems findet eine Austrocknung der bei der Sanierungsmaßnahme eingetragenen Baufeuchte statt. Gemessen wird mit kombinierten Porenluftfeuchte-/Temperatursensoren im Stirnholz des Balkenkopfes und im Luftraum an der Stirnseite.

### C. Vergleich von hygrothermischen Messungen und Simulationen

Anhand des Vergleichs von Berechnungsergebnissen mit Messwerten werden die Grenzen numerischer Simulationen deutlich. Verwendet werden dazu die Messungen an Balkenköpfen in einem Schulgebäude nahe Cottbus. Mit Beginn des Schulbetriebes nach einer umfassenden energetischen Sanierungsmaßnahme beginnt die Aufzeichnung der Messwerte. Neben den Messungen innerhalb der Konstruktion werden Innenklimadaten sowie Außenlufttemperatur- und -luftfeuchte erfasst.

Abbildung 2 zeigt den Verlauf der relativen Porenluftfeuchte im Stirnholz ausgewählter Balkenköpfe im Jahr 2014. Die Auflager dieser Balkenköpfe haben unterschiedliche Konstruktionseigenschaften. Balken S01 ist der Referenzbalken, an dem zum Vergleich keine Fußbodenheizung vorhanden ist. S06 und S07 unterliegen dem Wärmeenergieeinfluss aus der Fußbodenheizung. An S07 ist der Auflagerbereich nicht mit Sand, wie im Bestand, sondern mit einer Perliteschüttung ausgeführt worden. Im blauen Kurvenverlauf ist das Ergebnis der Simulation unter

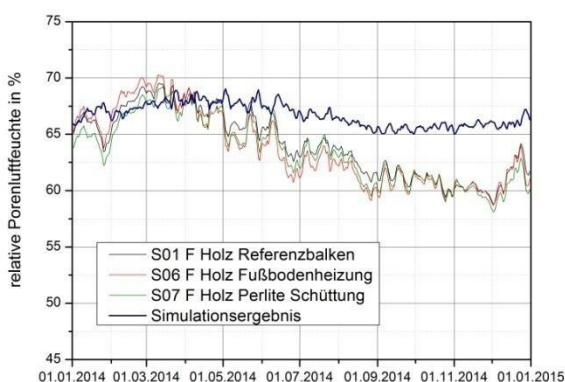


Fig. 6. Abb. 2: Gegenüberstellung der gemessenen und berechneten Porenluftfeuchte im Stirnholz der Balkenköpfe

Verwendung der Klimadaten des Standortes Cottbus und der Raumklimadaten des Klassenzimmers dargestellt. Die

Abweichung zwischen den Messungen und der Berechnung der Porenluftfeuchte variiert im Jahresverlauf und liegt bei diesem Beispiel bei maximal 5 %.

Das Simulationsergebnis der Temperatur in Abbildung 3 folgt hingegen dem Verlauf der Messergebnisse. In den Wintermonaten liegen Berechnung und Messung näher beieinander als in den Sommermonaten.

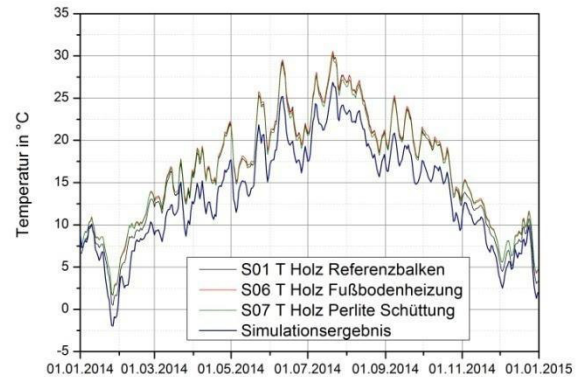


Fig. 7. Abb. 3: Gegenüberstellung der gemessenen und berechneten Temperaturen im Stirnholz der Balkenköpfe

### III. ZUSAMMENFASSUNG

Hygrothermische Messungen in Testhäusern zeigen, dass eine schadenfreie Applikation von Innendämmssystemen in Gebäuden mit historischen Holzbalkendecken möglich ist. Bei der Planung energetischer Sanierungsmaßnahmen ist eine Bewertung des Schadenrisikos mithilfe numerischer Simulationen möglich. Voraussetzung ist eine möglichst genaue Kenntnis der Konstruktion und der Materialeigenschaften der verwendeten Baustoffe. Forschungsbedarf besteht in der Weiterentwicklung numerischer Simulationssoftware.

### LITERATUR

- [1] WTA-Merkblatt 6-5: Innendämmung nach WTA II: Evaluation of internal insulation systems with numerical design methods. Fraunhofer IRB Verlag, Stuttgart
- [2] Ruisinger U. et al.: Holzbalkenaufklager in historischem Mauerwerk: Analyse, Bewertung. Mauerwerk-Kalender 2016, Verlag Ernst & Sohn, Berlin
- [3] Staar A., Strangfeld P., Bark T. 2016: Numerische Simulation am Praxisbeispiel der Hygrothermie von Holzbalkenköpfen. Beitrag zur BausIM 2016, TU Dresden
- [4] Grunewald et al. 2016. Delphin – Simulationsprogramm für den gekoppelten Wärme-, Luft-, Feuchte-, Schadstoff- und Salztransport. [www.bauklimatik-dresden.de](http://www.bauklimatik-dresden.de)
- [5] Anlauf, E; Staar A.: Energetische Sanierung eines denkmalgeschützten Sand-steingebäudes mittels Innendämmung – Messergebnisse zum hygrothermischen Verhalten der Holzbalkenköpfe. In: BUFAS Hrsg.: Altbausanitize 9: 25 Jahre Feuchte und Altbausanitize 25. Hanseatische Sanierungstage, Beuth Verlag 2014

# Untersuchungen zur Verbesserung der Wärmeübertragung durch die Nutzung von strukturierten Feinblechen - Experiments on Heat Transfer with Structured Metal Sheets

Prof. Dr.-Ing. habil. Sylvio Simon, MEng. Steffen Wichmann, beide BTU C-S, FG Gestaltung von Produktionssystemen / Werkzeugmaschinen (Design of production systems/ machine tools, member of Neseff)

Ass. Prof. Karel Fraňa, Dipl.-Ing. Josef Egert; Techn. Universität Liberec, Fakultät für Maschinenbau Department of Power Engineering Equipment, Faculty of Mechanical Engineering

**Abstract:** Structured sheets have addition to increased bending stiffness considerable potential for lightweight. Unsteady turbulent flows around the plain and hexagonal sheets were analyzed numerically and experimentally in order to determine the heat transfer intensity between sheet surfaces and surrounding air flows. To obtain experimental results for later validations of numerical results, a measurement facility was designed and constructed. Flow patterns around metal sheets were measured under various flow conditions e.g. the effects of different temperatures, heating powers and flow velocities on the heat transfer intensity were studied. Numerically provided results demonstrated a good match between theoretical calculations and experiments. For all investigated patterns, the structured hexagonal sheets achieved significantly higher heat transfer intensity than the plain sheets.

**Keywords:** lightweight construction, bending stiffness energy efficiency, Structured Metal Plate, Heat Transfer, CFD, Wind Tunnel

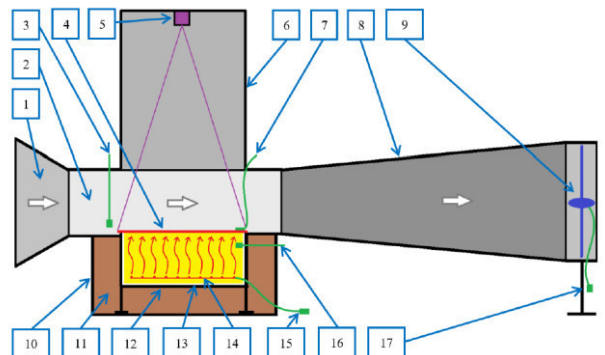
## I. INTRODUCTION

Strukturierte Feinbleche weisen durch ihre charakteristische Gestalt bereits verschiedene Leichtbauvorteile auf. Aktuelle Forschungen an der BTU CS beschäftigen sich mit dem Zusammenhang zwischen Strukturhöhe und Steifigkeitszunahme. Die vorhandene geringere Dehnsteifigkeit gegenüber glatten Blechen gleicher Materialstärke ermöglicht neuartige Verwendungsmöglichkeiten, bei der denen eine gewollte Verformung bei Überbeanspruchung vor einem Bruch eintreten soll. Zu den bisher vermuteten, jedoch noch nicht wissenschaftlich nachgewiesenen Eigenschaften gehört auch die Verbesserung der Wärmeübertragung durch die Anwendung strukturierter Bleche an der Übergangsstelle zwischen den beiden Medien.

## II. FORMULATION

Im Rahmen einer sehr umfangreichen Versuchsserie wurde in einem extra für diese Untersuchungen konzipierten Strömungsversuchstand Strömungsmessungen und Wärmeübergangsmessungen vorgenommen. Des Weiteren wurde mittels Laser die vorhandene Strömung visualisiert, um Verwirbelungen sichtbar zu machen. Die ermittelten Ergebnisse wurden zur Verifikation einer Strömungssimulation genutzt, die es künftig ermöglicht, die Effizienz Wärmeübertragung unter Nutzung strukturierter Bleche vorher zu bestimmen. Die Abbildung zeigt den prinzipiellen Aufbau des Versuchsstandes.

## III. MAIN RESULT



Die ermittelten Ergebnisse bestätigen, dass sich durch die Ausbildung einer turbulenten Strömung über den strukturierten Blechen die Wärmeübertragung gegenüber glatten Blechen verbessert. Die Nutzung von strukturierten Blechen in Wärmeüberträgern sollte bei Neukonstruktionen berücksichtigt werden.

# Energieeffizienz in der Maschinenkonstruktion - Energy Efficiency in the Design of Machinery

Prof. Dr.-Ing. habil. Sylvio Simon, MEng. Steffen Wichmann, beide BTU C-S, FG Gestaltung von Produktionssystemen / Werkzeugmaschinen (Design of production systems/ machine tools, member of Neseff)

Prof. Dr.-Ing. Thomas Meißner, MEng. Stephan Hernschier, MEng. Michael Weist; alle BTU C-S, Institut für Maschinenbau und Management, Mitglied von neseff (Institute for mechanical engineering and management; member of neseff)

**Abstract:** Die konsequente Anwendung von Gestaltungsrichtlinien im Bezug auf die Masse der verwendeten Maschinenelemente hilft energieeffiziente Produkte zu gestalten. Maschinenelemente wie Schrauben, berührungslose Dichtungen oder Radialwellendichtringe können dabei einen entsprechenden Beitrag leisten.

**Keywords:** gewichtsoptimierte Konstruktion, Leichtbau, Schrauben, Radialwellendichtringe, berührungslose Dichtungen

## I. INTRODUCTION

Durch die Gestaltung von Maschinen und Produkten wird sowohl der Energiebedarf während der Nutzung als auch der Energiebedarf zur Herstellung und Entsorgung festgelegt. Während der Energiebedarf bei der Produktnutzung von der spezifischen Nutzung abhängt, fallen bei der Bewegung des Produktes Energieverbräuche an, die direkt von der Produktmasse abhängen. Bei der Gestaltung der Produkte und Maschinen sind dabei die optimalen Bedingungen für Produkterstellung, Produktnutzung und Produktentsorgung zu ermitteln und umzusetzen.

## II. FORMULATION

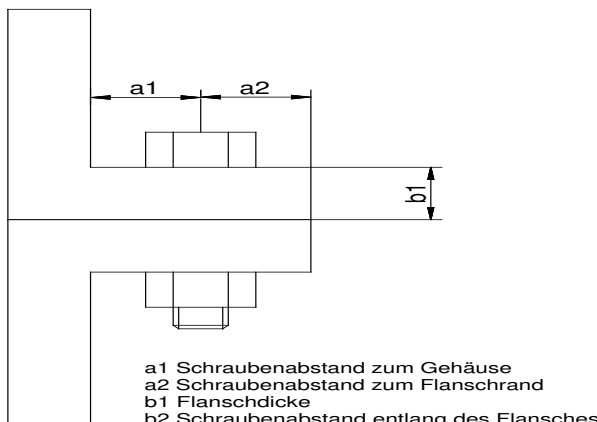
Exemplarisch ist zum Beispiel bei der Konstruktion eines Getriebes die richtige Auswahl des Gehäusewerkstoffes, der Wellen- und Maschinenelementwerkstoffe und die optimale Gestaltung. Durch hoch beanspruchbare Wellenwerkstoffe können Wälzlagern klein und damit gewichtssparend dimensioniert werden. Die dazugehörigen Wellenabdichtungen

versuchen geringere Reibmomente und damit geringere Verluste. Abgesehen davon benötigen kleinere Getriebegehäuse auch entsprechend reduzierte Ölmengen. Insgesamt gibt es verschiedene konstruktive Möglichkeiten das Produktgewicht gering zu halten und den Produktwirkungsgrad entsprechend optimal zu gestalten. Als Mitglied im internationalen Netzwerk neseff liegt uns die Ausbildung der Studierenden mit einem Fokus auf Energieeffizienz der Produkte sehr am Herzen.

Bei der Gestaltung von Gehäuseverschraubungen ist eine Vielzahl an variablen Parametern zu berücksichtigen. Hier kommt es drauf an, dass fertigungstechnisch realisierbare mit dem Minimum an Produktmasse entsprechend des

Auslegungskriterien umzusetzen. Die wichtigsten Parameter hängen dabei direkt vom Schraubendurchmesser ab. Eine hohe

Festigkeit des Schraubenwerkstoffes wie 12.9 oder 14.9 führt dabei zu kleinen Schraubendurchmessern und damit auch zu reduzierten Schraubenmassen. Von der optimalen Gestaltung von Schraubverbindungen und ausgewählten Maschinenelementen handelt unser Tagungsbeitrag.



# Energieeffizienz in der spanenden Bearbeitung - Energy Efficiency in Metal-cutting Manufacturing

Prof. Dr.-Ing. habil. Sylvio Simon, M.Eng. Steffen Wichmann, Dr.-Ing. Matthias Führer  
Ingenieurbüro Führer, BTU C-S, FG Gestaltung von Produktionssystemen /  
Werkzeugmaschinen (Design of production systems/ machine tools, member of Neseff), Döbeln

**Abstract:** Energieeffiziente Fertigungsprozesse berücksichtigen alle Energieverbräuche im Zusammenhang mit der Produktherstellung. Im Zerspanprozess können das Schnittkraftreduzierungen sein, die ihren Beitrag zur Energieeffizienz leisten. Außerdem reduziert der Einsatz von aussteuerbaren Werkzeugen Nebenzeiten und kann deutlich zur Qualitätserhöhung beitragen, wenn Umspannprozesse in der Bearbeitung entfallen.

**Keywords:** energieeffiziente Fertigung, Zerspanprozess, aussteuerbare Werkzeuge, Qualitätserhöhung, Schnittkraftreduzierung, Minimalmengenschmierung

## I. INTRODUCTION

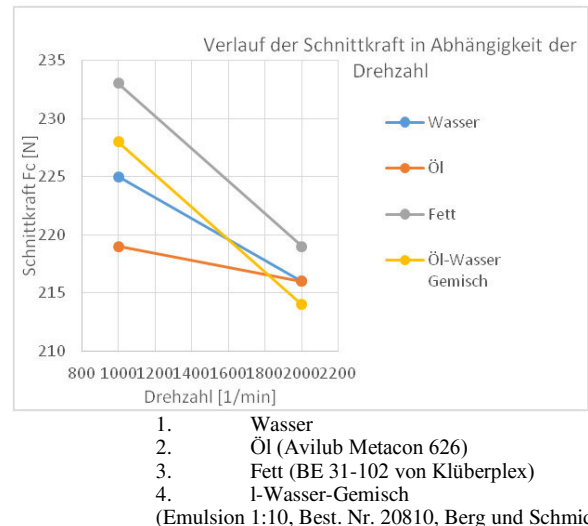
Für die Formgebung von Werkstücken, aber auch von Werkzeugen sind die Verfahren des Spanens von elementarer Bedeutung. Erste additive Fertigungen über den Versuchsmaßstab hinaus können und sollen nicht das Spanen ersetzen. Die Möglichkeiten der Optimierung der spanenden Verfahren waren und sind dabei abhängig vom jeweiligen Entwicklungsstand z.B. der Maschinentechnik, der Schneidwerkstoffe oder der Steuerungssysteme. Insgesamt wurde durch die Reduzierung der Bearbeitungszeit auch stets Energie eingespart, wobei sich die Betrachtungsweise von den einzelnen Fertigungsschritten hin zum Produktlebenszyklus erweitert hat.

## II. FORMULATION

Die Verkürzung von Bearbeitungszeiten aber auch die Optimierung der Bearbeitungsverfahren sind für den Energiebedarf bei der Produktherstellung von großer Wichtigkeit. Eine Analyse der Energieverbräuche zeigt dabei, dass endkonturnahe Guss- und Schmiedeteile deutlich reduzierte Energieverbräuche im Herstellungsprozess aufweisen. Die spanende Bearbeitung ist meist der größte Kostenanteil in der Erzeugnisfertigung. Aussteuerbare Werkzeuge können hier helfen, Zeiten und Kosten zu reduzieren.

Unter dem Gesichtspunkt der klassischen Nassbearbeitung mit hocheffizienten Kühlsmierstoffen und optimalen Werkzeugen besteht das Problem in der zielgenauen

Zuführung des Kühlsmierstoffes genau in die Trennstelle zwischen Werkzeug und entstehenden Span, wobei die Spanfließbedingungen positiv beeinflusst werden sollen. Hierfür sind technisch entsprechende Hochdruckpumpen für die Kühlsmierstoffzuführung sowie die nachfolgende Filterung, Kühlung und Kühlsmierstoffrückführung erforderlich. Deren Energiebedarf ist, auf den Gesamtprozess der spanenden Bearbeitung bezogen, mit 20 % schon erheblich.



1. Wasser
2. Öl (Avilub Metacon 626)
3. Fett (BE 31-102 von Klüberplex)
4. 1-Wasser-Gemisch  
(Emulsion 1:10, Best. Nr. 20810, Berg und Schmid)

## III. MAIN RESULT

Untersuchungen im Werkzeugmaschinenlabor der Brandenburgischen Technischen Universität Cottbus – Senftenberg zur Wirkung von verschiedenen Kühlsmierstoffen beim Drehprozess brachte interessante Ergebnisse. Zerspan wurde der Werkstoff S 235, die entstehenden Schnittkraftkomponenten wurden mit einem

Schnittkraftmessgerät von der Firma TeLC erfasst. Während der Versuche kamen unter anderem folgende Kühlsmierstoffe zum Einsatz:

# Vorbereitung des Werkzeugmaschinenlabor der BTU-CS, Campus SFB für Energieeffizienzmessungen in Maschinenparks und Ermittlung der Energieeffizienz am Beispiel ausgewählter LED Beleuchtung

Prof. Dr.-Ing. habil. Sylvio Simon, MEng. Steffen Wichmann, beide BTU C-S, FG Gestaltung von Produktionssystemen / Werkzeugmaschinen (Design of production systems/ machine tools, member of Neseff)

Prof. Dr.-Ing. Erhard Stein, MEng. Sindy Schmidt, BEng. Philipp Heise, alle BTU C-S, FG Mess- und Sensortechnik

**Abstract:** Um den gesamten Energiebedarf für die Herstellung von Produkten zu erfassen, wird exemplarisch das Werkzeugmaschinenlabor der BTU C-S mit aktueller Messtechnik ausgestattet. Diese ermöglicht auch, mögliche Beeinflussungen der Maschinen untereinander sichtbar zu machen. Bei der Ausrüstung von Werkzeugmaschinen mit LED Beleuchtung sind Besonderheiten zu beachten.

**Keywords:** Energieeffizienz, Werkzeugmaschinen, Messtechnik, LED Beleuchtung.

## I. INTRODUCTION

Das Werkzeugmaschinenlabor am Campus Senftenberg der Brandenburgischen Technischen Universität Cottbus – Senftenberg beinhaltet verschiedene Maschinen, die in der metallverarbeitenden Industrie eingesetzt werden. Neben dem Ziel der studentischen Ausbildung im Bachelor- und Masterkurs Maschinenbau waren Einzeluntersuchungen an diesen Maschinen zur Optimierung der Bearbeitungsprozesse und zur Reduzierung des Energieverbrauches der Bearbeitung bis die Schwerpunktthemen. Mit der Gründung des internationalen Netzwerkes Energieversorgung und Energieeffizienz – Neseff rücken jedoch weitere Fragestellungen in den Vordergrund.

## II. FORMULATION

Die gegenseitige Beeinflussung der Maschinen durch ihre unterschiedliche Stromaufnahme, ihre unterschiedliche

elektro- und schaltungstechnische Ausstattung soll zukünftig als Demonstrationslabor für die studentische Ausbildung als auch für betriebliche Fragestellungen dienen. Die BTU C-S betreibt bereits erfolgreich ein An-Institut – Griplab – welches sich mit der Simulation von Energieübertragungsnetzen und mit den internationalen Stromflüssen beschäftigt.

Für die Bestimmung der Energieeffizienz von Werkzeugmaschinen, wird ein Messsystem benötigt welches die Stromaufnahme der einzelnen Maschinen bestimmen kann. Dabei sollen die anfallenden Daten zentral auf einer Basisstation gespeichert und von dieser analysiert werden. Durch die Analyse können Optimierungsvorschläge generiert werden. Es ist z.B. möglich durch intelligentes Aufteilen der einzelnen Verbraucher bereits eine Blindstromkompensation vorzunehmen. Besonders die energietechnischen Auswirkungen einer Arbeitsplatzbeleuchtung mit LED werden im Vortrag dargestellt.

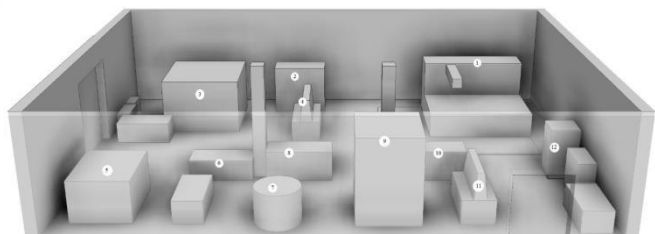


**Abbildung 1: räumliche Darstellung des WZM-Labors (A.Riethmüller)**

# Создание системы слежения за Солнцем на базе платформы Arduino

Воротынцев Д.В.

Кафедра Гидроэнергетики и возобновляемых источников  
энергии  
НИУ Московский Энергетический Институт  
Москва, Россия  
Dvr.energy@gmail.com

Васьков А.Г., к.т.н., доцент

Кафедра Гидроэнергетики и возобновляемых источников  
энергии  
НИУ Московский Энергетический Институт  
Москва, Россия  
VaskovAG@mpei.ru

**Аннотация:** В данной работе рассмотрено создание портативного солнечного трекера на базе платформы Arduino. Приведены алгоритмы работы устройства и результаты полевых испытаний. В заключении делается вывод о рациональности применения систем слежения за Солнцем.

**Ключевые слова:** система слежения за Солнцем, трекер, Arduino.

## I. Введение.

Система слежения за Солнцем (трекер) – это устройство, которое устанавливает фотоэлектрические модули в оптимальное положение по критерию максимизации вырабатываемой мощности. Среднегодовой прирост выработанной энергии в районах с большой облачностью может достигать 20%, в солнечных районах – 30-40%. [1] Трекеру не нужно быть очень точным для того, чтобы быть эффективным. Некоторые авторы утверждают, что отклонение в 10 градусов от оптимального угла наклона уменьшит выработку фотоэлектрических преобразователей всего на 1,5%. [2]

## II. Описание алгоритма слежения за Солнцем

В данной работе был создан комбинированный двухосный активный трекер, состоящий из Arduino Mega, двух сервомоторов, трех фотодиодов и солнечной панели номинальной мощностью 2 Вт

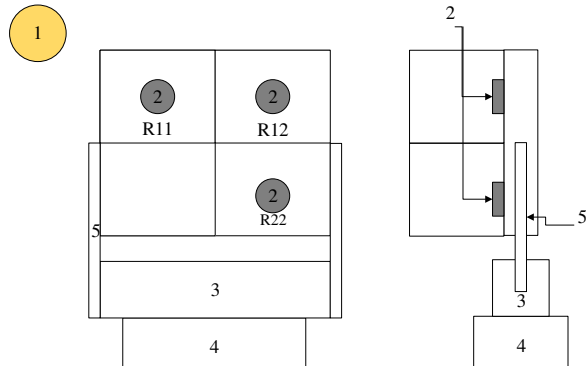


Рисунок 1. Схема двухосного активного трекера, следящего за самой яркой точкой на небосводе. Обозначения: 1 - источник света, 2 - фотодиоды, 3 - сервомотор(изменение угла наклона), 4 - сервомотор(изменение азимута), 5 - крепления.

Разработанный трекер работал в четырех режимах:

Горизонтальное положение приемной площадки(далее - ПП)

Оптимальный годовой угол ПП

Работа по заданному календарному графику

Поиск наиболее яркой точки на небосводе

Это было сделано для того, чтобы провести сравнение вырабатываемой солнечной панелью мощности при использовании различных систем слежения за Солнцем и при установке в оптимальное годовое положение.

В начале работы трекер устанавливается в положение при котором азимут ПП равняется 180 градусам(направление на юг), угол наклона - 0 градусов. Такое положение соответствует горизонтальной площадке.

После каждого изменения положения трекера производится десятисекундная задержка, необходимая для стабилизации показаний приборов, и измеряется мощность, вырабатываемая солнечной панелью. Для этого к солнечной панели последовательно были подключены два резистора номиналом 22 и 47 Ом(суммарное сопротивление - 69 Ом - находится близко к точке максимального КПД применяемой солнечной панели). К резистору номиналом 22 Ом подключен вольтметр. Показания вольтметра снимаются каждые 10 секунд в течении 30 секунд, затем усредняются. Вырабатываемая мощность может быть найдена по формуле:

$$P = \left(\frac{U_v}{22}\right)^2 * (22 + 47)$$

где  $U_v$  - усредненное показание вольтметра.

После этого при помощи встроенной функции Ардуино, определяется текущее время и, на основании этой информации, по сохраненному массиву положений Солнца, определяется оптимальный угол наклона и азимут ПП(работа трекера по заданному календарному графику):

$$\beta_{\text{пп}} = 90^\circ - a_c$$
$$A_{\text{пп}} = A_c$$

где  $\beta_{\text{пп}}$  - угол наклона приемной площадки,  $a_c$  - высота Солнца,  $A_{\text{пп}}$  и  $A_c$  - азимут ПП и Солнца соответственно.

Затем производится корректировка положения ПП при помощи алгоритма поиска наиболее яркой точке на небосводе. Угол  $\phi$  и  $\Delta R$  задаются пользователем. В данной работе  $\phi=5^\circ$ ,  $\Delta R=0,1*R_{12}$ .

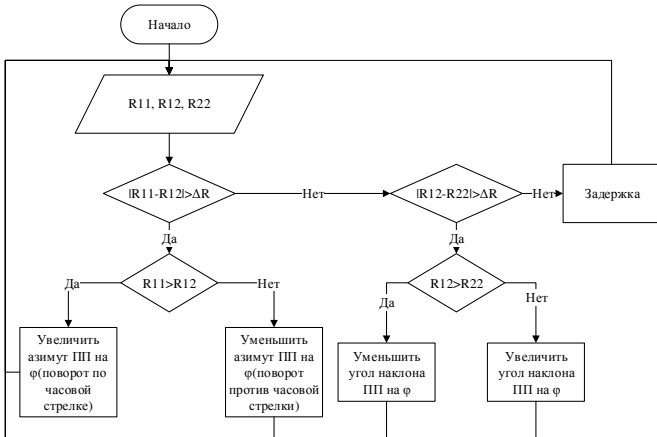


Рисунок 2. Алгоритм поиска наиболее яркой точки на небосводе.

После этого трекер устанавливается в оптимальное годовое положение для Москвы - угол наклона 50 градусов, азимут - 180 градусов.

Вся полученная информация(азимут, угол наклона для каждого измерения и вырабатываемая мощность при различных положениях ПП) отправляется через интернет соединение на сервер для дальнейшей обработки. Измерения производились каждый час.



Рисунок 3. Разработанная система.

### III. Полученные результаты.

Трекер был испытан 8 мая 2016 года в Московской области в условиях значительной облачности.

Система поиска наиболее яркой точки на небосводе не изменяла положения ПП по сравнению с заданным календарным графиком(выработанная при этом мощность так же не отличалась). Это можно объяснить малой точностью фотодиодов и большим выбранным  $\Delta R$ .

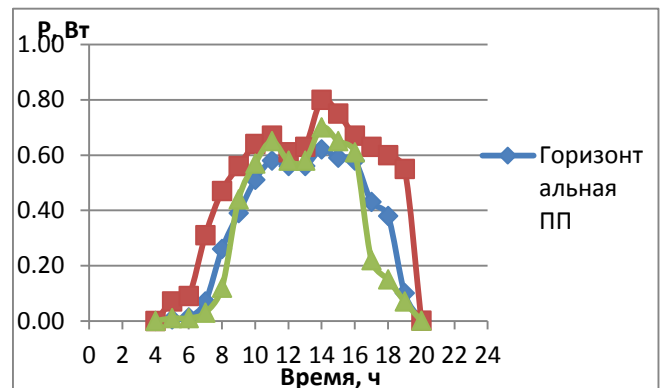


Рисунок 4. Выработанная мощность в течении световых суток

Для полноценной оценки эффективности работы трекера необходимо провести серию экспериментов при различных погодных условиях, но пока что на основании проведенного опыта можно сделать несколько выводов:

1. Система слежения за Солнцем увеличивает вырабатываемую мощность солнечной батареи. В данном случае, в условии значительной облачности, прирост выработки по сравнению с годовым оптимальным углом составил 49%, что согласуется с теоретическим расчетом для данного месяца.

2. Наибольший прирост выработки при использовании трекера наблюдается в утренние и вечерние часы (с 5 до 9 и с 16 до 19 часов), что соответствует периоду утренних и вечерних пиков нагрузки в большинстве энергосистем

### IV. Вывод.

Системы слежения за Солнцем могут увеличивать выработку солнечных панелей на 30-40%, что было продемонстрировано на практике в условиях данного эксперимента. Однако, рациональность использования подобных систем должна быть доказана с экономической точки зрения. В анализе должны быть учтены множество факторов, таких как потребляемая сервомоторами мощность, амортизационные издержки на оборудование и затраты на эксплуатацию. Только после детального анализа можно делать вывод о выгодности применения трекров в данных условиях.

### ЛИТЕРАТУРА

- [1] A review of principle and sun-tracking methods for maximizing solar systems output. Hossein Mousazadeh, Alireza Keyhani, Arzhang Javadi, Hossein Mobli, Karen Abrinia , Ahmad Sharifi, 2009
- [2] Tracstar. Should you install a solar tracker?; 2007. <http://www.helmholz.us/ smallpowersystems>.

# Generalization of the Data on Heat Transfer and Resistance for a Flow in Plate Heat Exchangers

M. Yu. Yurkina, Vas.S. Beliayev, A.L. Efimov

Department of Heat-and-Mass Exchange Processes and Installations  
National Research University MPEI  
Moscow, Russia

YurkinaMY@mpei.ru, BeliayevVasS@mpei.ru, EfimovAL@mpei.ru

**Abstract** — Calculation of modern heat exchangers is carried out, as a rule, according to computer programs of developers and their subsidiaries.

**Keywords** — *heat exchange, hydraulic resistance, lamellar heat exchangers.*

## I. INTRODUCTION

The dependences on heat exchange and hydraulic resistance of such devices put in algorithms of programs in an explicit form are inaccessible to the user. Therefore in need of comparison of devices, various producers, it is necessary to address directly on firms that is extremely inconvenient. Especially, if it is required to carry out multiple calculations.

## II. RESULTS

General view of dependences, discharged by us on a basis generalizations results, executed by means of the computer program of Sondex (type of plates – TL) for the compelled current of liquids following [1]:

$$Nu = A Re^{n} Pr^{0.4} \left( \frac{2F_0}{f_0} \right)^p X_{t0} \quad (1)$$

$$\xi = B Re^m Re_k^{mk} \left( \frac{2F_0}{f_0} \right)^q X_0 \quad (2)$$

where  $X_{t0}$ ,  $X_0$  – correction coefficients for taking note on heat exchange and hydraulic resistance of unevenness of distribution of streams of heat carriers on width and depth of packages of plates.

Values of constants to formulas (1) and (2) are given in tab. 1, and geometrical characteristics of heat exchangers – to tab. 2. Generalization is executed in the ranges of change of numbers of  $Re=300 \div 60000$  and  $Pr=1,5 \div 10$ . The generalized dependences for heat exchangers are presented in fig. 1.

Table 1. Constants to formulas (1) and (2)

A	n	p	B	m	$m_k$	q
0,0385	0,73	0,22	0,36	-0,037	0,012	0,011

Table 2. Geometrical characteristics

Тип	d, м	$D_{vz}$ , м	$F_0, \text{м}^2$	$2F_0/f_0$	$X_{t0}$	$X_0$
S20A	0,48	0,05	0,021	918	0,970	1,022
S4A	0,48	0,032	0,042	318	1,038	0,949
S8A	0,48	0,032	0,084	635	0,925	0,898
S7A	0,48	0,50	0,073	319	1,076	1,357
S14	0,48	0,50	0,15	655	0,966	0,848
S47	0,48	0,1	0,5	1162	0,941	1,014
S21	0,48	0,1	0,24	577	0,970	1,000
S62	0,48	0,150	0,68	1220	1,038	1,204
S86	0,48	0,150	0,9	1670	1,076	0,970
S41	0,48	0,150	0,45	850	0,905	0,949
S65	0,48	0,200	0,68	886	0,966	0,848

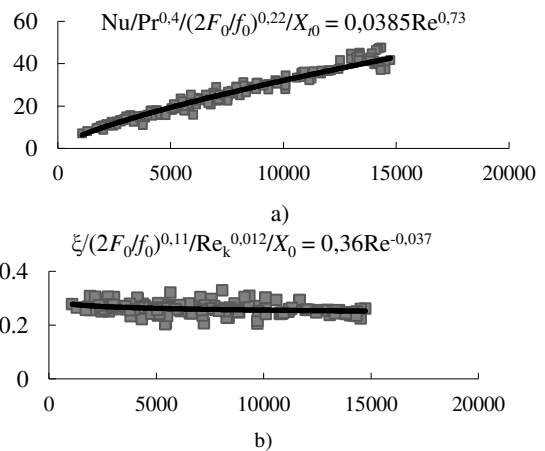


Figure 1 – The generalized dependences on heat exchange (a) and hydraulic resistance (b) at the compelled current of liquid (on abscissa axis values of numbers of  $Re$ , on ordinate axis — a dimensionless complex in the studied ranges are postponed)

## III.CONCLUSION

Comparison of the taught results with data of publications of foreign authors has shown that at the compelled current of single-phase liquids in channels of lamellar heat exchangers have used the same numbers of similarity of  $Nu$ ,  $Re$  and  $Pr$  [2-4]. Difference consists only that they accepted the characteristic cross size of channels of lamellar heat exchangers to equal two distances between the next plates (as for a flat crack), and we defined him as the elation off our cross narrow sections of the channel to the moistened perimete. Besides, the exponent at Prandtl's numbers is accepted by them equal 0,333. In works [2 - 4] the exponent at Prandtl's numbers is accepted, as well as in our works, equal 0,4. Fortaking note of relative length of the channel in [9, 10] the same as in dependences (1) and (2), the relation  $2F_0/f_0$  is entered.

## REFERENCES

- [1] Industrial power system and heating engineer: Help series: In 4 books / Under a general edition of A.V. Klimenko and V. M. Zorin. M.: MPEI Publishing house, (2007).
- [2] Arsenyev O. P. Vzaimosvyaz of transfer of heat and an impulse in channels of lamellar heatexchange devices//Integrirovannie technologists and a =nergosberezeniye. – Kharkiv: NTU "HPI", (2011), No. 1. Page 3 – 8.
- [3] Arsenyev O. P. The generalized equation for calculation of hydraulic resistance of channels of lamellar heat exchangers//Integrirovannie technologists and energy saving – Kharkiv: NTU "HPI", (2010), No. 4. Page 112 – 117.
- [4] G.A. Longo, A. Gasparello, R. Sartori. Experimental heat transfer coefficient during refrigerant vaporization and condensation inside herringbone-type plate heat exchangers with enhanced surfaces. Int. J. Heat Mass Transfer 47(2004) 4125 – 4136

# Increasing Efficiency of fuel Supply Systems at Thermal Power Plant

Y. Zhigulina<sup>1</sup>, V. Khromchenkov, V. Krivokon

Dept. of Industrial Heat Power Engineering Systems  
Moscow Power Engineering Institute  
[Zhigulina.kate@gmail.com](mailto:Zhigulina.kate@gmail.com)<sup>1</sup>

**Abstract**— The article is devoted to a problem of rationalization of fuel consumption at heat supply sources. Some original schemes of receiving and storing the liquefied natural gas as alternative reserve fuel generated by means of application of expansion turbines are proposed.

**Keywords**— thermal power plant, natural gas, turboexpanders, methane, black oil.

## I. INTRODUCTION

Natural gas is the main fuel for the majority of district-heating plants and thermal power plants at the European part of Russia. Black oil is usually used there as the reserve fuel. It causes the expensive maintenance of black oil economy. Even while storing one has to keep black oil fluid and because of that there is necessity of its constant heating and circulation all year round. Besides oil-fired boilers have lower efficiency than gas-fired ones due to sediments of combustion products at heat exchange surface areas, higher temperature of the exhaust fumes and etc.

In our research we propose the technical solution that allows to generate, to store and to use the liquefied natural gas as the reserve fuel at heat supply souses instead of black oil.

## II. APPLICATION OF TURBO EXPANDERS AT TPP

Heat supply sources consume natural gas of low pressure (a little more than 1 atm.). At the same time the pressure of natural gas arriving at heat supply sources is about 0,5-1,2 MPa. Usage of turbo expanders for capturing the energy that is otherwise lost in the gas pressure letdown process, allows you to produce power and to cool the gas deeply.

Natural gas delivered to consumers, is a mixture of hydrocarbons, with a predominant share of methane (50 - 99%), as well as nitrogen, carbon dioxide and others. Cooling the gas by reducing its pressure via the turbo expander will condense some high-boiling fractions of hydrocarbons.

Fig.1 and 2 contains the obtained diagrams of two compositions of real gas (from Ishimbay-Magnitogorsk pipeline and Moscow region gas networks) with different contents of high-boiling components (temperature - entropy and enthalpy - entropy). The gas composition influences much to the isobars course in the two-phase field. In this area where the isobars have knees in two-phase field (under the saturation curve) methane begins to condense.

So if working on gas with a lot of high-boiling fractions, we can condense them even at atmospheric pressure at the temperature level of about -65°C, whereas in the case of low-boiling gas only at -130°C. This means that, additional cooling of the gas should be done in order to obtain the necessary

amount of liquefied gas. It will complicate the technological scheme.

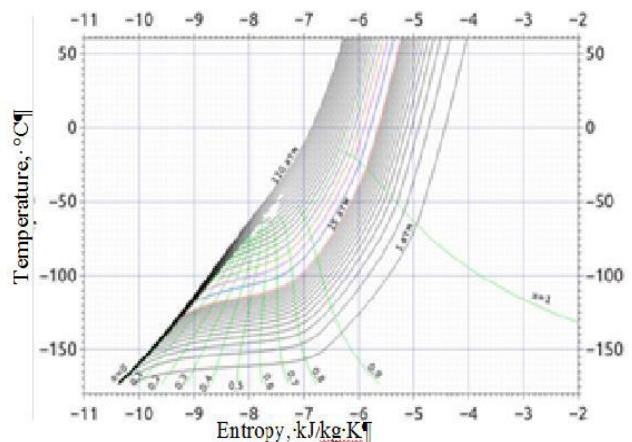


Fig.1 Thermodynamic diagrams of real natural gas (Ishimbay-Magnitogorsk pipeline)

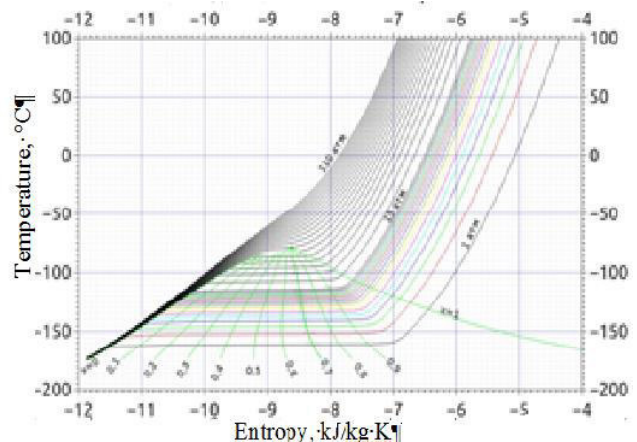


Fig.2 Thermodynamic diagrams of real natural gas (Moscow region gas networks)

## III. CALCULATION OF THE DEVELOPED SCHEMES

The calculation of the developed schemes (fig. 3a,b) was performed using the following data of Moscow TPP-23: the annual natural gas and black oil consumption, the composition and the technical characteristics of the main equipment.

The calculations were done using the comprehensive process modeling via Aspen Hysys. The calculations shows

that it will take a little less than 9 months to accumulate the necessary amount of the reserve fuel.

This scheme cannot be used if work on natural gas with composition no. 2 consisting from 98% of methane. The problem is that the temperature level is not low enough for the methane condensation. So it was decided to use cold recovery, providing the preliminary cooling of the gas before the expander. The condensation outlet is almost 3 times bigger, then it was in the first scheme, so in this case the accumulation period of the reserve fuel is 3 months.

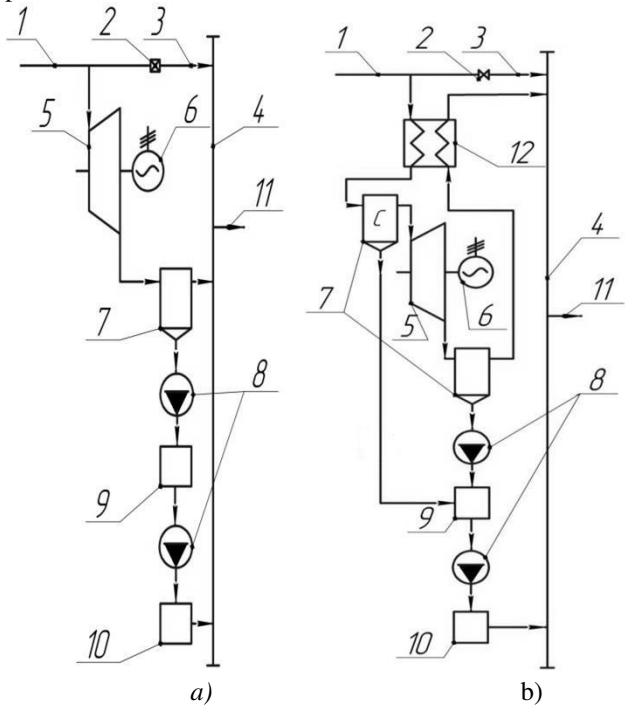


Fig 3. Schematic diagrams of scheme 1 (a) and scheme 2 (b)

*1 — high pressure gas pipeline, 2 — throttle valve, 3 — bypass, 4 — low pressure pipeline, 5 — expansion machine, 6 — electric generator, 7 — separator, 8 — pump, 9 — storage tank, 10 — gasifier, 11 — to the consumer of natural gas, 12 — heat exchanger*

The calculations for nine different compositions of natural gas were done for estimation of the feasibility of the first scheme usage.

#### IV. CONCLUSIONS

- The possibility of usage of liquefied natural gas as the reserve fuel at gas oil-fired thermal power plants (TPP) and boiler plants in Russia is considered.
  - The estimation of the annual amounts of black oil and natural gas that are needed to ensure the reliable operation of several power plants in Russia has been done.
  - Fundamental technical solutions for reserving at TPP the necessary amounts of liquefied gas are presented. The evaluation confirms the effectiveness of the technical ability to use liquefied natural gas as a backup fuel reconstructed and newly designed gas power station.
  - The calculations showed that the first scheme can be applied only when work on natural gas with a high content of high-boiling fractions (more than 4-6 %).
  - The increase of pressure of natural gas in the high-pressure pipeline from 9 up to 12 atm leads to the increase of mass fraction of the condensate in the circuit 1 for 1.6%, and in the circuit 2 for 0,43%.
  - The increase of the total mass fraction of hydrocarbons except methane involves a higher output of condensate (for example, when the total share of these components is increased for a 1%, the output of the condensate increases at 0.2%).

# District Heating And City Energy Supply: Outlining A New Model and Main Principles

E. Gasho

Dept. of Industrial Heat Power Engineering Systems  
Moscow Power Engineering Institute

**Abstract –** The article is devoted to the problems of thermal modernization of existing and insulation of new buildings where it is technically and economically feasible, with non-expensive regulation. Technically and economically optimized district and decentralized heating systems.

**Keywords-** energysaving, heat supply system, district heating, waste heating.

## I. INTRODUCTION

The table 1 contains the existing problems of heat supply systems in cities. These problems are caused due to significant differences of operating conditions.

**Table 1.**

Technical solutions	Effects
Substantial (to 2/3) rate of industrial heat consumption with stable loads schedule	Constant load for boilers and turbines during the year
Enlargement of buildings, urban concentration and centralization of heating systems	Reduction of specific heating energy cost in 3-4 times
The use of industrial reversionary energy resources, heat from cogeneration plant	Reduction of primary energy consumption
Spread of cogeneration (combined heat and power)	Up to 30% of fossil fuels savings
Cumulative effects: the consistent operation of thermal power plants, fuel savings, low fares	30-35 million tons of coal equivalent per year savings

## II. INFLUENCING FACTORS ON THE SIDE OF CONSUMERS

- Thermal protection improvement in buildings
- Reconstruction and decommissioning of outdated boilers and turbines with gas turbines and CCGT
- Increasing the quantity of new (renovated) buildings
- Reconstruction of buildings, including replacement of engineering communications and lighting systems
- The growing number of shopping and office, entertainment centers with a predominance of electrical load
- The growth of electricity consuming equipment in households buildings (including air-conditioning)

- Equipping cogeneration units with large boiler gas turbines
- Peak accumulating energy sources of different capacity in urban areas
- Use of industrial CHP, heat recycling CHPP, other secondary energy resources
- The growth of peak electrical loads of different nature
- The use of local resources for the development of additional heat and electricity generation

Table 2 contains the new principles of Energy model in sources, network and consumers.

## III. INFLUENCING FACTORS ON THE SIDE OF GENERATION

- Growth of distributed generation" plants of different capacity (including renewables)

**Table 2.**

<b>sources</b>	<b>network</b>	<b>consumers</b>
Modernization of N/Q energy parameters depending on load graphs		Optimization of heat consumption in buildings (including renovation and modernization of buildings)
Three-generation in the cities of the southern part of the country (+ heat pump cooling-supply systems)	Technologically optimal rate of centralization and regulatory systems	The presence of peak-power devices to large consumers
Local, renewable fuels (peat, municipal waste, waste water, recycling of vent-emissions)	The optimal rate of distributed energy sources of different origin	Demand management methods (e.g. Broad tariff menu for promotion of energy saving)
Rational development of heat supply from nuclear sources (	Automated system linking modes of consumption and generation (smart grid)	

#### IV. INFLUENCING FACTORS ON THE SIDE OF GENERATION

- Use of combined energy sources with equipment adequate to energy load structure and climate (steam-, gas turbines, hybrid, etc)
- Informational-analytical systems of accounting and monitoring, billing.
- Recoverable heat utilization systems
- Use of local fuel, renewables, combined and hybrid systems
- Nuclear heat generation of different origin (ATPP, AEC, PATÈS)
- Construction of thermal power station with an increased share of electrical power (steam-gas)
- Access control systems for heat consumption
- Optimal schematic solutions for cities of different sizes and in different climatic zones
- Three-generation (heat, power and chill) for large southern cities, heat pumps for balancing the peak loads
- Peak accumulating systems for large energy peak consumers like shopping malls

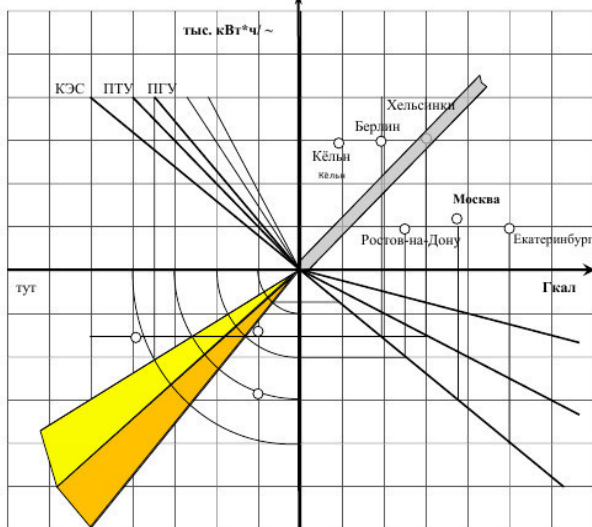


Fig.1. Zones of optimal energy sources

#### REFERENCES

- [1] E. Gasho, M. Stepanow. Energieeffizienz: die gesetzgebende Basis, die Maßnahmen der staatlichen Politik, die wirtschaftlichen und geschäftlichen Praktiken. Nachhaltige Entwicklung in Russland. Berlin-St. Petersburg, 2013, 45-55
- [2] E. Gasho, Y. Repezkaya Programme der energieeinsparung sind aufgeleest – wie weiter (наем.языке)//Wostok. 2011. №2.

# Energy efficiency of ventilation system

M.N. Stepanenko<sup>1</sup>, A. Ya. Shelginskii, Yu. V. Yavorovskii  
Dept. of Industrial Heat Power Engineering Systems  
Moscow Power Engineering Institute  
Moscow, Russia  
[maggynikolaevna@gmail.com](mailto:maggynikolaevna@gmail.com)<sup>1</sup>

**Abstract**— Energy efficiency analysis of ventilation emission usage for heating intake air of various units including waste heat exchangers and the heat pump was carried out. The mathematical model and the calculation algorithm of the considered ventilation system have been proposed.

**Keywords**— *heat pump, airflow system, energy consumption, calculation algorithm, mathematical model.*

## I. INTRODUCTION

The need for energy efficient heat recovery is ever growing. The rise in energy prices and further environmental commitments places an increasing burden on organisations as they seek to reduce energy consumption. The heat recovery ventilation system provide the most effective and energy efficient ventilation, helping reduce energy use and consumption.

To conserve heat in the ventilation and air conditioning systems are often considered the possibility of recycling the heat removed from the air space. Combined use of heat exchangers (HRV) and heat pumps in ventilation and air conditioning systems for the recycling of heat from the air in addition to the general method of partial recycle more and more attention.

However, when using the HRV and heat pump systems to be considered such an important factor in the system, as the growth of the aerodynamic resistance of electricity consumption in the fan drive for growth in the entire ventilation system, and the additional cost of the compressor drive heat pumps. In addition, it is necessary to take into account the fact that by using fossil fuel unit costs in the toe on average production of 1 kWh of electricity to 2.32 times higher than the cost of production of 1 kWh of heat. Besides, it is necessary to take into account the ratio of the heat rates, and electricity in certain regions. Most of the professionals involved in the development and improvement of ventilation systems do not account for all factors that significantly affect the economic effect of the introduction and use of specifications and heat pump systems.

## II. FORMULATION

To evaluate the feasibility of using schemes with energy saving measures necessary to determine the main load of the object (the need for heat, electricity and others.), Operating costs and to evaluate capital investments. Produced for this calculation are multiple-choice and time-consuming. Software module block diagram significantly reduces the amount of time for calculation. A separate software module (this is due to the peculiarities of calculation of each scheme) was written for each of the schemes

under consideration, with the consistency and the main stages of computation are the same for all of them.

For comparative analysis of energy consumption were considered four options of ventilation systems. The mathematical model of the ventilation system, including: definition of the parameters of supply and exhaust air, the characterization of the heat exchanger depending on the thermophysical properties of air and heat loads, the pressure loss across the air path, the definition of required thermophysical characteristics of heat pump systems.

Features calculations heat transfer surface having a temperature below the dew point temperature of the cooled air have been addressed by using water drop ratio:

$$\zeta = \frac{H_2 - H_{2x}}{C_{par} \cdot (t_2 - t_{2x})} \quad (1)$$

where  $\zeta$  – water drop ratio representing the relation of amount of full heat of the obvious heat transferred in the heat exchange device to quantity;  $C_{par}$  – specific heat of moist air at an average temperature of device kJ / (kg K);  $H_2, t_2$  и  $H_{2x}, t_{2x}$  – enthalpy and temperature of moist air at inlet and outlet from device, kJ / (kg K).

## III. CONCLUSION

The following results were obtained based on a mathematical model:

The Most efficiency of ventilation system for the climatic conditions of the central regions of the Russian Federation is combined use of heat pumps and heat recovery. Its use reduces the cost of conventional fuel by 65%, the cost of the primary conventional fuel by 70% compared without the use of energy-saving measures.

A comparison of the values of the conditional and contingent primary fuel costs, with additional costs for the production of additional electricity shows the need for an integrated approach to the feasibility study of modernization of air ventilation.

## IV. REFERENCES

- [1.] M.N. Stepanenko, A. Ya. Shelginskii. Using heat ventilation emissions in buildings ventilation systems. Safety and Security of Energy Magazine. 2014. № 2 (25). c. 42 – 45. (in Russian).
- [2.] M.N. Stepanenko, A. Ya. Shelginskii, Yu. V. Yavorovskii Energy consumption when using a heat vent emissions // Industrial power Magazine. 2016. №3. C. 8-14. (in Russian).

# Ermittlung des Absorptionskoeffizienten für Transparente Körper

E. Voelker

Institute für Simulative Untersuchungen im Bauwesen  
Brandenburgische Technische Universität  
Cottbus, Germany  
eduard.voelker@b-tu.de

W. Glasov

Moskauer Energetische Universität  
Lehrstuhl für Thermodynamische Prozesse und Anlagen  
Moskau, Russland

**Abstract**— Auf der Suche nach alternativen Energiequellen bleibt die Sonnenenergie als eine der wichtigsten Quellen. Die Aufgabe der Wissenschaftler und Ingenieure ist es, die Sonnenenergie effektiv und kostengünstig nutzbar zu machen. Ein Behälter mit Wasser und einer transparenten Abdeckung bietet die einfachste Form, Sonnenenergie einzufangen und zu speichern. Es ist anzunehmen, dass in so einem Wasserspeicher, wie im Gewässer eine starke Temperaturschichtung geben wird. Diese wirkt sich unterschiedlich auf die Wärmeverluste aus. So sind im oberen Bereich des Speichers höhere Verluste zu erwarten. Der Speicher besteht aus einer geschlossenen Konstruktion aus Porenbeton, Wärmedämmung und Edelstahl. Die obere Abdeckung besteht aus einer lichtdurchlässigen 2-fach verglasten Glasscheibe. Die eingefangen Wärme soll gespeichert werden und bei Bedarf zur Versorgung der schwimmenden Bauten dienen. Da es im See keine großen Verschattungen gibt, eignet sich dieser Einsatzort besonders. Es soll jedoch vorher berechnet werden, wie effektiv diese einfache Methode bezüglich der Aufnahme und des Speicherns von Sonnenenergie sein kann.

**Keywords**— Absorptionskoeffizient; Strahlung; Methode; Transparente Körper; Wellenlängenbereich

## I. EINFÜHRUNG

Für die Berechnung der Temperaturverteilung, infolge der Temperaturstrahlung im transparenten Körper bedarf es einen Absorptionskoeffizienten  $k$ , der ein bestimmtes solares Spektrum abdeckt.

$$\frac{\partial T}{\partial t} = a \cdot \frac{\partial^2 T}{\partial x^2} + \frac{(k \cdot q)}{\rho C} \cdot e^{-kx} \quad (1)$$

Die Bildung eines Mittelwertes aus den einzelnen gemessenen spektralen Absorptionskoeffizienten kommt nicht infrage, da der Verlauf der spektralen Absorptionskoeffizienten über weite Wellenlängen nicht linear ist. Zur Ermittlung eines Absorptionskoeffizienten im sichtbaren Wellenlängenbereich werden jeweils eine analytische und eine experimentelle Methoden vorgestellt.

## II. ANALYTISCHE FORMULIERUNG

In der analytischen Methode wird der sichtbare Wellenlängenbereich in acht Bereiche mit einem Intervall von jeweils  $0,05 \mu\text{m}$ , als Differenz zwischen den Messwerten unterteilt. Es werden so zusagen 8 Sonnenstrahlen mit dazugehöriger Intensität erzeugt. Jeder dieser Strahlen wird auf eine vorgegebene Tiefe absorbiert. Aus der Summe der absorbierten Wärmeenergie wird dann ein Absorptionskoeffizient für diesen Wellenlängenbereich ermittelt. Dabei macht der Anteil an extraterrestrischer

Strahlung im visuellen Bereich  $E_v$  46% der gesamten Strahlung aus.

$$E_v = \int_{0,4}^{0,8} E_0(\lambda) d\lambda \quad (2)$$

Die gesamte Strahlung, die die Erde außerhalb der Erdatmosphäre erreicht beträgt ca.  $1368 \text{ W/m}^2$  und ist auch als Solarkonstante  $E_s$  bekannt[1]. Die einzelnen Wärmeströme im vorgegebenen Intervall von  $0,05\mu\text{m}$  setzen sich aus dem Flächenintegral zusammen.

$$q_i = \int_{\lambda 1}^{\lambda 2} \frac{\left( \frac{c1}{(\lambda \cdot 10^{-6})^5 \cdot (\frac{c2}{e^{\lambda \cdot 10^{-6} \cdot T - 1}})} \right)^{-4 \cdot \pi \cdot (Rs)^2}}{F} \cdot 10^{-6} \cdot K d\lambda \quad (3)$$

wobei mit dem Koeffizienten  $K$  die Absorption der Strahlungsenergie durch atmosphärische Gase berücksichtigt wird.

Summe der absorbierten Wärmeenergie wird folgender Formel berechnet:

$$q_a = \sum_{i=1}^n [(1 - e^{-k[i] \cdot 1,86}) \cdot q_{[i]}] \quad (4)$$

Durch die Umstellung nach  $k$  bekommt man einen Absorptionskoeffizienten für den sichtbaren Wellenlängenbereich.

## III. EXPERIMENTALE FORMULIERUNG

Die experimentelle Ermittlung des Absorptionskoeffizienten im sichtbaren Wellenlängenbereich basiert auf der Herleitung aus der Wärmetransportgleichung. Unter der Annahme, dass die Wärmeleitung im transparenten Körper kein Einfluss auf die Temperaturverteilung infolge von Wärmestrahlung hat. Dieser Fall tritt im instationären Wärmetransport auf, wenn die Wärmeleitung langsamer voranschreitet als die Wärmestrahlung. Somit wird aus der zeitlichen Differenz zwischen zwei Temperaturmesspunkten der Absorptionskoeffizient ermittelt.

$$t_1 \cdot \frac{q}{\rho C} e^{-kx_1} = t_2 \cdot \frac{q}{\rho C} e^{-kx_2} \Rightarrow \frac{t_1}{t_2} = \frac{e^{-kx_1}}{e^{-kx_2}} = e^{-kx_2 + kx_1}$$

## QUELLENANGABE

- [1] Hans Dieter Baehr, Karl Stephan: Wärme- und Stoffübertragung, 6. Auflage, 2008 Springer-Verlag, Berlin Heidelberg.
- [2] Wasilij Glasov, Moskauer Energetisches Institut: persönliche Mitteilung 2012 (В.С. Глазов, к.т.н., доц. «НИУ «МЭИ»)

# Feasibility Study for Renewable Sources of Energy Usage in Decentralized Power Generating System in the Batakan Settlement

N. Karpov, P. Krapivko, Y. Myravitsky, G. Derygina  
 Dept. of Hydro Power Engineering and Renewable Energy Sources  
 Moscow Power Engineering Institute  
 Moscow, Russia  
 KarpovND@mpei.ru

**Abstract**—Power supply of the decentralized regions, including the object in Batakan settlement (Zabaikalskiy kray, Gazimurskiy region) is currently provided by diesel generators. The main problems of isolated users power supply are: the high cost of diesel fuel transportation, dependence on its delivery, the environmental damage caused by exhausts and noise. The diesel fuel costs growth promotes to cost raising of power energy, produced by diesel power stations. The paper provides the method of implementation justification of wind power and sun power generations into the local power generating system (LPGS) in accordance with the current Russian and international standards.

**Keywords**—local power generating systems; wind power generators, solar photoelectric plants; diesel generators, power efficiency

## I. DESCRIPTION OF THE EXISTING POWER SUPPLY SYSTEM

The existing power supply system of the Batakan settlement consists of two diesel generators of 200 kW power, and also two reserve diesel generators 25 kW each. The equipment was installed in 1982-1983 years, which means its deterioration. Currently about 600 people are living here. There are administrative building, school, kindergarten, ambulance feldsher's station, fire station, gas station and some power-saw benches. The total annual power consumption in the settlement for 2015 year was 2.5 mil kWh. Months power consumption of the Batakan settlement is represented in fig. 1.

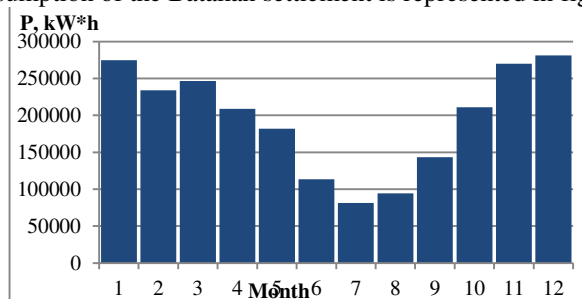


Fig. 1. Months power consumption in the Batakan settlement for 2015 year

## II. JUSTIFICATION OF WIND TURBINES (WTG) USAGE FEASIBILITY

Based on the performed researches, absence of meteorological stations has been revealed. In that case calculations and analysis of wind resources [1] have been made using the meteorological station (MS) data with 6-th hours observational series of wind speed during 2015 year, based on the “Raspisanie pogodi” website data [2] (table I).

TABLE I. Primary wind statistical characteristics in the Batakan settlement

Characteristic	Value
Average wind speed at a height of 10 m, m/s	2,05
Mean-square deviation, m/s	1,79
Wind Variation factor	0,84
Maximum wind speed, m/s	13

Annual average specific energy, kWh/m <sup>2</sup>	235,9
--	-------

On the first stage of WTG selection the following requirements shall be considered: WTG singular rated capacitance with mounting and transportation possibility; WTG class according to IEC 61400-1; climatic category according to GOST 51991-2002.

During designing of the WTG, which may be added to the local power system of the Batakan settlement, 4 WTG models with singular rated capacitance from 100 kW to 330 kW, TFC modification have been selected: AeronauticaWindPower AW29-225, Fuhrländer FL250, Nordex N29/250, Vestas V29.

The final choice of WTG model on the assumed WPS location shall be performed after technical and economic justification. Large WTGs amount may be reduced according to maximum value of capacity factor, r.u.:

$$k_{wtg}^{c.f.} = \frac{P_{wtg}^{year}}{N_{wtg}^{inst} \cdot 8760}, \quad (1)$$

where  $P_{wtg}^{year}$  - WTG annual energy output.

The value of specific energy from the propeller disk area can be also be reviewed as an energy efficiency criterion, according to GOST 51991-2002:

$$P_{wtg}^{sp} = \frac{P_{wtg}^{year}}{F_{wtg}}, \quad (2)$$

where  $F_{wtg}$  – propeller disk area for propeller type WTG, It is calculated by the formula:

$$F_{wtg} = \frac{\pi \cdot D_{wtg}^2}{4}, \quad (3)$$

Energy efficiency calculation results for selected isolated operating WTG models are represented in the table II.

TABLE II. WTG capacity factor.

Manufacturer	Model	$k_{wtg}^{c.f.}$ , r.u.	$P_{wtg}^{sp}$ , kWh/m <sup>2</sup>
Aeronautica	AW29-225	0,11	114,3
Fuhrländer	FL 250	0,11	119
Nordex	N29/250	0,13	129
Vestas	V29	0,13	136

Considering the load curve, aerodynamic losses for adjacent WTG blur, ice formation losses and others, value of the capacity factor will be lower for 10%. In accordance with the act №47 from the 23th of January 2015 [3] considering the objects of wind generation, independently on installed capacity value, capacity factor value shall not be lower than 0.27. So, It has been decided not to use wind power generation in the Batakan settlement.

## III. JUSTIFICATION OF SOLAR PHOTOELECTRIC PLANTS (SPEP) USAGE FEASIBILITY

Designing of photoelectric power plants (PEPP) begins with location selection. Further selection of models and their amount

shall be made. The SPEP location has to comply to the international standard IEC 62257-7-1 and It shall be selected around the object according to the following criteria:

1. Solar insolation high rate;
2. Terrain form simplicity, in other words – minimal adjacent solar power plants blur. Self-purification possibility, ease mounting shall be considered;
3. Poorness of the soil, deep underground water;
4. Electrical substation with sufficient transfer capability for SPEP connection shall be located nearby;
5. Infrastructure presence (transportation, roads which help to decrease building cost).

SPEP location has been selected nearby diesel power station (DPS). There is enough space for solar modules park deployment with selected power of 400 kW.

For the solar photoelectric plants usage feasibility it is required:

1. To learn the actual offers of manufacturer companies and chose appropriate equipment;
2. To establish the location of solar equipment mounting;
3. To define SPEP capacity factor value.

Insolation source information may be received using the data of the closest actinometrical station (AS) in the Borzya settlement, Chita region, in 250 km from the. Height difference is 70 meters [4]. Basic energy characteristics of insolation in the Batakan s. according to actinometrical station in Borzya are represented in table III.

TABLE III. Basic energy characteristics of insolation.

No	Name	Region	$\phi$ n.l.	$\Psi$ e.l.	Year
72	Borzya	Chita	50,3	116,4	
	total		$P_{\Sigma}$ , kW·h/m <sup>2</sup>		1442
	direct		$P_{\text{normal beam}}$ , kW·h/m <sup>2</sup>		850
	diffused		$P_{\text{diff}}$ , kW·h/m <sup>2</sup>		592
	Albedo		r, r.u.		0,32

After energy resources in the Batakan settlement has been analyzed, we may talk about insolation high rate.

During the SPEP designing, which may be added to the local power system of the Batakan settlement, silicic micromirph, monocrystal and polycrystal panels, and also heterostructure (thin-film + monocrystal silicon) were studied and reviewed as the most widely used and the most available to purchase in Russia. Four modules of SPEP have been selected, their parameters are represented in the table IV.

TABLE IV. Photoelectric modules.

Model (Manufacture)	P, W	Type	Surface area, m <sup>2</sup>	Efficiency, %
SFM23054 (Jingyang SE Co, China)	200	Monocrystal Si	1,7	17
BRS150M(BPS TECH, China)	150	Polycrystal Si	1	17
Hevel HJT (Hevel Solar, Russia)	260	Heterostructure	1,64	20
Hevel MSI (Hevel Solar, Russia)	125	micromorph Si	1,43	>20

SPEP model selection is performed according to the criterion of energy efficiency, r.u:

$$k_{\text{SPEP}}^{\text{c.f.}} = \frac{P_{\text{SPEP}}^{\text{year}}}{N_{\text{SPEP}}^{\text{inst}} \cdot 8760} , \quad (4)$$

where  $P_{\text{SPEP}}^{\text{year}}$  annual SPEP energy output:

$$P_{\text{SPEP}}^{\text{year}} = P_{\text{year}}^{\text{hs}} \cdot \eta \cdot F_{\text{SPEP}} , \quad (5)$$

where  $P_{\text{year}}^{\text{hs}}$  insolation to horizontal surface of 1 m<sup>2</sup> with average cloud;

$\eta$  – efficiency of SPEP plan, inverters and batteries;  
 $F_{\text{SPEP}}$  – total solar panel square [5].

Capacity factor calculation results for selected models of SPEP are represented in table V.

TABLE V. SPEP capacity factor

Model (country)	$k^{\text{c.f.}}, \text{r.u.}$	$\eta, \text{r.u.}$
SFM23054 (China)	0,21	0,15
BRS150M (China)	0,16	0,15
Hevel HJT (Russia)	0,19	0,18
Hevel MSI (Russia)	0,34	0,18

In accordance with the act №47[3] from the 23th of January considering the objects of solar generation, independently on installed capacity value, capacity factor value has to be not lower than 0.14. In that case using solar generation in the Batakan settlement is reasonable.

Photoelectric models of Russian manufacturer company Hevel – Hevel MSI have been selected as the final variant. The penetration rate of DPS generation from the energy consumption graphic at the expense of SPEP has been made. Its value is 45% on year. Diesel fuel economy equals to 35%.

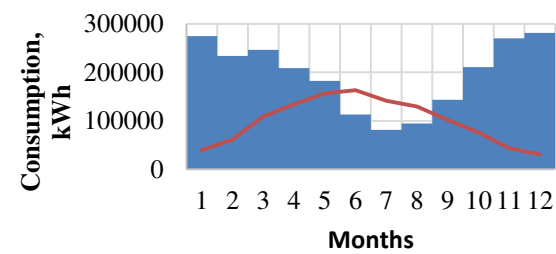


Fig 2. Months power consumption in the Batakan settlement considering SPEP generation

#### IV. CONCLUSIONS

This method allows to perform preliminary efficiency estimation of wind and solar generation integration into local power generating system considering capacity factor value in accordance with the act №47 from the 23th of January 2015 year.

Wind power generators integration into the LPGS of the Batakan settlement is pointless because of low rate of WTG capacity factor. Integration of photoelectric modules Hevel MSI with amount of 3200 units allows to decrease diesel fuel consumption for 35%.

#### REFERENCES

- [1] Derugina G.V., Malinin N.K., Pugachev R.V., Shestopalova T.A. Basic Wind Characteristics. Wind resources and their calculation methods: study guide/ - M.: MPEI publishing, 2012
- [2] Russian meteorological website “Weather timetable”: <http://rp5.ru>
- [3] Act from the 23th of January 2015 №47 “About introduction of changes to some Russian Federation government acts considering stimulation of renewable sources of energy usage around retail markets of electrical energy”.
- [4] Data base, “Scientific USSR climate guidebook”, NVIE department, IEE, MPEI (TU), 2004
- [5] Solar energetics: study guide for universities / V.I. Vissarionov, G.V. Derugina, V.A. Kuznecova, N.K. Malinin; edited by V.I. Vissarionov. – M.: Publishing house MPEI, 2008. – 276c.

# Application of Heat Pumps in Hot Water Systems.

A.V. Martinov

Dept. of Industrial Heat Power Systems  
Moscow Power Engineering Institute  
Moscow, Russia

A.I. Rozhkova

Dept. of Industrial Heat Power Systems  
Moscow Power Engineering Institute  
Moscow, Russia  
Rozhkova.aleksandra@list.ru

**Abstract** —The article assesses the work of heat pump installations in the DHW system. Consider the principle of the heat pump, and also put forward the problem of energy saving. Due to the fact that bacteria are contained in water and the water on GOST can not be lower than 60 °C, proposed water purification system to increase the installation of energy efficiency and reduction of the water temperature.

**Keywords**— *heat pump; problem of energy saving; water purification system; energy efficiency.*

## I. INTRODUCTION

When we using domestic hot water systems there are a number of difficulties, such as large heat consumption on maintaining the desired temperature in the circulation circuit, the tangible consumption electricity for the circulation and complexity the operation and installation of the system caused by necessity of install automatic balancing valve in every riser for the organization of uniform circulation of water in all risers.

There is great potential opportunities the use of energy around us, and the heat pump is the most successful way to realize this potential. Today actual is solutions to environmental problems: instead of traditional burning fossil fuels - the use of alternative energy sources. In the case of heat pumps nonconventional energy source is a low potential heat. This heat is a natural and artificial origin, that is area of application of heat pumps is expanding significantly.

The use of heat pumps DHW system is possible both in new and existing buildings. The main advantage of the heat pump is a high efficiency compared to other methods of heating water. The report reviews the DHW circuit with heat pump type "air-water."

The ideal low potential heat source should provide a stable high temperature during the heating season, not be corrosive and polluting, have favorable characteristics, do not require a significant investment and maintenance costs. The heat source is a key factor in determining the performance of the heat pump.

As the temperature chart for hot water supply has a temperature of 70 ÷ 80 °C. High cost of power spent on heating, so it is advisable to reduce the temperature to 40 ÷ 60 ° C. This will lead to a reduction of power consumption for heating and to increase efficiency. But decrease in temperature of hot water without precleaning is not possible in accordance with GOST. Therefore, to solve the problem is possible by means one of the pre-treatment technologies, and thus it is possible to reduce the temperature of hot water up to 40 ÷ 60 ° C and hot water to obtain a highly efficient system.

## II. FORMULATION

Hot Water System is designed to provide consumers with hot water for technological, sanitary and hygienic purposes. When using hot water systems there are a number difficulties, such as the high costs of heat to maintain the desired temperature in the circulation circuit, tangible costs of electricity for the circulation caused by the need to install automatic balancing valve in every riser for the organization of a uniform circulation of water in all risers. Heat pump solves some of the above problems. Therefore, it is promising and rational exploitation of DHW systems.

There is great potential opportunities the use of energy around us, and the heat pump is the most successful way to realize this potential. Today actual is solutions to environmental problems: instead of traditional burning fossil fuels - the use of alternative energy sources. In the case of heat pumps nonconventional energy source is a low potential heat. This heat is a natural and artificial origin, that is area of application of heat pumps is expanding significantly.

The use of heat pumps in the industry is a solution of the problem of heat recovery and industrial heating. Due to the company's own heat emitted from the of technological processes of may be implemented industrial heating and DHW. Fuel costs for heating and process heating processes in various industries is 30-40% of the total fuel cost.

Function heat pumps are divided into only used for heating or hot water supply systems and integrated systems based on heat pumps. Second provide for space heating, cooling, preparation hot water sometimes and recycle exhaust air. Water is heated by heat transfer from overheating and heat condenser.

The use of heat pumps DHW system is possible both in new and existing buildings. The main advantage of the heat pump is a high efficiency compared to other methods of heating water. Saving 70% of the costs, the heat pump provides a year-round hot water. Due to the high efficiency, at a rate of 1 kW of electricity can get 3-5 kW of heat for heating water. Also, modern control systems designed to save energy depending on the time of day, the ambient temperature, the hot water flow rate.

As a low potential heat source in small systems based on heat pumps use the outdoor and exhaust air, soil and underground water, to high power systems used sea, lake and river water, geothermal and ground water. [1] The ideal low potential heat source should provide a stable high temperature during the heating season, not be corrosive and polluting, have

favorable characteristics, do not require a significant investment and servicing costs. Low potential heat source is a key factor in determining the performance of the heat pump.

Figure 1 is a schematic diagram of a heat pump for hot water. Refrigerant at high pressure through a throttle (4) enters the evaporator (1), where due to a sharp decrease in pressure causes the evaporation process. When the refrigerant extracts heat from the inner walls of the evaporator, and the evaporator in turn takes heat from N, in this case from the air. The compressor (2) gathers the refrigerant from the evaporator, compresses it, due to which the pressure and temperature of the refrigerant rises sharply and fed to the condenser (3).

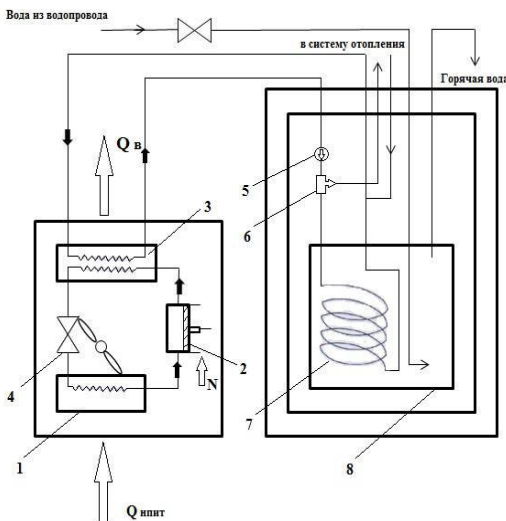


Fig. 1. Schematic diagram of the heat pump for hot water  
1 - evaporator; 2 - the compressor; 3 - the condenser; 4 - throttle;  
- pump; 6 - three way valve;  
7 - serpentine; 8 - water tub.

Furthermore, in the condenser, heated by compression refrigerant gives up heat to the heating circuit and becomes a liquid. The coolant with a pump (5) passes through the three-way valve (6), which regulates the flow of hot water in a heating system or coil (7). Water from the water enters the water tank (8), via which the coil is heated and rises. The heated water is taken from the top of the water tank and is supplied to the domestic needs. Since the system is a closed loop, then there is a constant circulation of water; wherein the hot water is discharged from the top on one pipe, it comes in its place on the other cold. The water tank is gradually heated to Th.

In a typical hot water temperature schedule hot water has a temperature of  $70 \div 80^\circ\text{C}$ . [2] This requires a large power expenditure. It is therefore advisable to lower the temperature of hot water up to  $40 \div 60^\circ\text{C}$ , resulting in a reduction of power consumption for hot water supply and to increase efficiency. But the decrease in temperature of hot water without pre-treatment is impossible in accordance with GOST. It is therefore necessary to provide for the environmental clean tap water from bacteria. There are a variety of water treatment methods such as the iodization of water, treatment with

ultraviolet light or the reverse osmosis method. water treatment method by applying ultraviolet is considered to be the safest. Also, the reverse osmosis method is the most efficient method of purifying water from microorganisms. In addition, iodination of water is used when a large volume of water. After purification, can reduce the hot water temperature to  $40 \div 60^\circ\text{C}$  and have a highly efficient domestic hot water system.

## ICONCLUSIONS:

1. The used heat pumps in domestic hot water systems allow you to adjust the hot water temperature in the range  $40 \div 60^\circ\text{C}$ , which leads to increased energy efficiency hot water systems.

2. The introduction of special environmental clean tap water provides reliable protection against bacteria.

## REFERENCES

- [1] Sokolov E.Y., Brodyansky V.M. "Energy bases transformation of heat and cooling processes", M : Energoizdat 1981.
- [2] Sokolov E.Y. "District heating and heat networks", M. Energy 1975

# Influence of Vibration Loads on the Efficiency of the Thin-film Heat Insulating Coatings for Protection of Power Equipment and Pipelines

P.A. Koroleva<sup>1</sup>, N.A. Loginova<sup>1</sup>, E.K. Völker<sup>2</sup>

Dept. of Industrial Heat Power Engineering Systems<sup>1</sup>

Moscow Power Engineering Institute<sup>1</sup>, Brandenburgische Technische Universität<sup>2</sup>

Moscow, Russia<sup>1</sup>, Cottbus, Germany<sup>2</sup>

malenkov.as.ya.ru@yandex.ru<sup>1</sup>

**Abstract** — In the paper it is described a study of thermophysical properties of thin-film heat insulating coatings (THIC), in the conditions attached vibration loads. Was measured thermal conductivity of THIC before and after exposure of vibration loads. The effective thickness of the insulation layer of THIC was calculated before the vibration load and thereafter, and also the insulation layer of mineral wool under the same conditions. The comparison of THIC and mineral wool was conducted and a result shows the efficiency of thin-film heat insulating coatings. All calculations are based on data from experimental systems used in this study and on the data previously conducted experiments with mineral wool.

**Keywords**— *thin-film heat insulating coatings (THIC); vibration loads; thermal insulation material; microspheres; thermal conductivity ; energy efficiency.*

## I. INTRODUCTION

Thermal insulation materials - an important element of energy saving, luxury housing, conservation of ecological stability. Currently in the field of energy many kinds of thermal insulation materials are used, like domestic and foreign manufacturers. However, the used materials are not sufficiently effective, they have a short lifespan, are not subject to dismantling and do not ensure compliance of normative losses. And also do not meet the requirements, which are characterized by low value of thermal conductivity and good mechanical properties, for example, such as resistance to vibration loads. Some of these drawbacks led to the development of a new type of heat insulating coating - the thin-film insulating coating. This type of insulation material has a number of advantages, in which other kinds of thermal insulation coatings are inferior to him. In most cases, the manufacturers companies in evaluating the thermal conductivity of the insulating material do not take into account effects of mechanical characteristics, including vibratory loads. This affects on the above permitted heat loss during the operation of thermal power equipment and pipelines. However, the specific dependency of effects of vibration on insulating properties of thin-film insulating coatings have not been in the technical literature. In this article you can see the advantages of using the THIC for the protection of power equipment and pipelines.

This study was supported financially by the Ministry of Education and Science of the Russian Federation under agreement no. 14.577.21.0119 dated October 20, 2014 ("Development of a Novel Insulation Structure for Heat Protection of the Equipment Operated at Temperatures up to

700°C," unique applied research identifier RFMEFI57714X0119)."

## II. DESCRIPTION OF EXPERIMENTAL SAMPLES AND INSTALLATIONS

The effectiveness of using of any heat insulation material is based on the result of its physical characteristics. The air is known to be a poor conductor of heat, so most of the insulating material contains a lot of air or gas, which is also a poor conductor of heat. The thin-film heat insulating coating (THIC) are created by using vacuum-processed hollow microspheres or gas-filled microspheres and various binder [1]. Production of experimental samples of THIC was carried out manually, insulating mixture which based on an inorganic binder and microspheres put in conductor. For the manufacture of experimental samples for the vibration test must be: a mixture of thermal insulation based on glass hollow microspheres brand K-25 and aluminophosphate binder with a ratio of 12: 1 by volume. continuity and uniformity of the insulating layers must be provided.

Prepared samples measuring  $100 \times 100 \times 12$  are fastened to the metal plates by special adhesive composition. In this paper we were investigated the mechanical and thermal properties of THIC-based glass hollow microspheres brand K-25 before and after exposure to vibration by a vibration table SignalStar Scalar, model V400LT / DSA1-2K.Ser.№3654, made by Data Physics Corporation, USA. The principle of operation is based on giving reciprocating oscillation in the vertical plane of the platform of vibration table and fixed on its production equipment (in our case it is a metal substrates on which the test specimens are fixed). Vibration table works in conjunction with additional equipment, such as: informational ABACUS converter, uninterruptible power supply and a PC. Also, measuring scales were used in the experiments, on which the weighing of samples were conducted for the analysis of the influence of random factors, as well as before and after testing the effects of sinusoidal vibration. Before and after the Vibration test the thermal conductivity of samples was measured by measuring of a stationary heat flow by method plate.

### III. EXPERIMENTAL RESEARCH

Modern requirements for thermal insulation coatings are characterized not only by the low value of thermal conductivity, and high mechanical properties, resistance to alternating loads and vibrations. In the course of the research we determined the value of the thermal conductivity before and after exposure to vibration loads, and also the products were examined for the presence of damage. Selection of test parameters is based on selecting a group of mechanical performance of products, in consequence of which the selected one or another mode of vibration tests. Selection of groups depends on the location and area of application of articles. Groups of mechanical performance of the products is determined in accordance with GOST (State All-Union standard) 30631-99 [2]. The selected group of mechanical performance is indicating on choose one or the other mode of vibration tests. Insulating constructions based on THIC are designed for high temperature power equipment and pipelines, respectively, groups of mechanical performance M5 and M2 are the most suitable [2], which involve work of the equipment and piping under the conditions defined for them, namely: The test was performed on 10 samples at a frequency 100 Hz at an amplitude of displacement of at least 0.5 mm for 6 hours. Samples were tested on vibration loads under normal climatic conditions: air temperature from 21 to 23 °C, relative humidity of air 25 to 38%, atmospheric pressure 93 to 101 kPa.

Samples were installed on vibration table in a horizontal position which characterizes the approximate position of exploitation.

### IV. RESEARCH RESULTS

Thermal insulation construction shall provide the normative level of heat loss of power equipment and pipelines, safe temperature of their outer surfaces for the human, the required parameters of coolant during operation. As a result of tests, the values of thermal conductivity for THIC before and after impact to vibration loads were obtained. The values of the thermal conductivity before the impact of vibration loads are next:

THIC based on aluminophosphate binder  $\lambda = 0,05 \text{ W} / (\text{m} \cdot {}^\circ\text{C})$ .

Mineral wool  $\lambda = 0,049, \text{W} / (\text{m} \cdot {}^\circ\text{C})$ .

After impact of vibration loads:

THIC based on aluminophosphate binder  $\lambda = 0,05 \text{ W} / (\text{m} \cdot {}^\circ\text{C})$ .

Mineral wool  $\lambda = 0,064 \text{ W} / (\text{m} \cdot {}^\circ\text{C})$ .

It was found that the thermal conductivity of THIC remained unchanged, while the coefficient of thermal conductivity in mineral wool increased by 30%.

Also, there was obtained their visual characteristic, which showed that all the samples of heat-insulating material able to withstand the destructive action of vibration at a frequency of 100 Hz and a displacement amplitude of not less than 0.5 mm for 6 hours. In order to compare the efficiency of heat-insulating material the calculation of insulation layer thickness was made for constructions before the impact of vibrations and after it. Was made the calculation of the thickness of thermal

insulating coatings on the basis of mineral wool as the most commonly used material, the results of which revealed that the required thickness of the thermal insulating layer of THIC 10-30% less than the thickness of the insulating layer based on mineral wool [3].

### V. CONCLUSION

After analysis of the existing kinds of thermal insulation coatings relevance was found in the development of new thermal insulation layer on the basis of the microspheres, after which a method for a determination the effectiveness of thermal insulation coatings with exposed to vibration loads was proposed.

After conducting experimental studies it was found that the thermal conductivity of the mineral wool after the vibration has increased by 30%, while the coefficient of thermal conductivity of THIC remained unchanged.

A calculation of thick insulation layer of structures based on THIC and mineral wool was made. According to results of the calculation it was shown that the required thickness of thermal insulation layer of THIC for the energy equipment and piping exposed to vibration loads is 10-30% less than the thickness of the insulation based on mineral wool. It shows the efficiency of THIC thermal insulation constructions.

### REFERENCES

- [1] Loginova N.A «Determining the efficiency of thin-film heat insulating coatings applied to heating systems». Dissertation.
- [2] GOST (State All-Union standard) 30631-99.
- [3] SNiP 41-03-2003. "Thermal insulation of equipment and pipelines".

# Application of Passive House Modeling Software to Design Residential and Public Buildings

I. Kalyakin, A. Ashikhmina, I. Sultanguzin<sup>1</sup>, A. Fedyukhin, Yu. Yavorovsky

Dept. of Industrial Heat Power Engineering Systems

National Research University "Moscow Power Engineering Institute"

Moscow, Russia

SultanguzinIA@mpei.ru<sup>1</sup>

**Abstract — An alternative method of modeling residential and public buildings is introduced in this paper. Topicality of the developing passive house conception for conditions of Russian climate using designPH and PHPP software is represented.**

**Keywords — residential and public buildings; passive house; designPH and PHPP; mathematical modeling; energy efficiency.**

## I. INTRODUCTION

Nowadays a problem of energy efficient houses design is of current importance and requires a systemic approach. The highest standard for such kind of buildings – a passive house, which basic criteria are: specific space heating demand up to 15 kWh/(m<sup>2</sup>a), total primary energy rate up to 120 kWh/(m<sup>2</sup>a) [1,2]. There is still no passive house in Russia, but principles, components and design methods are already in use in some new buildings. Usually the use of separate components doesn't help to achieve this standard. A detailed design based on use of all components together allows to achieve a passive house standard.

## II. TOPICALITY

The mathematical model helps us to connect all components of building energy system: source, consumer and connections between them. A modeling energy efficient houses in PHPP (Passive House Planning Package) and designPH software allows not only to estimate an energy balance of the building, but, more over, take into account geometrical characteristics, eliminate thermal bridges, which is quite actual for the considered construction industry, where we have a large variety of architectural solutions.

PHPP is a multipurpose tool, which can be used both in residential and public buildings. The canteen of International Children Centre «ARTEK», which is located in the Crimea, can be considered as an example of public building. The task was to make a reconstruction with the purpose of its year-round exploitation. A set of energy – saving procedures was suggested: a combined use of heat pumps in «floor heating» and «ceiling cooling» systems, solar collectors and sewage water heat recovery for hot-water supply, external walls and roof insulation, modern glazing and ventilation system with heat recovery.

As a result, calculations using traditional method showed, that space heating demand can be decreased by 50%, hot-water supply by 33%, ventilation by 80% and air cooling demand by 60%.

PHPP allows to get more accurate values of energy demands of the canteen energy system taking into account transmission heat losses, constructive properties and climate of building location.

## III. COMPARRISON WITH TRADITIONAL METHOD

Requirements to thermal protection and energy consumption are getting more severe year by year. At the same time technological progress doesn't stand still. A new, more efficient materials and equipment are being developed and that is why energy parameters values (thermal conductivity, specific space heating demand, etc.) don't coincide with standard values, while traditional calculating methods for heating demand don't give us correct results of low energy consuming buildings analysis [3]. In this situation the mathematical modeling is required. And it is necessary to make an optimization of selection of energy equipment (heat pumps, combined extract and input ventilation with heat recovery, solar collectors and cell panels, etc.) and heat - insulating materials.

## IV. CONCLUSION

It is necessary to achieve the passive house standard or, at least, get near to it when designing new or reconstructing old buildings. It will help to decrease operating costs due to contraction of energy resources, while investment costs increase comparatively low.

## REFERENCES

- [1] Feist V. The main theses of passive house design. – M.: LLC «KONTI PRINT», 2015. – 144 p.
- [2] Pilipenko A.O. The development of theoretical and practical bases of the passive house conception // Architecture and construction. – № 1. – 2014.
- [3] Elokhov A.E. Passive houses. Comparative analysis of calculation methods // High technology buildings. – Summer 2013. – P. 36 – 44.

# Scientific Center «Wear Resistance» of National Research University «MPEI»

A.V. Ryzhenkov

Scientific Center «Wear resistance»  
Moscow Power Engineering Institute  
Moscow, Russia  
ryzhenkovav@mpei.ru

**Abstract -** The National Research University "Moscow Power Engineering Institute" scientific center "Improving wear resistance and reliability of the power equipment of thermal and electrical power stations" (short SC "Wear resistance") has been existing at since 1995. The main activity of the Research Center is to create conditions for effective development and implementation of innovative technologies to improve reliability and life-time of heat engineering and other equipment for the fuel and energy complex and its units such as turbines, compressors, stop-regulating valves, pumps, heat exchangers, piping tubes, etc.

**Key words -** Scientific Center, MPEI, effective, thermal power plant, heat supply system, wear resistance, erosion, corrosion.

## I INTRODUCTION

At present the staff of The Scientific Centre "Wear resistance" consists of more than 100 employees including professors (2), PhD (sci) (2) and candidates (14), scientific researcher (12), engineers (67), postgraduates (7) and masters.

In 2005, for the successful results in researching, developing and implementation of high technologies improving life-time and reliability of equipment into the Russian energy sector our colleagues were awarded with the Russian Federation Government Prize in Science and Technology field.

The Scientific Center has a modern, unique scientific research and testing platform. The installed equipment permit to solve the following tasks:

- to study properties of structural material surfaces;
- to develop effective methods and techniques of hardening;
- to perform micro- and nano-composite saving coatings which as a whole essentially change properties traditional structural materials; with that both life-time of units is increased and their effectiveness is grown as well.

The Scientific Centre "Wear resistance" actively cooperates with young scientists (students, postgraduate from other universities), which are involved in the scientific and technical seminars, conferences, exhibitions and R & Ds.

## II SCIENTIFIC CENTER ACHIEVEMENTS

On the base of new developed techniques and instrumentation and equipment the following achievements were reached:

- increase of the erosion, abrasive, cavitation resistance of turbin main elements , boilers, pumps, stop-regulating valves etc., not less than 3 times.;

- almost complete stopping of corrosion processes in the paths of heating equipment and also heating and water supply systems;

- removing accumulated deposits and preventing the accumulation of new ones over the paths of TPP and NPP equipment and heat supply systems as well;

- reduction of hydraulic resistance of equipment and pipelines in the water transport systems and carbohydrates by 30 ÷ 40%;

- reduction of adhesion level of ice and frost on the metal surfaces, which improves heat transfer equipment effectiveness up to 40%, and also to decreases ice mass accumulation by 90%;

- removal of heat losses to the normative values, grow of energy efficiency and life-time (not less than 1.5 times) for heat transfers and TPP equipment and also heat supply systems on the bases of application of the developed thin-film thermal insulation coatings.

## III PROVEN TECHNOLOGIES

Under performing different tasks and R&Ds the following technologies were tested and proven:

- Technology of protecting the steam turbines blades from erosion, based on using micro- and nanoscale modifications of functional surfaces.
- Technology of improving energy efficiency and reliability of heat and water supply system in operating (SAW technology) (figure 1, 2).



Figure 1. Drops of water on the metal surface after SAW technology.

#### IV CONCLUSION

In conclusion it necessary to underline that SC is a modern institution of innovative technologies platform for research and development in the Russian energy sector. Besides this SC gives opportunities to students to reach progress and success in their scientific carrier.



Figure 2. Mobile unit using to treat pipeline systems.

- The technology of reducing the heat power equipment losses on the basis of using the structured thin film thermal insulation coatings.
- Technology of increasing the power unit efficiency, based on reforming film condensation into drop type one.
- Technology of increasing stop valves operation ability, based on the use of wear-resistant coatings.
- Technology of improving the tribological characteristics of the heat power equipment functional surfaces on the basis of "slippery" coatings (figure 3).



Figure 3. Industrial issue turbine blades with "slippery" coating.

- Technology of the effective protection of the heat power equipment from atmospheric corrosion during repairs and long downtimes.
  - Combat technology to the phenomena of icing on the elements of electric and thermal power equipment.
  - Technology of energy consumption reducing for operating pumps in pipeline systems.
  - Technology of electric power producing on the basis of the pipelines system overpressure recovery.
  - Technology of preventing the icing phenomena of electric and thermal power equipment elements.

# Die Energiewende in Deutschland – Ziele und Status Quo-Analyse

D. Großmann

Brandenburgische Technische Universität Cottbus –  
Senftenberg, Fachgebiet Management regionaler  
Energieversorgungsstrukturen, Deutschland  
[doreen.grossmann@b-tu.de](mailto:doreen.grossmann@b-tu.de)

M. Nagel

Brandenburgische Technische Universität Cottbus –  
Senftenberg, Fachgebiet Management regionaler  
Energieversorgungsstrukturen, Deutschland  
[marius.nagel@b-tu.de](mailto:marius.nagel@b-tu.de)

**Abstrakt**— Mit dem Energiekonzept hat die Bundesregierung im Jahr 2010 die Energiewende in Deutschland eingeleitet. Die deutschen Energie- und Klimaschutzziele sehen eine deutliche Reduzierung der Treibhausgasemissionen vor; geplant ist eine Reduzierung um 80 % bis zum Jahr 2050 (im Vergleich zum Basisjahr 1990). Um dies erreichen zu können, soll einerseits die Energieeffizienz gesteigert und andererseits erneuerbarer Energien verstärkt genutzt werden. Erste Erfolge der festgelegten Instrumente zur Zielerreichung sind bereits derzeit erkennbar. Im Jahr 2014 wurde die elektrische Energie bspw. zu 25 % aus erneuerbaren Energien erzeugt; im Verkehrsbereich sank der Endenergieverbrauch pro Personenkilometer um ca. 35 % von 1990 bis 2013. Auch beim Wirtschaftswachstum kann eine Entkopplung vom Energieverbrauch festgestellt werden.

**Keywords**—Energiewende, Energieträger, Energieverbrauch, Importabhängigkeit, Deutschland

## I. EINLEITUNG

Mit dem Energiekonzept hat die Bundesregierung im Jahr 2010 einen mittel- bis langfristigen Umbau der Energieversorgungsstrukturen beschlossen [1]. Ziel ist eine „zuverlässige, wirtschaftliche und umweltverträgliche Energieversorgung“ zu sichern [1]. Dabei ist das Hauptziel der deutschen Energie- und Klimapolitik die Treibhausgasemissionen um 80 % bis zum Jahr 2050 im Vergleich zum Basisjahr 1990 zu reduzieren. Um dies zu erreichen, wurden verschiedene Teilziele definiert, die den Weg bis zum Jahr 2050 zeichnen sollen. Eine Ursache für den beschlossenen Umbau war die Feststellung, dass im Jahr 2010 die deutschen Treibhausgasemissionen zu 80 % durch die Energieerzeugung verursacht wurden. Dieser Beitrag erläutert die von der deutschen Bundesregierung im Jahr 2010 beschlossenen Teilziele des Energiekonzeptes und beleuchtet den Energieverbrauch nach eingesetzten Energieträgern und stellt die Importabhängigkeit Deutschlands in der zeitlichen Entwicklung dar. Abschließend werden die Teilziele des Energiekonzepts dem derzeitigen Status Quo gegenübergestellt.

## II. TEILZIELE DER DEUTSCHEN ENERGIE- UND KLIMAPOLITIK:

Der Umbau der Energieversorgung in Deutschland wird auch als Energiewende bezeichnet. Die Energiewende basiert auf zwei Elementen: der Erhöhung der Energieeffizienz und dem Einsatz von Erneuerbaren Energien. Eine wichtige Voraussetzung für das Gelingen der Energiewende ist allerdings, dass die Energiepreise wettbewerbsfähig bleiben und ein hohes Wohlstandsniveau gesichert wird [1]. Folgende Teilziele wurden zur Minderung der Treibhausgasemission festgelegt [1]:

1. Reduzierung der Treibhausgasemissionen (gegenüber 1990) um bis zu -40 % bis zum Jahr 2020 und -55% bis zum Jahr 2030,
2. der Anteil Erneuerbarer Energien soll am Bruttoendenergieverbrauch 18 % bis zum Jahr 2020; 30 % bis zum Jahr 2030 und 60 % bis zum Jahr 2050 betragen;
3. der Anteil Erneuerbarer Energien soll am Bruttostromverbrauch 35 % bis zum Jahr 2020; 50 % bis zum Jahr 2030 und 80 % bis zum Jahr 2050 betragen,
4. Verringerung des Stromverbrauchs (gegenüber 2008) um 10 % bis 2020 und 25 % bis 2050;
5. Verringerung des Endenergieverbrauchs im Verkehr (gegenüber 2005) um 10 % bis 2020 und 40 % bis 2050;
6. Verringerung des Primärenergieverbrauchs (gegenüber 2008) um 20 % bis 2020 und 50 % bis 2050;
7. Steigerung der Endenergieproduktivität jährlich um 2,1 %
8. Steigerung der Sanierungsrate von Gebäuden von derzeit weniger als 1 % pro Jahr auf 2% pro Jahr

## III. ENERGIEVERBRAUCH IN DER ZEITLICHEN ENTWICKLUNG:

Der nächste Abschnitt geht folgenden Fragen nach:

1. Welcher Energieträger wird zur Energieerzeugung in Deutschland am häufigsten genutzt?
2. Wie sind die Voraussetzungen Deutschlands zur Erreichung der Ziele des Energiekonzeptes?
3. Ist bereits eine Änderung der Energieträgerzusammensetzung erkennbar?

Nachfolgend werden der End- und der Primärenergieverbrauch nach Energieträgern in der zeitlichen Entwicklung betrachtet. Zunächst werden jedoch die Begriffe End- und Primärenergie kurz definiert.

Endenergie ist die Energieform, die Endverbraucher beziehen, um ihre gewünschten Bedürfnisse oder Ziele (warmer Raum, warmes Wasser oder Strom um fernzusehen) decken zu können. Endenergie ist i.d.R. bereits mehrfach umgewandelt und gelangt in direkt nutzbarer Form (bspw. als Fernwärme, Heizöl oder Strom) zu den Verbrauchern.

Primärenergie hingegen ist die Energieform vor jeglichem Umwandlungsprozess; hier liegt der Energieträger in seiner natürlichen Form vor, bspw. das Roherdöl in seiner natürlichen Umgebung. Der Aufwand für die Gewinnung, dem Transport, der Aufbereitung der Primärenergieträger bis hin zum nutzbaren Endenergiträgern wird mit festgelegten Primärenergiefaktoren berücksichtigt. Die verbrauchte Endenergie wird mit Primärenergiefaktoren beaufschlagt um den natürlichen (Primär)Energiegehalt der genutzten Endenergiträger rechnerisch zu erhalten.

Im Jahr 1990 wurden 9.473 PJ Endenergie in Deutschland verbraucht, die zu 42 % aus Erdöl, 20 % aus Gasen (Erdgas und Naturgasen), zu 17 % aus Strom, zu 9 % aus Braunkohle, zu 6 % aus Steinkohle und zu ca. 2 % aus Erneuerbare Energien erzeugt wurden [2]. Im Jahr 2013 betrug der Endenergieverbrauch mit 9.269 PJ nur unwesentlich weniger als 1990 [2]. Allerdings änderte sich die Zusammensetzung der zur Erzeugung genutzten Energieträger. Der Anteil an Erdöl, Braunkohle und Steinkohle verringerte sich (Erdöl 37 %, Braunkohle 1 %, Steinkohle 4 %); dafür stieg die Nutzung an Gasen, Strom und Erneuerbaren Energien an (Gasen 27 %, Strom 20 % und Erneuerbaren Energien 6 %) [2].

Im Gegensatz zum Endenergieverbrauch kann bei der Primärenergie eine stetige Reduzierung des Energieverbrauchs seit 1990 festgestellt werden. So betrug im Jahr 1990 der Primärenergieverbrauch 14.905 PJ; im Jahr 2014 waren es hingegen nur 13.076 PJ [2]. Auch die Zusammensetzung der Primärenergieerzeugung veränderte sich. Der Anteil an Mineralölen stagnierte bei 35 %. Auch der Einsatz der Steinkohle blieb relativ unverändert (15 % 1990 und 13 % 2014) [2]. Die Nutzung von Braunkohle und Kernenergie sank (Braunkohle von 21 % auf 12 % und Kernenergie von 11 % auf 8 % vom Jahr 1990 zum Jahr 2014) [2]. Zugenommen hat hingegen die Nutzung von Erdgas und Erneuerbaren Energien (Erdgas von 15 % auf 20 % und Erneuerbaren Energien von 1 % auf 6 % vom Jahr 1990 auf 2014) [2].

#### IV. IMPORTABHÄNGIGKEIT IN DER ZEITLICHEN ENTWICKLUNG:

Deutschland musste im Jahr 2013 71 % der zur Primärenergieerzeugung notwendigen Energieträger importieren; 1990 betrug der Anteil lediglich 57 % [2]. Ein Grund für die Erhöhung der Importabhängigkeit ist die Verringerung des inländischen Steinkohleabbaus. Wurden im Jahr 1990 nur 8 % der Steinkohle importiert, waren es 2013 bereits 87 %. Mineralöl und Kernenergie werden fast vollständig importiert. Auch Gase werden größtenteils importiert (2013 zu 87 %). Lediglich beim fossilen Energieträger Braunkohle kann Deutschland auf ausreichende inländische Ressourcen zurückgreifen.

#### V. STATUS QUO DER ENERGIEWENDE:

Beim Vergleich des Endenergieverbrauchs und des Bruttoinlandsprodukts in der zeitlichen Entwicklung konnte festgestellt werden, dass sich das Wirtschaftswachstum vom Endenergieverbrauch entkoppelt hat.

Der Endenergieverbrauch pro Bruttoinlandsprodukt reduzierte sich stetig, so sank dieser von 4,8 GJ/ 1.000 € im Jahr 1990 auf 3,9 J/ 1.000 € bzw. 3,4 GJ/ 1.000 € in den Jahren 2000 und 2013 ab [3]. Dieser Trend bestätigte sich auch beim Primärenergieverbrauch pro Bruttoinlandsprodukt.

Ebenso konnte ein Rückgang des Endenergieverbrauchs von 1990 bis 2013 im Bereich der Haushalte (von 859 MJ auf 665 MJ pro m<sup>2</sup> Wohnfläche) sowie im Verkehrssektor (von 55 MJ auf 34 MJ pro 100 zurückgelegte Personenkilometer) [3] festgestellt werden.

Auch eine Zunahme des Anteils Erneuerbarer Energien konnte in allen Verbrauchssektoren verzeichnet werden. Als Zwischenziel legte die Bundesregierung ein Anteil von 18 % am Bruttoendenergieverbrauch im Jahr 2020 fest; im Jahr 2013 betrug dieser bereits 12 % [4]. Der hohe Anteil an

Erneuerbaren Energie beim Endenergieverbrauch wird dominiert durch die Stromerzeugung. Im Jahr 2013 wurden bereits 25 % der elektrischen Energie durch Erneuerbare Energien erzeugt; im Jahr 2020 sollen es jedoch mindestens 35 % sein [4]. Beim Wärmeverbrauch wurden 2013 lediglich 9 % durch Erneuerbare Energien erzeugt. Noch geringer ist der Anteil im Verkehrssektor, hier waren es nur 6 % [4].

Der **Primärenergieverbrauch** pro Einwohner sank von 1990 von 187 GJ/Einwohner auf 171 GJ/Einwohner im Jahr 2013 ab [4]. Dies spiegelte sich auch bei den Treibhausgasemissionen wider. Im Vergleich zum Jahr 1990 sanken die Treibhausgasemissionen um 23 % ab; dadurch wurden 2013 220 Mio. t CO<sub>2</sub>-Äquivalente weniger emittiert wie 1990 [2]. Pro Einwohner reduzierte sich der Treibhausgas-ausstoß von 1990 bis 2013 um 27 % und ging von 16 auf 12 t CO<sub>2</sub>-Äquivalente zurück. Im Jahr 2020 sollen die Treibhausgasemissionen gemäß dem Energiekonzept der Bundesregierung um 40 % zum Vergleichsjahr gesunken sein [4].

#### VI. FAZIT

Mit dem Energiekonzept hat die Bundesregierung im Jahr 2010 ambitionierte Energie- und Klimaschutzziele festgelegt, die zu einem grundlegenden Umbau der Energieversorgungsstrukturen führt bzw. noch führen wird. Die Energiewende hat bereits begonnen; erste Erfolge sind sichtbar bspw. bei der Reduzierung der Treibhausgasemissionen oder dem Anteil an Erneuerbaren Energien bei der elektrischen Energie.

Auch im Bereich des Wärmeverbrauchs nimmt der Anteil an erneuerbaren Energien stetig zu; allerdings liegt dieser noch deutlich unter dem Anteil der elektrischen Energie. Beim Wärmeverbrauch dominiert die Gebäudewärme (Raumwärme und Warmwassererzeugung). Bei bestehenden Immobilien, die sich zum Größenteil in Privatbesitz befinden, setzt die Bundesregierung nicht auf die Durchsetzung von Ordnungsrecht zur Reduzierung des Endenergieverbrauchs, sondern auf Aufklärung durch Beratungsangebote und Anreizsetzung zur Förderung von Sanierungsmaßnahmen. Lediglich im Neubaubereich muss geltendes Recht eingehalten werden. So schreibt das Erneuerbare-Energien-Wärmegeetz (EEWärmeG) die Nutzung eines gewissen Anteils an Erneuerbarer Energien zur Wärmeerzeugung vor.

Damit die festgelegten Energie- und Klimaschutzziele der Bundesregierung eingehalten werden können, sind verstärkte Anstrengungen nötig. Besonders der Bereich der Effizienzsteigerung bietet ein enormes Potential, das bisher mit den gewählten Instrumenten der Bundesregierung zur Umsetzung der Energiewende zu wenig Beachtung geschenkt wurde.

#### REFERENCES

- [1] Bundesregierung (2010): Energiekonzept für eine umweltschonende, zuverlässige und bezahlbare Energieversorgung.
- [2] BMWi (2015): Bundesministerium für Wirtschaft und Energie: Energiedaten. Nationale und Internationale Entwicklung. Stand: 19.05.2015, Berlin.
- [3] AGEB (2015): AG Energiebilanzen e.V.. Auswertungstabellen zur Energiebilanz Deutschland. 1990 bis 2014. Stand: August 2015.
- [4] BMWi (2014): Bundesministerium für Wirtschaft und Energie: Die Energie der Zukunft. Erster Fortschrittsbericht zur Energiewende, Stand Dezember2014,Berlin

# Structurally Weak Areas Benchmark Energy Distribution Networks Based on Statistical Analysis

M. Plenz<sup>1</sup>, K. Lehmann

Brandenburg University of Technology, Electrical Power Systems

Großenhainer Str. 57, 01968 Senftenberg, Germany

[maik.plenz@b-tu.de](mailto:maik.plenz@b-tu.de)<sup>1</sup>

**Abstract**—A statistical simplification of existing distribution grid over several voltage levels based on different statistical network models allows immediate identification of possible energy feed-in areas (or self-sufficient areas) and critical parts of energy supply system in low voltage (LV) or medium voltage (MV) areas in Eastern Germany. This work presents this new model approach in the context of structurally weak areas.

**Keywords**—structurally weak areas; statistical distribution grid model; energy supply system.

## I. INTRODUCTION

The German energy policy is driven by three major concerns: the supply reliability, economic efficiency and environmental impact. Another aim is lowering the energy consumption about 25 % as well as adjusting the energy system to renewable energy generators until 2050. Decentralized power generation, short-time energy self-sufficient areas or so-called virtual power plants are major challenges of the distribution system operators.

Reference grid models or a statistical simplification of existing distribution grid allows identification of the static condition of distribution network systems. This enables distribution system operators or planner to fast extract critical grid areas as well as to give an estimated active power flux. The focus of this paper on structurally weak areas is based on the high ratio of renewable energy production to low demand in Eastern Germany.

## II. MODEL DESIGN AND THEORETICAL APPROACH

At first the compiled method or model is classified among existing traditional supply grid models. The definition of structurally weak areas forms the second part of this section.

### A. Traditional Network Models

There are several traditional methods to simplify energy supply network. The necessity concerning reduction of existing complex energy supply network originates from the following reasons:

- The vast computational and human resources need to evaluate and analyse the complete network structure of distributional grid with its operating equipment.
- The time invariant network structure caused by constant changes due to load and power production variations.

Within this contribution regarding their different models, which are classified by their grade of complexity, a new model is planned. Next to existing Case-By-Case-Analysis [1], these basic network models can be categorised into two classes: the real parameter based models (represented by artificial network models [2], synthetic network models [3] and reference networks [4], [5]) and abstract models (e.g. [6]). In general all models following the target of network simulation is to analyse the systems' behaviour due to parameter changes.

The planned network model based on statistical analysis (called sdg-models: statistical distribution grid models) and combines the benefits of all models in a way of statistical

analysis and optimization, especially for structurally weak areas.

The main contrast to previous research can be found in several numbers of parameters, the complexity of the model, the implementation of the medium-voltage level and the aim of the following research.

### B. Structurally weak areas

The research focus of this work can be retrieved in the distribution grid of Eastern Germany (especially Saxony, Brandenburg, Thuringia). These federal states are universally characterized as structurally weak regions in Germany. A coherent standard and comparable definition or limitation in terms of weak structured in general or specific structurally weak areas are not uniform available in literature. The terminology is rather used as a mono-causal argument for the implementation of certain development ideas. According to sources [7], [8], structurally weak areas show a number of characteristics:

- low regional economic performance and low GDP / head,
- high rate of unemployment combined with lower qualification level of unemployed people or workers,
- low innovative capacity, defined by a lesser extent distinctive research and development intensity, resulting in low number of R & D employees,
- limited social capital and below-average wealth,
- low private household incomes (with impact on purchasing power),
- lots of under-capitalised local authorities and companies and
- monostructural regional economic and corporate landscape.

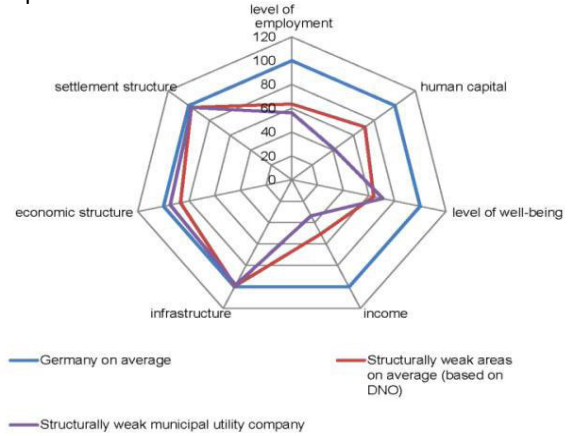


Figure 1: Comparison of Germany, the analysed structurally weak areas and an exemplary municipal utility company in structurally weak areas (based on datasets starting in 2012)

Some indicators listed above are quantitatively occupied with current information. Figure 1 shows all of these indicators, which establish the classification of regions in these structurally

weak areas. Therefore the selection refers to the quantitatively detectable information. Qualitative indices are completely eliminated due to lack of opportunities for comparison. The transformation of notions into quantitative magnitudes and information took place within the framework of existing research.

### III. STATISTICAL MODEL AND RESULTS

In order to allow a statistically significant amount of structurally weak network areas, 20 rural area-, 21 village-, 20 small town- and 9 city- low voltage and medium voltage grid structures have been recorded, analyzed and evaluated on basis of 37 parameters, for example inhabitants per household connections, (figure 2), apparent power of the station (S), outgoing feeders, amount of overhead lines, wire cross-section of household connections, building floor area and load distribution factor.

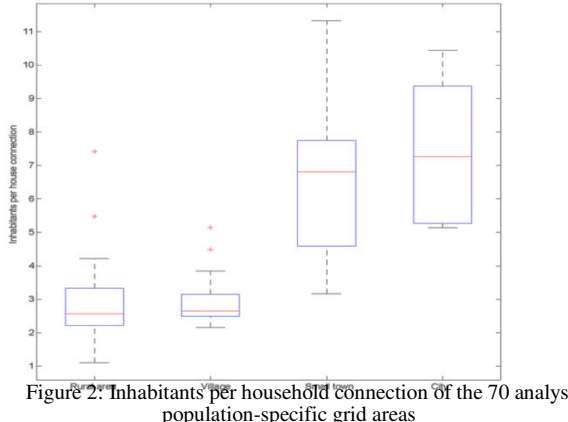


Figure 2: Inhabitants per household connection of the 70 analysed population-specific grid areas

The load distribution factor defines the positing of a synthetic or equivalent load on feeders (starting on low/medium voltage substation), which approximate the cumulated feeder load. That describes the distribution of nodes (section nodes  $K$ , general cable impedance  $R$ ,  $l_n$  length of the feeder segment and  $R'_n$  - cable impedance of the feeder segment) on grid radiation segment and summation of connected homogeneous loads or generations.

$$\varepsilon = \frac{1}{K \cdot R} \sum_{k=1}^K \sum_{n=1}^k R'_n \cdot l_n \quad (1)$$

$$\varepsilon = \frac{1}{K \cdot l_S} \sum_{n=1}^K l_n \quad (2)$$

Equitation 2, short form of (1), adjusted by assumptions that  $R$  is described by  $R'_n$  and the section length  $l_S$ . With a mean and a standard deviation ( $\varepsilon \pm \sigma$ ) between  $0.57 \pm 0.065$  (rural) and  $0.59 \pm 0.076$  (city), the load distribution factor illustrates a relatively homogeneous equivalent load in the middle of the feeder.

These parameters describe both the energy related and geographically/ structural occurrences of the regions and the associated networks. The development process of these statistical distribution grid models for low and medium voltage level use geo-information systems and databases of the network operators involved. The formation of statistical distribution grid models is based in the use of the arithmetic mean. In addition cluster analysis and neuronal networks are integrated to optimize the approach applied. The real representation of the sdg-models strongly depends on the 37 network parameters.

Some example results of the LV-/MV-grid analysis are shown in table 1.

Table I: Characteristics of network operation resources

Voltage level	Grid characteristics		
	Network operating resource	Characteristic I	Characteristic II
LV	Cable	NAYY 4x120 mm <sup>2</sup>	Length = 0.5 km
LV	Transformer	S = 0.4 MVA	4-7 outgoing feeders
MV	Cable	NA2XS2Y 3x1x150 mm <sup>2</sup>	Length = 5 km
MV	Transformer	S = 31.5 MVA	Length ≈ 40 km (section)

In conclusion the development of the resulting sdg-models allows:

- Low – voltage: four population-specific classes, each with a sdg-model
- Medium – voltage: one average sdg-model with 3 statistical variations by the reference parameter ("distance of transformer connection")

### IV. CONCLUSION

The chosen model network approach provides a detailed picture of the average LV / MV grids in the investigated areas. These statistical distribution grids (of the structurally weak areas) are the first reference grids, which describes the complete areas of one national DNO (Distribution Network Operator). Sensitive tests with future load reductions and share of renewable energies shows different effects in the sdg-models. It can be noted that the deviations from the voltage band of the LV networks can be found in rural or village networks, with long feeders and transformer with low apparent power stats. The medium voltage level recorded a different overloading level of grid equipment, however in slightly linked networks with increased central renewable supply. To optimize the results, extreme value networks are formed, which have a strong focus on maximum feed-in of renewable energies and minimal (resources technically) equipped distribution networks. A specific PowerFactory algorithm that analyses the correlating influence of the 37 parameters on the results of dynamic network calculations is also planned in the future.

### V. REFERENCES

- [1] T. Lühn et al. "Multi-Criteria Analysis of Grid Expansion Concepts on the Low Voltage Level," Zeitschrift für Energiewirtschaft, Volume 3, Springer Verlag, Wiesbaden, 2014.
- [2] C. Hille et al. „Technological Options for Extension of the German Distribution Network - Market Analysis and Assessment (in German: Technologieoptionen für den Verteilungsnetzausbau in Deutschland - Marktanalyse und Bewertung).“ Internationaler ETG-Kongress Berlin 2013, VDE-Verlag GmbH: Berlin, 2013.
- [3] M. Mohrmann et al. „Development and application of a database for assessing the development needs of low-voltage networks.“ In: Internationaler ETG-Kongress 2012, Berlin, VDE-Verlag GmbH: Berlin, 2012.
- [4] G. Kerber „Capacitance of Low-Voltage Distribution Networks for the feeding-in from Photovoltaic Systems“ (in German: Aufnahmefähigkeit von Niederspannungsverteilnetzen für die Einspeisung aus Photovoltaikkleinanlagen.) [doctoral thesis] Der Andere Verlag, Uelvensbüll.
- [5] CIGRE Task Force C6.04.02 “Benchmark Systems for Network Integration of Renewable and Distributed Energy Resources”, CIGRE, 2013.
- [6] J. Schumacher „Digital Simulation of Renewable Energy Supply Systems“ (in German: Digitale Simulation regenerativer elektrischer Energieversorgungssysteme.) [doctoral thesis] Universität Oldenburg, Oldenburg, 1991.
- [7] P. Cloke „Conceptualizing rurality“ In: Cloke, P.; Marsden, T.; Mooney, P. (Eds.): Handbook of Rural Studies, p. 18-28, SAGE Publications Ltd, London, 2006.
- [8] E. Engelke „Examples of sustainable regional development: Recommendations for rural areas“ (in German: „Beispiele nachhaltiger Regionalentwicklung: Empfehlungen für den ländlichen Raum“), Raabe Verlag, Stuttgart 19

# Modellierung des kombinierten Wärmeaustauschers in der Kontaktzone des Radiators und der Hüllfläche des Gebäudes

V. Glazov<sup>1</sup>, E. Klooz<sup>2</sup>, P. Vernitskas<sup>3</sup>

<sup>1)</sup> - National research University "MPEI", Moscow, Russia, [GlazovVS@mpei.ru](mailto:GlazovVS@mpei.ru)

<sup>2)</sup> - Brandenburg technical university, Cottbus, Germany, [eklooz@freenet.de](mailto:eklooz@freenet.de) ;

<sup>3)</sup> - Euroasian national university of name L.N. Gumileva, Astana, Kazakhstan, [www.bio.kz@mail.ru](http://www.bio.kz@mail.ru).

**Abstrakt:** Die Resultate der experimentellen und numerischen Studien in Heizkörperbereich. Eine Methode um die zusätzlichen Wärmeverluste auf der Wandseite hinter dem Heizkörper zu minimieren.

**Schlüsselwörter:** kombinierter Wärmeübertrag, zusätzliche Wärmeverluste, Radiator.

## I. EINLEITUNG

Zur korrekten Berechnung der installierten Heizungsleistung [1] ist es unabdingbar die Größe der zusätzlichen Wärmeverluste der sich an der Hüllflächen befindlichen Heizkörper (HK) zu kennen [2]. Die Analyse der existierenden Methoden [3, 4] zur Bestimmung der zusätzlichen Wärmeverluste, zeigt, dass jene beachtenswert sind und daher einen schmalen Anwendungsbereich haben. Diese Methoden wurden in Experimenten bestätigt [5].

Zu den mathematischen Modellen, die zur Grundlage die eingangs erwähnten Methoden haben, werden hier einige Kommentare und Bemerkungen vorgenommen:

- Der Wärmeaustausch an der Kontaktstelle des hinter dem Radiator befindlichen Bereichs (BhR) mit dem Heizkörper (HK) wird beschrieben, wie der Wärmeaustausch zwischen parallelen, flachen und isothermen Oberflächen endlicher Größe, getrennt durch eine strahlungsdurchlässige Umgebung. Die Form einiger existierender Heizvorrichtungen (z.B. Säulengusseisenradiatoren) und die Messung der Temperaturfelder der wärmeaustauschenden Oberflächen zeigt die Ungenauigkeit einer solchen Berechnungsweise auf.

- Der konvektive Anteil des Wärmestroms wird mittels empirischer Formel bestimmt. Diese Formel wird häufig bei Prozessen verwendet, die bei vertikalen Spalten auftreten. Der Raum zwischen den Säulen des Radiators und des hinter dem Radiator befindlichen Bereiches kann nur bei sehr großem Abstand als Spalt angesehen werden.

- Die Wärmeleitung durch den des hinter dem Radiator befindlichen Bereichs (BhR) wird betrachtet wie ein eindimensionaler Prozess bei stationären Bedingungen 1er und 2er Art. Die Strahlungskomponente des Wärmestromes wird linearisiert oder wie eine oberflächige Wärmequelle betrachtet. Diese Betrachtungsweise erfordert die Betrachtung nach der Normalverteilung, die leider nicht die Wärmestrahlungseigenschaften der Oberfläche berücksichtigen.

- Wärmeverluste durch die Kontaktstelle (KS) mit Zwischenböden und Fenstern werden nicht berücksichtigt, da diese in keinem Verhältnis zum BhR stehen, der bestimmt wird durch HK auf KS.

- Als erstes folgt darauf das Erfordernis dieser Methoden, zur Ermittlung der zusätzlichen Wärmeverluste über die Hüllflächen, weiter zu verbessern. Des Weiteren, solange sich in alten Häusern («Хрущевки») – diese machen ca. 50% des

gesamten Häuserbestandes in der russischen Föderation aus – die Heizkörper in Nischen der Hüllfläche mit kleinem Wärmedurchgangswiderstand befinden, erfordert es Konzepte zur Senkung der zusätzlichen Wärmeverluste in den erwähnten Gebäuden.

## II. ZIELSETZUNG

Entwicklung eines mathematischen Models zum kombinierten Wärmeaustausch in der Kontaktzone des Heizkörpers mit einer einfigen Hüllfläche. Das Modell soll den dreidimensionalen Wärmeübergang zwischen Hüllfläche und Zwischenböden, den konvektiven Wärmeübergang zwischen nichtisothermer Oberfläche des BhR und HK, sowie den Strahlungsaustausch, unter Beachtung der geometrischen und strahlungstechnischen Besonderheiten der Heizkörperoberfläche und der Hüllfläche, berücksichtigen.

Eine gegenüberstellende Analyse der Berechnungsergebnisse und des Versuches, durchgeführt in der Fensterbrettzone. Als Berechnungsinstrument dient das Modellierungsprogramm „PHOENICS“.

## III. FAZIT

1. Die Überprüfung der Resultate des mathematischen Modells zum Wärmeaustausch in der Kontaktzone BhR-HK und der experimentell gewonnenen Daten zeigt eine 7%-ige Diskrepanz im Temperaturfeld auf. Dies bekräftigt den Einfluss des „Schwarzgrades“ der Oberfläche des BhR auf die zusätzlichen Wärmeverluste in der Zone des HK.

2. Es kann eine Methodik zur Bestimmung und Senkung der zusätzlichen Wärmeverluste über den BhR mit Berücksichtigung der Form des HK und seinen strahlungstechnischen Eigenschaften, vorgeschlagen werden.

## LITERATUR

- [1] Russische Norm СНиП 41-01- Beheizung, Belüftung und Klimatisierung
- [2] Bogoslovski B.N: Bauphysik : Lehrbuch für Universitäten; 1982, S. 415
- [3] Raltschuk N.T: Untersuchung zusätzlicher Wärmeverluste in Abhängigkeit vom Aufbau der Heizkörper // Information für Bau und Architekturuniversitäten; 1984, S. 35-37.
- [4] Berschidskij G.A: Untersuchung des Einflusses der Luftströme von Heizkörpern und Lüftungsanlagen auf das Mikroklima eines Gebäudes. Thesis zum Erwerb des wissenschaftlichen Grades «Kandidat der technischen Wissenschaften», 1971
- [5] Kotljarowa N.S: Modellierung von Temperaturfeldern der Hüllfläche in der Zone des Heizkörpers. Thesis zum Erwerb des wissenschaftlichen Grades «Kandidat der technischen Wissenschaften», Rostow am Don, 1998, S-165

# Definition of Annual Efficiency Rate of the Water-water Heat Pump

A. Malakhova

Faculty for Architecture, Civil Engineering and Urban  
Planning  
Brandenburg University of Technology  
Cottbus- Senftenberg, Germany  
Anna.Malakhova@b-tu.de

H. Stopp

Faculty for Architecture, Civil Engineering and Urban  
Planning  
Brandenburg University of Technology  
Cottbus- Senftenberg, Germany  
Horst.Stopp@b-tu.de

**Abstract**— Straightforward procedure to determine the annual coefficient of efficiency of the water-water heat pump using water of artificial lake on Lusatia Lakeland is introduced.

Yearlong measurements of parameters were carried out and analyzed direct on floating object supplied with heat energy from water-water compression heat pump. Room climate of the touristic house was observed and the imperfections of comfort conditions in the summer time were determined. Economic analysis is introduced.

**Keywords**— heat pump; yearlong monitoring; efficiency rate of heat pump, water as an energy source

## I. INTRODUCTION

Implementation of the sustainable energy supply is not only the main rule for greatest energy concerns of the world, but also a significant part of regulations of developed countries today. Among them are Germany, which rate of achievement in field of renewable energies is more than impressive. According to Renewable Energy Law (EEG) and Federal Ministry for Economic Affairs and Energy of German, a part of renewable energies should run up to about 45% of the total energy generation in the country in year 2025. Specifications and requirements to sustainable applications are becoming more tightly every year.

The efficiency of heat pump application, which uses network electrical power and water of an artificial lake as low energy source to supply one of the touristic houses constructed directly on the water is considered. Coefficient of performance of heat pump compared with standard rate.

Annual rate of efficiency, which has direct influence on economics, was obtained by using of experimental approach and long monitoring with every-minute-parameters.

## II. FORMULATION

The theoretical parameter to obtain efficiency rate of heat pump may be useful only when choosing the installation. If there is existing equipment, it is advisable to define the real indicator of the efficiency of the heat pump. The following statements allow defining the instant (1), the time interval(2) and the annual (3) rate of the effectiveness according to [2]:

$$COP = \frac{Qi}{Ni} \quad (1)$$

*Qi*-instant value of produced heat energy;

*Ni*-instant value of power energy in compressor.

$$\dot{\epsilon} = \frac{Qt}{Nt} \quad .(2)$$

*Qt*-effectiveness of heat pump in time interval;

*Qt*- value of produced heat energy in time interval;

*Nt*- value of power energy of compressor in time interval.

$$JAZ = \frac{Qa}{Na} \quad (3)$$

*JAZ*-Jahresarbeitszahl (german)- the annual rate of efficiency;

*Qa*-amount of heat energy, annual;

*Na*-amount of power energy of compressor and pump of brine loop, annual.

Every minute data were obtained by carrying out the annual monitoring indicators of heat supply systems for:

- temperature of the forward and reverse heating circuit;
- temperature of the forward and reverse brine loop;
- consumption of the circulation pump brine circuit
- water consumption in the heating circuit;
- electric energy consumption in the compressor of the heat pump;
- room temperature;
- relative humidity of indoor air.

When the study of heating system of floating house, the following characteristics have been noticed:

### Advantages:

- Direct coupling to energy source
- Effective heat-mass transfer and heat removal due to properties of water comparing with using of ground as a source
- Achievement of comfortable room climate in heating season

### Disadvantages:

- Deficiency of passive cooling
- Wrong selection of heat pump meaning energy power, as a result- significant kicks in procedure behavior, run out of compressor and decrease of coefficient of performance

### III. MAIN RESULT

Calculation of efficiency of the heat pump, based on the experimental method, revealed the dependence of coefficient of transformation to the water temperature of the lake and the outside air. Moreover, the minimum rate of heat transformation ratio was about 2.0, and a maximum of 4.5. Being instantaneous, these indicators cannot fully assess the efficiency of the entire heating system for a long period.

When calculating the annual efficiency have been obtained the generated thermal energy, the consumption of electrical energy of compressor and power consumption of electrical pump of brine loop, counted via flow rates and pump load "WILO" curves provided by the manufacturer.

Calculations showed that the annual rate of efficiency is slightly lower than standard rate. Constituting 2.63 annual rate in 2015 is very different from the set 3.8. This fact has a direct impact on energy costs.

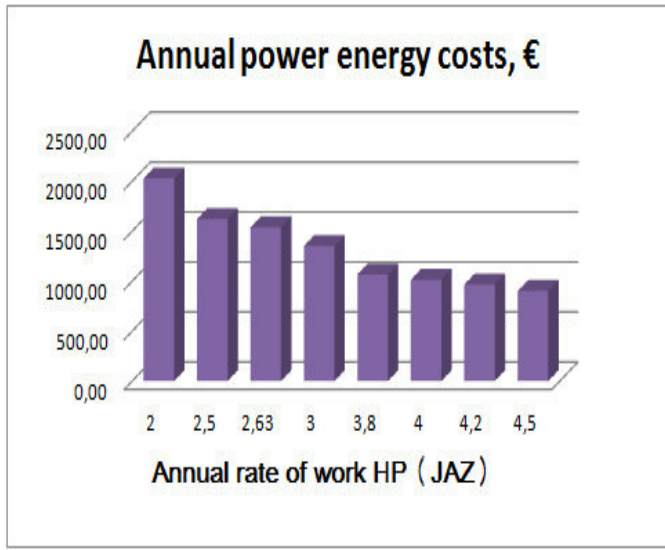


Fig.1 Dependence of annual costs of electricity on annual energy efficiency index of the heat pump

Taking the cost of 1 kW-hours of electrical energy equal to 28.81 cents for 2015, it can be received an annual cost of electricity expended heating system (energy consumption of pump in brine loop is taken into account) in value of 1539 Euro.

Recounting energy costs at standard indicators of efficiency, we get 1067 euro annually.

It is obvious that the greater efficiency of the heat pump system increases annual energy savings, and therefore energy costs. In this case, if the heat pump efficiency has been raised to the regulatory, savings would have amounted to about 500 euro per year.

The following graph shows the dependence of annual costs of electricity on annual energy efficiency index of the heat pump in the euro.

### IV. CONCLUSION

The experimental method allowed determining the annual performance of the heat pump installation. Economic analysis shows how energy costs go down with an increasing of the annual performance of the installation at least until the standard performance.

As a result of this analysis and the conclusions offered some measures to improve the energy efficiency of the installation, namely:

- Use the installation with smaller capacity
- The use of two-stage heat pump with active cooling function of the building in summer
- The intensification of heat and mass transfer processes in the submerged heat exchanger by increasing the heat transfer area.

### REFERENCES

- [1] Соколов Е.Я., Бродянский В.М. Энергетические основы трансформации тепла и процессов охлаждения. Учеб. пособие для вузов. — 2-е изд., перераб. — М.: Энергоиздат, 1981
- [2] Stefan Sobotta "PraxisWärmepumpe". 2, überarbeitete und erweiterte Auflage, DIN Deutsches Institut Für Normung e.V., Beuth Verlag GmbH Berlin Wien Zürich2015,
- [3] BMWi Energiekosten, 2015
- [4] A. Malakhova Strangfeld, P.; Stopp, H.: Optimization of two underwater heat exchangers as brine loops of Heat Pump for energy supply of floating house. XXII International Conference of students and postgraduates, National Research University (Moscow Power Engineering Institute), Moscow 2016
- [5] S. Dietzmann,B. Schmidt Messtechnische Untersuchung von Wärmeübertragern und Wärmepumpe für schwimmende Häuser am Geierswalder See unter Einbeziehung der Thermal-Response-Methode, Masterthesis, Germany 2014
- [6] X.Chen, G.Zang, J.Peng, X.Lin, T.Liu. The performance of an open-loop lake water heat pump system in south China. Elsevier, Applied Thermal engineering 26(2006) 2255-2261

# Ways to Increase the Effectiveness of Top Pressure Recovery Turbine application

V. Khromchenkov, Y. Zhigulina  
Dept. of Industrial Heat Power Engineering Systems  
Moscow Power Engineering Institute  
Moscow, Russia

**Abstract** - The paper describes methods how to increase the effectiveness of top pressure recovery turbine (TRT) application when using a wet cleaning of blast furnace gas. Three ways to increase the temperature of cool blast furnace gas before TRT are proposed.

**Keywords** - top pressure recovery turbine, saturated blast furnace gas, gas scrubbing.

## I. INTRODUCTION

Dozens of gas top pressure recovery turbines are exploited in our country and abroad today. These units use the excess pressure of blast furnace gas. The cost of electricity generated this way significantly lower than in comparison with electricity generated at TPP, and may be further reduced by improving the how of turbines themselves and their usage patterns.

Blast furnace gas used for the needs of consumers as fuel, is scrubbed, after that its temperature reduces from 200 - 300 °C to 35-40°C and it becomes saturated. The process of gas cleaning itself does not require such a reduction of the temperature. It is done only to reduce the moisture content of blast furnace gas delivered to the consumers.

When operating on cold saturated blast furnace gas the main problem is to ensure the purity of a flowing part of the turbine. This problem is solved by installing the washing system of the guide vanes of the first turbine stage, which ensures the purity of the blades.

## II. INCREASE THE TRT CAPACITY

Expansion process of the saturated gas differs much from the expansion of dry gas. It is accompanied by a continuous condensation of water vapor with release of latent heat of vaporization which is taken by the gas. The tests confirmed the results of researches on the definition influence of the saturated blast furnace gas parameters before TRT on its capacity and the temperature of the gas at the turbine output. These studies have shown [1] that the temperature increasing of saturated blast furnace gas before TRT up to 35- 40°C to 60 - 70°C leads to a significant increase in power of the turbine (15 - 20%).

There are three ways to increase the temperature of the saturated blast-furnace gas at the TRTinput: temperature rise of cooling water for gas scrubbing, the reduction of its flow rate, low parameters steam feeding at the TRTinput.

## III. FIRST METHOD

The first of these methods is simple and can be realized by complete or partial disconnection of water in cooling tower. In

this case, the economic effect of the higher gas temperature before TRT (and, as a consequence, increase the power of the turbine) increases further due to the reduction or complete elimination of energy costs for water supply to the cooling tower. The water is cooled partially or completely while staying in the radial settling tanks or while transporting.

## IV. SECOND METHOD

The second method usage is associated with a significant reduction of cooling water consumption for gas scrubbing, and consequently, this means changes of the gas cleaning way (small-size scrubbers installation), and water recirculation.

The results of the required quantity of cooling water calculations (per 1 kg of dry gas) depending on the temperature of blast furnace gas and for different pressures of blast furnace gas at the outlet of the furnace are shown in the fig. 1. As can be seen from the figure the required quantity of cooling water at the cooling scrubber decreases in 3-4 times while increasing the gas temperature from 40 up to 60-75 °C, and to a large extent depends on the gas temperature and pressure. The absolute reduction of the specific consumption of cooling water practically does not depend on the gas temperature before the gas cleaning system, and depends only on its pressure. Consequently, the economic effect obtained by reducing the electricity consumption for recycled water pumping while increasing the blast furnace gas temperature constant and its constant consumption does not depend on its temperature prior the gas scrubbing.

## V. THIRD METHOD

The third method of saturation blast furnace gas temperature at the TRTinput increasing to before does not affect devices of gas cleaning and require minor capital costs for the steam line. Its application is limited mainly by the presence of a source of steam utilization, its location and must be justified by technical and economic calculation.

Currently, many metallurgical works have a significant amount of steam at low parameters (0,25—0,4 MPa), obtained mainly in evaporative cooling systems for process equipment, blast furnace hot-blast stoves etc. This steam is often not used or has seasonal consumers (mainly in winter for heating).

Cold blast furnace gas heats when mixing with steam due to partial condensation of the vapor with release of large amounts of latent heat of vaporization. As a result of this preheating, the gas always remains saturated. As shown by calculations, the blast furnace gas heating magnitude is

greatly influenced by its temperature and pressure before mixing, as well as by the amount of steam supplied.

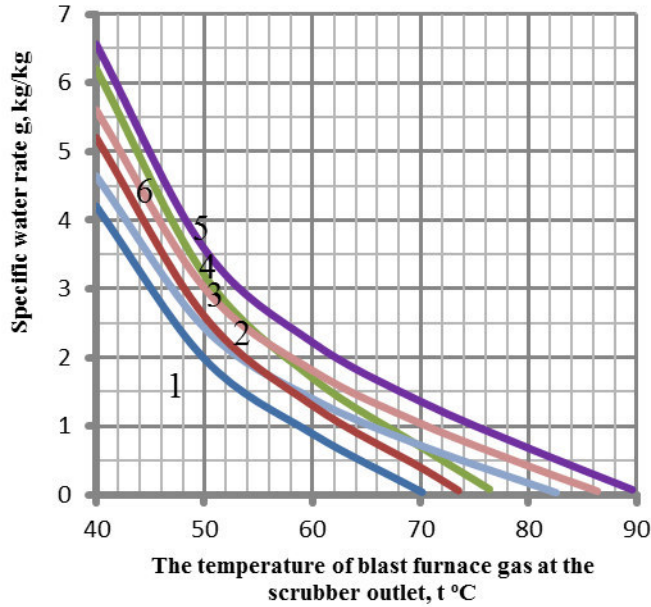


Fig.1. Cooling water consumption at the scrubber

1-2, 3-4, 5-6 at  $T_0 = 150, 200, 250^\circ\text{C}$ ;  
1, 3, 5 - at  $P_0 = 0,2 \text{ MPa}$ ;  
2, 4, 6 - at  $P_0 = 0,35 \text{ MPa}$ ;

The temperature of the steam does not influence much on the gas temperature after mixing. The fig.2 shows that the steam flow amount of 3-5% of the blast furnace gas consumption increases its temperature by 10-25 °C, depending on the gas parameters and, consequently, increases the useable work of the gas turbine from 8 to 19%.

The application efficiency of the third method, and the optimal amount of steam supply is depend on a number of factors. The main of them are the pressure and temperature of the blast furnace gas at the turbine input, the temperature of the exhaust fumes at the consumers, fuel and electricity fees, the distance to the steam source. It is obvious that the most economical is to use the steam from blast furnaces evaporative cooling. The turbine control system also influences much on the techno-economic performance. The

absence of the rotary guide blades at the first stage of TRT greatly reduces the effectiveness of the proposed method.

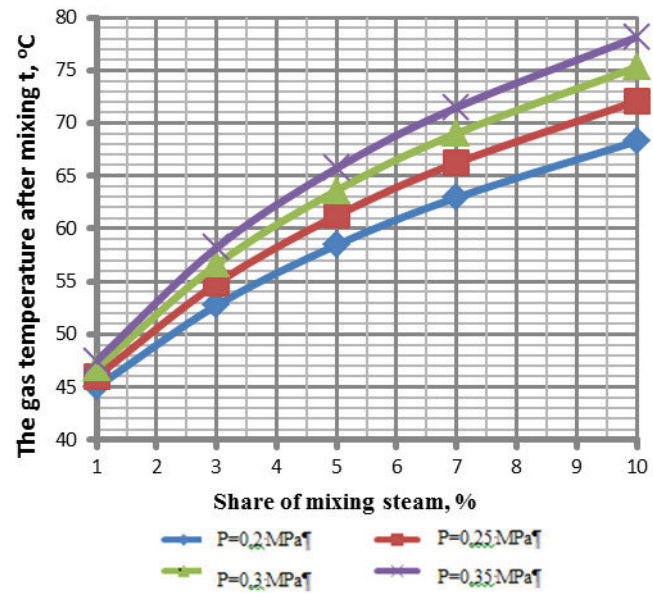


Fig. 2. The gas temperature after mixing with low parameters steam

## V. CONCLUSION

Thus, the energy and economic efficiency of TRT can be significantly increased by the temperature rise to the values at which the blast furnace gas is cooled in scrubbing system, delivering the water vapour from various rendering plants in blast furnace gas before TRT, combining the proposed ways, improving the design of TRT.

## REFERENCES:

- [1] Improving utilization of the excess pressure of blast furnace gas/ VG Khromchenkov V. G., B. V. Sazanov, D. B. Palitsin, V. A. Tolkushin. Industrial heat power energy, 1983 (in Russian)

Научное издание

**INTERNATIONAL ACADEMIC FORUM AMO – SPITSE – NESEFF (20–25  
June 2016, Moscow – Smolensk): Proceedings of the International Academic Forum  
AMO – SPITSE – NESEFF**

---

Формат 60x84<sup>1/8</sup>. Тираж 300 экз. Печ. л. 19,5

Издательство «Универсум»  
Отпечатано в издательском секторе филиала МЭИ в г. Смоленске  
214013 г. Смоленск, Энергетический проезд, 1

ISBN 978-5-91412-313-7

A standard linear barcode representing the ISBN number 978-5-91412-313-7. The barcode is composed of vertical black bars of varying widths on a white background.

9 785914 123137